UNIVERSIDAD POLITÉCNICA DE VALENCIA

DEPARTAMENTO DE TERMODINÁMICA APLICADA

Modelling and optimization of an adsorption cooling system for automotive applications

(*Doctoral Program of Energy Technology*)

Author

Maria Verde Trindade

Supervisor

Dr. Eng. José Miguel Corberán Salvador

Valencia, July 2015

Tesis doctoral

Modelling and optimization of an adsorption cooling system for automotive applications

Realizada por: Maria Verde Trindade

Dirigida por: Dr. D. José Miguel Corberán Salvador

Tribunal Calificador:

Presidente: Dr. D. Joan Carles Bruno Argilaguet

Secretario: Dr. D. José Gonzálvez Maciá

Vocales: Dr. D. José Ramón Garcia Cascales

Valencia, Julio 2015

“It's only those who do nothing that make no mistakes, I suppose.”

Joseph Conrad, *An Outcast of the Islands*

“I don't like work - no man does - but I like what is in the work - the chance to find yourself. Your own reality - for yourself not for others - what no other man can ever know. They can only see the mere show, and never can tell what it really means.”

Joseph Conrad, *Heart of Darkness*

ACKNOWLEDGEMENTS

I would like to express my deep appreciation and thanks to my thesis supervisor, Prof. José Miguel Corberán, for giving me the opportunity and motivation to undertake this work. His continuous encouragement, suggestions, advice and guidance throughout this entire course have been a beneficial contribution to this study.

Sincere gratitude is also due to Robert de Boer and Simon Smeding of the Energy Research Centre of the Netherlands (ECN), and also Angelo Freni and Alessio Sapienza of the Institute for Advanced Energy Technologies "Nicola Giordano" (CNR-ITAE) for their constant helpfulness and productive collaboration throughout this study.

I also would like to thank the members of the examination committee, for their attention and time.

In addition, I would like to acknowledge the support I have received from the Fundação para a Ciência e a Tecnologia (FCT) while pursuing this degree.

Special thanks to Isabel, Carolina and Ainoa for their friendship and cooperation.

Finally, I would like to thank my partner, Apollo. Without his love, patience and understanding, I certainly would have never succeeded in seeing this study to its end. It is to him, and my love for him, that I dedicate this work.

SUMMARY

This PhD study deals with the modelling of an adsorption system designed to provide air conditioning for vehicles, and is driven by the waste heat available from the water/glycol cooling circuit of the engine. The system is based on the sequential heating/cooling of two sorption beds containing a solid sorption material which desorbs or adsorbs water vapour. The condensation of the vapour is carried out by a cooling circuit while the subsequent evaporation of the condensed liquid is employed to produce the cooling effect, generating chilled water, which is then employed to cool down the air of the cabin.

The developed model is fully dynamic and is based on zero-dimensional lumped parameter models for all the necessary components of the overall system including the engine, the beds, the heating circuit, the cooling circuit, the chilled water circuit and the vehicle cabin. The sorption bed model takes into account the non-equilibrium of the adsorption and desorption processes and is able to work with any kind of adsorbent materials, but the study has been restricted to silica gel and zeolite which are among the most appropriate materials for this application. The model is employed to simulate a standard driving cycle of a vehicle, evaluating the instantaneous available heat from the engine cooling system and the dynamic behaviour of the described sorption A/C system, resulting in the estimation of the evolution of the cabin temperature along the cycle.

The model of the overall system has been developed under the MATLAB® Simulink® programming environment. The model of the adsorption system has been first validated against experimental results, showing its excellent capabilities to predict the dynamic behaviour of the system. The model was then used to analyse the influence of the main design parameters of the bed and the main operation parameters on the system's performance: cooling capacity and coefficient of performance (COP). This was done in order to provide rules for the optimal design and operation of this kind of systems.

Finally, the model has been employed to analyse the overall system (engine, adsorption system, heating and cooling circuits, chilled water circuit and cabin) performance along a standard driving cycle, under various operation strategies with regards to the initial state of the adsorbent material in the beds, and operation conditions both for a car and a truck. The results show the difficulties of activating the system at the initial periods of the cycle, when the engine is warming up, and the difficulties to synchronise the operation of the system with the availability of waste energy. They also highlight the limitation in capacity of the designed system, showing that it would not able to fulfil the comfort requirements inside the cabin in hot days or after soaking conditions.

Part of this PhD study was carried out in the frame of an R&D project called “Thermally Operated Mobile Air Conditioning Systems – TOPMACS”, financially supported by the EU under the FP6 program, which was devoted to the evaluation of the feasibility and performance of potential sorption system solutions for the air conditioning of vehicles.

RESUMEN

Esta tesis doctoral se centra en el modelado de un sistema de adsorción diseñado para proporcionar aire acondicionado de vehículos a partir del calor residual disponible en el circuito de refrigeración de agua/glicol del motor. El sistema se basa en el calentamiento/enfriamiento secuencial de dos reactores que contienen un material adsorbente sólido que desorbe o absorbe vapor de agua. La condensación del vapor se lleva a cabo mediante un circuito de refrigeración, mientras que la posterior evaporación del agua condensada se emplea para producir agua fría, que se emplea finalmente en enfriar el aire de la cabina.

El modelo desarrollado es completamente dinámico y se basa en modelos cero dimensionales de parámetros concentrados, para todos y cada uno de los componentes del sistema global incluyendo el motor, los reactores, el circuito de calentamiento, el circuito de enfriamiento, el circuito de agua fría y la cabina del vehículo. El modelo del reactor contempla el no equilibrio de los procesos de adsorción o desorción y es capaz de trabajar con cualquier par de materiales adsorbentes. No obstante el estudio se ha restringido a gel de sílice y zeolita que se encuentran entre los materiales más adecuados para esta aplicación. El modelo se emplea para simular un ciclo de conducción estándar del vehículo, evaluando el calor disponible instantáneamente en el sistema de refrigeración del motor, y el comportamiento dinámico del sistema descrito adsorción-Aire Acondicionado, permitiendo como resultado principal la estimación de la evolución de la temperatura de la cabina a lo largo el ciclo.

El modelo del sistema global se ha desarrollado en el marco del entorno de programación MATLAB® Simulink®. El modelo del sistema de adsorción se ha validado primero contra resultados experimentales demostrando las excelentes capacidades del modelo para predecir el comportamiento dinámico del sistema. A continuación, el modelo se ha aplicado para analizar la influencia de los principales parámetros de diseño del reactor, y de los principales parámetros de operación, sobre el rendimiento del sistema: la capacidad y coeficiente de

operación (COP), con el fin de proporcionar directrices para el diseño y operación óptima de este tipo de sistemas.

Por último, el modelo ha sido empleado para analizar el funcionamiento y prestaciones del sistema en su conjunto (motor, sistema de absorción, los circuitos de calefacción y refrigeración, circuito de agua fría, y la cabina) a lo largo de un ciclo de conducción estándar, bajo diferentes estrategias de operación en lo que se refiere al estado inicial del material adsorbente en los reactores, y las condiciones de operación, para el caso de un coche, y para el de un camión. Los resultados muestran las dificultades de la activación del sistema en los periodos iniciales del ciclo, cuando el motor se está calentando, y las dificultades para sincronizar el funcionamiento del sistema con la disponibilidad de energía térmica excedente del motor, así como la limitación en la capacidad de enfriamiento del sistema diseñado, que no resulta capaz de satisfacer los requerimientos mínimos de confort dentro de la cabina en los días calurosos o de enfriarlo con suficiente rapidez cuando el vehículo ha estado estacionado bajo el sol durante varias horas.

Parte de este estudio de doctorado se ha llevado a cabo en el marco de un proyecto de I + D denominado " Thermally Operated Mobile Air Conditioning Systems – TOPMACS", financiado parcialmente por la UE en el marco del programa FP6, y que perseguía la evaluación de la viabilidad y el potencial de aplicación de soluciones de sistemas de adsorción activadas por el calor residual del motor para el aire acondicionado de vehículos.

RESUM

Aquesta tesi doctoral es centra en el model d'un sistema d'adsorció dissenyat per a proporcionar aire acondicionat a vehicles a partir de la calor residual disponible al circuit de refrigeració d'aigua / glicol del motor. El sistema es basa en l'escalfament / refredament seqüencial de dos reactors que contenen un material adsorbent sòlid que desorbeix o absorbeix vapor d'aigua. La condensació del vapor es porta a terme mitjançant un circuit de refrigeració, mentre que la posterior evaporació de l'aigua condensada s'utilitza per a produir aigua freda, que s'empra finalment en refredar l'aire de la cabina.

El model desenvolupat és completament dinàmic i es basa en models zero dimensionals de paràmetres concentrats, per a tots i cada un dels components del sistema global incloent el motor, els reactors, el circuit d'escalfament, el circuit de refredament, el circuit d'aigua freda i la cabina del vehicle. El model del reactor contempla el no equilibri dels processos d'adsorció o desorció i és capaç de treballar amb qualsevol parell de materials adsorbents. No obstant això, l'estudi s'ha restringit a gel de sílice i zeolita que es troben entre els materials més adequats per a aquesta aplicació. El model s'utilitza per a simular un cicle de conducció estàndard del vehicle, avaluant la calor disponible instantàniament en el sistema de refrigeració del motor, i el comportament dinàmic del sistema descrit Adsorció-Aire Acondicionat, permetent com a resultat principal l'estimació de l'evolució de la temperatura de la cabina al llarg del cicle.

El model del sistema global s'ha desenvolupat en l'entorn de programació MATLAB® Simulink®. El model del sistema d'adsorció s'ha validat primer amb resultats experimentals demostrant les excel·lents capacitats del model per a predir el comportament dinàmic del sistema. A continuació, el model s'ha aplicat per analitzar la influència dels principals paràmetres de disseny del reactor, i dels principals paràmetres d'operació, sobre el rendiment del sistema: la capacitat i coeficient d'operació (COP), amb la finalitat de proporcionar directrius per al disseny i operació òptima d'aquest tipus de sistemes.

Finalment, el model ha estat utilitzat per analitzar el funcionament i prestacions del sistema en el seu conjunt (motor, sistema d'absorció, els circuits de calefacció i refrigeració, circuit d'aigua freda, i la cabina) al llarg d'un cicle de conducció estàndard, sota diferents estratègies d'operació pel que fa a l'estat inicial del material adsorbent en els reactors, i les condicions d'operació, per al cas d'un cotxe, i per al d'un camió. Els resultats mostren les dificultats de l'activació del sistema en els períodes inicials del cicle, quan el motor s'està escalfant, i les dificultats per sincronitzar el funcionament del sistema amb la disponibilitat d'energia tèrmica excedent del motor, així com la limitació en la capacitat de refredament del sistema dissenyat, que no resulta capaç de satisfer els requeriments mínims de confort dins de la cabina en els dies calorosos o de refredar amb suficient rapidesa quan el vehicle ha estat estacionat sota el sol durant diverses hores.

Part d'aquest estudi de doctorat s'ha dut a terme en el marc d'un projecte d'I + D denominat "Thermally Operated Mobile Air Conditioning Systems - TOPMACS", finançat parcialment per la UE en el marc del programa FP6, i que perseguia l'avaluació de la viabilitat i el potencial d'aplicació de solucions de sistemes d'adsorció activats per la calor residual del motor per a l'aire condicionat de vehicles.

GENERAL INDEX

FIGURE CAPTIONS

TABLE CAPTIONS

NOMENCLATURE

A	area [m^2]
A_c	cross-sectional area [m^2]
$A_{w,i}$	water side heat transfer area for one control volume (i) [m^2]
$A_{plate,i}$	plate heat transfer area for one control volume (i) [m^2]
$A_{unfin,i}$	unfinned surface heat transfer area for one control volume (i) [m^2]
$A_{fin,i}$	finned surface heat transfer area for one control volume (i) [m^2]
$A_{w,t}$	total heat transfer area for the water side [m^2]
cp	specific heat capacity [J kg^{-1} K^{-1}]
$cp_{ads,0}$	dry adsorbent specific heat capacity [J kg^{-1} K^{-1}]
$\overline{cp}_b$	equivalent heat capacity of the bed per adsorbent mass [J K^{-1}]
C	thermal capacity [J K^{-1}]
COP	coefficient of performance
$COP_{m,p}$	maximum practical coefficient of performance
COP_{max}	maximum theoretical coefficient of performance
D	depth [m]
D_h	hydraulic diameter [m]
e_{met}	water channel wall thickness [m]
H	height [m]
h	specific enthalpy [J kg^{-1}]
h	convective heat transfer coefficient [W m^{-2} K^{-1}]
$h_{eq,1}$	unfinned surface equivalent convection heat transfer coefficient [W m^{-2} K^{-1}]
$h_{eq,2}$	finned surface equivalent convection heat transfer coefficient [W m^{-2} K^{-1}]
k	thermal conductivity [W m^{-1} K^{-1}]
k_1	kinetic constant
k_2	kinetic constant
$\dot{Q}$	total heat transfer rate, W
$\dot{Q}_i$	total heat transfer rate in one control volume (i), W
$\dot{Q}_{cond}$	condenser capacity [W]
$\dot{Q}_{heat}$	bed heating capacity [W]
$\dot{Q}_{cool}$	bed cooling capacity [W]
$\dot{Q}_{chill}$	system cooling capacity [W]

$Q_{chill}\|_{m,p}$	maximum practical cooling capacity [W]
L_f	fin length [m]
m	mass [kg]
$m_{met,tot}$	total metal mass in the heat exchanger (including headers) [kg]
$m_{w,tot}$	total water mass in the heat exchanger (including headers) [kg]
$m_{ads,HE}$	total dry adsorbent mass per heat exchanger [kg]
$m_{met,HE}$	total metal mass per heat exchanger [kg]
$m_{ads,b}$	total mass of dry adsorbent packed in each bed [kg]
$\dot{m}$	mass flow rate [kg s^{-1}]
$\dot{m}_{evap,i}$	refrigerant flow entering the evaporator [kg s^{-1}]
$\dot{m}_{evap,o}$	refrigerant flow leaving the evaporator [kg s^{-1}]
$\dot{m}_{cond,i}$	refrigerant flow entering the condenser [kg s^{-1}]
$\dot{m}_{cond,o}$	refrigerant flow leaving the condenser [kg s^{-1}]
$\dot{m}_{evap}$	evaporation rate [kg s^{-1}]
$\dot{m}_{cond}$	condensation rate [kg s^{-1}]
M	molar mass [kg mol^{-1}]
N_{ch}	number of tube channels
N_{fins}	number of fins per channel tube
Nu	Nusselt number
p	channel pitch [m]
$P_{wet,ch}$	wetted perimeter of the channel [m]
P	pressure [mbar]
p_f	fin pitch [m]
R_{tot}	total thermal resistance [K W^{-1}]
R	universal gas constant [mbar m^3 kg^{-1} K^{-1}]
RH	relative humidity [%]
SCC	specific cooling power [W kg]
$SCC_{m,p}$	maximum practical specific cooling capacity [kW m^{-3}]
t	channel tube thickness [m]
t_f	fin thickness [m]
T	temperature, [K]
$T_{b,M}$	maximum bed temperature [K]

$T_{b,m}$	minimum bed temperature [K]
T_{env}	ambient temperature [K]
T_{cab}	cabin temperature [K]
T_{eng}	engine coolant water temperature [K]
$T_{w,i}$	inlet water temperature for the component in question [K]
$T_{w,o}$	outlet water temperature for the component in question [K]
$T_{wi,HE}$	water temperature at the inlet of the heat exchanger, [K]
$T_{wo,HE}$	water temperature at the outlet of the heat exchanger, [K]
T_{wi}	water temperature at the inlet of the bed [K]
T_{wo}	water temperature at the outlet of the bed [K]
U	heat transfer coefficient [W m^{-2} K^{-1}]
$UA_{total,HE}$	overall thermal conductance of the adsorbent heat exchanger [W/K]
UA_{comp}	component overall thermal conductance [W/K]
V	volume, m^3
V_{ch}	channel tube volume [m^3]
V_f	fin volume [m^3]
$V_{met,HE}$	non-adsorbent volume of the heat exchanger [m^3]
$V_{ads,HE}$	adsorbent volume in the heat exchanger [m^3]
$V_{w,HE}$	total volume of water in the heat exchanger [m^3]
V_{HE}	overall volume of the heat exchanger [m^3]
W	wide [m]
w	uptake [kg kg^{-1}]

Greek Letters

ρ	density [kg m^{-3}]
η_f	fin efficiency
ε	effectiveness
Δh_{des}	enthalpy of desorption [J kg^{-1}]
Δh_{ad}	enthalpy of adsorption [J kg^{-1}]
Δh_{fg}	enthalpy of vaporization [J kg^{-1}]
τ_{cycle}	full cycle time [s]

Subscripts

ads	adsorbent
a	non-condensable gases
b	bed
b1	bed 1
b2	bed 2
comp	component
C	condenser
cond	condenser
cw	bed cooling water
ch	channel tube
chill	chilled water
E	evaporator
evap	evaporator
eq	equilibrium
f	fin
HE	adsorbent bed heat exchanger
hw	bed heating water
(i)	control volume
l	liquid water
met	metal
max	maximum
min	minimum
port,i	inlet port
port,o	outlet port
s,i	inner wall surface
s,o	outer wall surface
sec	condenser secondary water
sat	saturation
v	water vapour
wch	water channel
w	secondary water
w-g	ethylene glycol-water mixture
wport,i	water inside the inlet port
wport,o	water inside the outlet port
wHE	water inside the adsorbent bed heat exchanger

1. INTRODUCTION AND OBJECTIVES

1.1. Motivation

In the past two decades, it was found that synthetic refrigerants played an important role in the depletion of the ozone layer, as well as in the increase of the global warming effect. CFCs and HCFCs, traditionally used as working fluids for refrigeration systems, have been prohibited for the protection of the ozone layer after stricter environmental regulations came into effect, first in Montreal in 1988 and afterwards in Kyoto in 1998. Since then, refrigeration technology has been experimenting with a large variety of alternative systems, in order to reduce energy consumption and minimize possible environmental impact.

One of the most promising alternatives for air conditioning and heat pump applications is the adsorption refrigeration technology, which offers significant advantages over traditional refrigeration systems. Recent research on adsorption refrigeration has mostly focused on developing more environmental friendly new systems that have high primary energy efficiency and are able to employ various kinds of driving energy, from solar energy to waste heat.

A basic adsorption refrigeration system consists of four main parts: a sorption bed (also called adsorber or adsorbent bed), a condenser, an evaporator and an expansion valve. The sorption bed is a process unit which is filled with an adsorbent material (such as zeolite, silica gel, active carbon, etc.). A heat exchanger fluid is used for heating or cooling the bed. As a principle, it operates by cycling adsorbate between bed, condenser, and evaporator.

An adsorption refrigeration system requires low grade energy for operating use. Hence, in such systems, the adsorption process plays the same role as the mechanical process in the traditional refrigeration systems by using energy in the form of heat rather than mechanical work, so that the working fluid can be circulated without any mechanical power.

Demir et al. [1] pointed out the most important advantages and disadvantages of adsorption systems. The main advantages of the adsorption heat pumps and adsorption refrigeration systems can be summarized as follows:

- They can operate with thermal driving energy sources such as waste heat, solar, and geothermal energies, etc.;
- They can work with low temperature driving energy sources;
- They do not require moving parts for the circulation of working fluid;
- They have long life time;
- They operate without noise and vibration;
- They have a simple working principle;
- They do not require frequent maintenance;
- They are environmentally friendly since do not contain any hazardous materials for the environment;
- They can be employed as thermal energy storage devices.

The main disadvantages of adsorption systems are the following:

- They have low coefficient of performance (COP) values;
- They work in an intermittent fashion;
- They require high technology and a special design to maintain high vacuum;
- They have large volume and weight when compared to traditional mechanical heat pump systems;
- They have low specific cooling power (SCP). The SCP is defined as the cooling power in watts per kilogram of adsorbent.

Several adsorption systems have already been built and tested in the recent years, showing encouraging results, but this technology still has to be improved. For instance, Wang et al. [2] mentioned several adsorption chillers which reached a commercial status. According to the author, adsorption chillers which were produced by the Nishiyodo Kuchouki Co. Ltd. appeared in the market in 1986. These chillers were driven by a heat source temperature from 50 to 90

ºC, and the temperature of the chilled water could be as low as 3ºC. When the chiller was driven by the hot water at 90 ºC, a COP of 0.7 could be reached. Mycom is a known company for producing silica gel–water adsorption chillers in Japan. The chillers produced can be powered by hot water at 75ºC and yield chilled water at 9 ºC with a reported COP of 0.6.

A mathematical model of the adsorption refrigeration system is usually employed to assist in the system design, to predict the system performance and to understand the adsorption/desorption phenomena in the bed. Also, by using an accurate simulation tool, the performance of the adsorption system can be improved by optimizing the operating conditions. The advantages of using numerical simulations are that large volumes of data can be generated at virtually no added cost, making the performance of parametric studies to optimize equipment performance much easier. Also, some parameters are difficult to test in the laboratory, and the experimental study could be expensive as well as time consuming.

Mathematical models are constantly being developed for predicting the performance of adsorption refrigeration systems. They provide fundamental understanding of the heat and mass transfer process in the bed and give useful guidelines regarding the system design. This PhD study focuses on two main objectives. The first one is to develop a model able to reproduce the dynamic behaviour of a double-bed adsorption cooling system. The second one is to use the developed model, after it has been validated by experimental data, to optimize the design and operation of the system, and improve its performance. In particular, the influence of parameter changes on the system performance in terms of cooling capacity and COP are analyzed. This can be achieved by estimating the cooling capacity and thermal efficiency limits, having as final goal a commercially attractive system, potentially able to compete with traditional air conditioning designs within the market.

1.2. Background and literature survey on adsorption refrigeration systems

1.2.1. Current status of the technology

Nowadays, several adsorption refrigeration systems are under development, as an alternative to traditional systems which require high energy consumption and emit ozone depleting gases (CFCs and HCFCs). A solid adsorption cooling system is a promising alternative to conventional vapour-compression systems, since it saves energy and minimizes environmental impact. This is possible since it can be driven either by waste heat sources or by renewable energy sources and uses no CFCs as refrigerant.

Research groups in China [3-8], Japan [9], The Netherlands [10], Italy [11] and France [12] have designed and tested several adsorption refrigeration systems. The systems mentioned above use waste heat as their driving energy source, and were designed for different kind of applications such as ice making, trigeneration and air conditioning.

Zhu et al. [3] designed a prototype of a zeolite-water adsorption chiller to be used on a fishing boat for preserving aquatic products. The system was designed to produce chilled water at about 5 ºC. The adsorption system was driven by the exhaust gas at 200 ºC from the engine, and then cooled at ambient temperature. The system comprised two adsorption units. Each unit consisted in a shell-and-tube heat exchanger filled with a synthetic zeolite 13X, a condenser/evaporator and a water tank. The condenser/evaporator was connected to the bed by a vapour line and immersed in the tank. The prototype system was tested under real conditions. The experimental results showed that when the temperature of the exhaust gas was increased, as a result of a higher engine load, the capacity of the unit became higher and the period of the cycle was shorter.

Wang et al. [4] designed an adsorption ice maker to be also used on a fishing boat. The system was driven by the exhaust gases from the engine. The

working pair employed was activated carbon and methanol. Before designing a suitable ice maker, the heat and mass transfer performances of a solidified bed and a granular bed were compared. They showed that the heat transfer coefficient in a solidified bed was much higher than in a granular bed, however, the performance of the solidified bed was inferior due to its low permeability. They pointed out the importance of mass transfer channels inside the bed to ensure that the adsorption rate would not be influenced by the low permeability. They also showed that the COP of a double-granular-bed system could be improved by 60% if heat and mass recovery was considered in the system. Finally, an adsorption ice maker which comprised of two solidified beds was designed and tested. The arrangement of the mass transfer channels in the beds was improved. Experimental results showed that an optimal ice production of 20 kg/h, a cooling power of 3 kW and a COP of 0.14 could be obtained with an evaporating temperature of 15 ºC.

Grisel et al. [10] designed and tested an adsorption cooling system driven by a low grade waste heat source. The system was designed to be implemented in a prototype trigeneration system. The system comprised of two sorption beds, an evaporator and a condenser. The working pair employed was silica gel and water. Each sorption bed consisted of six automotive plate-fin heat exchangers filled with about 1.45 kg of silica gel (type Sorbsil A). In order to avoid an internal pressure drop in the bed as well as to prevent a too large temperature difference, the adsorbent heat exchangers were connected in parallel. The reason behind this was to achieve the lowest possible cooling water temperature for both components. Also, heat recovery between both beds was applied before the operation mode of both beds was reversed. The heat recovery proved to increase considerably the thermal efficiency of the system in terms of COP. The system was designed to achieve a continuous cooling power of 5 kW; however, this value was only reached under ideal operating conditions. The experimental results showed that an average cooling power of 3.6 kW, a SCP of 208 W/kg, and a COP of 0.62 could be obtained under more realistic operating conditions.

Several authors developed adsorption cooling systems for automotive applications [5-9, 11, 12].

Jiangzhou et al. [5] developed an adsorption air conditioning system to produce chilled water for the fan coils of a locomotive driver cabin. The system was driven by exhaust heat from the engine. A lab-scale prototype was tested and the experimental results were discussed. The prototype comprised of an adsorber, a regenerator, a condenser and an evaporator. The working pair employed was zeolite as adsorbent and water as working fluid. The experimental results showed that the adsorption and desorption temperatures have significant influence on the performance. However, it was found that the condensing temperature had no effect on the COP of the system, contrasting most other adsorption systems discussed here.

In a subsequent study, Lu et al. [6] carried out an experimental test with an adsorption air conditioner similar to the one proposed by Jiangzhou et al. [5] under real operating conditions. The adsorption system was installed in a locomotive and tested under different running conditions. The results showed that the adsorption air conditioning system was able to provide a cooling capacity high enough to make the locomotive's driver cabin comfortable. However, the cooling power was strongly affected by the running conditions of the locomotive. Experimental results showed that a cooling power between 3 and 4.2 kW could be obtained under standard running conditions.

Wang et al. [7] developed a zeolite-water adsorption air conditioner driven by the exhaust gas from the engine of a locomotive (at 350-450 ºC). The author designed an adsorption system different from other double-bed adsorption air conditioning systems found in the literature [3, 4, 11, 12]. The main difference is that the system comprised of two identical vacuum chambers. Each adsorption/desorption chamber contained one adsorber, one condenser and one evaporator. Based on the experiments, the system was able to produce a cooling power of 3.2 kW and COP of 0.152 at an evaporating temperature of 8 ºC.

Zhang et al. [8] constructed and tested an adsorption air conditioner for an automobile, powered by the exhaust gas from a diesel engine. The system used zeolite 13X as adsorbent and water as adsorbate. The adsorber was a finned double-tube heat exchanger filled with adsorbent pellets. The experimental results were presented in comparison to simulation results obtained by a previously developed mathematical model. Results showed a generally good agreement between the experimental and the simulation results. According to the experiments, the system was able to produce a SCP of 25.7 W/kg and a COP of 0.38 at an evaporating temperature of 10 °C and a condensing temperature of 45 °C. The inlet temperature of the heating gases and cooling fluid was reported at 310 °C and 25 °C, respectively.

Suzuki [9] proposed a zeolite–water adsorption cooling system for automobile air conditioning purposes. The system was driven by the exhaust gas from an engine at high temperatures (400-600 ºC). A preliminary study was presented in order to assess the feasibility of adsorption systems in automobile air conditioning applications.

Vasta et al. [11] designed and tested a prototype of an adsorption chiller to be installed in a truck for mobile air conditioning purposes. The system used waste heat from the engine coolant loop and it was designed to produce about 2.5 kW of cooling power for the driver cabin. The system used a novel type of zeolite named FAM-Z02 as the adsorbent and water as the adsorbate. The experiments with this prototype were performed in two sections: (i) the prototype was tested at the laboratory in simulated conditions (ii) the prototype was installed on a truck cabin and tested in real conditions. The onboard prototype was composed of two beds, a compact evaporator and a condenser. Each sorption bed contained finned flat-tube heat exchangers packed with zeolite grains. The compact evaporator and condenser were built by using finned-tube heat exchangers. The total weight of the prototype was 60 kg and its size was 170 dm^3, measurements which were deemed suitable for mobile applications. Experiments carried out in the laboratory showed that the system was able to produce an adequate cooling power of 1-2.3 kW, a SCP of 300-600 W/kg and a COP of 0.25-0.45 at normal climate driving conditions (condensing

temperature at 28 ºC and heating temperature at 90 ºC). The experiments with the prototype installed in the truck cabin showed that the system was able to deliver cold air at 9 ºC with a cooling power of 2 kW in non-favourable operating conditions.

Poyelle et al. [12] designed and tested a zeolite-water adsorption air conditioning system driven by a high temperature heat source (at 230 ºC). The adsorption air conditioner prototype contained two beds, operating out of phase, one condenser and one evaporator. The beds operated with a internal heat and mass recovery cycle in order to enhance the performance of the system. Also, the authors developed a consolidated adsorbent composite with good heat transfer properties which was used in the beds. Each bed comprised of a tubular heat exchanger filled with 5 kg of pure zeolite, 1.3 kg of binder, and 1.8 kg of expanded natural graphite. They noted that the addition of graphite resulted in an increase of the effective thermal conductivity of the adsorbent (from 0.1 W m^{-1} K^{-1} for a granular bed to 5 W m^{-1} K^{-1} for the adsorbent composite), as well as an improved heat transfer coefficient between the tube wall and the adsorbent (from 30 W m^{-2} K^{-1} to 500-1000 W m^{-2} K^{-1}). However, the mass transfer characterized by the effective permeability decreased due to material consolidation (from 10^{-9} m^2 to 10^{-12} m^2). To overcome the problem of low permeability, arteries were designed in the consolidated bed to decrease mass transfer resistance. Experiments carried out with a total heat and mass recovery time of 10 min and a cycle time of 60 min showed that a SCP of 97 W/kg and COP of 0.41 could be achieved at an evaporating temperature of 4 ºC. At a higher evaporating temperature (25-30 ºC), the system could reach a COP of 0.68 and a SCP of 135 W/kg. Authors also put forward a mathematic model to predict the performance of the system, which was validated by experimental results. Furthermore, the model predicted that a SCP of 600 W/kg and a COP of 0.7 could be reached if the mass transfer performance of the system was improved by using a certain new adsorbent material with enhanced mass transfer properties.

Recently, several interesting review articles [1, 2, 13, 14, 15, 16, 17] have been published, giving an overview of the adsorption cooling systems which have

been developed up to now, and an analysis of their advantages and their disadvantages. Adsorption cooling systems still present some drawbacks such as low SCP and COP. However, alternatives have been studied in order to increase the performance of the machines.

Many researchers have proposed advanced adsorption cycles such as heat recovery cycles [18-20], mass recovery cycles [21, 22], heat and mass recovery cycles [23-25], multi-stage cycles [26-29] and multi-bed cycles [30-32] in order to improve the COP and provide a continuous cooling output. The continuity of the cooling process is generally provided by increasing the number of beds [1]. The increase of COP is obtained by recycling otherwise wasted heat that is rejected from the bed being cooled by transferring it to the bed being heated. This increases the COP of the cycle since the required amount of external heat input is reduced. A heat transfer fluid is used to transfer heat between the beds. When recycled heat is supplied uniformly to the beds, the process is called uniform-temperature heat recovery [13]. This type of advanced cycle results in the enhancement of the COP up to 50% for a two-bed machine [1,13]. Besides the utilization of heat recovery cycles, it is possible to increase the cooling power of the system by using a refrigerant mass recovery process between the two beds. The mass recovery cycle increases the cyclic adsorption capacity and the SCP is improved accordingly. It could also increase the ability of the adsorption cooling system to use low grade heat [15]. Both SCP and COP of the system could be improved if the heat and the mass recovery cycle are simultaneously used and combined into the heat and mass recovery cycle. Lastly, the use of multi-bed and multi-stage cycles can also improve the performance of an adsorption cooling system. The main goal of these advanced cycles is to lower the driving source temperature, especially at temperatures lower than 80 ºC [15], and to enhance the waste heat utilization capability. However, additional beds and heat exchangers in these type of advanced cycles could result in the increase of production cost and the enlargement of the chiller size.

Furthermore, the efficiency of the adsorption system can be improved by enhancing the heat and mass transfer process in the bed in order to speed up

the adsorption/desorption phenomena. There are two common ways to enhance the heat and mass transfer in a sorption bed: one is the improvement of the thermo-physical properties of the adsorbent, and the other is to optimize the bed design.

Since the thermal conductivity of adsorbents is generally low, the heat is transferred slowly through the bed, and consequently, the adsorption/desorption cycle time becomes longer [1]. This could negatively affect the performance of the adsorption system. However, it is possible to enhance the heat transfer in the adsorption system by improving the thermal conductivity of the adsorbent. This could be achieved by adding good thermally conductive materials such as expanded graphite and carbon fibre into the adsorbent [1, 14, 15]. In addition, mixing the different size of adsorbent particles together could also strengthen the heat transfer process [15]. Consolidating the adsorbent and/or mixing it with a metallic foam additive is another good method to improve the heat transfer performance of the bed [14, 15]. On the other hand, mass transfer depends on the adsorbate flow through the bed (interparticle flow) and through the adsorbent (intraparticle diffusion) [1]. As such, consolidation of the adsorbent results in decreasing permeability of adsorbate through the adsorbent particles [12]. Therefore, these methods are more effective only when the mass transfer is not the main factor to impact on the performance of the adsorption system. If the influence of the mass transfer is relatively high, the mass transfer must be enhanced as along with the heat transfer. Reducing the thickness of the adsorbent layer would be one simple and commonly used method, however the effective capacity of the bed and the filling amount of the adsorbent would decrease [15].

Another approach for heat transfer enhancement in the bed consists of improving the sorption bed design, for example by using extended surfaces (i.e. fins or similar surfaces) which can increase the effective heat transfer area. However, the disadvantage of this technology is that it also increases the thermal capacity of the bed. On the other hand, a low ratio of metal-to-adsorbent heat capacity and a low secondary fluid heat capacity can also improve the system performance [15]. Also, the heat transfer in the bed can be

enhanced by reducing the contact heat resistance between the adsorbent and the metal [15]. The mass transfer through the bed can be improved by creating voids in the bed [1].

1.2.2. Review of mathematical models

The performance analysis of adsorption refrigeration systems has been investigated by many researchers. Most research on these systems is related to the development of mathematical models in order to predict the behaviour of the adsorption cooling system, and to improve the system's performance by optimizing the operating conditions, such as temperature levels, mass flow rate and cycle time.

Various types of mathematical models have been proposed and used to carry out critical investigations on adsorption refrigeration. In this chapter, a review of the present state of mathematical modelling of such systems is presented. Validation with experimental data is an important step in mathematical modelling development, and therefore comparisons with experimental results have been considered where possible. The models have been classified based on complexity. The development of those models can be classified into two branches: (i) thermodynamic models (ii) dynamic models.

Thermodynamic models form the simplest category, in which the heat and transfer mechanism is generally not examined. As expected, these models can be used to obtain a theoretical limit regarding performance and capacity of a system, but are not able to identify causes of poor performance when examining experimental data. Several thermodynamic models can be found in the literature [33, 34, 35, 36].

Dynamic models are more complex, can subsequently be divided into two further categories. The first category is the lumped parameters models, also known as zero-dimensional models. This category is characterized by the temperature or mass content of the adsorbed phase depending only on the time variable. The second category is comprised of models that include one or more

space dimensions for the temperature or mass content of adsorbate, in addition to the time variable. Consequently, they can be divided into one-, two- or three-dimensional models, depending on how many dimensions they include.

1.2.2.1. Thermodynamic models

Cacciola et al. [33, 34, 35] proposed thermodynamic models to predict the performance of an adsorption heat pump machine. However, in their analysis, the performance of the system is limited by the heat transfer inside the sorption bed only, and an equilibrium adsorption state was assumed.

Cacciola et al. [33] presented a non-dimensional model based on thermodynamic analysis in order to simulate the transient behaviour of a recuperative two-bed zeolite-water adsorption heat pump. In the model, two main assumptions were made: (a) uniform temperature in each bed; (b) the adsorption process was at equilibrium. The governing energy balance equations were derived taking into account the efficiencies of the system components. The equation were transformed to a non-dimensional form and solved numerically. The model was tested using design data taken from Douss et al. [37] and good qualitative agreement was obtained.

Cacciola et al. [34] developed a thermodynamic model to predict the performance of a reversible adsorption heat pump and find the most efficient working pair for domestic applications. The model was used to compare the performance of different adsorbent-adsorbate pairs: two zeolite-water pairs (4A and 13X type) and one activated carbon-methanol pair. The results showed an optimum desorption temperatures of 200 $^{\circ}$C for the zeolite-water pairs and 120 $^{\circ}$C for the activated carbon-methanol pair, with an evaporator temperature of 5 $^{\circ}$C and a condenser temperature of 55 $^{\circ}$C. They concluded that zeolite-water is the most suitable pair for air conditioning purposes, since a higher COP and specific cooling power is obtained, in comparison with the activated carbon-methanol pair.

The optimization of the design of an adsorption heat pump based on thermodynamic analysis was investigated by Cacciola et al. [35] and Benthem et al. [36].

Cacciola et al. [35] developed a thermodynamic model to study the effect of the bed design on the performance of a zeolite-water adsorption heat pump. In their model, the cycle time is limited only by the heat transfer inside the bed. Their results were presented in terms of COP and specific power, which was defined as the ratio between the useful energy and the cycle time per unit of adsorbent mass. The results showed that the COP and the specific power decreased with the increase in the heat capacity ratio between the metal and the dry adsorbent.

Benthem et al. [36] performed an optimization study of the design of a zeolite-water adsorption heat pump. The bed was heated by using oil from a boiler and cooled by using an external heat exchanger. The system operated in counter phase with internal heat recovery from the hot, desorbed bed to the cold, adsorbed bed. A detailed thermodynamic model was used for the optimization of the design of all the system components (boiler, condenser exchanger and evaporator). All the principal components of the machine were designed in order to obtain a constant heat production. To achieve this goal, a system with an automatic bypass of the external heat exchanger was proposed and the sizes of the condenser cooler and the exchanger were optimized. The experimental results showed that the average power of the system increased to 13.1 kW starting from 9 kW for almost 70% of the cycle time. To further improve the power of the system, the effect of the global heat transfer coefficient of the bed on the performance was analyzed. It was shown that the average power of the system increased and the cycle time was shortened by the enhancement of the heat transfer coefficient.

All the models mentioned above are highly interesting, since they help understand the feasibility of using an adsorption cooling system. However, they do not provide information on the dynamic performance, which is highly dependent on the transient behaviour of the various internal and external

interactions between the adsorbent and heat exchanger fluids, and is necessary for the design and optimization of the system.

1.2.2.2. Dynamic models

Modern developments are focusing on dynamic models which give a more clear idea about the dynamic behaviour of the transient heat and mass transfer processes present in the sorption bed. Several dynamic models can be found in the literature [7, 9, 20, 37-64]. Most of the proposed models have been used to investigate conventional double-bed adsorption cooling systems [7, 20, 37-50, 63]. Some of the dynamic models found in the literature have already been validated with experimental data [7, 37-39, 42, 44, 48-54, 63]. Differences among the aforementioned models generally occur in the simplifying assumptions, numerical resolution method, components design and application of the modelled system. The majority of researchers propose zero-dimensional models [7, 9, 37-44, 49, 51, 52, 63] while some have focused on one-dimensional models [45, 55-57, 61, 64] and others on two-dimensional models [20, 46, 47, 50, 54, 58-60, 62]. Three-dimensional models can also be found in the literature [48, 53].

Some of the above dynamic models [20, 37, 42, 44, 49, 50, 56, 57, 59, 61, 62] assume that thermodynamic equilibrium exists between the adsorbent and adsorbate. Therefore, it is assumed that there exists no resistance to mass transfer between the adsorbate and the adsorbent. In this case, the adsorption process is represented by the adsorption equilibrium equation for the adsorbent/adsorbate pair in question. However, in most of the models found in the literature [7, 9, 38-41, 43, 45-48, 51-55, 58, 60, 63, 64], the adsorption process is interpreted by a non-equilibrium model which takes into account the mass transfer resistance inside the adsorbent particles, as proposed by Sakoda et al. [52].

Sakoda et al. [52] proposed a zero-dimensional heat and mass transfer model to predict the performance of a small scale solar cooling unit. The adsorption/desorption process was described by a non-equilibrium model which

takes into account the mass transfer resistance inside the packed bed. A linear driving force (LDF) model was proposed in order to interpret the adsorption process. In the model, the adsorption uptake was approximately given by the LDF equation represented by the difference between the amount adsorbed and the amount adsorbed in equilibrium at certain pressure conditions. The simplified model, which takes into account both adsorption properties and apparatus characteristics, was used to predict the dynamic behaviour of the experiments. A comparison between the predicted results and those obtained experimentally was presented. The experimental results were well interpreted by the model.

Suzuki [9] employed a similar model to Sakoda et al. [52] to predict the performance of a waste heat driven adsorption cooling system for automotive applications. The model was simplified by assuming a constant regeneration temperature. The basic equations were written for the adsorbing process; however, no details were outlined with respect to the evaporator and condenser modelling. No validation was presented in this paper, and the model was too simplified to predict the performance of the system. The effects of the overall heat transfer coefficient between the bed and cooling/heating fluid on the performance of the system were studied. It was found that the overall heat transfer coefficient and the cycle time has the most significant effect on the SCP. The author believes that quicker cycle times with higher heat transfer coefficients provide a higher SCP, which results in smaller amounts of adsorbent for the required cooling capacity. The author also indicates the need for further investigation on the effect of the temperature behaviour of the exhaust gases on the automobile's available waste heat. This effect was not considered in his study.

Sami et al. [42] presented a zero-dimensional dynamic model to study a single and/or double-bed adsorption system with heat recovery. The systems examined used activated carbon and methanol as the working pair. A detailed energy balance model for the adsorber, evaporator and condenser was presented. However, the model was simplified by assuming that the adsorption equilibrium was maintained during the whole process. A comparison between

the predicted results and those obtained experimentally was presented. The simulation results showed that the model was able to predict the dynamic behaviour of the systems and compared well with the presented experimental data.

Wang et al. [7] proposed a zero-dimensional dynamic model to predict the performance of an adsorption air conditioner driven by waste heat. A non-equilibrium adsorption model which takes into account the mass transfer resistance inside the bed was assumed. The model takes into account the energy balance in the adsorber, evaporator and condenser. Simulation results compared to experimental data indicate that the model was able to predict the dynamic performance of the adsorption system accurately, and also compared well with the limited experimental data presented. According to the simulation, the cooling power and COP reached 10.184 kW and 0.2237, respectively, for design working conditions of 450 ºC gas inlet temperature, 40 °C cooling temperature and 6.5 °C chilled water temperature.

Miyazaki et al. [39] proposed an improved zero- dimensional heat and mass transfer model that was able to simulate the transient behaviour of a silica gel-water double-bed adsorption chiller. A detailed energy and mass balance model was presented for the sorption bed, evaporator and condenser. In order to take into account the mass transfer limitations in the bed, a non-equilibrium adsorption process was assumed by using the LDF model [52]. The model was validated with experimental data. A new cycle time allocation was proposed in order to enhance system performance. The temperature profile for different components of the system according to the new cycle time allocation was presented. It was observed that the new cycle time smoothens the delivered chilled water temperature, especially during the switching processes (pre-heating or pre-cooling time). The new cycle time allocation improved the system performance in terms of both COP and cooling power. The cooling power was increased up to 6% with the new cycle time allocation. Furthermore, it was observed that the COP increases with the increase of the cycle time, since there is lower consumption of driving heat source with longer duration cycles.

On the other hand, for low cycle times the COP decreases abruptly since there is not enough time for adsorption or desorption to occur satisfactorily.

Schicktanz et al. [38] developed an improved zero-dimensional dynamic model, which can reproduce the dynamic behaviour of a tested silica gel-water adsorption chiller. A detailed heat and mass transfer model was presented for the adsorber, condenser and evaporator. The adsorption model takes into account mass and energy conservation, and a linear driving force approach [52] was assumed in order to take into account the mass transfer resistance in the adsorber. The simulation results were validated by measured data coming from an adsorption chiller. The measured and simulated results showed very good agreement. From an energetic point of view, the maximum uncertainty was 6%. Dynamically, the uncertainty between measurement and simulation was 15%.

Chua et al. [48] studied a double-bed silica gel-water adsorption chiller using a three-dimensional heat and mass transfer model. The model takes into account both energy and mass resistance within the sorption bed. Furthermore, the model takes into account the energy transfer in the fins, which intensify the heat transfer in the bed. A detailed heat and mass transfer model for the bed, condenser and evaporator was presented. The model results were compared with experimental data. The model prediction agrees very well with the experimental data. The model was used to study the effect of the cycle time on the cooling capacity and on the COP. Authors showed that the cooling capacity might decrease if the cycle time is not optimized. The simulation results revealed that the average cooling capacity was maximized at a cycle time between 230 s and 650 s.

Zhang [53] developed a three-dimensional heat and mass transfer model to predict the performance of an adsorption cooling system driven by the waste heat of an engine. The adsorber was a cylindrical double-tube divided in equal compartments by twelve radial fins. Each compartment was filled with the same amount of adsorbent, specifically 13X-type zeolite, and water was used as working fluid. Both adsorption and desorption processes take place in all the compartments at the same time. Therefore, unlike a two-bed configuration, the

system works in an intermittent way. This configuration was chosen due to its mechanical simplicity, which would ensure fewer malfunctions, especially in harsh or isolated environments. The model was divided into four submodels describing heat transfer in heating/cooling fluids, heat transfer in the metal tube, heat transfer in the fins and heat and mass transfer in the adsorbent. The model takes into account both internal and external mass resistances in the adsorber. A linear driving force equation was employed in order to account for the mass transfer resistances within the adsorber, as proposed by Sakoda et al. [52]. The model was validated by experimental results, showing good agreement between simulated and experimental bed temperatures and cycle times. The author suggests that the model could be used to optimize adsorption systems operating with low-grade heat, and study the kinetics between adsorbate and adsorbent in terms of mass transfer.

Intensive studies have been focused on optimizing the performance of an adsorption cooling system [20, 37, 40, 41, 43-47, 49, 50, 55, 58, 59, 61-64]. The performance of an adsorption cooling system is affected mainly by adsorption/adsorbate properties, configuration parameters and operating conditions. The influence of the operating conditions on the performance has been investigated by various research groups [37, 40, 41, 43, 45, 50, 58]. Similarly, many researchers have conducted parametric studies to analyze the effect of the system design on the performance [37, 40, 41, 44, 46, 47, 49, 55, 59, 61-64].

Saha et al. [43] studied the influence of operating temperatures, water flow rates and cycle times on the cooling power and COP of a double-bed silica gel – water adsorption chiller, using a zero-dimensional dynamic model. The adsorption/desorption process is described by a non-equilibrium model which takes into account the mass transfer resistance inside the bed [52]. The heat and mass balance in the adsorber, condenser and evaporator were taken in consideration; however, they were not detailed enough for a dynamic analysis of the system performance. It was shown that the system performance could be improved by optimizing several operating parameters such as operating temperatures, water flow rate and cycle time. It was also shown that the most

influential parameter is the operating temperatures, followed by water flow rates. Cycle time is less influential in quantitative terms but qualitatively is very important.

Cho et al. [44] proposed a zero-dimensional dynamic model to study the effect of the operating conditions and heat transfer rate of the condenser, evaporator and adsorber on a system's cooling capacity and cycle time. The system in question was a double-bed silica gel-water adsorption chiller. They showed that the condenser heat transfer rate is the most sensitive variable; furthermore, the effect of the evaporator heat transfer rate on the performance is insignificant. They also showed that the cycle time increases significantly with a large value of heat transfer rate. It was also reported that the cooling performance can be improved by increasing the heat transfer rates of the condenser and adsorber.

Hajji et al. [45] proposed a one-dimensional heat and mass transfer model to analyze the effect of the operating temperatures and design parameters on the performance of a zeolite – water adsorption cooling system. Their model was simplified by considering only a convection term for the heat flow. The heat and mass transfer equations were arranged in a dimensionless form. They observed that the temperature difference between the condenser and the evaporator has an important effect on the system performance, since a decrease improves significantly the COP. Nevertheless, the effect of the cooling (ambient) temperature is not as important. They showed that an excessively long cycle time is responsible for a lower COP. A study of the influence of the design parameters, namely the inert portion of the adsorbent container, the heat transfer rate and the total surface area on the system performance was presented as well. It was observed that the influence of the thermal capacity of the inert portion of the adsorbent container is small, and the heat transfer rate and surface area have a strong effect on the COP.

Douss et al. [37] studied the effect of the operating temperatures and design parameters on the dynamic behaviour of a two-bed zeolite-water adsorption heat pump with an internal heat recovery. They developed a zero-dimensional dynamic model, and they assumed that each component of the system

(adsorber, evaporator and condenser) is homogeneous. They reported some numerical instability, particularly at small time steps. However, the model was validated by experimental results. The effect of the heat transfer coefficient of the system components on the performance was also studied. Results showed that the temperature of the zeolite is not a sensitive variable, the heat transfer coefficient of the components is a sensitive variable, and the pressure is the most sensitive variable. The authors pointed out that the evaporator heat transfer coefficient affects the capacity greatly. For example, if the evaporator is undersized, the evaporation temperature of the water is much lower than the evaporation load, which decreases the performance of the cycle by decreasing the mass of the evaporated water.

Liu et al. [58] studied the effect of the operating conditions on the performance of a zeolite-water adsorption cooling system based on a mathematical model. The model proposed is a two-dimensional dynamic model, and takes into account both heat and mass limitations present in the bed. They used a non-equilibrium model known as LDF model [52], in order to take into account the mass transfer resistance within the adsorbent particles. The model for the bed involved the heat and mass conservation equations for the heat exchange fluid, metal, and adsorbent material in the bed. The heat losses during the adsorption process were neglected, as well as the thermal resistance between the metal tube and the adsorbent. A detailed model for the condenser and evaporator was considered in the study. However, the model was not validated by experimental results. Nevertheless, authors conducted a useful parametric study on the thermal performance of a zeolite-water cooling cycle. The results obtained show that the adsorption temperature, generation temperature, condensing temperature and evaporating temperature have significant effects on the COP and SCP. The cycle time decreases with an increase in fluid velocity, but this effect will be reduced for fluid velocities larger than 0.5 m/s. The optimum value of fluid velocity lies within 0.1-0.5 m/s. From a physical design point of view, authors suggest it is also important to study the effects of heat exchanger parameters on the system performance.

Miyazaki et al. [40] analyzed the effects of a number of heat exchanger parameters and operating conditions on the performance of a two-bed silica gel-water adsorption chiller. They developed a zero-dimensional heat and mass transfer model of a commercial adsorption chiller. They proposed a new technique for the optimization analysis called particle swarm optimization (PSO). The PSO controls all variables simultaneously to search for the optimum cycle time, which maximizes the specific cooling capacity (SCC) with randomly distributed particles within a preset range. The effect of the bed heat capacity and the bed number of transfer units (NTU) on the COP and optimum SCC was investigated. They showed that a larger NTU resulted in a decrease of the COP due to a shorter cycle time; however, the maximum SCC was improved. On the other hand, both the COP and optimum SCC were increased by a smaller bed heat capacity ratio.

Zhang et al. [41] proposed a zero-dimensional heat and mass transfer model and studied the effect of the operating temperatures and the overall heat transfer coefficient on the performance of a zeolite-water waste heat adsorption cooling system driven by an engine's exhaust gases. A detailed model was presented for the bed; however, no details were outlined with respect to the heat and mass balance in the condenser and evaporator. A non-equilibrium state was assumed, and the adsorption rate was defined by a LDF model [52]. However, the model was simplified by assuming that the adsorbed phase was liquid and the specific heat of the adsorbent is constant. A numerical analysis was presented, but the model was not validated by experimental results. In order to optimize the system performance, the authors analyzed the influence of the parameter changes on the system coefficients. Four system coefficients were defined as the key parameters, such as: coefficient of performance (COP), specific cooling power (SCP), coefficient of waste heat cooling (WCOP), and coefficient of waste heat recovery (WCOE). The overall heat transfer coefficient was defined by the authors as the overall heat transfer coefficient between the bed and the heating/ cooling fluid on the basis of the unit weight of adsorbent. The author showed that the heat transfer coefficient value has a big impact on the system performance, especially on the SCP. The influence of operating temperatures, namely the evaporator temperature, the condenser temperature,

the heating/cooling fluid inlet temperature and the maximum adsorption/desorption temperature on the system coefficients were analyzed as well. In general, the analysis shows that the SCP is more sensitive to changes in the operating temperatures than the COP, WCOP, and WCOE.

Alam et al. [46, 47, 49], Zheng et al. [50] and Voyiatzis et al. [55] introduced a non-dimensional switching frequency, which is inversely proportional to the cycle time, to find the optimum design and/or operating conditions of a system.

Zheng et al. [50] have studied the effect of the switching speed on the performance of a double-bed activated carbon-ammonia adsorption heat pump. They developed a two-dimensional dynamic model which takes into account non-dimensional parameters such as bed-switching speed, the number of transfer units, the adsorbent Biot number, the contact Biot number, the inert material alpha number, the refrigerant alpha number, the beta number and the lambda number. They investigated the effect of the bed cycling speed on the system performance, at different regeneration and ambient temperatures. They showed that at each regeneration temperature and ambient temperature, the COP initially increases with low bed cycling speeds, reaches a maximum and then decreases as the beds are cycled faster. A similar behaviour can be seen for the cooling power; however, the bed cycling speeds for optimum COP and cooling power are different. The optimum bed cycling speed, at which the COP is optimized, is linearly related to the regeneration temperature and the ambient temperature. When the ambient temperature decreases, the beds should be cycled faster.

Alam et al. [46] investigated the influence of the heat exchanger design parameters on the performance of a two-bed silica gel – water adsorption chiller as well as on the switching frequency. They performed parametric analyses, by using a two-dimensional heat and mass transfer model, in order to obtain the optimum switching frequency for different design and operating conditions. They showed that the optimum switching frequency is strongly dependent on the heat exchanger design parameters. The optimum switching frequency increases with the increasing of the adsorbent number of transfer units (NTU) and the ratio of

fluid channel radius to the adsorbent thickness (Hr), but decreases with the bed Biot number (Bi) and the heat exchanger aspect ratio (Ar). Furthermore, it was observed that the COP and cooling capacity are not optimized at a single optimum switching frequency.

In a subsequent study, Alam et al. [47] introduced a new profit function to determine a single optimum point for switching frequency, based on a similar model to Alam et al. [46]. The proposed profit function takes into account the heat input/output price and the availability of heat input. The effect of the heat exchanger design parameters on the profit function as well as on the switching frequency was analyzed. For a given set of non-dimensional parameters, such as the NTU, the bed Biot number (Bi), the heat exchanger aspect ratio (Ar), the ratio of fluid channel radius to the adsorbent thickness (Hr), the fluid alpha number ($\alpha_{f\text{-}a}$) and the inert material alpha number ($\alpha_{m\text{-}a}$), the profit function is maximized in order to determine the optimum switching frequency of the system. Authors observed that the profit and the optimum switching frequency increases with increasing the NTU and Hr and decreases with the increasing of Bi number, Ar ratio, fluid and inert alpha number.

Alam et al. [49] developed a zero-dimensional dynamic model to predict the optimum design conditions of a double-bed silica gel – water adsorption chiller. Their model takes into account the energy and mass balance in the adsorber, condenser and evaporator, and a uniform temperature and pressure through the whole adsorber was assumed. A set of non-dimensional parameters were considered for the parametric studies. The model was validated with experimental data. An optimization study was performed, analyzing the effect of the switching frequency on the COP and cooling power. It was found that the switching frequency is one of the most influential operating parameters. Both COP and non-dimensional cooling capacity (NCC) have an optimum switching frequency, but they are not optimized at the same switching frequency. It was concluded that the performance of the system can be improved by setting the switching frequency properly. Authors also investigated the effect of the number of transfer units (NTU) of the system components on the overall system performance. They observed that the performance of the system in terms of

COP and cooling power is strongly affected by the adsorber NTU. However, the condenser NTU is a less significant parameter.

Following Alam et al. [46, 47, 49], Voyiatzis et al. [55] analyzed the effects of heat exchanger design and switching frequency on the performance of a silica gel-water adsorption chiller, using a similar technique. They proposed a one-dimensional model for the simulation of the system, which takes into account the heat and mass transfer resistance in the sorption bed. A set of non dimensional parameters such as the Fourier, the Nusselt, the Biot and the Stefan numbers, as well as the space velocity of the fluid were defined for the parametric analyses. They showed that system performance can be improved by increasing either the bed Fourier number or the thermo-fluid Nusselt number. Furthermore, the system performance can be also increased by decreasing either the thermofluid Fourier number or the bed Biot number. It was also showed that an increase of the space velocity results in an increase of the cooling capacity and a decrease of the COP. In addition, they observed that for all the parameters exists an optimum switching frequency, however, the COP and NSCC (non-dimensional specific cooling capacity) are not optimized at the same switching frequency.

Marletta et al. [59] proposed a two-dimensional heat and mass transfer model to predict the performance of an innovative consolidated bed developed at CNR-ITAE research institute. The performance of the CNR-ITAE bed type was compared with conventional bed configurations found in the literature, such as the pure powder type and the consolidated powder type. Authors studied the effect of the heat transfer coefficient and thermal conductivity on the performance of different bed configurations. They showed that the proposed CNR-ITAE bed type performs better than the other bed configurations mentioned above. The good heat transfer conditions provided by the metal-bound consolidated powder arrangement proposed by CNR-ITAE allows a shorter cycle time and a higher SCP than other bed configurations available in the literature.

Apart from the conventional adsorption cooling system, some researchers proposed new cycle time configurations such as heat and mass recovery cycles in order to improve the system performance in terms of cooling capacity and COP. For instance, Maggio et al. [20] proposed a two-dimensional heat and mass transfer model of a zeolite-water adsorption machine, with internal heat recovery, using two consolidated beds. The performance of the system was compared to a single bed configuration. The simulation results showed that the COP and cycle time of the system increased with respect to the single bed configuration while on the contrary, the specific cooling power decreased. Furthermore, a parametric analysis was carried out in order to study the influence of parameters such as the minimum temperature difference between the two beds at the end of the heat recover step, the metal/adsorbent heat transfer coefficient, the adsorbent thickness and the vapour permeability of the bed on the performance of the machine. Authors observed that all the design parameters have an important role in the operation of the system, helping to define the bed design that maximizes the performance as well as the most profitable heat recovery conditions.

1.3. Purpose and objectives of the PhD study

This research started within the framework of an R&D project called “Thermally Operated Mobile Air Conditioning Systems - TOPMACS”, financially supported by the EC under the FP6 program [65]. The project aimed at the development of double-bed adsorption cooling systems driven by low temperature energy coming from the engine coolant loop, for automotive air conditioning applications. The prototype systems were designed to be fitted on a passenger vehicle and a commercial truck.

The main aim of this PhD study is to develop a lumped parameter model capable of reproducing the dynamic behaviour of a double-bed adsorption cooling system, and to employ it as a simulation tool to assist the design and optimize the operation of this type of adsorption systems.

The first specific objective is to develop a model for each system component in order to capture the principal physical phenomena occurring there. This will allow to understand the non-equilibrium adsorption/desorption process in transient regime. It will also allow for an accurate characterization of the equilibrium state of the adsorbent material and working fluid used in the system, as well as for a detailed evaluation of the working fluid flow between the components, also in non-steady state. In a similar way, the dynamic behaviour of the operation of the valves between the system's components will be examined. Detailed models of the various heat exchangers employed in the system and their behaviour in transient regime is another objective relative to the development of the model of the sorption system.

The second specific objective is to validate the developed model with experimental measurements in dynamic conditions, and assess different operation strategies of the system, such as the inclusion of an additional heat recovery process. The experimental data used for the validation process described above were obtained at the ECN research institute (Energy research Centre of the Netherlands, Petten, The Netherlands).

The third specific objective is to perform a parametric study in order to assist the design and optimize the operation of the system. The effect of the cycle time on the system performance will be investigated in order to find an optimum value that makes the system achieve the best performance. Moreover, an alternative system layout for the adsorption A/C system will be studied in order to further increase the system performance.

After the completion of the objectives mentioned above, the last objective is to incorporate the developed dynamic model into the global model of the vehicle of the TOPMACS project [65], in order to predict the performance of the system prototype at different working and driving conditions. It will also allow to investigate the influence of different start-up conditions on the system performance.

In parallel to the development of the overall system model, a separate analytical model will be developed in order to study the influence of the main bed design parameters on the overall thermal conductance of the bed. Moreover, the model will be employed to investigate the influence of the bed design parameters and operating temperatures on the maximum performance of the system that could be achieved with a properly designed and operated system.

2. ADSORPTION COOLING SYSTEM THEORY

2.1. Adsorption concept

Adsorption, also known as physisorption, is the process by which molecules of a fluid are fixed on the walls of a solid material. The adsorbed molecules undergo no chemical reaction but simply lose energy when being fixed: adsorption, the phase change from fluid to adsorbate (adsorbed phase) is exothermic. Moreover, this process is reversible. The adsorption process is represented in Fig. 1.

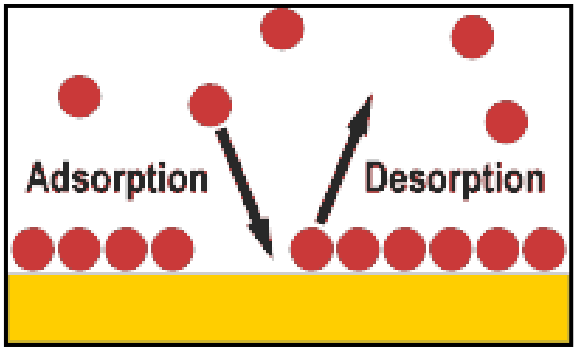

Fig. 1. Adsorption/desorption process.

Physisorption is a general phenomenon: it occurs whenever an adsorbable gas (the adsorptive) is brought into contact with the surface of a solid (the adsorbent). The interfacial layer comprises of two regions: the surface layer of the adsorbent (often called the adsorbent surface) and the adsorption space in which enrichment of the adsorptive can occur. The material in the state adsorbed is known as the adsorbate, as distinct from the adsorptive, i.e., the substance in the fluid capable of being adsorbed. In physisorption the adsorption process is based on intermolecular forces. The forces involved in physisorption include both van der Waals forces (dipole-repulsion) and electrostatic interactions comprising polarization, dipole, and quadrupole interactions [66-69].

This PhD study focuses on adsorption cooling systems mainly used for automotive air conditioning purposes: a pure refrigerant vapour that can easily

be condensed at ambient temperature and a microporous adsorbent with a large adsorption capacity.

Different terms associated with adsorption systems can be found in the literature. To prevent misunderstanding, the most common terms used in this study and their specific meaning are described below:

Physisorption: Solid/vapour sorption without chemical reaction between adsorbent and adsorbate.
Adsorption: Solid/vapour sorption.
Adsorbate: The vapour being accumulated in the adsorbent (i.e. substance in the adsorbed state).
Adsorbent: Sorption material used to adsorb/ desorb the adsorbate.
Uptake: The amount of adsorbate which is adsorbed in the adsorbent per amount of dry adsorbent.
Adsorbent bed heat exchanger: The heat exchanger in which the adsorbent is packed.
Sorption bed: Process unit comprised of adsorbent bed heat exchangers.
Refrigerant: The vapour that circulates through the refrigeration system (i.e. working fluid).

2.2. Basic adsorption cooling system

A basic adsorption cooling system usually consists of four main parts: a sorption bed, a condenser, an expansion valve and an evaporator. A design scheme of a basic adsorption cooling system is shown in Fig. 2(a). The sorption bed desorbs the refrigerant when heated and adsorbs refrigerant when cooled. In this manner, the bed operates as a thermal compressor to drive the refrigerant around the system and therefore cool the desired space. The refrigerant is desorbed from the bed as it is being heated to drive the refrigerant out of the bed. The refrigerant vapour is conducted to a condenser where it is cooled and condensed to liquid. The refrigerant condensate then expands to a lower pressure through an expansion device. Then, the low pressure condensate is

conducted to an evaporator. The low pressure condensate is vaporized in the evaporator by taking heat from the space to be conditioned through a cooling medium (chilled water or air). When further heating no longer produces desorbed refrigerant from the bed, the bed is isolated and allowed to return to the adsorption conditions. When the adsorption conditions are established in the bed, the refrigerant vapour from the evaporator is reintroduced to the bed to complete the cycle. The basic adsorption cooling system performs a closed cycle.

An idealized thermodynamic cycle of a basic adsorption cooling system is illustrated in Fig. 2(b).

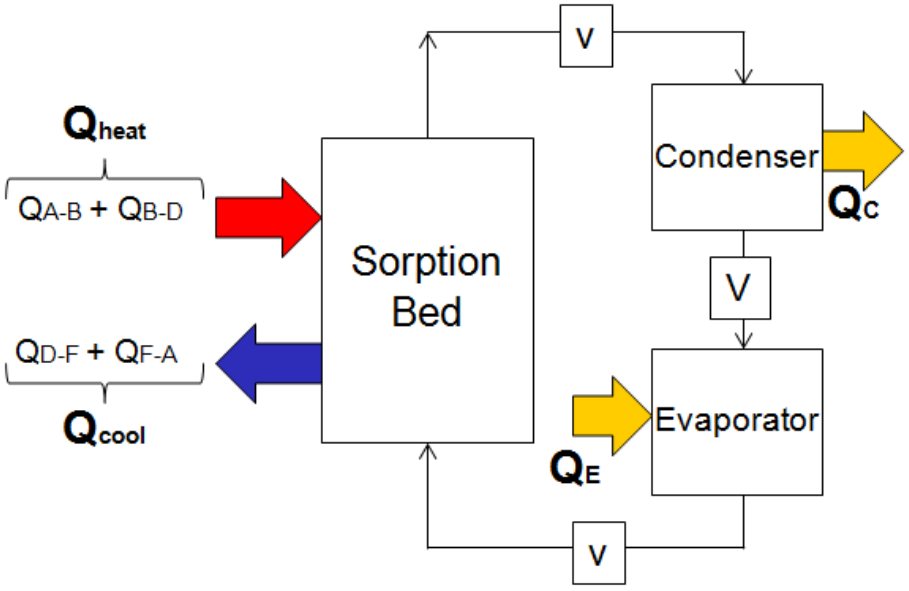

(a)

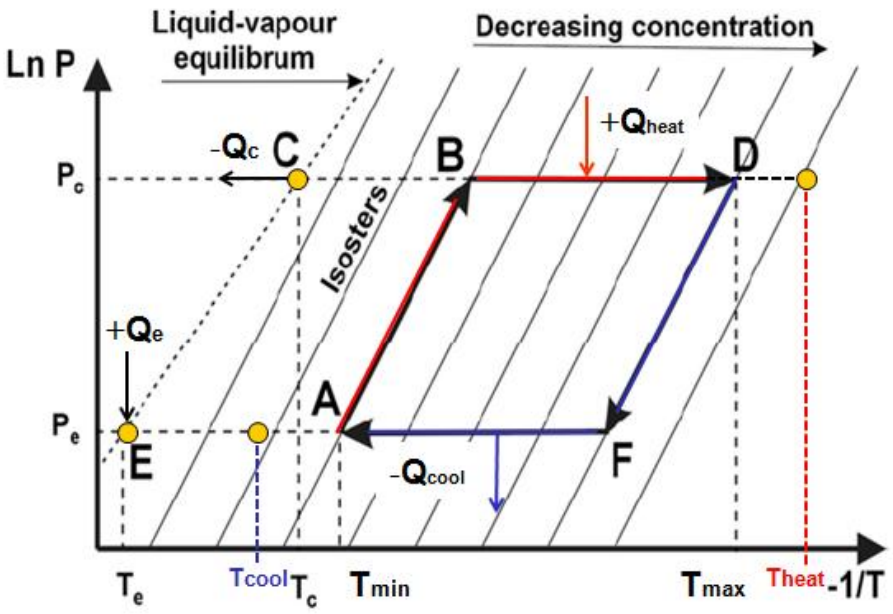

(b)

Fig. 2. Schematic diagram: (a) Basic adsorption cooling system, (b) Ideal basic cycle in a Dühring diagram: Saturation liquid-vapour curve for the refrigerant (EC, dashed line), isoster curves (thin lines), and adsorption cycle (bold line). Heating period: step A-B and step B-D; Cooling period: step D-F and step F-A.

The ideal adsorption cycle, illustrated in Fig. 2(b), may include the following stages:

Stage 1 - Isosteric Heating ($T_A \rightarrow T_B$): A typical idealized basic cycle starts at a T_A and pressure P_E. T_A is equal to the minimum of the bed while P_E represents the pressure of the evaporator. During the regeneration phase of the cycle (A-B), the bed is connected to a heat source at temperature T_{heat} and it receives an amount of heat Q_{A-B}. Consequently, the pressure of the bed increases as the temperature of the bed is being increased. The cycle moves along an adsorption isoster to reach the temperature T_B and the pressure P_C which represents the pressure of the condenser. There is no mass transfer during this stage of isosteric heating.

Stage 2 - Isobaric Desorption ($T_B \rightarrow T_D$): During this stage of the cycle, the bed receives an amount of heat Q_{B-D} at constant pressure P_C. The temperature is raised to T_D which is equal to the maximum temperature of the bed. This is the isobaric desorption step which results with the condensation of the refrigerant (i.e. desorbed vapour) in the condenser at pressure P_C.

Stage 3 - Isosteric Cooling ($T_D \rightarrow T_F$): During the second period of the cycle, the bed temperature decreases from T_D to T_F since the bed is being cooled by a low temperature heat source at T_{cool} and dissipating heat Q_{D-F}. Meanwhile, the pressure drops to P_E once again as the temperature of the bed is decreased. There is no mass transfer during this stage of isosteric cooling.

Stage 4 – Isobaric Adsorption ($T_F \rightarrow T_A$): The final step occurs at constant pressure P_E while the temperature decreases from T_F to T_A. Hence, the bed dissipates heat Q_{F-A}. The refrigerant (condensate) leaving the condenser is vaporized in the evaporator. The same amount of refrigerant vaporized is once again adsorbed by the bed. This is the isobaric adsorption step. At this step, the evaporator absorbs heat Q_E from the space to be conditioned, producing a cooling effect.

The efficiency of a basic cycle is very low and the cooling capacity is not continuous. In order to obtain a continuous and stable cooling effect, generally two beds are used in the adsorption cooling system. In a typical two-bed cycle, one bed is heated during the desorption period and the other bed is cooled during the adsorption period. The heating and cooling phases are reversed when the beds reach the maximum and minimum temperature limits of the adsorption cycle. Alternatives to improve the efficiency of a basic cycle include the use of a heat recovery cycle, a heat and mass recovery cycle, multi-bed and multi-stage cycle, etc…

2.3. Adsorption cooling system for automotive air conditioning purposes

2.3.1. Traditional MAC system environmental impacts

Europe is making a huge effort to reduce Greenhouse gas emissions. The recent European Union directive on mobile air conditioning (MAC) phases out systems using HFC-134a as refrigerant for new cars placed on the EU market from 2008 onwards. The end date of the phase-out period was proposed to be 2012 [70].

Recent technology in MAC systems is represented by vapour compression cycles that use R134a as refrigerant. The primary energy source for these systems is mechanical power produced by the engine to drive the compressor, and electric power to run the fans, which is again derived from the engine itself. MAC systems have a considerable impact on fuel consumption. For a B class car on an urban cycle under heavy ambient conditions, it can increase car fuel consumption up to 70%. From EU estimations, the CO_2 emissions increase due to the use of MAC ranges from 4% to 8% on a yearly basis. This means, with the same hypothesis as before, an increase in CO_2 emissions from 5 to 10 million tons of CO_2 per year in Europe only. To give an idea, this amount of CO_2 is equivalent to having from 2.500.000 to 5.000.000 “additional cars” on European roads, each with 16.000 km per year and with CO_2 emissions equal to 120 grams/km [71].

Additionally, MAC systems have significant impact on the environment due to leakages. Every year, between 750 and 2500 tons of R134a are emitted in the atmosphere, just because of leakages. Taking into account the GWP, this is equivalent to about 1 to 3 millions of tons of CO_2. This is just for leakages and servicing, without taking into account the problem of end of life recovery [71].

Hence, the environmental impact of traditional MAC systems is twofold:

- *Direct impact*, due to leakages of the refrigerant fluid into the atmosphere. These leakages may be caused by poorly designed, badly maintained installations, or by refrigeration units abandoned at the end of their life without recovering or recycling the refrigerant fluid. Depending on the fluid, these leakages may have an influence on ozone depletion and/ or on global warming by the greenhouse effect [71].

- *Indirect Impact*, which is related to the energy necessary to run the MAC systems. This energy is both mechanical and electrical, and it is produced by burning an extra amount of fuel, requiring a more powerful engine and increasing fuel consumption. This generates additional emissions of CO_2 (carbon dioxide) into the atmosphere. By the simple fact of consuming energy over its life cycle, any refrigeration unit contributes to climate change [71].

Part of the PhD work presented here has been carried out in the frame of a R&D project called “Thermally Operated Mobile Air Conditioning Systems – TOPMACS” financially supported by the EC under the FP6 program [65]. All participants in the TOPMAC project [65] are listed in Table 1. The project focuses on the design and development of innovative MAC systems for automotive applications with a reduced impact on the environment, both direct and indirect.

Within the frame of the Topmacs project [65], an adsorption cooling system for air conditioning purposes which employs the waste heat from the engine coolant loop to cool the car cabin has been realized at the ECN facilities (Energy research Centre of the Netherlands - ECN). The application of adsorption refrigeration to automotive air conditioning has high potential, since it uses water as working fluid and it can be powered by the waste heat from the engine without using up any mechanical energy output from the engine, therefore resulting in fuel consumption reduction.

Table 1. List of participants on the Topmacs project.

Participant name	Participant short name	Country
Centro Ricerche Fiat	**CRF**	Italy
Iveco	**IVC**	Italy
Valeo Thermique Habitacle	**VTH**	France
Enginion AG	**EAG**	Denmark
Treibacher Industrie AG	**TIAG**	Germany
Energy Research Centre of the Netherlands	**ECN**	Netherlands
Istituto di Tecnologie Avanzate per l'Energia "Nicola Giordano"	**CNR-ITAE**	Italy
University of Warwick	**UW**	United Kingdom
Institut fur Kernenergetik und Energiesysteme, Universitat Stuttgart	**IKE-USTUTT**	Germany
Universidad Politécnica de Valencia	**UPV**	Spain

2.3.2. Operating principle

The developed adsorption cooling system is based on the utilization of the waste heat contained in the engine coolant instead of the exhaust gases. A previous study within the Topmacs project [65] allowed to conclude that the potential of heat recovery from the engine coolant was much higher than that from the exhaust gases, and the size of the beds could also be much smaller.

The main source of waste heat from the engine is the engine cooling water. The cooling water temperature at the outlet of the engine normally lies between 90-95 ºC for cars. The water temperature could be increased by heat recovery from the exhaust gases. However, this option was not considered in the final design of the system because of the inherent increase in costs and complexity of the system.

A detailed scheme of the developed adsorption chiller is shown in Fig. 3. The system prototype comprises of two sorption beds connected to a condenser and an evaporator, an expansion device plus four check valves. The system involves three independent secondary water loops: a secondary water loop to heat the bed (Heating Water Loop, in Fig. 3), a secondary water loop to cool first the condenser and then the bed (Cooling Water Loop, in Fig. 3), and a

secondary water loop to provide heat to the refrigerant in the evaporator (Chilled Water Loop, in Fig. 3). The sorption beds operate in counter-phase in order to allow a continuous useful effect: while one bed is in cooling phase, the other is in heating phase.

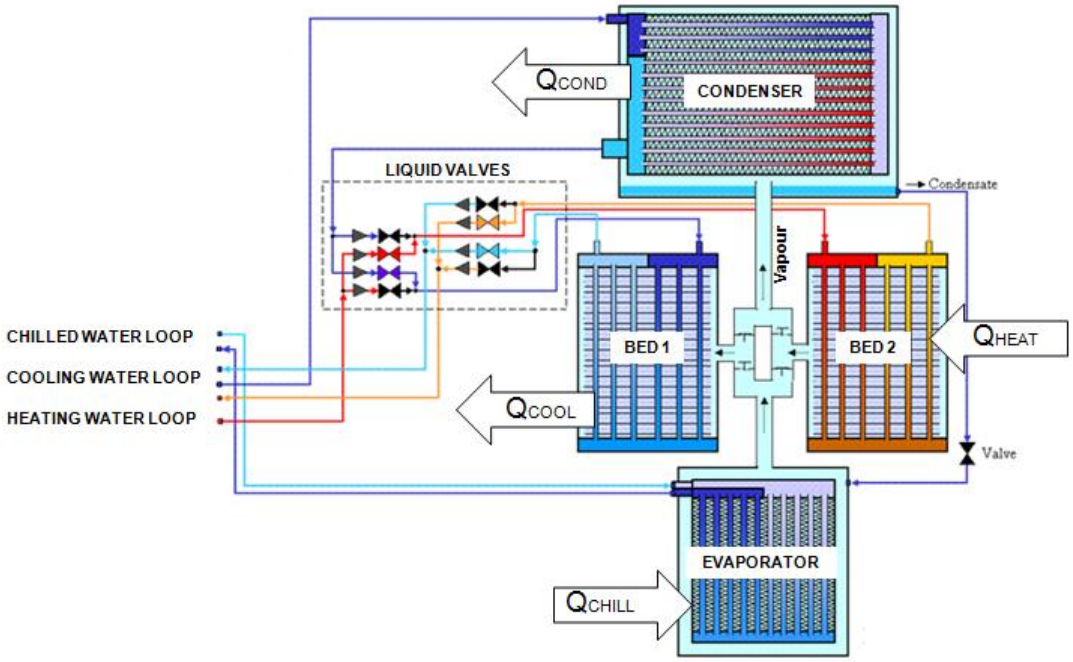

Fig. 3. Layout of the adsorption chiller: Detailed view.

Fig. 4 shows how the adsorption air conditioning system is implemented in the car. The operation of the system is cyclic, and each cycle involves the following steps. One of the beds (Bed 2, in Fig. 4) is heated up by heating water from the outlet of the engine. The adsorbent starts to desorb the water vapour inside the bed. The bed pressure increases due to the water vapour and the valve between the bed and the condenser opens (the communication valve with the evaporator is kept closed). The water vapour condenses in the condenser, releasing its latent heat of condensation to the cooling water circuit. Liquid water passes from the condenser to the evaporator through an expansion device. At the same time, the other bed (Bed 1, in Fig. 4) is being cooled down thanks to an auxiliary cooler (Radiator, in Fig. 4) which dissipates the heat to the ambient. The bed starts to adsorb the water vapour, and then the pressure decreases because the bed valves are all closed. When the bed pressure becomes lower than the one in the evaporator, the communication valve between the bed and

the evaporator opens, and the bed starts to adsorb the water vapour coming from the evaporator, producing the evaporation of the water in it. During the evaporation stage, the water absorbs heat from the space to be conditioned, producing the cooling effect which flows through the cabin cooler (Air Cooler, in Fig. 4). Then, the water from the auxiliary cooler is conducted to Bed 2, which is dry and hot, cooling it down, decreasing its pressure and activating the adsorption from the evaporator. At the same time, Bed 1, which is full and cooled, is heated up to increase its pressure and activate the desorption process.

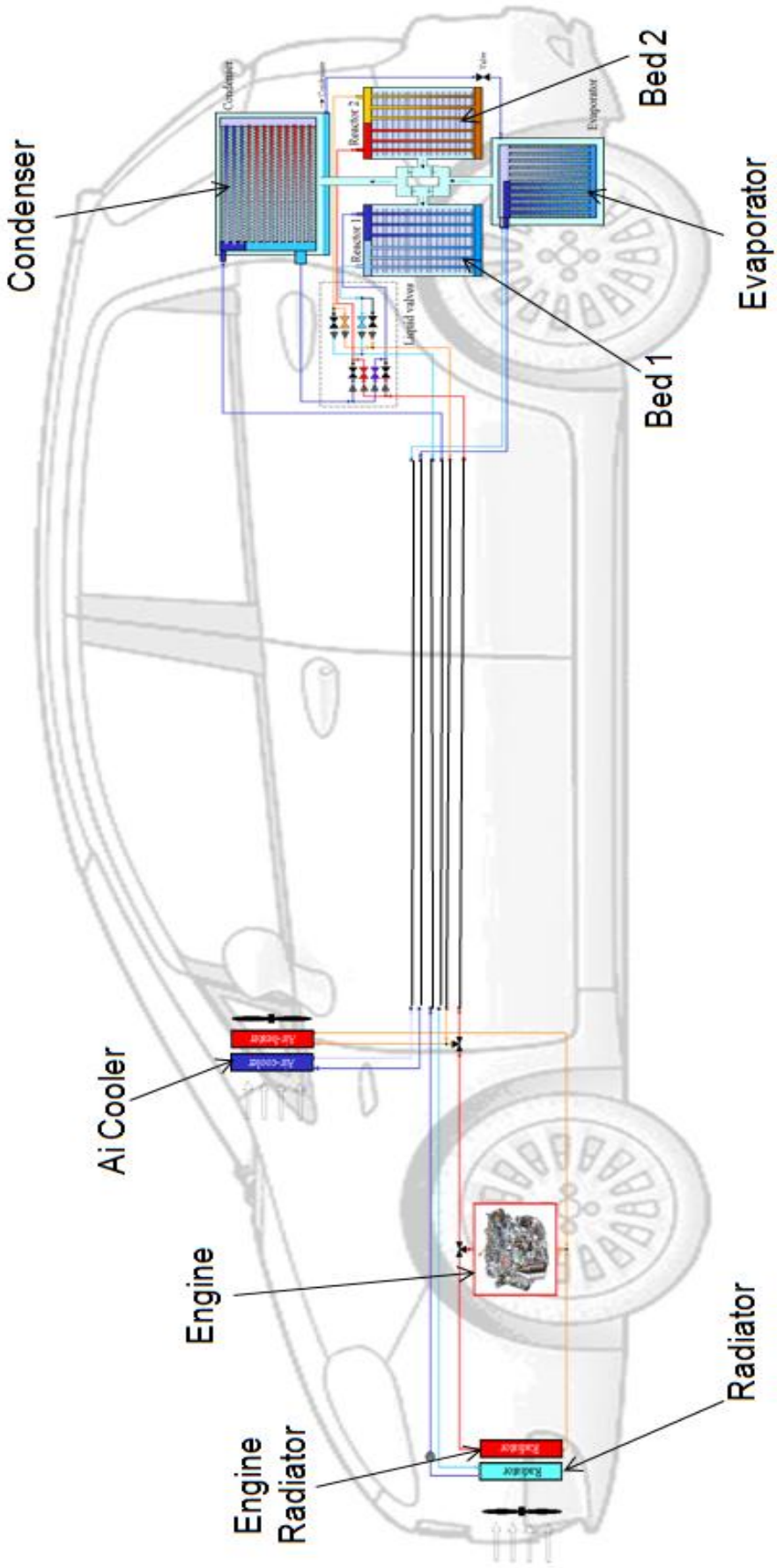

Fig. 4. Scheme of the onboard adsorption air conditioning system implemented in the car.

2.3.3. Working pair

The working pair employed in the adsorption cooling system plays an important role in the system's performance. The most common adsorbent/adsorbate pairs used in adsorption cooling systems are: zeolite-water, active carbon – methanol, silica gel-water and carbon-ammonia.

According to the working principle of the adsorption cooling system for the targeted application, the adsorbent should have the following characteristics [72]:

- high surface area,
- small pore size,
- low regeneration temperature,
- high adsorption capacity,
- large change of adsorption capacity with temperature variation
- good compatibility with the refrigerant
- cheap,
- non-toxic
- chemically and physically stable in working conditions.

Taking into account the criteria mentioned above, the selected adsorbent for the adsorption cooling system under study was decided to be a type of silica gel named Sorbsil A. The specific adsorbent material was specifically designed for adsorption machines driven by low temperature heat sources. This type of adsorbent can be efficiently used with a maximum desorption temperature of 80-90 ºC, which is suitable for utilization of the heat coming from the engine coolant loop.

Additionally, the system under study used water as adsorbate (refrigerant) due to its safety, simplicity, zero toxicity, low cost and high heat of evaporation (about 2500 kJ/kg). However, a drawback of using water is the low working pressures (0.01-0.1 bar) which can limit mass transfer processes especially

during the adsorption phase [72]. The amount of water that is reversibly adsorbed, and thus causes the desired chilling effect, depends on the temperature levels of the waste heat, cooling water, condenser and evaporator, but also on the adsorption properties of the silica gel.

2.3.4. Real adsorption cycle on the Dühring diagram

Fig. 5 shows an example of the temperature-pressure evolution of the studied system, obtained experimentally, on a Dühring diagram. The diagram shows the equilibrium data of the working pair (i.e. Sorbsil A/water) in the form of isosters. The isosters are straight lines with a slope depending on the water content in the adsorbent (uptake).

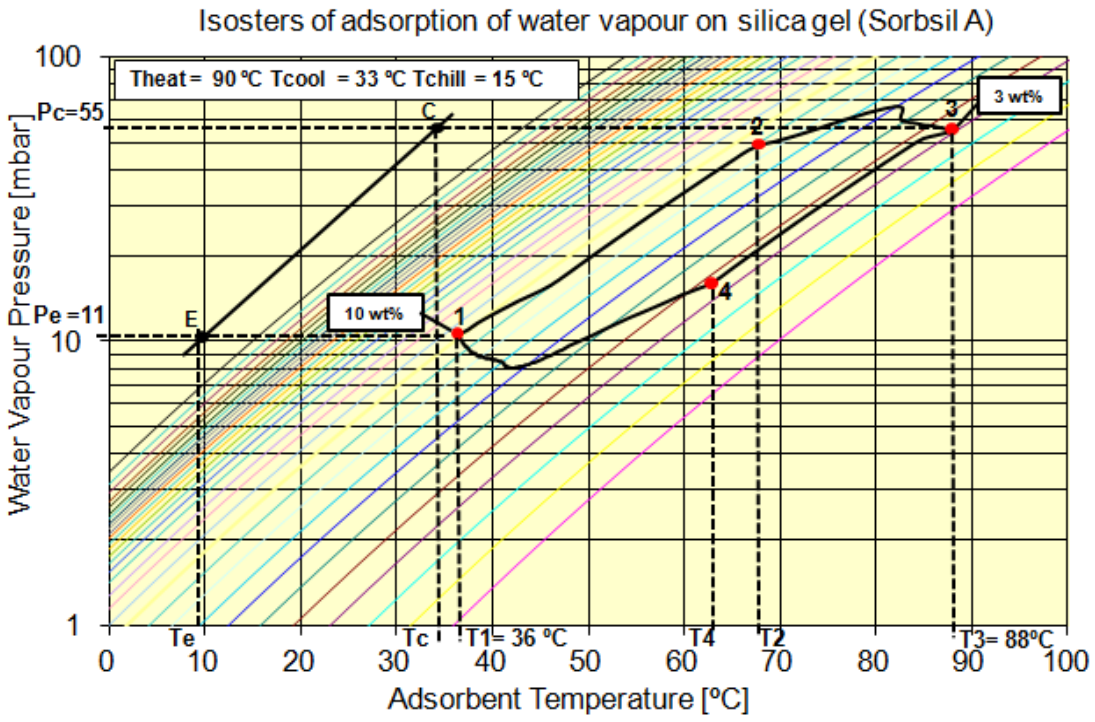

Fig. 5. Real adsorption cycle of the adsorption system under study in a Dühring diagram: Saturation liquid-vapour curve for the water (EC, bold line), isosters (thin lines), and adsorption cycle (bold line). Heating period: step 1-2 and step 2-3; cooling period: step 3-4 and step 4-1.

As it can be seen on Fig. 5, T_{heat} is the maximum temperature up to which the bed can be heated by the heating water (heat source at 90 ºC) while the

temperature T_{cool} is the minimum temperature up to which the bed can be cooled down by the cooling water (heat sink at 33 ºC). The temperature T_E is the highest saturation temperature of the refrigerant in the evaporator (at approximately 9 ºC) and it corresponds to a pressure P_E. The temperature T_C is the minimum saturation temperature of the refrigerant in the condenser (at approximately 35 ºC) and it corresponds to a pressure P_C. The temperature T_1 is the minimum temperature within the adsorption cycle. The temperature T_2 is the minimum temperature where desorption occurs at condenser pressure P_C. The temperature T_3 is the maximum temperature within the heating period. The temperature T_4 is the maximum temperature where adsorption occurs at evaporator pressure P_E. The maximum uptake w_{max} within the cycle appears at the temperature T_1 and pressure P_E while the minimum uptake w_{min} appears at the temperature T_3 at a pressure P_C. The resulting total uptake variation is defined as $\Delta w = w_{max} - w_{min}$. Moreover, in the range of the operating conditions of the operating cycle in case, the water uptake changes from 3% to about 10% wt (based on dry silica gel mass). So in this case, a variation of 7% of the water uptake is causing the chilling effect.

3. EXPERIMENTAL SETUP

3.1. Prototype system description

3.1.1. Introduction

Two different prototypes of an adsorption chiller for mobile air conditioning purposes were built and tested under the framework of the Topmacs project [65]. The two adsorption chiller prototypes were specifically designed to be installed in a car and a truck, respectively. They were designed to be driven by the low grade waste heat from the vehicle's engine coolant loop. The temperature at the outlet of the engine normally lies between 90–95 °C for cars and 80–90 ºC for trucks. A great amount of thermal energy can be therefore recovered from the engine's coolant loop at those temperatures. The coolant temperature, usually water, can subsequently be increased by heat recovery from the exhaust gases in order to provide an increased temperature heat source. However, this option was not considered in the final design of the system, because of the inherent increase in cost and complexity.

The amount of water that is reversibly adsorbed, and thus causes the cooling effect, depends not only on the temperature levels of the external water circuits, but also on the physical properties of the adsorbent. The adsorbent material used was silica gel for the car prototype and zeolite for the truck prototype. Both adsorption systems used water as adsorbate. The adsorbent/adsorbate pairs chosen can operate at low temperatures, therefore they are suitable for using with a low temperature heat source.

For the truck prototype, the two beds were built using a novel functionalized material called AQSOA®-FAM-Z02, specifically designed by Mitsubishi Corporation [73] for adsorption machines driven by low temperature heat sources. A previous work demonstrated that the zeolite material FAM-Z02 can be efficiently used with a maximum desorption temperature of 80–90 ºC, which is suitable for utilization of the heat coming from the engine coolant loop [74].

The experimental characterization of the truck prototype system has been carried out at the CNR-ITAE laboratories. A detailed description of the adsorption chiller prototype specifically designed to be implemented in a truck can be found in the literature [70, 11].

The adsorbent material employed in the car prototype was a silica gel of 0.2 - 1.0 mm grain size named Sorbsil A, manufactured by Ineos Group Limited [75]. The car prototype has been experimentally evaluated at the ECN laboratories. In this chapter of the PhD study, a detailed experimental characterization of the adsorption chiller prototype specifically designed and built to be installed on a Fiat Grande Punto car is presented. Part of the information shown in this chapter has been provided by the ECN research institute [76], where the PhD author spent several months as part of her thesis.

3.1.2. Principle of the system operation

The main components of the adsorption chiller prototype are: the condenser, the evaporator and the thermal compressor, which consists of two sorption beds named bed 1 and bed 2. Furthermore, the prototype has four check valves to direct the refrigerant vapour flow (named vapour valves), a condensate valve connected to a liquid level control in the evaporator and four three way valves (named liquid valves) to direct the heating and cooling water circuits alternately to both sorption beds. The vapour and liquid valves are necessary to switch between adsorption and desorption mode. Fig. 6 shows the design of the onboard adsorption chiller prototype.

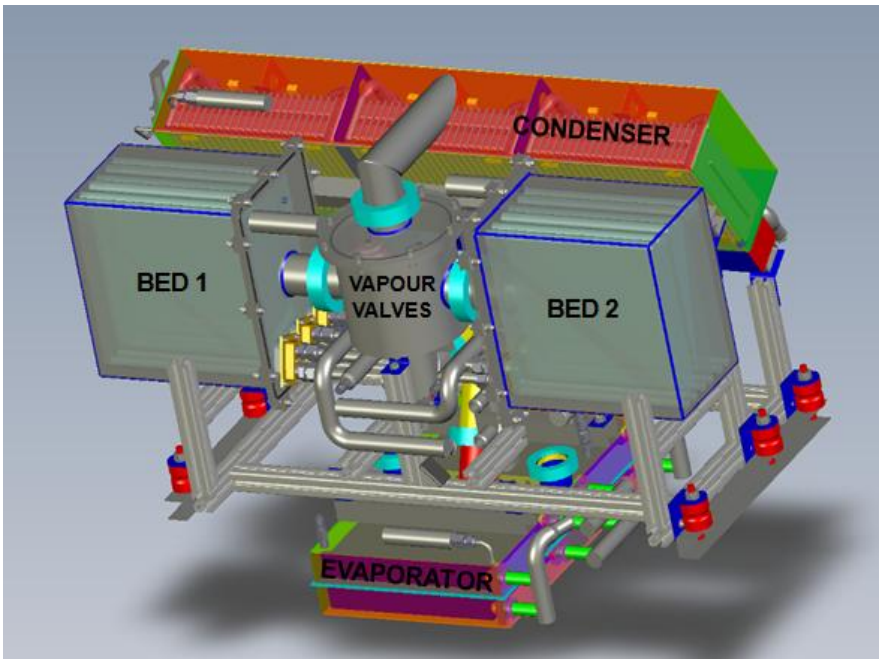

(a)

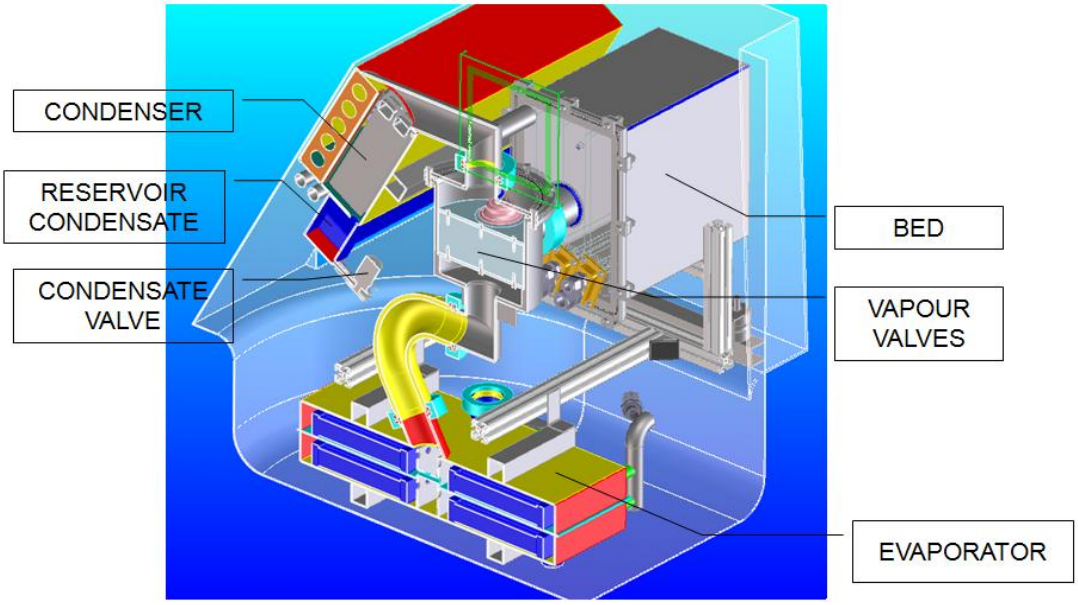

(b)

Fig. 6. Design drawing of the onboard adsorption chiller prototype: (a) Full view, (b) Cross-section.

Fig. 7(a) shows an actual picture of the onboard adsorption chiller prototype. As it can be seen, the adsorption chiller is connected to three secondary water circuits for heating, cooling, and chilled water. The heating water is send to one of the two beds, depending on the position of the liquid valves. The cooling water is first send to the condenser and then through the valves to the other

bed. The chilled water circuit is directly fed into the evaporator. The sorption beds operate in counter-phase in order to allow a continuous useful effect: one bed is in cooling mode while the other in regeneration mode. The prototype in question is designed to be placed in the trunk of a European compact car (Fiat Grande Punto), as mentioned above. Fig. 7(b) shows a picture of the onboard prototype installed in the vehicle. It is possible to recognize the central vapour house and the two beds located in the trunk of the car. Moreover, the evaporator is placed below the spare wheel space, and the condenser is placed between the beds and the back seats. The overall weight of the onboard prototype is 86 kg, not including the weight of the water in the circuits for heating, cooling and chilling, the refrigerant water in the evaporator, and also excluding the thermal insulation.

(a)

(b)

Fig. 7. Picture of the onboard adsorption chiller: (a) in the laboratory and (b) installed in the vehicle.

3.2. System components design and specifications

3.2.1. Thermal compressor

The thermal compressor section of the adsorption chiller prototype consists of two sorption beds. Fig. 8 shows the design of the thermal compressor. As it can be seen in Fig. 8(a), the beds are connected to a central vapour housing that contains the gravity operated refrigerant check valves. Each bed has three brazed type flat-tube fin heat exchangers connected in parallel, as it can be seen in Fig. 8(b). This particular type of heat exchanger is normally used as evaporator in a conventional automotive air conditioning system, and it was manufactured by Denso Corporation [77]. Each heat exchanger is filled with silica gel (Sorbsil A) grains and sealed with metal gauze. The weight of each aluminium heat exchanger (excluding the headers) is 1.012 kg and the fin side of each heat exchanger is filled with 1 kg of silica gel grains. The adsorbent/heat exchanger assembly is named here as adsorbent bed heat

exchanger. The system has a full parallel flow, and the header which divides the flow is placed outside the aluminium containment.

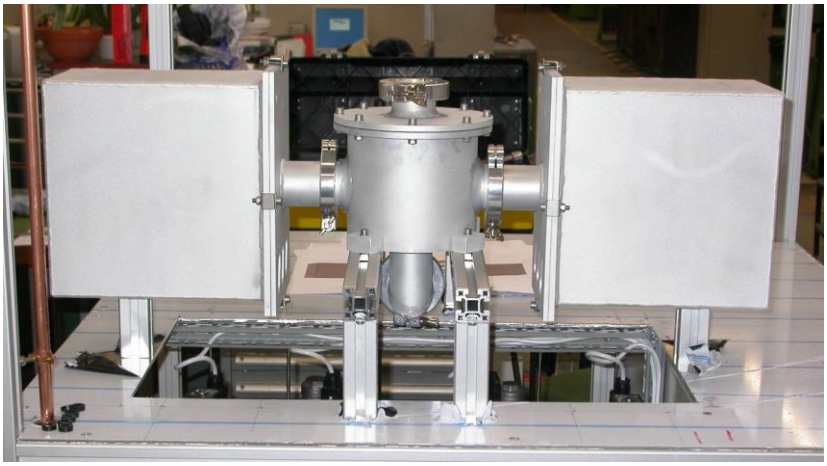

(a)

(b)

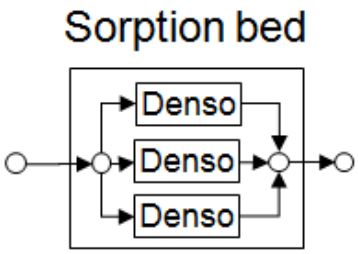

(c)

Fig. 8. Thermal compressor design: (a) Two identical containments (i.e. beds) connected to the central vapour housing. (b) Single bed, comprised of three Denso heat exchangers, and inlet/outlet header. (c) Bed water flow arrangement scheme.

3.2.2. Evaporator

In order to save space, the evaporator is made up of two sections built on top of each other, as seen in Fig. 9. Each section has two heat exchangers which are connected in parallel. The heat exchangers used to built the evaporator are four compact heater cores used for automotive applications and fabricated by Valeo [78]. The upper section has a fixed maximum water level. The lower section has

two temperature controlled level sensors with a set point at 1/3 of the heat exchangers' fin height. The condensate enters the evaporator at the top, and when the maximum level is reached, the water flows to the bottom. The containment shell is made of 2 mm thick stainless steel.

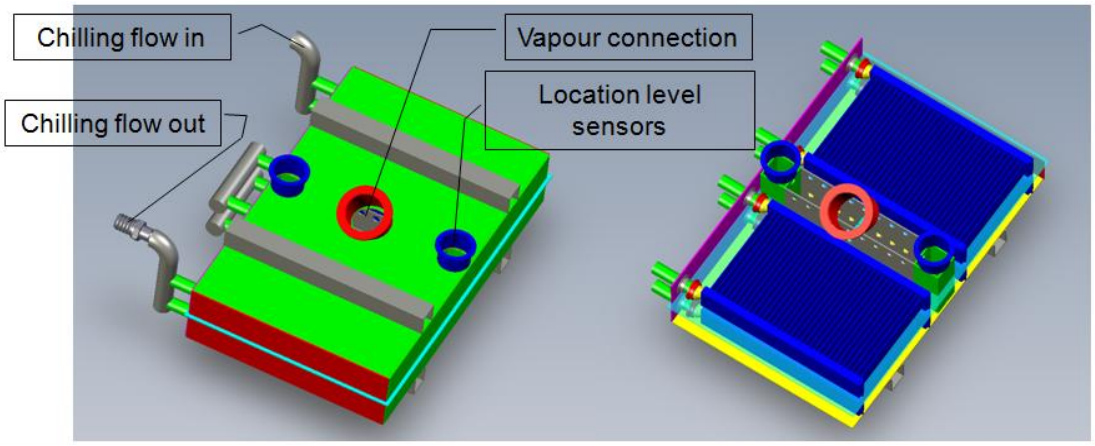

(a)

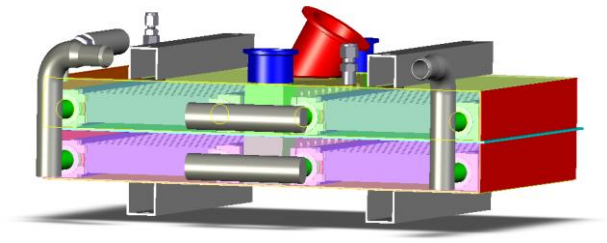

(b)

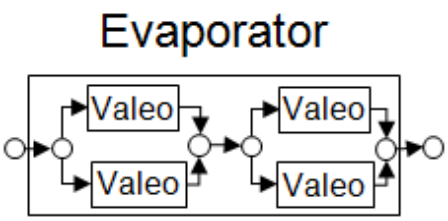

(c)

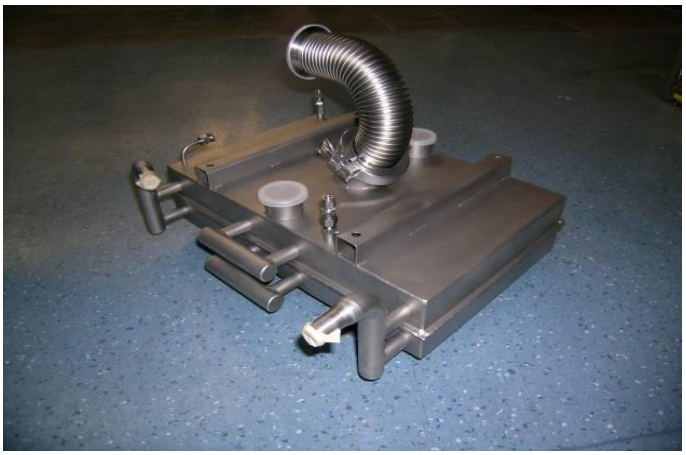

(d)

Fig. 9. Evaporator: (a) Design scheme, full view (b) Design scheme, side section view, (c) Water flow arrangement scheme, (d) Actual picture.

3.2.3. Condenser

The condenser is made up of three heat exchangers connected in parallel flow and contained in a stainless steel compartment, as seen in Fig. 10. The heat exchangers used to built the condenser are evaporators fabricated by Behr [79], another known manufacturer of automotive applications equipment. The condenser has internal reinforcements to withstand the forces of the internal vacuum. Once condensed, the condensate falls in a reservoir at the bottom of the housing. Even with the car moving, an amount of water will stay in the centre of the reservoir and will maintain the necessary pressure difference between condenser and evaporator. Non condensable gasses gather at the top of the housing and can be sucked away by a small sprinkler pipe. The outer shell is made of 2 mm stainless steel.

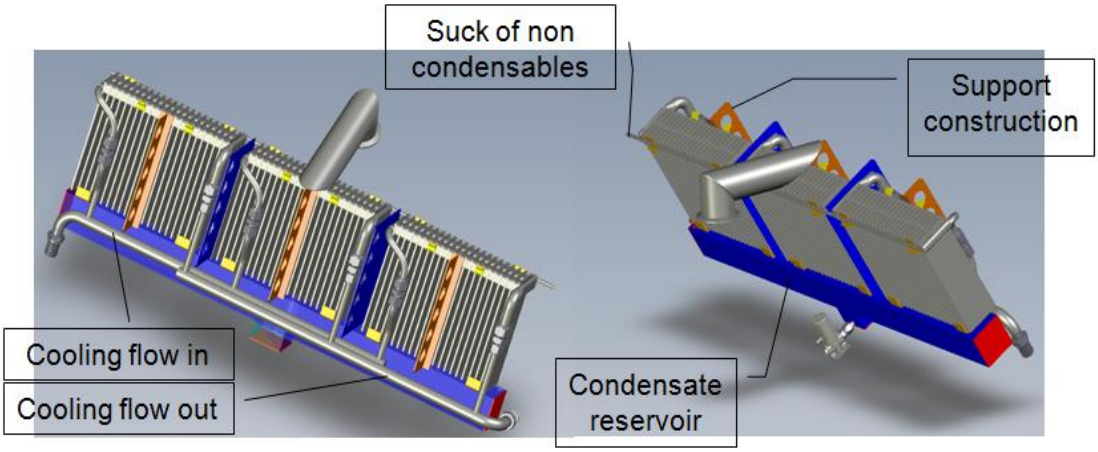

(a)

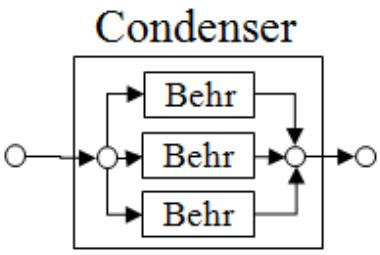

(c) (d)

Fig. 10. Condenser: (a) Design scheme, back view, (b) Design scheme, front section view, (c) Water flow arrangement scheme, (d) Actual picture.

3.2.4. Tubing and valves (liquid and vapour)

The adsorption chiller prototype uses the following control valves: four vapour check valves connected between the beds and the condenser/evaporator; four electromagnetic 3-way liquid valves and one liquid level control valve which is a small electromagnetic valve. Flexible rubber hoses are used to connect in series the cooling circuit of the bed after the condenser. This kind of tube is also used to connect the system with the car's water circuits.

3.3. System control

A good system control is necessary to realize maximum hardware performance. Not only the heat production of a car depends on the number of revolutions of the engine, but also the flow rate corresponds with the number of rotations. Therefore, the speed of the car plays an important role in determining the amount of available cooling. Because a heat, cool or chill water storage is too heavy for a car application, the control of the system has to be very flexible. Table 2 summarizes the system control strategies which have been used.

Table 2. Summary of the system control.

	Control Strategy
Timing liquid valves	Switching between beds is done using the difference between inlet and outlet temperatures of the heating/cooling water circuit of the beds. This is combined with a maximum allowable switching time. Fixed time control as back-up Heat recovery by delayed switching between inlet and outlet valves of the heating/cooling water circuit.
Level control evaporator	Level controller based on evaporation at thermocouples.
Vapour valves	Self actuating check valve.

A PLC system is installed to control the electrical equipment such as pumps and liquid valves, and to acquire readings from the temperature, pressure and flow sensors. The repeated heating and cooling of the beds is controlled by four electromagnetic three-way liquid valves. A design scheme of the liquid valves is presented in Fig. 11. The system can be operated either on fixed times for the beds' heating and cooling, or on flexible timing, where the switching of the valves is controlled by the actual temperature differences between the inlet and outlet temperature of the heating and cooling circuit. As an example, when both differences between inlet and outlet are less than 1K, the valves at the inlet are switched. The valves at the outlet are switched with a time delay with respect to the inlet valves. This time delay prevents hot water at high temperature to be sent directly to the cooling circuit and cooling water to be sent to the heating circuit. In this mode, a part of the sensible heat contained in the water circuits is recovered.

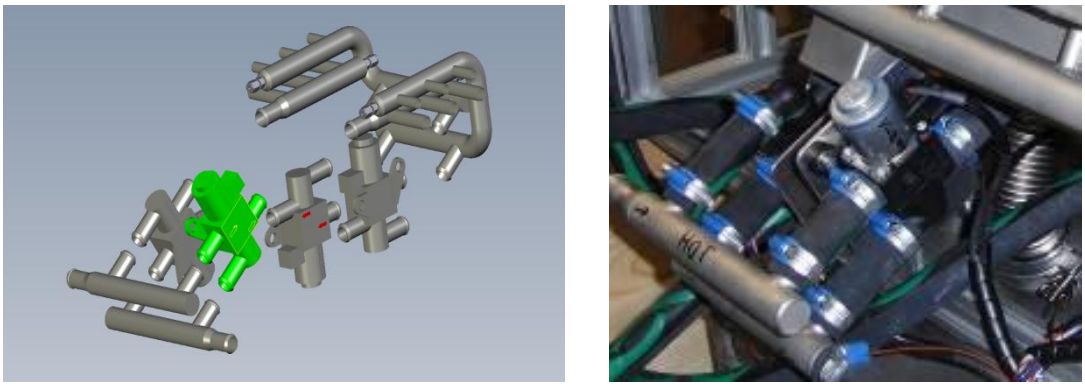

(a) (b)

Fig. 11. Liquid valves: (a) Design scheme, (b) Actual picture.

3.4. Experimental procedure

3.4.1. Laboratory tests

Several experiments were carried out using an ECN test rig to interface the adsorption prototype with the external heat sources/sinks and to simulate the cooling load. The external heating energy was provided by electric heaters placed in an open storage tank, and the external cooling energy was provided by a roof top cooler with an additional compression cooler. Thermostatic baths were used to reheat the chilled water circuit. All secondary water circuits (heating, cooling and chilled water circuit) contained a temperature controlled water storage and a pump. To determine the thermal powers, each circuit was equipped with a flow sensor (Burkert), temperature sensors (PT100) at the inlet and outlet, and a wet pressure difference sensor to measure the pressure drop. Furthermore, temperature and pressure sensors were also installed inside the beds, the evaporator and the condenser. All sensors for the measurements were checked before and corrected for deviations. The lay-out and instrumentation of the heating, cooling and chilled water circuits are shown in Fig. 12. Each one of the two beds is indicated by the numbers E440 and E430.

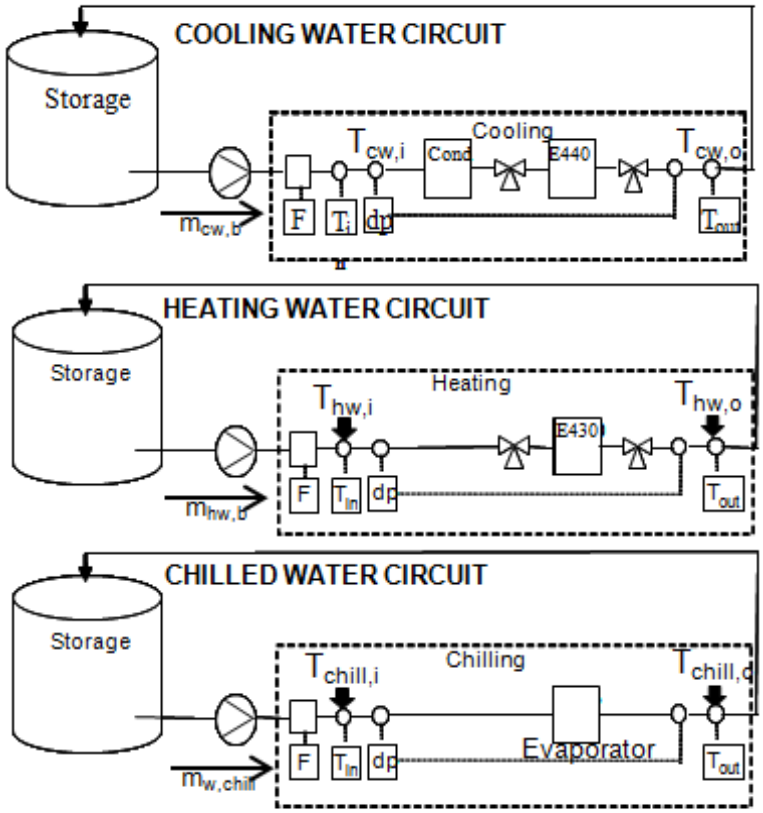

Fig. 12. Basic layout of the secondary water circuits (heating, cooling and chilled water circuits).

The test rig allows the fully automatic operation of the system and the management of different control strategies. Components installed (heat exchangers, temperature and pressure sensors, flow meters, valves and pumps) are electronically managed. A data acquisition and control system was realized by a specific software written in the Labview® language.

All the tests were carried out following a specific testing procedure:

- Setting of the operating conditions: the operating conditions tested were set by thermostatic controllers and external electric energy sources and sinks;
- Reaching of stable conditions: the system was operated until reaching stable periodical conditions in terms of temperature and pressure of each component;

- Data treatment for the last two cycles: to get a high reliability of the achieved results, after reaching stable conditions, two further cycles were performed and the corresponding thermal powers were calculated by a specific excel spreadsheet.

3.4.2. Settable operating conditions

The experimental tests have been performed at different operating conditions in order to assess the performance of the system. Table 3 reports the settable temperatures and flow rates for the heating, cooling and chilled water. The operating conditions described below were used to generate a set of experimental data that was later used for the validation of the mathematical model of the adsorption system (see chapter 6).

Table 3. Settable operating conditions.

Heating Water In (Heating water loop)		Cooling Water In (Cond+Bed cooling loop)		Chilled Water In (chilled water loop)	
Temp [ºC]	**Flow [kg/s]**	**Temp [ºC]**	**Flow [kg/s]**	**Temp [ºC]**	**Flow [kg/s]**
90	0.20	33	0.20	15	0.13
Total Cycle Time: 6 min					

4. OPTIMIZATION STUDY OF THE ADSORBENT BED HEAT EXCHANGER DESIGN

4.1. Introduction

Research activity on thermally driven adsorption cooling systems has received much attention in the recent years. Adsorption systems have the benefits of being environmentally friendly, since they do not use highly ozone depleting refrigerants, and they can be operated with low grade heat sources (<100 ºC) [80]. Moreover, such systems have the benefits of energy saving, noise and vibration free operation, simple control, and do not require moving parts [1, 80]. These features make them suitable for applications in automotive air conditioning using waste heat, normally coming from the engine operation.

Although adsorption systems present all the benefits mentioned before, they usually have the drawbacks of low overall efficiency and high investment costs relative to traditional electrically-driven refrigeration systems. The adsorption systems must have their size and cost reduced in order to make this technology more commercially viable. Therefore, the research activity on such systems is mainly focused on enhancing their performance. The most promising solution to achieve this goal is the enhancement of the heat and mass transfer in the sorption bed. Good heat transfer performance of the bed will increase the total heat transfer coefficient and the rate of heat transferred between the adsorbent and the heat transfer fluid [15]. In a similar view, a good mass transfer performance will reduce the diffusion time of the adsorbate in the adsorbent and shorten the adsorption/desorption cycle time [15], which will then cause an increase of the performance of the system.

The heat and mass transfer enhancement in the bed can be achieved by improving the thermal-physical characteristics of the adsorbent material. For example, directly synthesize the adsorbent material on conductive substrates in order to guarantee both high heat and mass transfer efficiency [80]. Another method to enhance the heat transfer in the bed consists of using extended

surfaces in order to increase the heat transfer area. Several types of extended surfaces such as finned tubes, plate heat exchangers and plate-fin heat exchangers are commonly used to increase the heat transfer rate in the bed [14]. However, Raymond et al. [81] pointed out the fact that any extended surfaces will detrimentally affect the COP of the system. As the bed is thermally cycled, the energy stored in the inert metal heat exchanger during the desorption stage will be rejected to the environment as the bed is cooled during the subsequent adsorption stage. Therefore, extended surfaces utilize heat that would otherwise regenerate the refrigerant supply and produce cooling. The author suggested that an optimum design of the bed is needed to balance the increased heat transfer area by using extended surfaces against the poorer COP resulting from the larger heat input.

Hence, an optimization of the bed design is required when using extended surfaces. As the sorption bed design should meet some minimum requirements of heat and mass transfer, the design criteria should involve the following thermal considerations: (i) good heat transfer rate from the heat exchanger fluid to the adsorbent; (ii) high permeability within the bed so that vapour can pass through the voids between the adsorbent grains in order to minimize the mass transfer resistances; (iii) low thermal capacity of the heat exchanger to avoid heat losses and (iv) the thermal mass of any non-adsorbent component must be minimized, as well as the dimensions of the system. Therefore, the sorption bed design should be considered carefully for each system application.

This chapter relates to the design optimization of a sorption bed which was specifically designed to be part of an adsorption cooling system for automobile air conditioning applications under the framework of the Topmacs project [65]. This bed configuration is based on a flat tube–fin heat exchanger filled with silica gel grains. This type of heat exchanger has been selected to perform a design optimization study. An analytical model has been developed in order to estimate the overall thermal conductance of the adsorbent bed heat exchanger by using a thermal resistance network. The bed thermal conductance should be high, in order to yield the greatest possible change in uptake, thus maximizing the cooling production of the system. A parametric study was performed using

the model to determine the effect of the geometrical and thermal parameters on the specific thermal conductance of the adsorbent bed heat exchanger. Since most of the design parameters of the bed under consideration are not optimized to reach the maximum system performance, it is important to know which are those parameters that mostly affect the cooling capacity and the COP. Therefore, another parametric study has been carried out by using the same model in order to evaluate the effect of the design parameters on the system performance. The system performance was evaluated in terms of maximum specific cooling capacity and maximum coefficient of performance that can be achieved in practical operation of the system as it will be described later on.

4.2. Literature review on sorption bed design

Over the past decades, many researchers have proposed various types of sorption bed designs in order to improve the heat transfer in the bed. However, most of the purposed bed designs are not optimized for automotive air conditioning applications.

For instance, Zhang [8] developed a double tube heat exchanger packed with zeolite pallets where axial metal fins were used in order to enhance the heat conduction in the bed. Critoph et al. [82] developed a prototype that was composed of monolithic carbon discs and aluminium fins. The monolithic carbon was mixed with an organic binder. Restuccia et al. [61] designed a coated heat exchanger which was made of finned tubes where zeolite was firmly bounded to the metal of the heat exchanger. Guilleminot et al. [83] studied a consolidated composite compound made from a mixture of zeolite with copper foam which increased the thermal conductivity of the bed. Gui et al. [84] designed a slim wall shell tube sorption heat exchanger in order to improve the heat transfer rate. Saha et al. [85] employed activated carbon fibers, as adsorbent, which were packed tightly inside oxygen-free copper fins. Bou et al. [86] developed a coated heat exchanger where the adsorbent was inserted in an expanded graphite plate. Lambert et al. [87] used annular fins interspersed with metal wool to improve sorption bed heat transfer.

There is a limited number of researchers that have investigated the effect of the bed design parameters on the overall heat transfer rate and hence how it affects the system performance.

For instance, Niazmand et al. [62] developed a two-dimensional heat and mass transfer model for a sorption bed with annular fins, which considers both internal and external resistances of bed particles. The effects of bed configurations such as fin spacing, bed height and particle size on the system performance were investigated. They showed that the cooling capacity can be increased by the increase of the number of fins and the decrease of the fins height. They found that the COP can be reduced by the use of fins; however, for a given cooling capacity, the bed size can be reduced dramatically when fins are employed, with a small sacrifice in cooling production. Furthermore, they found an optimum value for the particle diameter which maximizes the cooling capacity; however, the COP of the system is slightly influenced by the particle diameter.

Khan et al. [29] studied the effect of overall thermal conductance and adsorbent mass on the performance of a two-stage adsorption chiller with re-heat. The authors found that the COP of the system using re-heat can be significantly increased compared to the system without re-heat, at the cost of slightly lower cooling capacity. The effect of the sorption bed and evaporator overall thermal conductance values and adsorbent mass on the system performance were also investigated. They found that performance can be strongly influenced by the bed overall thermal conductance and slightly influenced by the overall thermal conductance of the evaporator. Furthermore, they showed that COP can be increased by the reduction of the adsorbent mass.

Rezk et al. [63] developed a lumped analytical simulation model for a silica gel/water adsorption chiller with mass and heat recovery. The effect of changing fin spacing on the cooling capacity and COP was investigated by using the simulation model. They showed that the cooling capacity increased by 3% and the COP decreased 2.3% when varying the fin spacing from its design value to a minimum permissible.

Solmus et al. [64] developed a one-dimensional local thermal non-equilibrium model in order to study the heat and mass transfer mechanisms inside a cylindrical sorption bed. The model takes into account both internal and external mass transfer resistances. The influence of several design parameters such as the adsorbent particle diameter, bed thickness, bed porosity, adsorbent thermal conductivity on the transient distributions of temperature, pressure and amount adsorbed in the radial direction of the cylindrical bed were investigated. They showed that the performance can be improved by reducing any significant heat transfer resistances and internal mass transfer resistances but not external mass transfer resistances.

Raymond et al. [81] developed a sorption bed thermal resistance model for a adsorption heat pump. The effects of fin pitch and fin height and other parameters on the performance were investigated in order to find the optimum heat exchanger geometry that achieves a desirable balance of thermal conductance and COP. This study was performed for two different working pairs. They found that the geometry that achieves this balance was significantly different for the two working pairs studied as a result of their different densities, wall contact resistances and effective conductivities of the adsorbent materials.

4.3. Design of the adsorbent bed heat exchanger under study

This chapter illustrates the geometrical and thermal considerations of sorption bed design using the plate-and-fin geometry as a base-case. The base-case bed corresponds to a single adsorbent bed heat exchanger, which was specifically designed and realized by the ECN research institute under the framework of the TOPMACS project [65] (see chapter 3). However, the analysis can also be applied with modifications to other bed designs employing fin surfaces.

The heat exchanger under consideration is a brazed type flat-tube fin heat exchanger. The employed heat exchangers were manufactured by Denso [77]

and are made of aluminium, which has lower density compared with other materials. In this way, the heat capacity of the metal in the bed could be minimized. Fig. 13(a) shows an actual picture of the heat exchanger used for the bed manufacture. The silica gel (type Sorbsil A) was packed in the interstices between the fins. Fig. 13(b) shows an actual picture of the adsorbent bed heat exchanger. The heat transfer fluid selected for heating and/or cooling the bed is pure water.

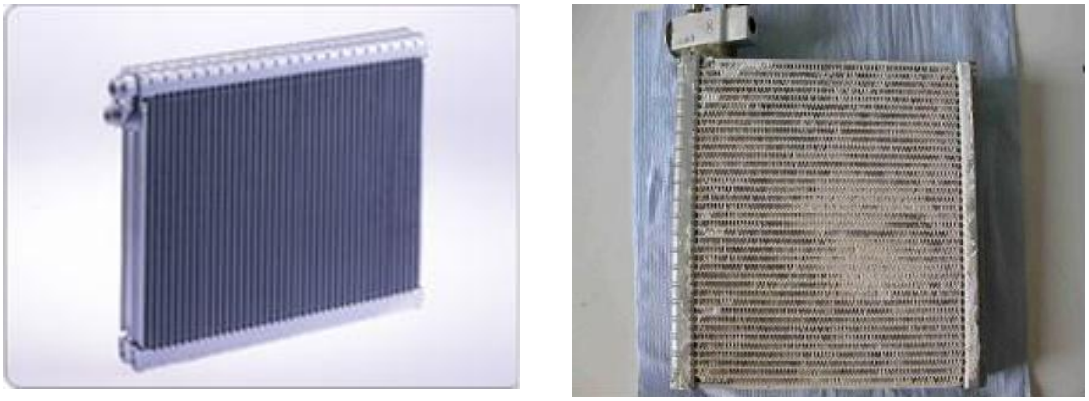

(a) (b)

Fig. 13. (a) Brazed type flat-tube fin heat exchanger [10]; (b) Actual picture of the adsorbent bed heat exchanger.

Fig. 14 shows the design parameters of the flat-tube fin heat exchanger under consideration. Physically, the heat exchanger is constructed by flat channel tubes covered with uniformly spaced rectangular fins to increase the heat transfer area on the air side which will be employed to increase the heat transfer to the adsorbent. Each channel tube comprises of two flat plates and an interplate channel, which carries the heat transfer fluid (i.e. water) for heating or cooling the packed adsorbent in a cyclic manner. The heat is transferred from the water to the adsorbent through the plates and fins. The number of channels determines the total heat transfer surface. The geometrical parameters of the heat exchanger are detailed on Table 4.

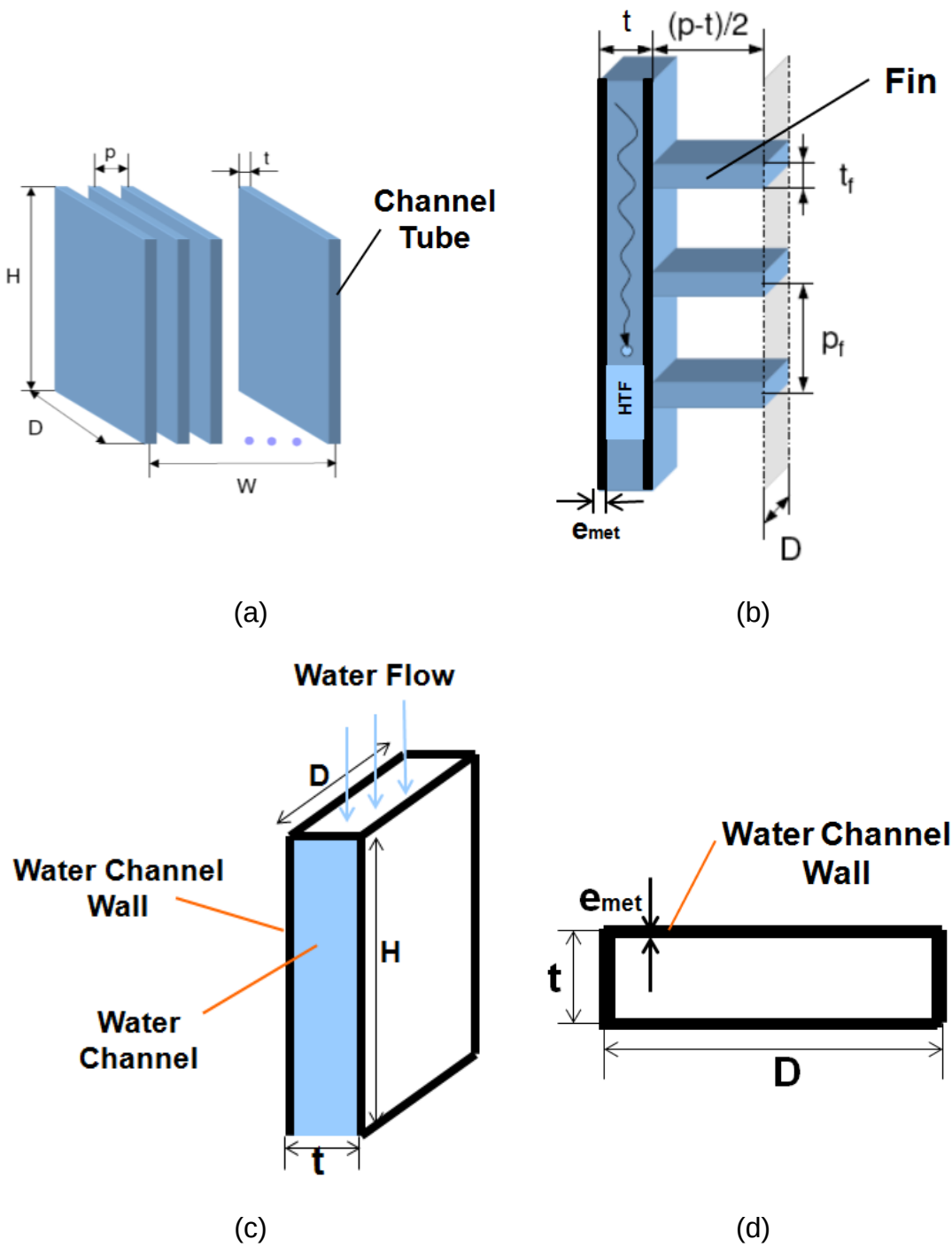

Fig. 14. Design sketch of the tube-fin heat exchanger: (a) core; (b) single channel tube and fins; (c) side view of a channel tube; (d) cross view of a channel tube.

Where: W is the heat exchanger wide; H is the heat exchanger height; D is the heat exchanger depth; t is the total channel tube thickness; p is the channel pitch; t_f is the fin thickness; p_f is the fin pitch; e_{met} is the thickness of the water channel wall (i.e. thickness of a single plate).

Table 4. Geometrical parameters for the base-case bed.

Parameters	Value	Units
Depth, D	0.038	m
Height, H	0.210	m
Wide, W	0.255	m
Channel Pitch, p	0.0067	m
Channel Thickness, t	0.0017	m
Fin Pitch, p_f	0.0015	m
Fin Thickness, t_f	0.0001	m
Water Channel Wall Thickness, e_{met}	0.0003	m
Number of tube channels, N_{ch}	38	-

The adsorbent bed heat exchanger comprises two parts: the non-adsorbent part, which includes the channel tubes plus fins, and the adsorbent part.

The non-adsorbent volume of the heat exchanger corresponds to the total volume of channels plus the total volume of fins. Hence, the volume of the heat exchanger $V_{met,HE}$ is given by the following equation:

$$V_{met,HE} = N_{ch} \cdot (V_{ch} + N_{fins} \cdot V_f) \tag{4.1}$$

where the volume of a single channel tube and fin, respectively, may be expressed as:

$$V_{ch} = 2 \cdot e_{met} \cdot (D + t) \cdot H \tag{4.2}$$

$$V_f = (p - t) \cdot t_f \cdot D \tag{4.3}$$

and the total number of channel tubes N_{ch} and the total number of fins per channel tube N_{fins} are given by:

$$N_{ch} = \frac{W}{p} \tag{4.4}$$

$$N_{fins} = \frac{H}{p_f} \tag{4.5}$$

Replacing Eqs. (4.2) to Eq.(4.5) into Eq. (4.1), it follows that:

$$V_{met,HE} = \frac{W}{p} \cdot \left[2 \cdot e_{met} \cdot (D + t) \cdot H + \frac{H}{p_f} \cdot \left((p - t) \cdot t_f \cdot D\right)\right] \tag{4.6}$$

Hence, the metal mass of the heat exchanger can be estimated as:

$$m_{met,HE} = V_{met,HE} \cdot \rho_{met} \tag{4.7}$$

On the other hand, the adsorbent volume of the heat exchanger is obtained by calculating the free space between the fins. This approximation is valid by supposing that the adsorbent is in its pelletized form. The adsorbent volume of the heat exchanger $V_{ads,HE}$ can be estimated by the following equation:

$$V_{ads,HE} = N_{ch} + (V_{free} - N_{fins} \cdot V_f) \tag{4.8}$$

where the free space between the fins for a single plate V_{free} is given by:

$$V_{free} = (p - t) \cdot D \cdot H \tag{4.9}$$

Replacing Eqs. (4.3) to (4.5) and Eq. (4.9) into Eq. (4.8) and rearranging, the following equation is obtained:

$$V_{ads,HE} = W \cdot D \cdot H \cdot \left[\left(1 - \frac{t}{p}\right) \cdot \left(1 - \frac{t_f}{p_f}\right)\right] \tag{4.10}$$

Since the overall volume of the heat exchanger V_{HE} may be expressed as:

$$V_{HE} = W \cdot D \cdot H \tag{4.11}$$

it follows that,

$$V_{ads,HE} = V_{HE} \cdot \left[\left(1 - \frac{t}{p}\right) \cdot \left(1 - \frac{t_f}{p_f}\right)\right] \tag{4.12}$$

Hence, the overall volume of the heat exchanger V_{HE} can be expressed as:

$$V_{HE} = \frac{V_{ads,HE}}{\left[\left(1 - \frac{t}{p}\right) \cdot \left(1 - \frac{t_f}{p_f}\right)\right]} \tag{4.13}$$

On the other hand, the adsorbent volume $V_{ads,HE}$ can also be expressed as:

$$V_{ads,HE} = \frac{m_{ads,HE}}{\rho_{ads}} \tag{4.14}$$

Replacing Eq. (4.14) into Eq. (4.13), yields the overall volume of the heat exchanger which is required to allocate a given mass of adsorbent:

$$V_{HE} = \frac{m_{ads,HE}}{\rho_{ads}\left[\left(1 - \frac{t}{p}\right) \cdot \left(1 - \frac{t_f}{p_f}\right)\right]} \tag{4.15}$$

The total volume of water which circulates through the channel tubes of the heat exchanger $V_{w,HE}$ can be estimated by:

$$V_{w,HE} = N_{ch} \cdot A_{c,wch} \cdot H \tag{4.16}$$

where the cross-sectional area of a single water channel $A_{c,wch}$ is given by:

$$A_{c,wch} = (D - 2 \cdot e_{met}) \cdot (t - 2 \cdot e_{met}) \tag{4.17}$$

Therefore, the total volume of water in the heat exchanger $V_{w,HE}$ can be estimated by:

$$V_{w,HE} = \frac{W}{p} \cdot (D - 2 \cdot e_{met}) \cdot (t - 2 \cdot e_{met}) \cdot H \tag{4.18}$$

Hence, the total mass of water in the heat exchanger can be estimated as:

$$m_{w,HE} = V_{w,HE} \cdot \rho_w \tag{4.19}$$

The total heat transfer area of the water side is given by:

$$A_{w,t} = N_{ch} \cdot P_{wet,ch} \cdot H \tag{4.20}$$

where $P_{wet,ch}$ is the wetted perimeter of the channel.

Taking into account that the adsorbent is only placed at both sides of the channel tube (with depth D), the total heat transfer area of the water side $A_{w,t}$ can be written as follows:

$$A_{w,t} = \frac{W}{p} \cdot 2 \cdot D \cdot H = \frac{2}{p} \cdot V_{HE} \tag{4.21}$$

Eq. (4.21) can be combined with Eq. (4.15) to obtain:

$$A_{w,t} = \frac{2 \cdot m_{ads,HE}}{p \cdot \rho_{ads} \left[\left(1 - \frac{t}{p}\right) \cdot \left(1 - \frac{t_f}{p_f}\right)\right]} \tag{4.22}$$

The equation mentioned above provides the relationship between the available heat transfer area of the water side with the adsorbent mass and the design parameters of the heat exchanger.

4.4. Heat transfer model

4.4.1. Heat transfer paths

The schematic diagram of the modelled adsorbent bed heat exchanger is shown in Fig. 15. As it can be seen, the bed can be divided into three parts. One is the adsorbent part, which is filled with adsorbent particles. The second one is the metal part, which comprises the plates and fin surfaces. Finally, the third one is the heat transfer fluid.

The adsorbent is in contact with a plate (i.e. “wall”) that separates it from the fluid. The role of the heat transfer fluid (i.e. water) is to cool down or heat up the adsorbent particles, which causes the adsorbent mass to adsorb refrigerant vapour from the evaporator or to desorb the refrigerant to the condenser.

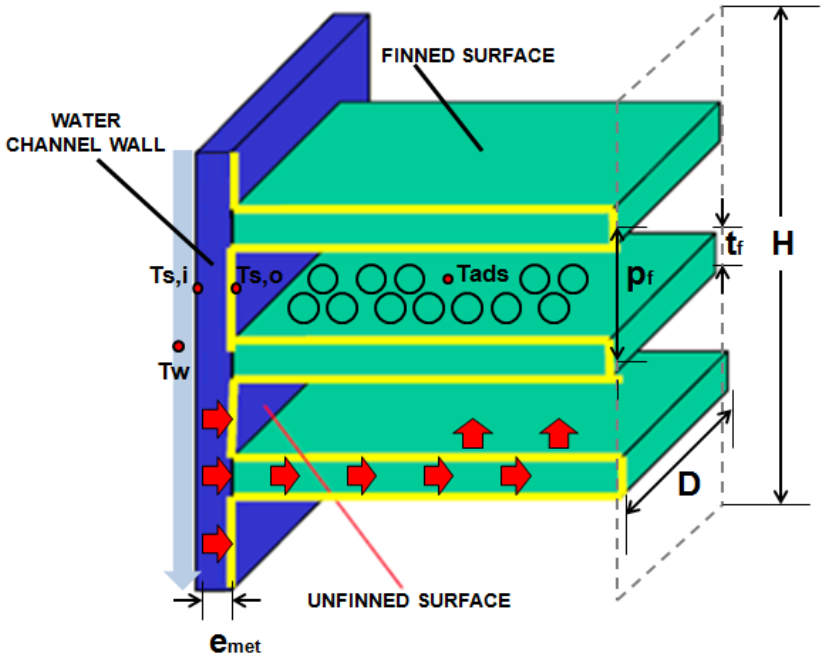

Fig. 15. Schematic diagram of the modelled adsorbent bed heat exchanger.

Where: T_w is the water temperature; $T_{s,i}$ is the inner wall surface temperature; $T_{s,o}$ is the outer wall surface temperature; T_{ads} is the adsorbent temperature.

The heat is transferred from the water to the adsorbent through the following paths:

- Firstly, the heat is transferred from the heat transfer fluid (hot or cold water) at T_w to the inner wall surface at $T_{s,i}$ by convection, with a convective heat transfer coefficient h_w.
- Secondly, the heat is transferred across the plate by conduction with a thermal conductivity of k_{met}.
- Finally, the heat is transferred from the outer wall surface at $T_{s,o}$ to the adsorbent at T_{ads} through two parallel heat flow paths: by conduction from the finned surface (i.e. fins) and by conduction from the unfinned surface (i.e. the wall surface between the fins).

4.4.2. Model assumptions

The equations governing the heat transfer process were developed using the control volume (i) approach as illustrated in Fig. 16.

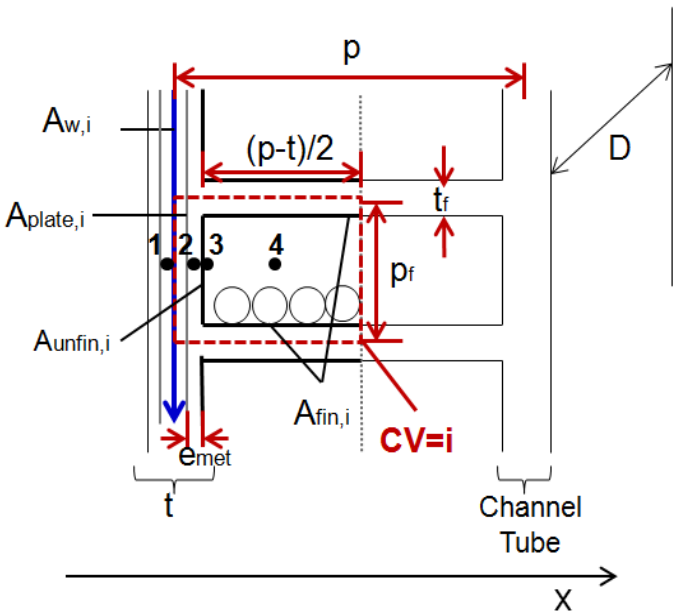

Fig. 16. Adsorbent bed heat exchanger control volume (i).

Where: 1 – T_w: Water temperature; 2 – $T_{s,i}$: Inner wall surface temperature; 3 – $T_{s,o}$: Outer wall surface temperature; 4 – T_{ads}: Adsorbent temperature.

In this analysis, the following assumptions are considered:

- The heat is transferred through the plate under one-dimensional conditions in the longitudinal (x) direction,
- The thermal conductivity of the metal is constant,
- The overall heat transfer coefficient is uniform along the heat exchanger,
- The heat transfer area of the plate $A_{plate,i}$ is equal to the heat transfer area of the water side $A_{w,i}$,
- The base of the fins are at the same temperature as the surface to which they are attached (i.e. at temperature $T_{s,o}$),
- The equivalent convection heat transfer coefficient h_{eq} is uniform over the surface. The heat conduction from the wall in contact with the adsorbent will be evaluated through an equivalent convection heat transfer coefficient, with different values for the adsorbent close to the water channel and for the adsorbent in between the fins.

4.4.3. Overall thermal conductance estimation

Under these assumptions, a simple thermal resistance network can be used to determine the overall thermal conductance of the adsorbent bed heat exchanger. The thermal circuit and the resistance for each element is represented in Fig. 17. The equivalent thermal circuit includes the following resistances to heat flow: (i) convection resistance at the inner wall surface; (ii) conduction resistance through the plate; (iii) convection resistances for the unfinned surface as well as along the fins, which act in parallel.

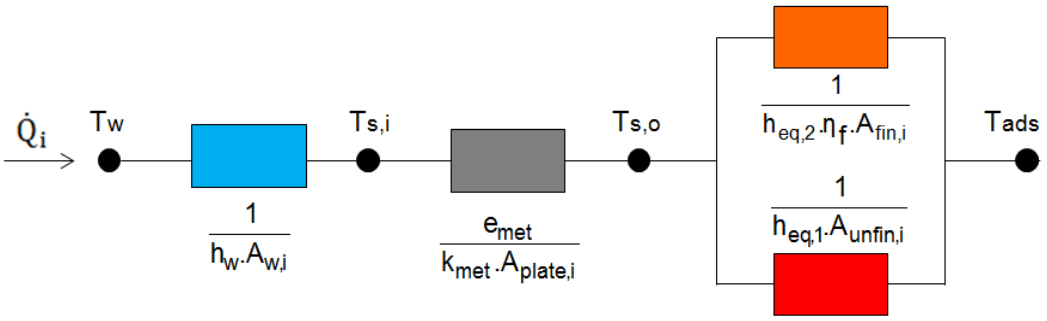

Fig. 17. Heat Transfer through the adsorbent bed heat exchanger in one control volume (i): Equivalent thermal circuit.

Therefore, the total thermal resistance from the water to the adsorbent in one control volume i (see Fig. 16) can be written in the following way:

$$R_{tot} = \frac{1}{h_w \cdot A_{w,i}} + \frac{e_{met}}{k_{met} \cdot A_{plate,i}} + \frac{1}{h_{eq,1} \cdot A_{unfin,i} + h_{eq,2} \cdot \eta_f \cdot A_{fin,i}} \qquad (4.23)$$

where the heat transfer area A for the water side, unfinned and finned surfaces, respectively, may be approximated as:

$$A_{w,i} = A_{plate,i} = p_f \cdot D \qquad (4.24)$$

$$A_{unfin,i} = (p_f - t_f) \cdot D \qquad (4.25)$$

$$A_{fin,i} = 2 \cdot \left(\frac{p - t}{2}\right) \cdot D \qquad (4.26)$$

The equivalent convection heat transfer coefficients for the unfinned and finned surfaces, $h_{eq,1}$ and $h_{eq,2}$, are estimated by assuming an average thermal conductivity and thickness. In order to apply the fin efficiency theory, the heat transfer by conduction from the wall surface (unfinned and finned surfaces) to the adsorbent has been assumed to be equivalent to an equivalent heat transfer coefficient by convection from the wall surfaces to the adsorbent. The equivalent convection heat transfer coefficient can be estimated as the ratio of

the adsorbent thermal conductivity to the corresponding distance between the adsorbent at mean temperature T_{ads} and the outer wall surface temperature$T_{s,o}$.

The equivalent convection heat transfer coefficients h_{eq} in one control volume i are shown schematically in Fig. 18.

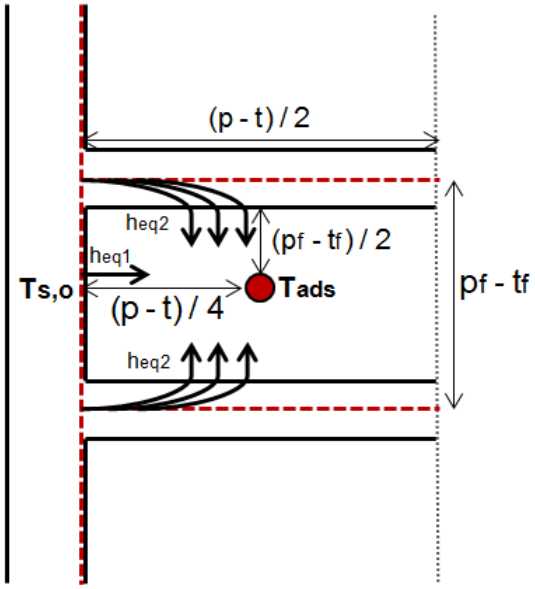

Fig. 18. Equivalent convection heat transfer coefficients estimation.

Therefore, the equivalent convection heat transfer coefficients for the unfinned and finned surfaces, respectively, can be estimated as:

$$h_{eq,1} = \frac{k_{ads}}{\left(\frac{p-t}{4}\right)} = \frac{4 \cdot k_{ads}}{(p-t)} \tag{4.27}$$

$$h_{eq,2} = \frac{k_{ads}}{\left(\frac{p_f - t_f}{2}\right)} = \frac{2 \cdot k_{ads}}{(p_f - t_f)} \tag{4.28}$$

The convective heat transfer coefficient on the water side h_w is estimated by assuming the hypothesis of fully developed laminar flow and a channel geometry similar to infinite parallel plates. Therefore, the convective heat

transfer coefficient on the water side h_w becomes a function of the Nusselt number Nu in the following way [88]:

$$h_w = k_w \cdot \frac{Nu}{D_h} \tag{4.29}$$

where D_h is the hydraulic diameter of the water channel and k_w is the thermal conductivity of the water.

The hydraulic diameter of the water channel may be expressed as:

$$D_h = \frac{4 \cdot A_{c,wch}}{P_{wet,ch}} = 2 \cdot (t - 2 \cdot e_{met}) \tag{4.30}$$

In Eq. (4.29), the Nu value corresponding to the channel geometry in question is 7.54 [88] assuming the hypothesis of laminar flow with uniform wall temperature.

Hence, Eq. (4.29) can be rewritten as:

$$h_w = k_w \cdot \frac{7.54}{2 \cdot (t - 2 \cdot e_{met})} \tag{4.31}$$

The total heat transfer from the water to the adsorbent in one control volume i (see Fig. 16) can be expressed as:

$$\dot{Q}_i = \frac{T_w - T_{ads}}{\frac{1}{A_{w,i}}\left[\frac{1}{h_w} + \frac{e_{met}}{k_{met}}\right] + \frac{1}{h_{eq,1} \cdot A_{unfin,i} + h_{eq,2} \cdot \eta_f \cdot A_{fin,i}}} \tag{4.32}$$

Substituting Eqs. (4.24) to (4.26) into Eq. (4.32), the obtained result is:

$$\dot{Q}_i = \frac{T_w - T_{ads}}{\frac{1}{p_f \cdot D}\left[\frac{1}{h_w} + \frac{e_{met}}{k_{met}}\right] + \frac{1}{h_{eq,1} \cdot (p_f - t_f) \cdot D + h_{eq,2} \cdot \eta_f \cdot (p - t) \cdot D}} \quad (4.33)$$

By combining and isolating $A_{w,i} = p_f \cdot D$ in the dominator, it follows that:

$$\dot{Q}_i = \frac{T_w - T_{ads}}{\frac{1}{A_{w,i}}\left[\frac{1}{h_w} + \frac{e_{met}}{k_{met}} + \frac{1}{h_{eq,1} \cdot \left(\frac{p_f - t_f}{p_f}\right) + h_{eq,2} \cdot \eta_f \cdot \left(\frac{p - t}{p_f}\right)}\right]} \quad (4.34)$$

Hence, the heat flux applied to the control volume (i) over interval $\Delta A_{w,i}$ may be expressed as:

$$q|_{\Delta A_{w,i}} = \frac{\dot{Q}_i}{\Delta A_{w,i}} = \frac{T_w - T_{ads}}{\frac{1}{h_w} + \frac{e_{met}}{k_{met}} + \left[\frac{1}{h_{eq,1} \cdot \left(\frac{p_f - t_f}{p_f}\right) + h_{eq,2} \cdot \eta_f \cdot \left(\frac{p - t}{p_f}\right)}\right]} \quad (4.35)$$

Finally, the heat transfer coefficient U for a differential element $\Delta A_{w,i}$ may be expressed as:

$$U|_{\Delta A_{w,i}} = \frac{q|_{\Delta A_{w,i}}}{T_w - T_{ads}} = \frac{1}{\frac{1}{h_w} + \frac{e_{met}}{k_{met}} + \left[\frac{1}{h_{eq,1} \cdot \left(\frac{p_f - t_f}{p_f}\right) + h_{eq,2} \cdot \eta_f \cdot \left(\frac{p - t}{p_f}\right)}\right]} \quad (4.36)$$

Substituting Eq. (4.27), Eq. (4.28) and Eq. (4.31) into Eq. (4.36), the obtained result is:

$$U|_{\Delta A_{w,i}} = \frac{q|_{\Delta A_{w,i}}}{T_w - T_{ads}} = \frac{1}{\frac{1}{\left[k_w \cdot \frac{7.54}{2 \cdot (t - 2 \cdot e_{met})}\right]} + \frac{e_{met}}{k_{met}} + \left[\frac{1}{\frac{4 \cdot k_{ads}}{(p - t)} \cdot \left(\frac{p_f - t_f}{p_f}\right) + \frac{2 \cdot k_{ads}}{(p_f - t_f)} \cdot \eta_f \cdot \left(\frac{p - t}{p_f}\right)}\right]} \quad (4.37)$$

Rearranging,

$$U|_{\Delta A_{w,i}} = \frac{1}{\frac{1}{\left[k_w \cdot \frac{7.54}{2 \cdot p \cdot \left(\frac{t}{p} - 2 \cdot \frac{e_{met}}{p}\right)}\right]} + \frac{e_{met}}{k_{met}} + \frac{p \cdot \left(1 - \frac{t}{p}\right)}{4 \cdot k_{ads} \cdot \left[\left(1 - \frac{t_f}{p_f}\right) + \frac{\eta_f}{2} \cdot \left[\frac{p^2 \cdot \left(1 - \frac{t}{p}\right)^2}{p_f{}^2 \cdot \left(1 - \frac{t_f}{p_f}\right)}\right]\right]}} \tag{4.38}$$

where the fin efficiency η_f may be defined as:

$$\eta_f = \frac{\tanh(m \cdot L_f)}{m \cdot L_f} \tag{4.39}$$

With

$$L_f = \frac{(p - t)}{2} \tag{4.40}$$

and

$$m = \sqrt{\frac{P_f \cdot h_{eq,2}}{A_{c,f} \cdot k_{met}}} = \sqrt{\frac{(2 \cdot D) \cdot h_{eq,2}}{(t_f \cdot D) \cdot k_{met}}} = \sqrt{\frac{4 \cdot k_{ads}}{k_{met} \cdot t_f \cdot (p_f - t_f)}} \tag{4.41}$$

Hence,

$$m \cdot L_f = \sqrt{\frac{4 \cdot k_{ads}}{k_{met} \cdot t_f \cdot (p_f - t_f)}} \cdot \frac{p - t}{2} \tag{4.42}$$

Rearranging, it follows that

$$m \cdot L_f = \frac{1}{2} \cdot \sqrt{\frac{4 \cdot k_{ads}}{k_{met}}} \cdot \sqrt{\frac{1}{\frac{p_f}{p}\left(\frac{t_f}{p}\right)^{-1} - 1}} \cdot \left(\frac{t_f}{p}\right)^{-1} \cdot \left(1 - \frac{t}{p}\right) \tag{4.43}$$

Assuming that the heat transfer coefficient of the bed is constant along the heat exchanger, the overall thermal conductance of the adsorbent bed heat exchanger $\mathrm{UA_{total,HE}}$ can be roughly estimated as:

$$\mathrm{UA_{total,HE}} = \int_0^{\Delta A_{w,i}} \mathrm{U|_{\Delta A_{w,i}}} dA_{w,t} = \mathrm{U|_{\Delta A_{w,i}}} \cdot \int_0^{\Delta A_{w,i}} dA_{w,i} = \mathrm{U|_{\Delta A_{w,i}}} \cdot A_{w,t} \quad (4.44)$$

where $\mathrm{A_{w,t}}$ is the total heat transfer area of the water.

By substituting Eq. (4.38) and Eq. (4.21) into Eq.(4.44), it follows that

$$\mathrm{UA_{total,HE}} = \frac{1}{\frac{1}{\left[k_w \cdot \frac{7.54}{2 \cdot p \cdot \left(\frac{t}{p} - 2 \cdot \frac{e_{met}}{p}\right)}\right]} + \frac{e_{met}}{k_{met}} + \frac{p \cdot \left(1 - \frac{t}{p}\right)}{4 \cdot k_{ads}\left[\left(1 - \frac{t_f}{p_f}\right) + \frac{\eta_f}{2} \cdot \left[\frac{p^2 \cdot \left(1 - \frac{t}{p}\right)^2}{p_f^2 \cdot \left(1 - \frac{t_f}{p_f}\right)}\right]\right]}} \cdot \frac{2}{p} \cdot V_{HE} \quad (4.45)$$

where $\mathrm{V_{HE}}$ is the overall volume of the heat exchanger.

Finally, the ‘specific thermal conductance’ defined here as the overall thermal conductance of the adsorbent bed heat exchanger divided by the volume of the heat exchanger can be determined by the following expression:

$$\frac{\mathrm{UA_{overall}}}{\mathrm{V_{HE}}} = \frac{1}{\frac{1}{\left[k_w \cdot \frac{7.54}{2 \cdot p \cdot \left(\frac{t}{p} - 2 \cdot \frac{e_{met}}{p}\right)}\right]} + \frac{e_{met}}{k_{met}} + \frac{p \cdot \left(1 - \frac{t}{p}\right)}{4 \cdot k_{ads}\left[\left(1 - \frac{t_f}{p_f}\right) + \frac{\eta_f}{2} \cdot \left[\frac{p^2 \cdot \left(1 - \frac{t}{p}\right)^2}{p_f^2 \cdot \left(1 - \frac{t_f}{p_f}\right)}\right]\right]}} \cdot \frac{2}{p} \quad (4.46)$$

As it can be observed, the specific thermal conductance of the adsorbent bed heat exchanger is a complex analytical expression which depends on the following geometrical and thermal parameters:

$$\frac{UA_{total,HE}}{V_{HE}} = f\left(k_w, k_{ads}, k_{met}, p, \frac{t}{p}, \frac{p_f}{p}, \frac{t_f}{p}, \frac{e_{met}}{p}\right) \quad (4.47)$$

The effect of the geometrical and thermal parameters mentioned above on the $UA_{total,HE}/V_{HE}$ will be investigated in subsection 4.5.2.

Notice that the fin efficiency η_f , in Eq.(4.46), is also a function of the following design parameters:

$$\eta_f = f\left(k_{ads}, k_{met}, \frac{t}{p}, \frac{p_f}{p}, \frac{t_f}{p}\right) \quad (4.48)$$

4.4.4. Performance estimation

The heart of the adsorption cooling system developed under the framework of the Topmacs project [65] is effectively the sorption bed which is composed of three unitary heat exchangers filled with adsorbent material as it can be seen in Fig. 8(b) of chapter 3. Clearly, the performance of the system as a whole depends on the performance of the aforementioned heat exchangers. To assist the system design process, an analytical model has been developed in order to estimate the performance of a single adsorbent bed heat exchanger.

A simple adsorption cooling system has been considered in this study. The system operates between three temperature levels, which correspond to the high, medium and low-temperature sources. A schematic diagram of the three temperature (3T) adsorption cooling system in consideration is shown in Fig. 19. Such system consists of an adsorbent bed heat exchanger (i.e. bed) at temperature T_b connected to the appropriate sources, a condenser at temperature T_{cond} and an evaporator at temperature T_{evap}. Basically the system operates by cycling adsorbate (i.e. refrigerant) between bed, condenser and evaporator. The bed switches between two modes: the heating phase and the cooling phase. The first one represents the desorption process and it occurs when the bed receives heat (Q_{heat}) from the high-temperature source (i.e. heating water) and releases heat (Q_{cond}) to the medium-temperature source.

The transfer of heat (Q_{cond}) to the medium-temperature source occurs during the condensation of the refrigerant in the condenser. The second phase represents the adsorption process and it occurs when the refrigerant is vaporized in the evaporator by taking heat (Q_{chill}) from the low-temperature source (i.e. chilled water) and the bed releases heat (Q_{cool}) to the medium-temperature source (i.e. cooling water). For an ideal 3T adsorption system, the bed switches from T_{heat} (desorption phase, $T_b=T_{heat}$) to T_{cool} (adsorption phase, $T_b=T_{cool}$).

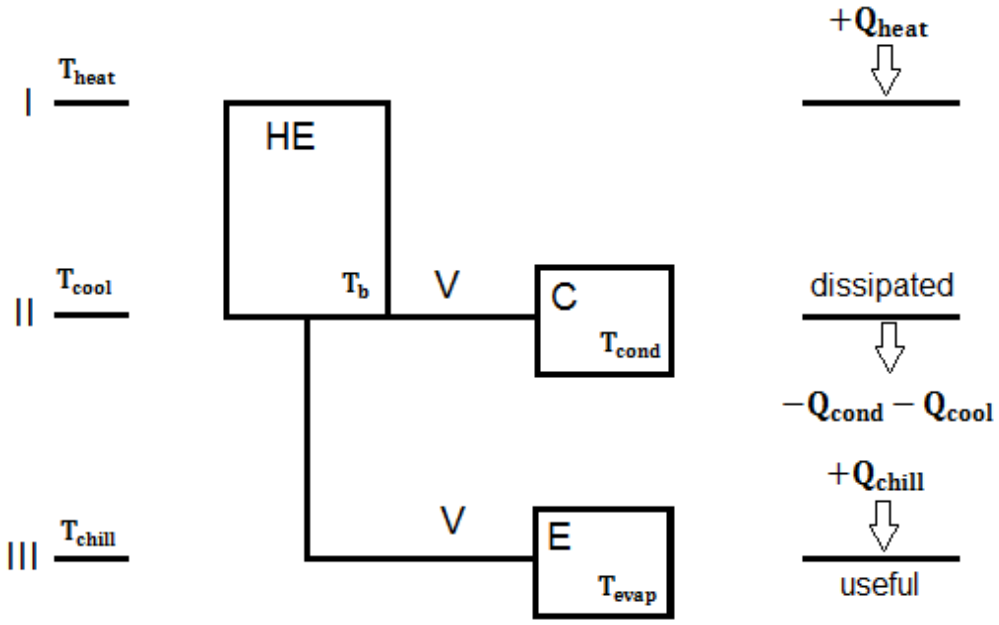

Fig. 19. Schematic diagram of the 3T adsorption cooling system under study.

Where: HE is the adsorbent bed heat exchanger (i.e. bed); C is the condenser; E is the evaporator; I is the high-temperature source; II is the medium-temperature source; III is the low-temperature source; Tb is the bed temperature; T_{cond} is the condenser temperature and T_{evap} is the evaporator temperature.

The performance of the adsorption system in consideration has been quantified by the maximum coefficient of performance ($COP_{m,p}$) and the maximum specific cooling capacity ($SCC_{m,p}$) that could be achieved in practical operation of the system as it will be described bed later on.

4.4.4.1. Maximum coefficient of performance

The coefficient of performance (COP) of the system can be defined as the ratio between the amount of cooling produced in the evaporator and the amount of heating that must be supplied to the bed during the heating phase:

$$\mathrm{COP} = \frac{\mathrm{Q_{chill}}}{\mathrm{Q_{heat}}} \tag{4.49}$$

In practice, the maximum coefficient of performance for the adsorption system in question can be approached by:

$$\mathrm{COP_{m,p}} = \frac{\mathrm{Q_{chill}}|_{\mathrm{m,p}}}{\mathrm{Q_{heat}}} = \frac{\mathrm{m_{ads,HE}} \cdot \Delta w \cdot \Delta \mathrm{h_{fg}}}{\mathrm{m_{ads,HE}} \cdot \Delta w \cdot \Delta \mathrm{h_{des}} + \left(\mathrm{m_{ads,HE}} \cdot \mathrm{cp_{ads,0}} + \mathrm{m_{w,tot}} \cdot \mathrm{cp_w} + \mathrm{m_{met,tot}} \cdot \mathrm{cp_{met}}\right) \cdot \Delta \mathrm{T_b}} \tag{4.50}$$

where $\mathrm{m_{ads,HE}}$ is the total mass of dry adsorbent in the heat exchanger [kg], $\mathrm{m_{met,tot}}$ is the total metal mass (including the inlet/outlet headers) of the heat exchanger [kg], $\mathrm{m_{w,tot}}$ is the total water mass (including the water in the headers) in the heat exchanger [kg], Δw is the maximum uptake variation in the bed [kg of adsorbate/Kg of dry adsorbent], $\Delta \mathrm{h_{fg}}$ is the enthalpy of vaporization of the refrigerant [J $\mathrm{kg^{-1}}$], $\Delta \mathrm{h_{des}}$ is the enthalpy of desorption of the adsorbent [J $\mathrm{kg^{-1}}$], $\Delta \mathrm{T_b}$ is the maximum temperature variation in the bed [K], $\mathrm{cp_{met}}$ is the metal specific heat [J $\mathrm{kg^{-1}}$ $\mathrm{K^{-1}}$], $\mathrm{cp_w}$ is the specific heat of the water [J $\mathrm{kg^{-1}}$ $\mathrm{K^{-1}}$] and $\mathrm{cp_{ads,0}}$ is the specific heat of the dry adsorbent [J $\mathrm{kg^{-1}}$ $\mathrm{K^{-1}}$].

In Eq. (4.50), $\mathrm{m_{ads,HE}} \cdot \Delta w$ corresponds to the mass of refrigerant [kg]. The term in the numerator of Eq. (4.50) represents the latent heat of vaporization of the cycled adsorbate (i.e. refrigerant) assuming that the adsorbent goes through the maximum possible uptake change, Δw. In the denominator of Eq. (4.50), the first term refers to the heat input required for the desorption of the same amount

of adsorbate/refrigerant, while the second term represents the sensible heat required to heat the adsorbent, the heat transfer fluid and the metallic parts of the heat exchanger along the heating phase, for the maximum bed temperature change, ΔT_b.

Dividing the numerator and the dominator by $m_{ads,HE} \cdot \Delta w \cdot \Delta h_{des}$ and rearranging, it follows that

$$COP_{m,p} = \frac{\frac{\Delta h_{fg}}{\Delta h_{des}}}{1 + \overline{cp}_b \cdot \left(\frac{\Delta T_b}{\Delta w \cdot \Delta h_{des}}\right)} \tag{4.51}$$

where the equivalent heat capacity of the bed per adsorbent mass, $\overline{cp}_b$, is given by:

$$\overline{cp}_b = \left[cp_{ads,0} + \left(\frac{m_{w,tot}}{m_{ads,HE}}\right) \cdot cp_w + \left(\frac{m_{met,tot}}{m_{ads,HE}}\right) \cdot cp_{met}\right] \tag{4.52}$$

According to literature, the maximum theoretical coefficient of performance of an adsorption system is defined by Sharonov et al. [89] as the ratio between the enthalpy of vaporization and the enthalpy of desorption:

$$COP_{max} = \frac{\Delta h_{fg}}{\Delta h_{des}} \tag{4.53}$$

Hence, Eq. (4.51) can be written as:

$$COP_{m,p} = \frac{COP_{max}}{1 + \overline{cp}_b \cdot \left(\frac{\Delta T_b}{\Delta w \cdot \Delta h_{des}}\right)} \tag{4.54}$$

The obtained expression for the maximum practical COP (given by Eq. (4.54)) takes into account all the heating/cooling losses of all masses present in the bed, i.e. metal, adsorbent and heat transfer fluid masses.

The practical COP will be lower than the maximum COP ($\mathrm{COP}_{\mathrm{m,p}}$) because of other irreversibilities such as pressure losses between the bed and the condenser/evaporator and heat losses.

The temperature and uptake variation in the bed during a full cycle time are shown in Fig. 20.

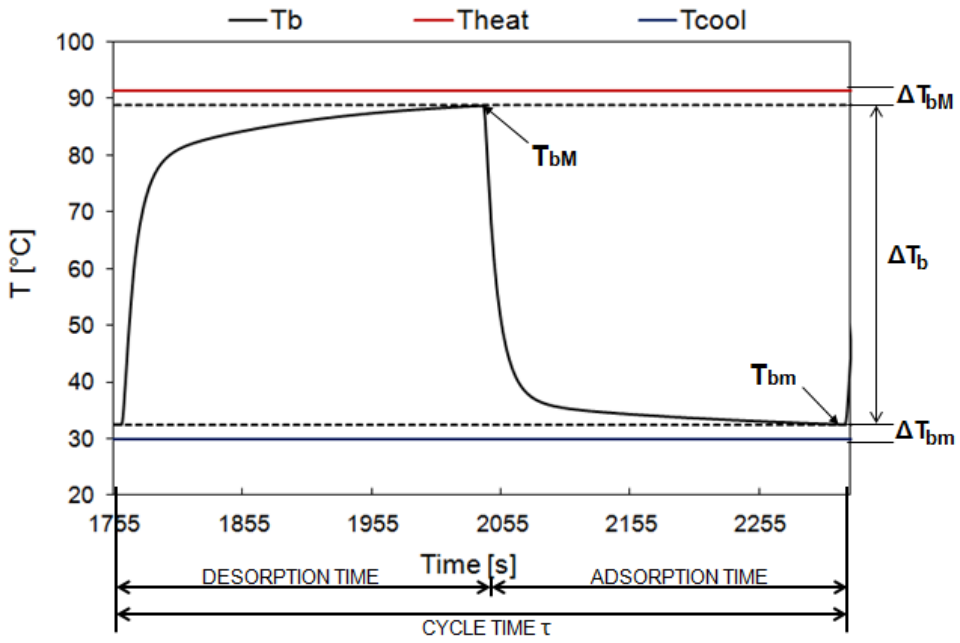

(a)

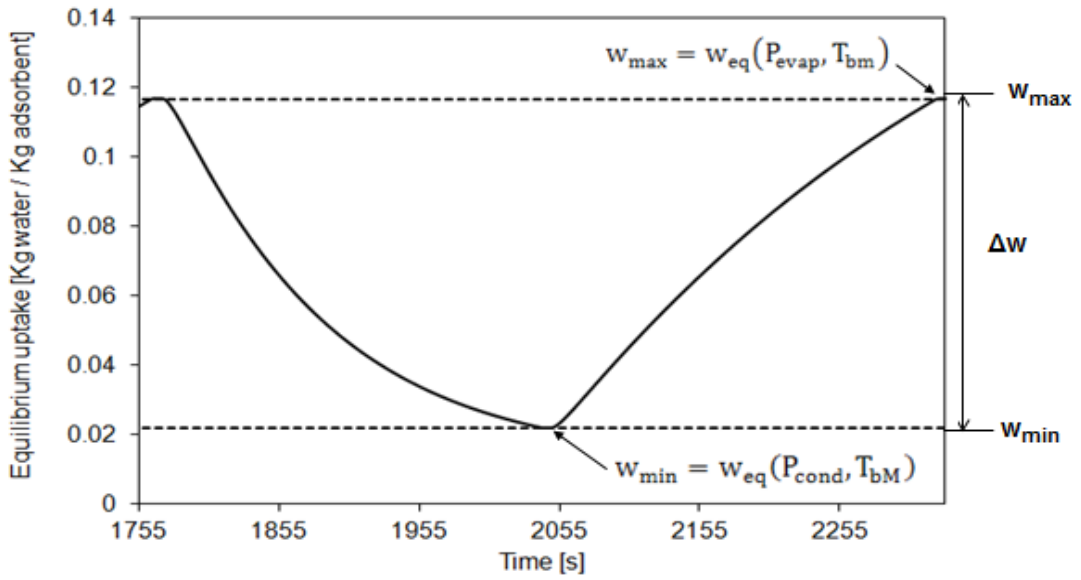

(b)

Fig. 20. Temperature and uptake variation in the bed during a full cycle time: (a) Maximum temperature variation estimation; (b) Maximum uptake variation estimation.

Where: $T_{b,M}$ is the maximum bed temperature; $T_{b,m}$ is the minimum bed temperature; T_{heat} is the heating water temperature; T_{cool} is the cooling water temperature; w_{max} is the maximum uptake; w_{min} is the minimum uptake.

The maximum temperature variation in the bed, ΔT_b , as illustrated in Fig. 20(a), can be defined as:

$$\Delta T_b = T_{b,M} - T_{b,m} \cong \varphi(T_{heat} - T_{cool}) \tag{4.55}$$

In practical operation of the system, the maximum and minimum bed temperatures do not achieve the temperatures of the external heating and cooling water sources, which correspond to T_{heat} and T_{cool} respectively. For this reason, the difference ΔT_b in Eq. (4.55) has to be corrected by a factor φ in order to take into account the asymptotic approach of $T_{b,M}$ and $T_{b,m}$ towards T_{heat} and T_{cool} .

However, the difference between the maximum bed temperature and the heating water temperature, as well as the difference between the minimum bed temperature and the cooling water temperature are small. This fact has been confirmed by simulation results obtained at constant operating conditions (cooling water temperature at 33 ºC, heating water temperature at 90 ºC and chilled water temperature at 15 ºC) as it can be seen in Fig. 21. The model used to generate these results will be described in chapter 5.

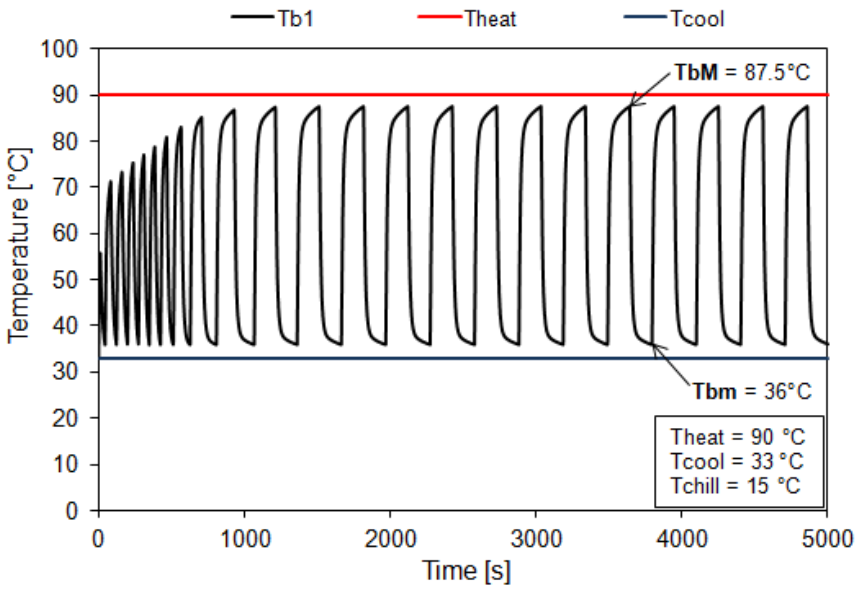

Fig. 21. Simulation results obtained at constant operating conditions: Bed temperature evolution.

From the simulation results, the correction factor φ mentioned in Eq. (4.55) is between 0.90 - 0.95. As such, it has been assumed that the factor φ has a value of 1, which means that the bed temperature difference, ΔT_b , is assumed to be equal to the difference between the maximum and minimum water temperature limits (T_{heat} and T_{cool} respectively):

$$\Delta T_b = T_{heat} - T_{cool} \tag{4.56}$$

The maximum uptake variation in the bed, Δw , will be the one corresponding to the difference of equilibrium uptakes between the end of the heating and cooling periods:

$$\Delta w = w_{max} - w_{min} \tag{4.57}$$

where the maximum and minimum uptakes, w_{max} and w_{min} , correspond to the uptake at equilibrium conditions.

The equilibrium uptake in the bed, w_{eq} , in kg of adsorbate/kg of dry adsorbent, depending on the temperature and pressure, can be estimated by the following equation [34]:

$$\ln P = a_0 + a_1 \cdot w_{eq} + a_2 \cdot {w_{eq}}^2 + a_3 \cdot {w_{eq}}^3 + \frac{b_0 + b_1 \cdot w_{eq} + b_2 \cdot {w_{eq}}^2 + b_3 \cdot {w_{eq}}^3}{T} \tag{4.58}$$

where the numerical values of the coefficients a and b (i = 0, 1, 2, 3) are taken from the literature [90] for the adsorbent/adsorbate pair under study.

Hence, the maximum and minimum bed uptakes, as illustrated in Fig. 20(b), are estimated by the above equation at the following hypothetical temperature and pressure conditions:

$$w_{max} = w_{eq}(P_{evap}, T_{bm}) \cong w_{eq}(P_{evap}, T_{cool}) \tag{4.59}$$

$$w_{min} = w_{eq}(P_{cond}, T_{bM}) \cong w_{eq}(P_{cond}, T_{heat}) \tag{4.60}$$

where P_{evap} and P_{cond} are the evaporator and condenser pressure, respectively. The most favourable conditions for the condenser and evaporator pressures are considered to be the saturation pressure corresponding to the saturation temperature in the condenser and the evaporator. These saturation

temperatures correspond to the temperatures of the cooling and chilled water loops.

The condenser and evaporator pressures, P_{evap} and P_{cond} , are estimated at the following hypothetical temperature conditions:

$$P_{evap} = P_{sat}(T_{evap}) \cong P_{sat}(T_{chill}) \tag{4.61}$$

$$P_{cond} = P_{sat}(T_{cond}) \cong P_{sat}(T_{cool}) \tag{4.62}$$

The desorption enthalpy Δh_{des} , in J/kg, at a specified uptake (w_{min}) can be estimated by the following equation [34]:

$$\Delta h_{des}(w_{min}) = -(b_0 + b_1 \cdot w_{min} + b_2 \cdot {w_{min}}^2 + b_3 \cdot {w_{min}}^3) \cdot \frac{R}{M_w} \tag{4.63}$$

where the numerical values of the coefficients b (i = 0, 1, 2, 3) are taken from the literature [90] for the adsorbent/adsorbate pair in question.

The specific heat of vaporization of the water Δh_{fg}, in J/kg, at a specified temperature (T) can be estimated by a simple linear regression as the following equation [91]:

$$\Delta h_{fg}(T) = 3159.2 \cdot 10^3 - 2406.7 \cdot T \tag{4.64}$$

In this PhD study, the specific heat of vaporization of the water is estimated at the following hypothetical temperature conditions:

$$\Delta h_{fg} = \Delta h_{fg}(T_{evap}) \cong \Delta h_{fg}(T_{chill}) \tag{4.65}$$

Taking into account all the hypotheses and definitions previously mentioned, it can be concluded that the maximum practical COP depends on the following bed design parameters:

$$\mathrm{COP_{m,p}} = \mathrm{f}\left(\frac{\Delta h_{fg}}{\Delta h_{des}}, \Delta h_{des}, \overline{cp}_b, T_{heat}, T_{cool}, T_{chill}\right) \tag{4.66}$$

The effect of the design parameters mentioned above on the $\mathrm{COP_{m,p}}$ will be investigated will be investigated in subsection 4.5.3. Notice that the equivalent heat capacity of the bed per adsorbent mass $\overline{cp}_b$, given by Eq. (4.52), is a function of the following bed design parameters:

$$\overline{cp}_b = \mathrm{f}\left(cp_{met}, cp_{ads}, cp_w, \frac{m_{w,tot}}{m_{ads,HE}}, \frac{m_{met,tot}}{m_{ads,HE}}\right) \tag{4.67}$$

4.4.4.2. Maximum specific cooling capacity

The total heat given by the heating water to the bed in order to desorb the refrigerant along the heating period can be estimated as:

$$Q_{heat} = \int_D^{\tau} UA_{total,HE} \cdot (T_{heat} - T_b)\, dt \tag{4.68}$$

Assuming that the overall heat transfer coefficient is constant along the heating period, it follows that:

$$Q_{heat} = UA_{total,HE} \cdot \left(T_{heat} - \widetilde{T}_b\right) \cdot \frac{\tau}{2} \tag{4.69}$$

where $\widetilde{T}_b$ is the mean temperature of the bed which is defined as:

$$\widetilde{T}_b = \frac{\int_0^{\frac{\tau}{2}} T_b\, dt}{\frac{\tau}{2}} \tag{4.70}$$

It can be understood, with the help of Fig. 20(a), that the mean temperature of the bed $\widetilde{T}_b$ depends on the maximum and minimum temperatures of the bed ($T_{b,M}$ and $T_{b,m}$), and it should be more close to $T_{b,M}$ since the bed is in heating mode. However, in order to simplify the calculus it has been assumed that $\widetilde{T}_b$ is the arithmetic mean between the heating and cooling water temperatures. Hence,

$$\widetilde{T}_b \cong \frac{T_{b,M} + T_{b,m}}{2} \cong \frac{T_{heat} + T_{cool}}{2} \tag{4.71}$$

Substituting Eq. (4.71) into Eq. (4.69), it follows that

$$Q_{heat} \cong UA_{total,HE} \cdot \left(\frac{T_{heat} + T_{cool}}{2}\right) \cdot \frac{\tau}{2} \tag{4.72}$$

On the other hand, the maximum practical COP taking into account the heating/cooling losses can be also expressed as:

$$COP_{m,p} = \frac{m_{ads} \cdot \Delta w \cdot \Delta h_{fg}}{Q_{heat}} \tag{4.73}$$

Substituting Eq. (4.72) into Eq. (4.73) and rearranging, the following relation can be found:

$$UA_{total,HE} \cdot \left(\frac{T_{heat} + T_{cool}}{2}\right) \cdot \frac{\tau}{2} = \frac{m_{ads} \cdot \Delta w \cdot \Delta h_{fg}}{COP_{m,p}} \tag{4.74}$$

Taking into account that the same amount of water desorbed is fully condensed and then evaporated, the maximum cooling capacity of the system can be evaluated as:

$$\dot{Q}_{chill}\big|_{m,p} = \frac{m_{ads} \cdot \Delta w \cdot \Delta h_{fg}}{\tau} = \frac{1}{2} \cdot UA_{total,HE} \cdot \left(\frac{T_{heat} + T_{cool}}{2}\right) \cdot COP_{m,p} \tag{4.75}$$

The above equation relates the maximum cooling capacity with the maximum coefficient of performance that could be achieved in practice.

Finally, the maximum cooling capacity per volume of heat exchanger, named here as maximum specific cooling capacity, $SCC_{m,p}$, can be estimated as:

$$SCC_{m,p} = \left.\frac{\dot{Q}_{chill}}{V_{HE}}\right|_{m,p} \cong \frac{1}{2} \cdot \frac{UA_{total,HE}}{V_{HE}} \cdot \left(\frac{T_{heat} + T_{cool}}{2}\right) \cdot COP_{m,p} \qquad (4.76)$$

Therefore, it can be concluded that the $SCC_{m,p}$ depends on the following bed design parameters:

$$SCC_{m,p} = f\left(\frac{\Delta h_{fg}}{\Delta h_{des}}, \Delta h_{des}, \overline{cp}_b, T_{heat}, T_{cool}, T_{chill}, k_w, k_{ads}, k_{met}, p, \frac{t}{p}, \frac{pf}{p}, \frac{tf}{p}, \frac{e_{met}}{p}\right) \qquad (4.77)$$

The effect of the design parameters shown above on the $SCC_{m,p}$ will be investigated in subsections 4.5.2 and 4.5.3.

4.5. Parametric studies

4.5.1. Base-case design parameters

In this PhD study, several parametric studies have been carried out with reference to a specific bed configuration, which have been discussed before (see section 4.3). This configuration is defined here as the base-case bed. The effect of various design parameters on the specific thermal conductance and system performance has been investigated. This was done with the aim of finding the optimal design which will allow the system to reach the best heat transfer performance. Unless stated otherwise, all the parameters related to geometrical aspects of the base-case bed are listed on the top side of Table 5, whereas other parameters, concerning the employed adsorbent (i.e. silica gel),

metal (i.e. aluminium) and the heat transfer fluid (i.e. water) are listed on the bottom side of Table 5.

For the parametric studies, nominal air conditioning conditions (i.e. for typical summer conditions) have been considered: heating water temperature of 90 ºC, ambient temperature of 33 ºC and evaporating temperature of 15ºC.

Two basic assumptions have been made in this analysis. The major assumption is about the effective adsorbent thermal conductivity of the bed, which is very difficult to estimate and depends on many factors such as gas pressure, porosity, etc. According to the literature [92], the effective thermal conductivity of a granular adsorbent bed (including adsorbent grains plus interparticle voids) varies from 0.06 W m^{-1} K^{-1} in case of very loose grains, to 0.2 W m^{-1} K^{-1} in case of compacted grains. Taking into account the above, the mean value within this range has been assumed for the effective adsorbent thermal conductivity of the bed, e.g. 0.13 W m^{-1} K^{-1}.

The second assumption concerns the value of the water thermal conductivity. This parameter has been estimated for a water temperature of 61.5 ºC, since it corresponds to the average temperature between heating the bed at 90 ºC and cooling the bed at 33 ºC.

Table 5. Base-case parameters values.

Geometrical Parameters	**Value**	**Units**	**Ref.**
Channel Pitch, p	0.0067	m	-
Channel Thickness/Pitch Ratio, t/p	0.2537	-	-
Fin Pitch/Channel Pitch Ratio, p_f/p	0.2239	-	-
Fin Thickness/Channel Pitch Ratio, t_f/p	0.0149	-	-
Water Channel Wall Thickness/Pitch Ratio, e_{met}/p	0.0448	-	-
Thermal Parameters			
Water Thermal Conductivity at 61.5 ºC, k_w	0.656	$W\ m^{-1}\ K^{-1}$	[93]
Water Specific Heat Capacity, cp_w	4182	$J\ kg^{-1}\ K^{-1}$	[94]
Enthalpy of Vaporization at 15 ºC, Δh_v	2465.7E03	$J\ kg^{-1}$	-
Adsorbent Thermal Conductivity, k_{ads}	0.13	$W\ m^{-1}\ K^{-1}$	-
Dry Adsorbent Specific Heat Capacity, $cp_{ads,0}$	750	$J\ kg^{-1}\ K^{-1}$	[90]
Desorption Enthalpy, Δh_{des}	3115.9E03	$J\ kg^{-1}$	-
Metal Thermal Conductivity, k_{met}	160	$W\ m^{-1}\ K^{-1}$	[94]
Metal Specific Heat Capacity, cp_{met}	890	$J\ kg^{-1}\ K^{-1}$	[94]
Other Design Parameters:			
Metal/Adsorbent Mass Ratio: $m_{met,tot}/m_{ads,HE}$	1.3156	-	-
Water/Adsorbent Mass Ratio: $m_{w,tot}/m_{ads,HE}$	0.5241	-	-

4.5.2. Effect of the bed design parameters on the bed specific thermal conductance and maximum specific cooling capacity

In the present study, the effect of the design parameters such as p, t/p, p_f/p, t_f/p, e_{met}/p, k_{ads}, k_{met} and k_w on the specific thermal conductance and maximum specific cooling capacity ($SCC_{m,p}$) will be discussed (Fig. 22-30). By means of changing one of the parameters mentioned before and keeping all the other parameters constant, it was possible to study its influence on the heat transfer performance of the system. Unless stated otherwise, the base-case parameter values adopted in the parametric studies are the ones reported on Table 5. As it can be seen from Eq. (4.76), the maximum specific cooling capacity is proportional to the specific thermal conductance. This conclusion will be confirmed in the following subsection, and this is the reason why both parameters have been studied together.

4.5.2.1. Geometrical parameters

The base-case value for the channel pitch is 6.7 mm, and this study will include a variation of this parameter from approximately half to double this value: 3-12 mm. The effect of the channel pitch (p) of the heat exchanger on the specific thermal conductance of the bed and the maximum specific cooling capacity ($SCC_{m,p}$) is presented in Fig. 22. In this figure, all parameters except p remained constant, and are equal to their base-case values given in Table 5. It may be seen from Fig. 22 that the channel pitch strongly affects both specific thermal conductance and maximum specific cooling capacity. As the channel pitch increases, the specific thermal conductance and the maximum specific cooling capacity decrease. This can be explained by the fact that the total thermal resistance increases with the channel pitch because the conductive path length increases. Reducing the distance between the water channels enhances the heat transfer performance since the conduction through the adsorbent is poor. Hence, for closely spaced channels the heat will be quickly transferred, and consequently the conduction through the adsorbent will improve. Thus, the design efforts should be focused on reducing the channel pitch; however, it should be taken into consideration that the adsorbent granules must still be able to fit in between the channels. Significant performance improvements could be achieved with channel pitches smaller than 0.004 m. For example, by reducing the channel pitch from its design value (p=0.0067 m) to a minimum permissible value (e.g. p=0.004 m), may increase the specific thermal conductance and maximum specific cooling capacity by approximately 2.5 times its original value. The maximum specific cooling capacity ranges from 1199 (for p=0.0067) to 3363 kW/m^3 (for p=0.004). For this reason, the following parametric studies (Figs. 23-30) have been carried out for both the channel pitch design value (p=0.0067 m) and the reduced pitch value (p=0.004), in order to compare both performances. The red dots and green dots shown on Figs. 23-30 indicate the obtained results for the bed configuration which has been taken as reference (i.e. base-case bed) and for the reduced pitch bed, respectively.

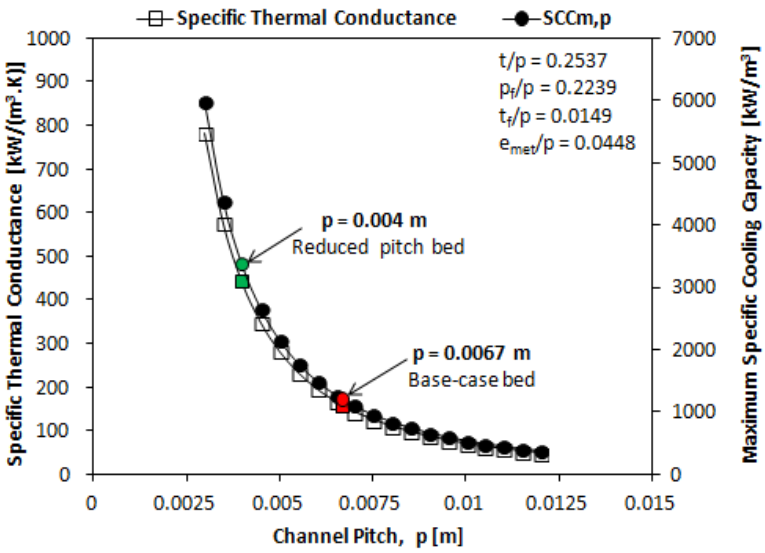

Fig. 22. Effect of p on specific thermal conductance of the bed and $SCC_{m,p}$.

The effect of the channel thickness/pitch ratio (t/p), which varies from 0.16 to 0.668, on the specific thermal conductance of the bed and the maximum specific cooling capacity is presented in Fig. 23. In this figure, all parameters except t/p remained constant and are equal to their base-case values, except p which corresponds to 0.0067 m (for base-case bed) in Fig. 23(a) and 0.004 m (for reduced pitch bed) in Fig. 23(b). It may be seen from Fig. 23 that the specific thermal conductance and maximum specific cooling capacity decrease as the channel thickness/pitch ratio increases, however, this variation is smoother than the previous one. This is due to the fact that reducing t/p enhances the convection heat transfer coefficient from the water side, and hence the overall heat transfer performance of the bed. Decreasing the channel thickness (t) by means of decreasing t/p results in an increase of the water velocity in the channels and hence a faster heat transfer rate from the water to the adsorbent. For the base-case bed, the maximum specific cooling capacity increases from 632 for a t/p of 0.668 to 1481 kW/m^3 for a t/p of 0.16, however, significant performance improvements could be achieved with a reduced pitch of 0.004 m. For the reduced pitch bed, the maximum specific cooling capacity increases from 1772 for a t/p of 0.668 to 4156 kW/m^3 for a t/p of 0.16, an improvement of more than 1.3 times of the original value.

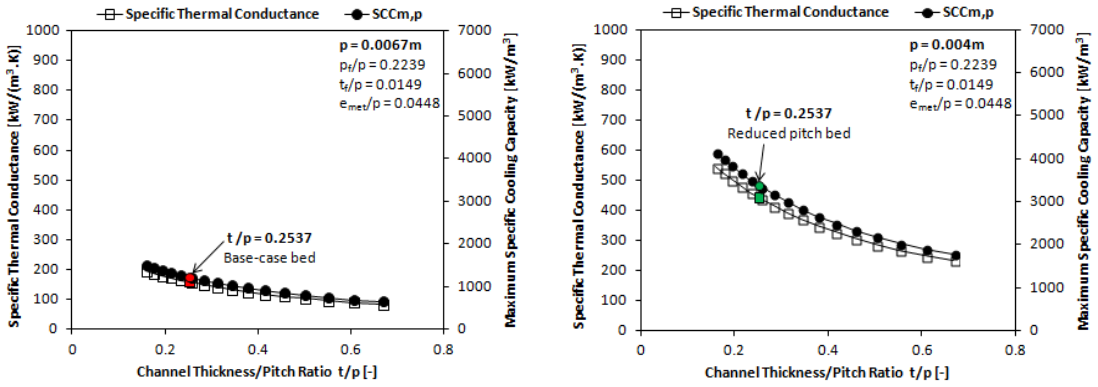

(a) (b)

Fig. 23. Effect of t/p on specific thermal conductance and $SCC_{m,p}$ for: (a) Base-case bed: p=0.0067 m; (b) Reduced pitch bed: p = 0.004 m.

The effect of the fin thickness/channel pitch ratio (t_f/p) in the studied range 0.005-0.0278, on the specific thermal conductance of the bed and the maximum specific cooling capacity is presented in Fig. 24. In this figure, all parameters except t_f/p remained constant, and are equal to their base-case values, except p which corresponds to 0.0067 m (base-case bed) in Fig. 24(a) and 0.004 m (reduced pitch bed) in Fig. 24(b). It may be seen from Fig. 24 that both specific thermal conductance and maximum specific cooling capacity slightly increase with the fin thickness/channel pitch ratio enhancement, however, it does not yield significant benefits. This can be explained by the fact that increasing the fin thickness (t_f) enhances the heat conduction along the fins improving the heat transfer to the adsorbent. Therefore, it is not convenient to decrease the fin thickness in order to accommodate more amount of adsorbent in the space between the fins, as it might decrease the temperature gradient through fins which would reflect in lower heat transfer rates from the fins to the adsorbent. For the base-case bed, the maximum specific cooling capacity increases from 1110 kW/m^3 for a t_f/p of 0.005 to 1258 kW/m^3 for a t_f/p of 0.0278, however, the performance could be significant enhanced with a reduced pitch of 0.004 m. In this case, the maximum specific cooling capacity increases from 3499 kW/m^3 for a t_f/p of 0.005 to 3966 kW/m^3 for a t_f/p of 0.0278, a 13.3 % of improvement.

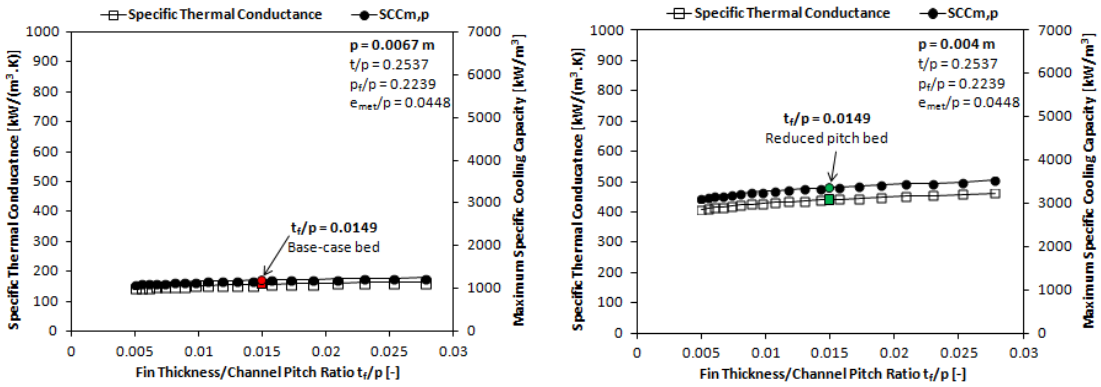

(a) (b)

Fig. 24. Effect of t_f/p on specific thermal conductance and $SCC_{m,p}$ for: (a) Base-case pitch: p=0.0067 m; (b) Reduced pitch: p = 0.004 m.

The effect of the fin pitch/channel pitch ratio (p_f/p), which varies from 0.1 to 0.555, on the specific thermal conductance of the bed and the maximum specific cooling capacity is presented in Fig. 25. In this figure, all parameters except p_f/p remained constant, and are equal to their base-case values, except p which corresponds to 0.0067 m (base-case bed) in Fig. 25(a) and 0.004 m (reduced pitch bed) in Fig. 25(b). It may be seen from Fig. 25 that the fin pitch/channel pitch ratio significantly affects both specific thermal conductance and the maximum specific cooling capacity. Decreasing p_f/p enhances the thermal conductance and the maximum specific cooling capacity. This can be explained by the fact that decreasing the fin pitch (p_f) by means of decreasing p_f/p results in increasing the number of fins, which will increase the heat transfer performance of the bed and hence the maximum specific cooling capacity. Thus, a better heat performance of the bed could be achieved by means of reducing the distance between the fins, however, a smaller adsorbent grain size must be considered in order to fit the adsorbent grains.

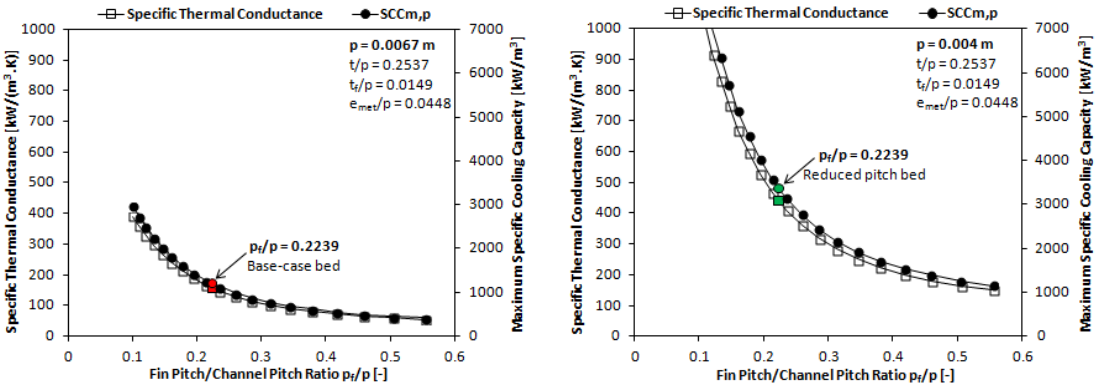

(a) (b)

Fig. 25. Effect of p_f/p on specific thermal conductance and $SCC_{m,p}$ for: (a) Base-case pitch: p=0.0067 m; (b) Reduced pitch: p = 0.004 m.

The effect of the water channel wall thickness/channel pitch ratio (e_{met}/p), which varies from 0.0298 to 0.0936, on the specific thermal conductance of the bed and maximum specific cooling capacity is presented in Fig. 26. In this figure, all parameters except e_{met}/p remained constant, and are equal to their base-case values, except p which corresponds to 0.0067 m (base-case bed) in Fig. 26(a) and 0.004 m (reduced pitch bed) in Fig. 26(b). It may be seen from Fig. 26 that the specific thermal conductance and maximum specific cooling capacity slightly increases as the water channel thickness/channel pitch ratio increases, however, it does not yield significant benefits. This may be explained by the fact that increasing the water channel wall thickness (e_{met}) enhances the water velocity in the channel for a fixed water mass flow rate, and hence the convection heat transfer coefficient from the water to the adsorbent. For the base-case bed, the maximum specific cooling capacity increases from 1150 kW/m^3 for a e_{met}/p of 0.0298 to 1391 kW/m^3 for a e_{met}/p of 0.0936, however, the enhancement with a reduced pitch of 0.004 m is much higher. In this case, the maximum specific cooling capacity increases from 3227 kW/m^3 for a e_{met}/p of 0.0298 to 3904 kW/m^3 for a e_{met}/p of 0.0936.

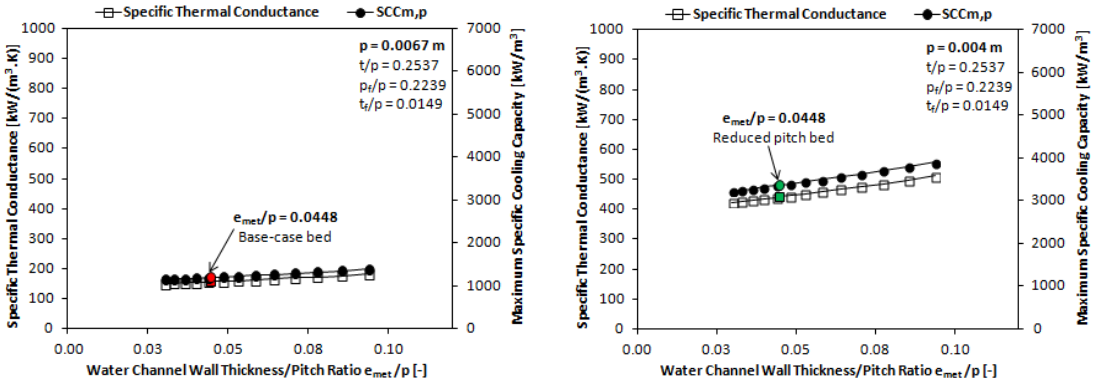

(a) (b)

Fig. 26. Effect of e_{met}/p on specific thermal conductance and $SCC_{m,p}$ for: (a) Base-case pitch: p=0.0067 m; (b) Reduced pitch: p = 0.004 m.

The combined effect of the t/p and p_f/p, which are the most important parameters affecting the specific thermal conductance of the bed, is presented in Fig. 27. This figure includes the base-case bed (p=0.0067) and the reduced pitch bed (p=0.004). It may be seen from Fig. 27 that the decreased t/p and p_f/p ratios positively affect the specific thermal conductance of the bed. Thus, decreasing t/p and p_f/p improves the specific thermal conductance of the bed. The effect is most apparent for t/p less than approximately 0.21 and p_f/p less than approximately 0.13. Fig. 27 suggests that there is a significant increase in specific thermal conductance for t/p less than 0.16 and pf/p less than 0.10. For the base-case bed, by decreasing the t/p and p_f/p from 0.25 and 0.22 to nearly 0.16 and 0.10, may increase the specific thermal conductance from 165 to 615 kW/m^3. However, higher performance improvements could be achieved with a reduced pitch of 0.004 m. In this case, by decreasing the t/p and p_f/p from 0.25 and 0.22 to nearly 0.16 and 0.10 may increase the specific thermal conductance from 463 to 1727 kW/m^3. This is a very significant improvement by almost three times its original value. Better performance for this type of bed could also be reached by significantly reducing the pitch, the water channel depth, and the fin pitch separation without affecting the equivalent adsorbent thermal conductivity. However, this would require a different technology for depositing the adsorbent between the fins.

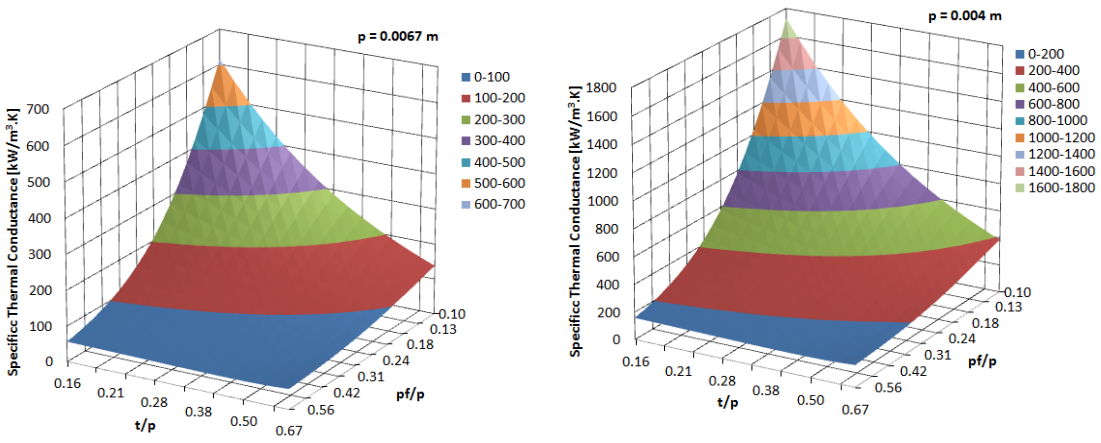

(a) (b)

Fig. 27. Effect of t/p and p_f/p on specific thermal conductance for: (a) Base-case bed: p=0.0067 m; (b) Reduced pitch: p = 0.004 m.

4.5.2.2. Thermal conductivity

The effect of the effective adsorbent thermal conductivity of the bed, which varies from 0.06 to 0.20 W m^{-1} K^{-1}, on the specific thermal conductance and maximum specific cooling capacity is presented in Fig. 28. In this figure, all parameters except the adsorbent thermal conductivity remained constant, and are equal to their base-case values, except p which corresponds to 0.0067 m (base-case bed) in Fig. 28(a) and 0.004 m (reduced pitch bed) in Fig. 28(b). It may be seen from Fig. 28 that the adsorbent thermal conductivity is a very sensitive parameter which positively affects the heat transfer performance. As expected, higher adsorbent thermal conductivity results in better the global performance. It has been found that an adsorbent thermal conductivity exceeding 0.15 W m^{-1} K^{-1} is desirable. The specific thermal conductance increases from 157 to 211.5 kW $m^{-3}.K^{-1}$ by increasing the adsorbent thermal conductivity from its design value, which corresponds to 0.13 W m^{-1} K^{-1} for the granular adsorbent bed under consideration, to 0.20 W m^{-1} K^{-1}. Obviously, the conduction through the adsorbent constitutes the major portion of the total thermal resistance in the bed. Hence, the design efforts should be focused on reducing the thermal resistance through the adsorbent. This could be achieved by mixing the adsorbent grains with metallic foam. This method may improve the heat transfer performance, since it will increase the adsorbent thermal

conductivity. Another method to improve the equivalent thermal conductivity of the bed is to decrease the intergranular porosity of the adsorbent by mixing together grains of various sizes [83]. Decreasing the intergranular porosity results in heat transfer improvement, since the vapour that surrounds the grains has low thermal conductivity.

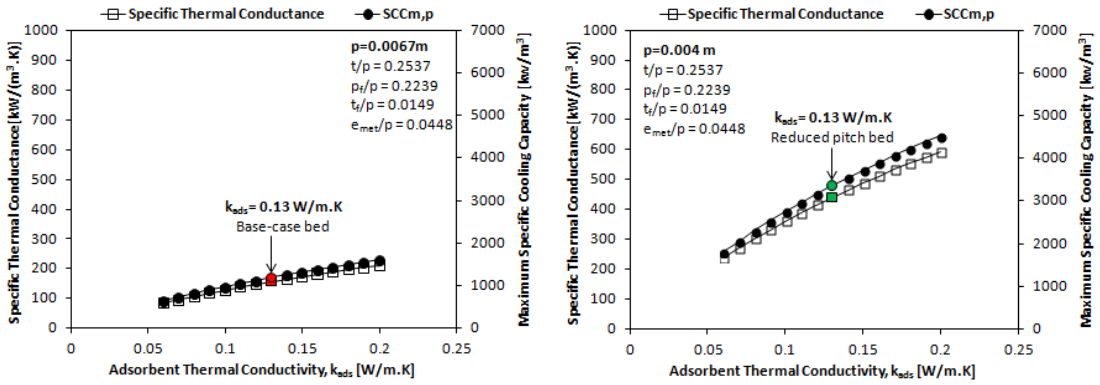

(a) (b)

Fig. 28. Effect of adsorbent thermal conductivity on specific thermal conductance and $SCC_{m,p}$ for: (a) Base-case pitch: p=0.0067 m; (b) Reduced pitch: p = 0.004 m.

The effect of the metal thermal conductivity of the bed, which varies from 20 to 400 W m^{-1} K^{-1}, on the specific thermal conductance of the bed and the maximum specific cooling capacity is presented in Fig. 29. In this figure, all parameters except the metal thermal conductivity remained constant, and are equal to their base-case values, except p which corresponds to 0.0067 m (base-case bed) in Fig. 29(a) and 0.004 m (reduced pitch bed) in Fig. 29(b). It may be seen from Fig. 29 that the metal thermal conductivity does not have a significant influence on the heat transfer performance. It has been found that a metal thermal conductivity of at least 140 W m^{-1} K^{-1} is desirable. Exceeding this value does not yield significant benefits. The specific thermal conductance just increases from 157 to 160 kW m^{-3} K^{-1} by increasing the metal thermal conductivity from its design value, which corresponds to 160 W m^{-1} K^{-1} for the aluminium used in the bed, to 400 W m^{-1} K^{-1}. Obviously, the plate-side conduction heat transfer resistance has a very small contribution on the total thermal resistance in the bed. Therefore, changing the metal material of the

heat exchanger from aluminium to copper, which has higher thermal conductance, will not result in a performance enhancement since its thermal capacitance its much larger and heat losses of alternative heating and cooling will increase. However, as observed before, the heat transfer performance of the bed and hence the maximum specific cooling capacity could be significantly improved by reducing the channel pitch from its design value to 0.004 m. In any case, it also can be seen that employing low conductivity materials like plastics could lead to an important loss of performance.

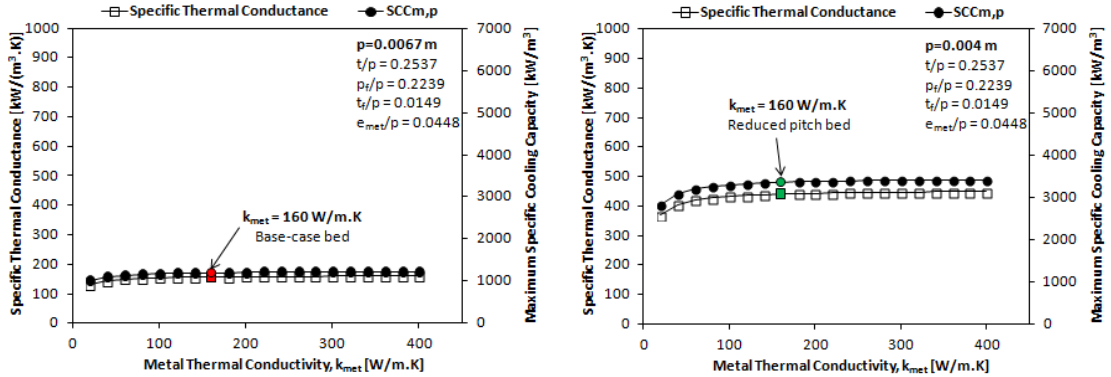

(a) (b)

Fig. 29. Effect of metal thermal conductivity on specific thermal conductance and $SCC_{m,p}$ for: (a) Base-case pitch: p=0.0067 m; (b) Reduced pitch: p = 0.004 m.

Finally, the effect of the heat transfer fluid thermal conductivity on the specific thermal conductance of the bed and the maximum specific cooling capacity, at different channel pitch values, is presented in Fig. 30. Two different heat transfer fluids have been analysed. The first one is pure water with thermal conductivity of 0.656 W m^{-1} K^{-1} at 66 ºC, which corresponds to the base-case, and the other one is a 30% ethylene glycol-water mixture with thermal conductivity of 0.5 W m^{-1} K^{-1} at 66 ºC [93]. It may be seen from Fig. 30 that the heat transfer fluid thermal conductivity does not have a significant influence on the performance. It is clear that fluid-side convection heat transfer resistance has a very small contribution on the total thermal resistance in the bed. Changing the heat transfer fluid from water to a mixture of glycol-water will result in a small decrease of the specific thermal conductance of the bed, and

hence on the temperature variation along the heat exchanger. Therefore, it will also have an influence on the actual heat transfer performance of the heat exchanger. This can be explained by the fact that the convective heat transfer coefficient of the fluid decreases with thermal conductivity, which results in lower heat transfer performance. On the other hand, an inappropriate increase of the convective heat transfer coefficient of the fluid due to fluid velocity increase (or the use of brine) could result in increased pressure losses in the channel. This would increase the pumping work, and therefore contribute negatively to the actual COP of the system.

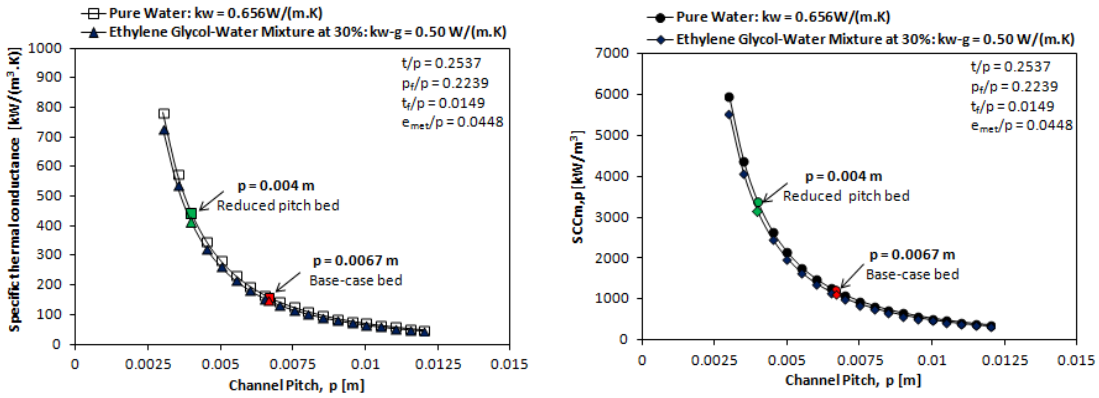

Fig. 30. Effect of the heat transfer fluid thermal conductivity values on: (a) Specific thermal conductance; (b) $SCC_{m,p}$.

4.5.3. Effect of the bed design parameters on the maximum system performance

In the present study, the effect of the design parameters such as Δh_{des}, $\frac{m_{w,tot}}{m_{ads,HE}}$, $\frac{m_{met,tot}}{m_{ads,HE}}$ and the operating temperatures on the maximum performance of the system in terms of $COP_{m,p}$ and $SCC_{m,p}$ will be discussed (Fig. 31-36). Unless stated otherwise, the base-case parameter values adopted in the parametric studies are reported on Table 5.

4.5.3.1. Desorption heat

The effect of the desorption heat on the $COP_{m,p}$ and $SCC_{m,p}$ is presented in Fig. 31. The maximum performance obtained for the Sorbsil A/water pair, which corresponds to the working pair used in the base-case bed, has been compared with other performances that may be achieved by using different working pairs. Several working pairs with different adsorption properties have been analysed and are reported on Table 6. The maximum and minimum uptakes as well as the desorption heat have been recalculated by using Eqs. (4.58) to (4.60) and Eq. (4.63), whose coefficients a, b have been taken from the literature [90, 92] for the working pairs under study. Moreover, the specific heat capacity considered for each adsorbent material has been taken from the literature [90, 92]. The equivalent thermal conductivity of the adsorbent has been assumed to be the same in all the cases and is equal to 0.13 $W.m^{-1}\ K^{-1}$. This is a strong assumption, which clearly affects the representative uncertainty of the obtained results.

Table 6. Adsorption properties for the working pairs under study.

Adsorbent	*Adsorbate*	$cp_{ads,0}$ [$J\ kg^{-1}\ K^{-1}$]	Δh_{des} [$kJ\ kg^{-1}$]	w_{min} [$kg\ kg^{-1}$]	w_{max} [$kg\ kg^{-1}$]	Δw [$kg\ kg^{-1}$]
Sorbsil A (silica gel)	water	750	3115.9	0.0205	0.1781	0.1576
SWS-1L (silica gel)	water	817	2610.4	0.1232	0.4554	0.3322
Zeolite 4A	water	980	7381.5	0.3449	0.3814	0.0365
FAM-Z02 (zeolite)	water	914	2795.1	0.0954	0.2996	0.2042

It may be seen from Fig. 31 that the desorption heat of the working pair has significant influence on the maximum performance of the system. The performance of the system increases with the decreasing of the desorption heat due to the fact that less heat input is required for the bed to absorb and adsorb the refrigerant. For example, changing the working pair used in the base-case bed, with desorption heat of 3115.9 kJ kg^{-1} with the SWS-1L/water pair, with desorption heat of 2610.4 kJ kg^{-1}, could increase both $COP_{m,p}$ and $SCC_{m,p}$ by approximately 38 %. For the base-case bed, the maximum practical COP is approximately 32% less than the maximum theoretical coefficient of performance defined according to literature [89] (see Eq. (4.53)) for the

reference operating conditions. Adsorbent/adsorbate pairs with higher desorption heat will result in a COP decrease due to higher heat losses. Therefore, it is convenient to choose a working pair with low desorption heat and low adsorbent specific heat capacity in order to reduce the heat losses. On the other hand, the adsorbent material should have good adsorption properties so that more amount of refrigerant is adsorbed/desorbed, and hence more cooling capacity is produced. The SWS-1L silica gel clearly demonstrates very good features for the application under study.

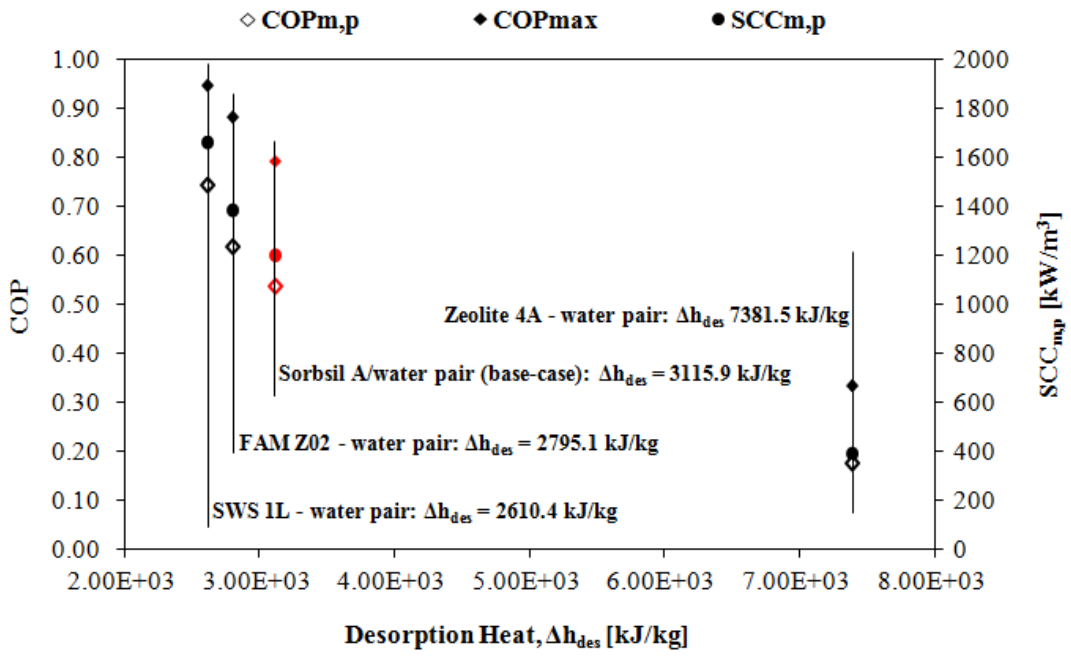

Fig. 31. Effect of the desorption heat for different adsorbent/adsorbate pairs on the maximum performance.

4.5.3.2. Heat transfer fluid/adsorbent mass ratio

The effect of the water/adsorbent mass ratio, which varies from 0.1 to 0.77 on the $COP_{m,p}$ and $SCC_{m,p}$ is presented in Fig. 32. It may be seen from Fig. 32 that the reduction of the water/adsorbent mass ratio positively affects both $COP_{m,p}$ and $SCC_{m,p}$. This can be easily explained by the fact that low amount of water in the heat exchanger requires less heat input for sensible heating the bed and hence increases the performance of the system. Therefore, the water/adsorbent

mass ratio should be kept as low as possible in order to avoid heat losses. This can only be accomplished by reducing the volume of the water channels and headers.

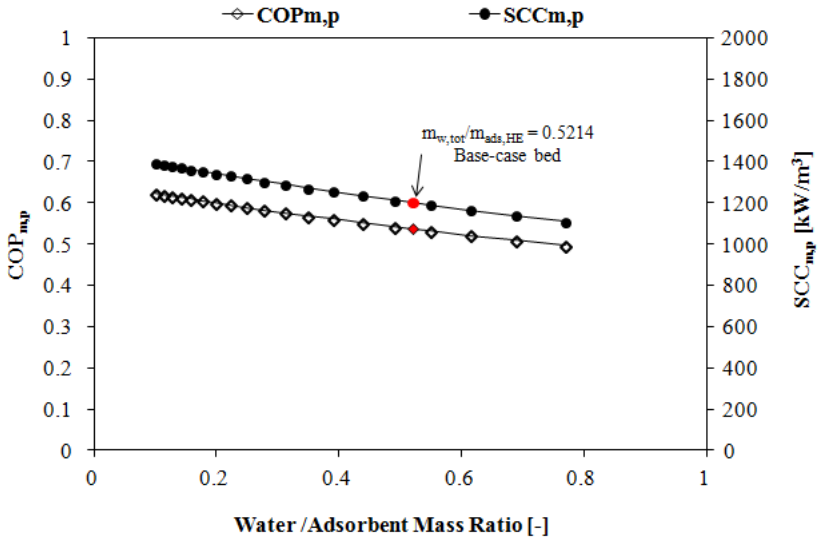

Fig. 32. Effect of the water/adsorbent mass ratio on the $COP_{m,p}$ and $SCC_{m,p}$.

4.5.3.3. Metal/adsorbent mass ratio

The effect of the water/adsorbent mass ratio, which varies from 0.1 to 2.66 on the $COP_{m,p}$ and $SCC_{m,p}$ is presented in Fig. 33. Decreasing the water/adsorbent mass ratio results in an increase of both $COP_{m,p}$ and $SCC_{m,p}$. The reason is that a small amount of metal requires relatively less heat input for heating the inert masses of the bed. In any case, by comparing Figs. 32 and 33, it can be seen that the effect of reducing the water mass is slightly higher than reducing the metal mass. Moreover, the performance of the system could be significantly enhanced by considering metal components and adsorbents for the bed manufacture that have low specific heat capacities in order to avoid heat losses and other energy losses associated to the alternate heating and cooling.

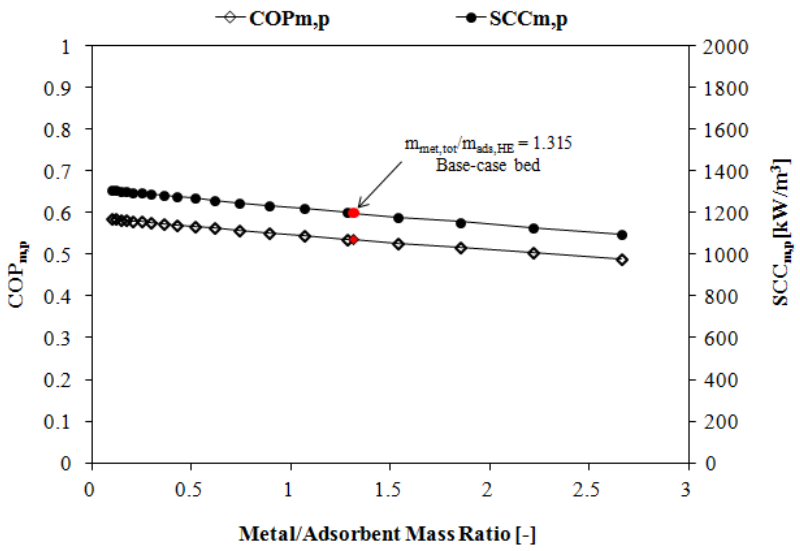

Fig. 33. Effect of the metal/adsorbent mass ratio on the $COP_{m,p}$ and $SCC_{m,p}$.

4.5.3.4. Operating temperatures

The effect of the heating water temperature, which varies from 70 to 120 ºC, on the maximum specific cooling capacity ($SCC_{m,p}$) and maximum coefficient of performance ($COP_{m,p}$) is presented in Fig. 34. As it can be seen from Fig. 34, the $SCC_{m,p}$ increases with higher heating water temperatures, however, the $COP_{m,p}$ of the system decreases. This can be explained by the fact that increasing the heating water temperature improves the cooling capacity due to enhancing the desorption rate. The negative effect of the heating water temperature increase on the $COP_{m,p}$ can be explained by the fact that more heat input is required for the bed to achieve a desired desorption temperature. Therefore, an optimum design should balance the increased cooling capacity due to higher heating water temperatures against the poorer $COP_{m,p}$ resulting from larger heat inputs. It seems that the $SCC_{m,p}$ is more sensitive to heating water temperature variations. For example, by increasing the heating water temperature from 70 to 120 ºC, the $COP_{m,p}$ decreases by 19.7 % from 0.57 to 0.46, but the $SCC_{m,p}$ increases by 88.7% from 836.5 to 1579 kW/m^3.

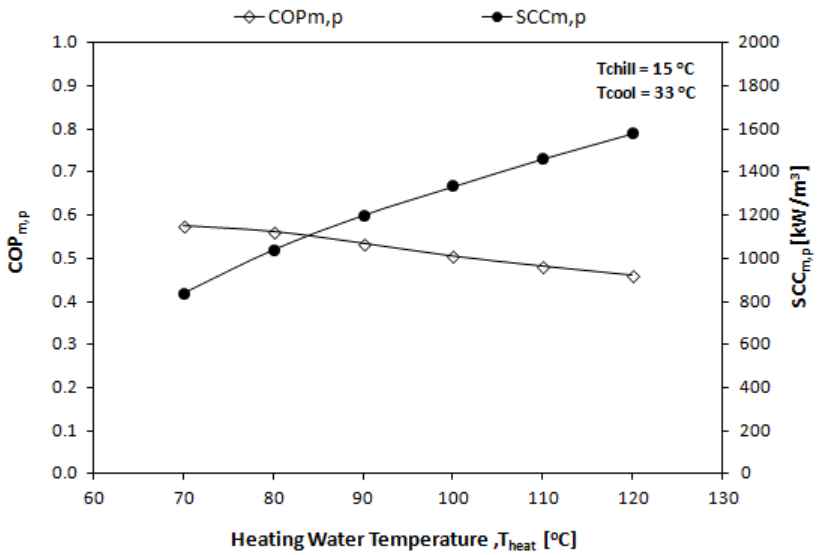

Fig. 34. Effect of the heating water temperature on the $COP_{m,p}$ and $SCC_{m,p}$.

The effect of the cooling water temperature variation from 20 to 40 ºC on the $SCC_{m,p}$ and $COP_{m,p}$ is presented in Fig. 35. As it can be seen from Fig. 35, lowering the cooling water temperatures not only increases the maximum specific cooling capacity but also increases the $COP_{m,p}$ of the system, due to the increase of the adsorption rate. This was something to be expected, as good adsorption rate means that more refrigerant is adsorbed/desorbed, and hence more energy is produced. The $SCC_{m,p}$ is more sensitive to cooling water temperature variations than $COP_{m,p}$. For example, by increasing the cooling water temperature from 20 to 40 ºC, the $COP_{m,p}$ decreases by 21.2 % from 0.58 to 0.45, while the $SCC_{m,p}$ by 43.70 % from 1588.3 to 894.1 kW/m^3. Taking into account that the lower the cooling water temperature, the higher is the cost of the heat rejection system, it should be designed to keep the maximum cooling temperature below 30 ºC.

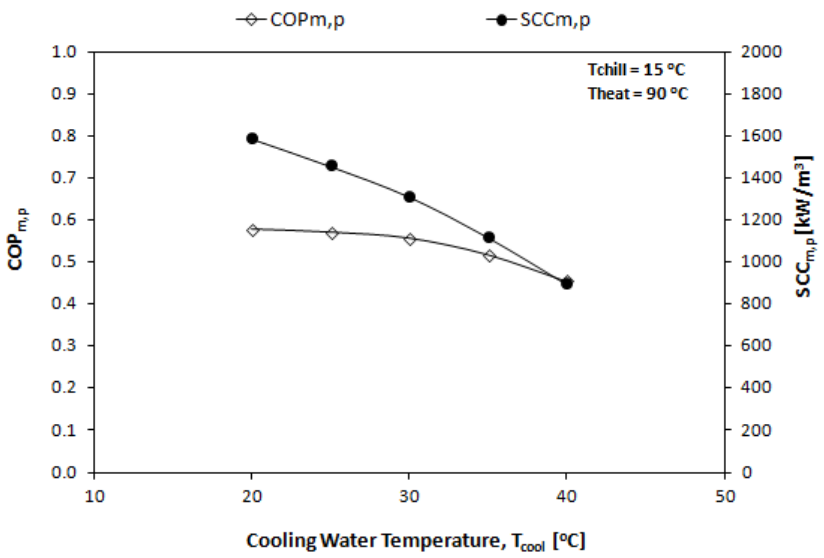

Fig. 35. Effect of the cooling water temperature on the $COP_{m,p}$ and $SCC_{m,p}$.

The effect of the chilled water temperature, which varies from 5 to 20 ºC on the $SCC_{m,p}$ and $COP_{m,p}$ is presented in Fig. 36. As it can be seen from Fig. 36, increasing the chilled water temperatures increases both $COP_{m,p}$ and $SCC_{m,p}$. As expected, both $COP_{m,p}$ and $SCC_{m,p}$ increase linearly when increasing the chilled water temperature. Decreasing the chilled water temperature results in less cooling energy produced, and therefore lower adsorption rates. For example, by decreasing the chilled water temperature from 20 to 5 ºC, both $COP_{m,p}$ and $SCC_{m,p}$ decreased by 28.9%. Each time the produced chilled water temperature decreases by 1 ºC, the system loses 0.011 of its $COP_{m,p}$ value.

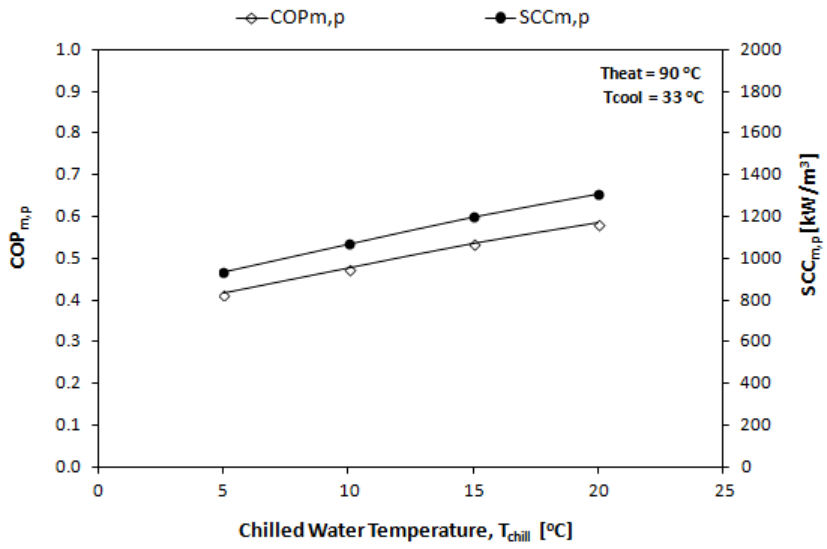

Fig. 36. Effect of the chilled water temperature on the $COP_{m,p}$ and $SCC_{m,p}$.

5. DESCRIPTION OF THE DYNAMIC MODEL

5.1. Introduction

In this chapter of the PhD study, a detailed and practical model of the silica gel-water adsorption cooling system that was developed in the framework of the Topmacs project [65] is presented. The adsorption cooling system in question was designed to be driven by waste heat coming from the engine coolant loop to cool the cabin of an automobile.

A non-equilibrium lumped parameter modelling approach has been employed for each component of the system, in such a way that they provide for a reasonable accuracy in the estimation of their performance, as well as a moderate calculation time.

As mentioned in chapter 1, many advanced models such as one-dimensional, two-dimensional and three-dimensional can be found in the literature [20, 45-48, 50, 53-62, 64]. However, in this PhD study, the main objective of the model is to reproduce the dynamic behaviour of the adsorption system and to predict accurately the overall performance of the system under different start-up conditions. Hence, due to the complexity of the system's application, advanced models cannot predict the dynamic behaviour of the entire system (engine, adsorption cooling system and cabin) under non-steady operating conditions. In this context, the general modelling approach is to use a zero-dimensional model (uniform temperature distribution in each operating unit at any instant) in order to simulate the dynamic behaviour of the entire system under real operating conditions.

The model of the adsorption system is completely dynamic and it is able to calculate the sequential operation of a double-bed adsorption chiller, calculate the condensation of the vapour at the condenser and the cooling effect produced at the evaporator. The governing equations are derived from the energy and mass balance for the various components of the system and by

using thermodynamic relationships. The form of these equations depends on whether the cycle step considered is a heating or a cooling step, and on the status of connection between the sorption bed and either the condenser/ evaporator, which is dictated by the internal pressure of these components. One difference between the presented model and the models appearing in the literature [7, 9, 20, 33-64] is that the flow between the components is based on the pressure difference between them. Also the pressure in the sorption bed is based on a state equation, as well as on mass conversation. This makes the model able to follow the full dynamics of the system. Moreover, different valve operation strategies or automatic operation (reed valves) could be analysed with the employed formulation model. In the following sections, the model equations and assumptions are presented, as well as the assumptions which have been made for each component of the system. Finally, the model has been validated by experimental data. The experimental tests were carried out on a lab-scale adsorption chiller prototype tested at the laboratories of the ECN research institute (Energy research Centre of the Netherlands, Petten, The Netherlands). Part of this study has been realized at ECN, where the PhD candidate acquired knowledge on measurement procedures.

5.2. Thermophysical properties of the adsorbent

5.2.1. Adsorption rate

A non-equilibrium adsorption/desorption process occurs in practical adsorption cooling systems. Therefore, a non-equilibrium model has been considered to describe the kinetic process of water adsorption on the adsorbent material (i.e. Sorbsil A silica gel). In this model, the adsorption rate, i.e. the change of water content in the packed bed with time, is expressed by the linear driving force (LDF) equation used by Sakoda et al. [51, 52] which takes into account the mass transfer resistance inside the packed bed. It has been assumed that the adsorption rate is proportional to the difference between the instantaneous uptake and the one that would be obtained at the equilibrium conditions. The water uptake (w) is defined as mass of adsorbed water per unit mass of dry

adsorbent [kg/kg]. Therefore, the adsorption rate, dw_b/dt , may be expressed in the following form [51]:

$$\frac{dw_b}{dt} = k_m\left(w_{eq} - w_b\right) \tag{5.1}$$

where w_{eq} is the adsorbed water uptake at equilibrium state at (T_b, P_b) and w_b is the adsorbed water uptake at the present state. The internal mass transfer coefficient, k_m , for adsorption is given by [51]:

$$k_m = \frac{15D_s}{{R_p}^2} \tag{5.2}$$

where R_p is the average radius of an adsorbent particle [m], and the surface diffusivity D_s is a function of the temperature [51]:

$$D_s = D_{s0} \cdot \exp\left(-\frac{E_a}{R \cdot T_b}\right) \tag{5.3}$$

where D_{s0} is a pre-exponent constant [m^2/s], E_a is the activation energy of surface diffusion [J/mol], R is the gas constant [J mol^{-1} K^{-1}] and T_b is the bed temperature [K].

Finally, Eqs. (5.2) to (5.3) may be combined and Eq. (5.1) simplified to:

$$\frac{dw_b}{dt} = k_1 \cdot e^{-k_2/T_b} \cdot \left(w_{eq} - w_b\right) \tag{5.4}$$

where

$$k_1 = \frac{15D_{s0}}{{R_p}^2} \tag{5.5}$$

$$k_2 = \frac{E_a}{R} \tag{5.6}$$

The values of the constants k_1 and k_2 depend on the nature of the adsorbent material and particle size. Unfortunately, it was not possible to estimate the constants k_1 and k_2 with sufficient accuracy because the required data for the kinetics of water adsorption on the adsorbent material under study (i.e. Sorbsil A silica gel) was not available in the literature. In order to resolve this issue, the constants k_1 and k_2 assume the values reported in the literature [7] for an adsorbent material with similar characteristics to the one considered. Then the Eq. (5.4) is multiplied by a correction factor in order to better fit the simulation results to the experimental data.

5.2.2. Adsorption equilibrium

The sorption properties of an adsorbent such as silica gel are determined by the water sorption isosteres, i.e. lines of constant water uptake as a function of the adsorbent temperature and water vapour pressure.

The adsorption equilibrium of water on the Sorbsil A silica gel has been experimentally characterized in a wide temperature and vapour pressure range at the laboratories of the CNR-ITAE research institute (Institute for Advanced Energy Technologies “Nicola Giordano” of the National Council of Research, Messina, Italy). The equilibrium data for the considered working pair can be represented by a set of isosteres. The isosteres in a diagram $\ln P$ versus $1/T$ are straight lines that may be represented in the form $\ln P = A(w) + B(w)/T$ [34], whose slopes are proportional to the enthalpy of adsorption and depend on the water content in the adsorbent (w). The isosteres of water adsorption on Sorbsil A in a Dühring diagram are shown in Fig. 37. The isosteres demonstrate the gradual decrease of the water uptake (w) with increasing adsorbent temperature (T) and reduction of water vapour pressure (P) (see, for instance, Fig. 37).

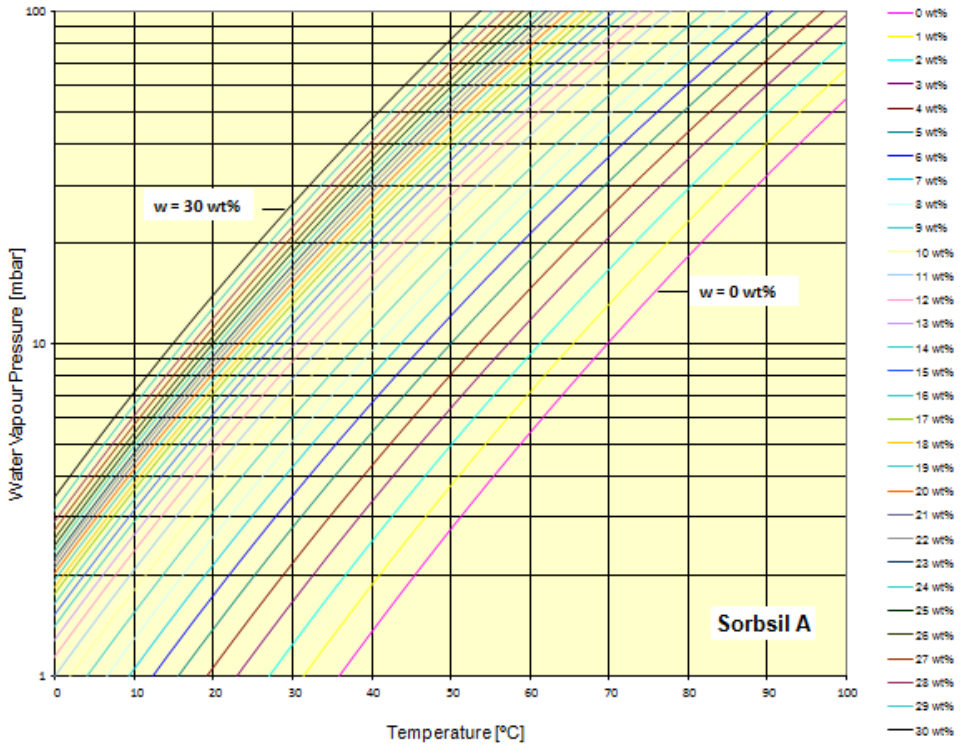

Fig. 37. Isosteres of sorption equilibrium of water vapour on Sorbsil A in a Dühring diagram.

Thus, the adsorption uptake at equilibrium conditions w_{eq} , in kg adsorbate / kg adsorbent, is estimated by the adsorption-equilibrium equation written in the following form [34]:

$$\ln P_b = A(w_{eq}) + \frac{B(w_{eq})}{T_b} \tag{5.7}$$

where P_b is the bed pressure [mbar] and T_b is the bed temperature [K]. The parameters A and B are characteristics of the adsorbent/adsorbate interaction and describe a set of isosteres.

Therefore, the parameters $A(w_{eq})$ and $B(w_{eq})$ in Eq. (5.7) are cubic polynomial functions defined as:

$$A(w_{eq}) = a_0 + a_1(w_{eq} \cdot 100) + a_2(w_{eq} \cdot 100)^2 + a_3(w_{eq} \cdot 100)^3 \tag{5.8}$$

$$B(w_{eq}) = b_0 + b_1(w_{eq} \cdot 100) + b_2(w_{eq} \cdot 100)^2 + b_3(w_{eq} \cdot 100)^3 \quad (5.9)$$

The numerical values of the coefficients a and b (i = 0, 1, 2, 3) are determined by a least squares fit to the experimental data for the silica gel / water pair under study, which can be found in Restuccia el al. [90].

5.2.3. Adsorption enthalpy

In this model, the adsorption enthalpy is not considered constant, as often occurs in the literature, but depends on the uptake. The adsorption enthalpy is a function of the amount of adsorbed water (w_b), and it is independent of the temperature. Thus, the isosteric enthalpy of adsorption Δh_{ad} (or alternatively the isosteric heat of adsorption), in J/kg, is defined by the following relationship [34]:

$$\Delta h_{ad}(w_b) = -(b_0 + b_1 w_b + b_2 {w_b}^2 + b_3 {w_b}^3) \cdot \frac{R}{M_w} \quad (5.10)$$

where R is the universal gas constant [J mol^{-1} K^{-1}], M_w is the water molar mass [kg/mol] and w_b is the water uptake at non-equilibrium conditions [kg/kg]. As mentioned previously, the numerical values of the coefficients b (i = 0, 1, 2, 3) can be found in the literature [90] for the silica gel/ water pair in question.

5.2.4. Equivalent specific heat of the adsorbent

The specific heat is an important property of the adsorbent as it provides information of the heat which is to be rejected or removed for a given temperature change in the adsorbent. However, a theoretical evaluation of the specific heat of the silica gel is not simple, as many different heat transfer mechanisms are involved in the porous adsorbent.

In this model, the equivalent specific heat of the adsorbent under study (i.e. Sorbsil A silica gel) has been considered constant with the temperature, and it only depends on the water uptake (w_b). Hence, the equivalent specific heat of the silica gel at different uptakes, in J kg^{-1} K^{-1}, is defined by the following equation [90]:

$$cp_{ads}(w_b) = \frac{cp_{ads,0} + cp_w \cdot w_b}{1 + w_b} \quad (5.11)$$

where $cp_{ads,0}$ is the specific heat of the dry adsorbent (750 J kg^{-1} K^{-1} for the silica gel) and cp_w is the specific heat of the liquid adsorbate (4190 J kg^{-1} K^{-1} for the water).

5.3. Thermodynamic properties of the refrigerant

The thermodynamic properties of the refrigerant (i.e. pure water), such as the latent heat of vaporization of the water (Δh_{fg}), the specific heat of the water vapour (cp_v) and the saturation temperature of the water (T_{sat}) are calculated by correlations presented in the following subsections, which have been taken from the literature [91].

5.3.1. Latent heat of vaporization

The specific heat of vaporization of the water Δh_{fg} is given by Eq. (4.64) which can be found in chapter 4 (see subsection 4.4.4.1).

5.3.2. Saturation temperature

The saturation temperature of the refrigerant, T_{sat}, in K, is estimated by the water liquid-vapour equilibrium equation:

$$\log(P) = c_0/T_{sat} + c_1 + c_2 \cdot T_{sat} + c_3 \cdot {T_{sat}}^2 + c_4 \cdot {T_{sat}}^3 + c_5 \cdot \log(T_{sat}) \quad (5.12)$$

where the numerical values of the constants c_i (i=0,1,2,3,4,5) are taken from the literature [91] for the refrigerant liquid-vapour equilibrium considered.

5.3.3. Specific heat of the vapour

The specific heat of the water vapour cp_v , in J kg^{-1} k^{-1}, can be expressed in the form:

$$cp_v(T) = CP_0 + CP_1 \cdot T + CP_2 \cdot T^2 + CP_3 \cdot T^3 + CP_4 \cdot T^4 + CP_5 \cdot T^5 \qquad (5.13)$$

where the coefficients CP_i (i=0,1,2,3,4,5) for the water vapour are reported in the literature [91].

5.4. Heat exchanger model

An alternative equation to the the standard NTU formulation has been developed to describe the heat exchanged between the system components and the heat transfer fluid (secondary water).

Since each component of the system is considered to be an instantaneous uniform temperature body, the standard NTU formulation can be employed to describe the heat transferred between the component in question (i.e. adsorbent bed heat exchanger, condenser, evaporator) and the heat transfer fluid under steady state conditions:

$$\dot{Q} = \varepsilon_{comp} \cdot \dot{m}_w \cdot cp_w \cdot (T_{w,i} - T_{comp}) \qquad (5.14)$$

where T_{comp} denotes the temperature of the component in question and $T_{w,i}$ denotes heat transfer fluid (water) temperature at the inlet conditions.

However, Eq. (5.14) only takes into account the temperature difference between the component and the heat transfer fluid at the inlet conditions. Under non-steady state, the heat transfer fluid temperature changes highly with the time. In

order to take into account the inlet and outlet temperatures of the heat transfer fluid, the basic equation for the sensible heat has been employed:

$$\dot{Q} = \dot{m}_w \cdot cp_w \cdot \left(T_{w,i} - T_{w,o}\right) \tag{5.15}$$

where $T_{w,i}$ and $T_{w,o}$ denotes inlet and outlet temperature of the heat transfer fluid (water).

The following approach has been developed by combining the Eq. (5.14), given by the standard NTU Method, with the Eq. (5.15):

$$\rightarrow \varepsilon_{comp} \cdot \dot{m}_w \cdot cp_w \cdot \left(T_{w,i} - T_{comp}\right) = \dot{m}_w \cdot cp_w \cdot \left(T_{w,i} - T_{w,o}\right) \tag{5.16}$$

The following equation can be employed to isolate the inlet temperature $T_{w,i}$ as a function of the outlet temperature $T_{w,o}$ and the effectiveness ε_{comp} :

$$T_{w,i} = \frac{T_{w,o} - \varepsilon_{comp} \cdot T_{comp}}{1 - \varepsilon_{comp}} \tag{5.17}$$

By substituting Eq. (5.17) in Eq. (5.14), the following equation is obtained:

$$\dot{Q} = \varepsilon_{comp} \cdot \dot{m}_w \cdot cp_w \cdot \left(\frac{T_{w,o} - T_{comp}}{1 - \varepsilon_{comp}}\right) \tag{5.18}$$

Eq. (5.18) provides a way to estimate the heat exchanged as a function of the temperature difference between the outlet temperature $T_{w,o}$ and the component temperature T_{comp}. Eq. (5.18) gives the same results as Eq. (5.14) under steady conditions. Furthermore, this guarantees that an average value between both equations is always valid for steady state conditions. So the following equation, which takes into account both inlet and outlet temperatures, is proposed:

$$\dot{Q} = \varepsilon_{comp} \cdot \dot{m}_w \cdot cp_w \cdot \left[\alpha \left(T_{w,i} - T_{comp}\right) + (1 - \alpha) \frac{\left(T_{w,o} - T_{comp}\right)}{\left(1 - \varepsilon_{comp}\right)}\right] \tag{5.19}$$

where ε_{comp} is the effectiveness of the component in question; $\dot{m}_w$ is the secondary water mass flow [kg/s]; T_{comp} is the temperature of the component; cp_w is the specific heat capacity of the water [J kg^{-1} K^{-1}] ; $T_{w,i}$ and $T_{w,o}$ are the inlet and outlet temperatures of the secondary water [K].

As the model is zero dimensional and includes no spatial variations of temperature, Eq. (5.19) is employed to account for the variations of temperature of the water along the component. The parameter α corresponds to the weighting factor of the temperature difference between the inlet and outlet water temperatures and the temperature of the component in question. This parameter was adjusted by comparing the numerical predictions with the experimental results. A value of α = 0.8, i.e. 80% of the inlet temperature difference and 20% of the outlet temperature difference was found to produce good results for a wide range of operating conditions.

The effectiveness of the component ε_{comp} could be chosen from the different cases of heat exchanger type and flow arrangements. However, as in the model it has been assumed that the secondary fluid has lower heat capacity than the component, and consequently that the component is only characterized by one single temperature T_{comp} , the convenient expression for the effectiveness is the one corresponding to the single stream heat exchanger [94]:

$$\varepsilon_{comp} = 1 - \exp(-NTU) = 1 - \exp\left(-\frac{UA_{comp}}{\dot{m}_w \cdot cp_w}\right) \tag{5.20}$$

where UA_{comp} is the overall thermal conductance of the component in question. Eq. (5.20) expresses the importance of heat transfer parameters, namely heat transfer area A and heat transfer coefficient U.

5.5. Sorption bed equations

5.5.1. Assumptions

The adsorption cooling system under study operate on an adsorption-desorption cycle which is carried out by two sorption beds that operate in counter-phase in order to allow a continuous useful cooling effect. As mentioned in chapter 3, each bed is composed of three tube-fin heat exchangers filled with adsorbent grains (silica gel) between the fins. The system is driven by a heat transfer fluid (secondary water), whose role is either to cool down or heat up the adsorbent particles, which in turn causes the heat exchanger to adsorb the refrigerant (water vapour) from the evaporator or to desorb the refrigerant to the condenser. Fig. 38 shows a design sketch of the modeled sorption bed. Fig. 39 shows a simplified schematic design of a single adsorbent bed heat exchanger. It is possible to recognize the main elements relevant to the model:

i. the heat transfer fluid (i.e. secondary water);
ii. the metal body of the heat exchanger which includes the fins and tubes;
iii. the porous adsorbent in the heat exchanger which is partially filled with water vapour in the empty spaces and liquid water in the adsorbed phase;
iv. the inlet and outlet headers of the bed, henceforth to be called inlet/outlet ports.

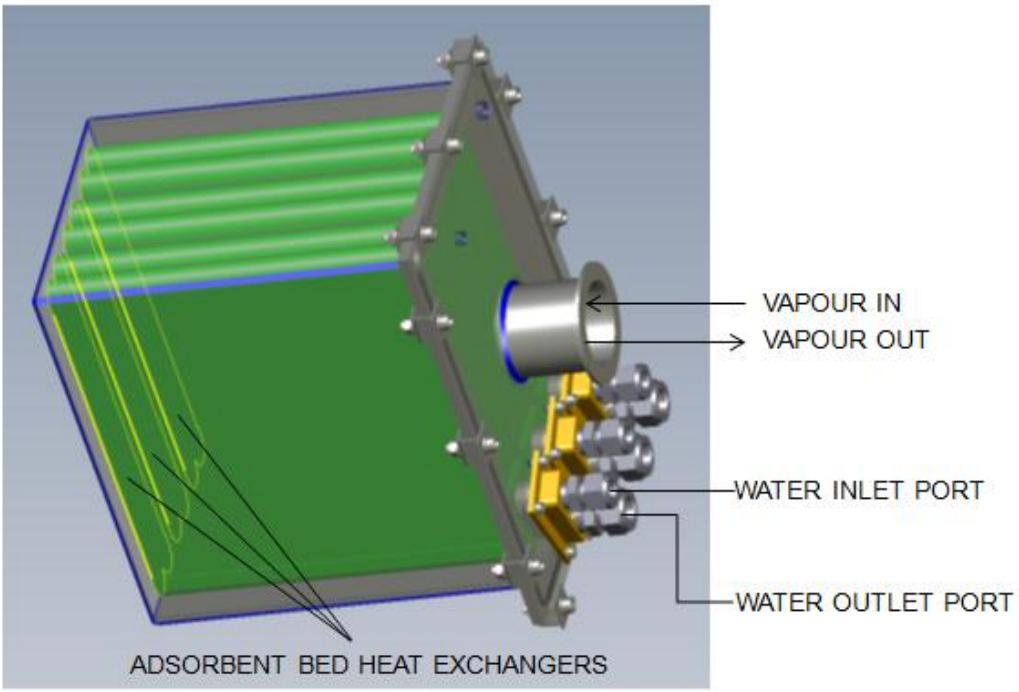

Fig. 38. Design sketch of the sorption bed under study.

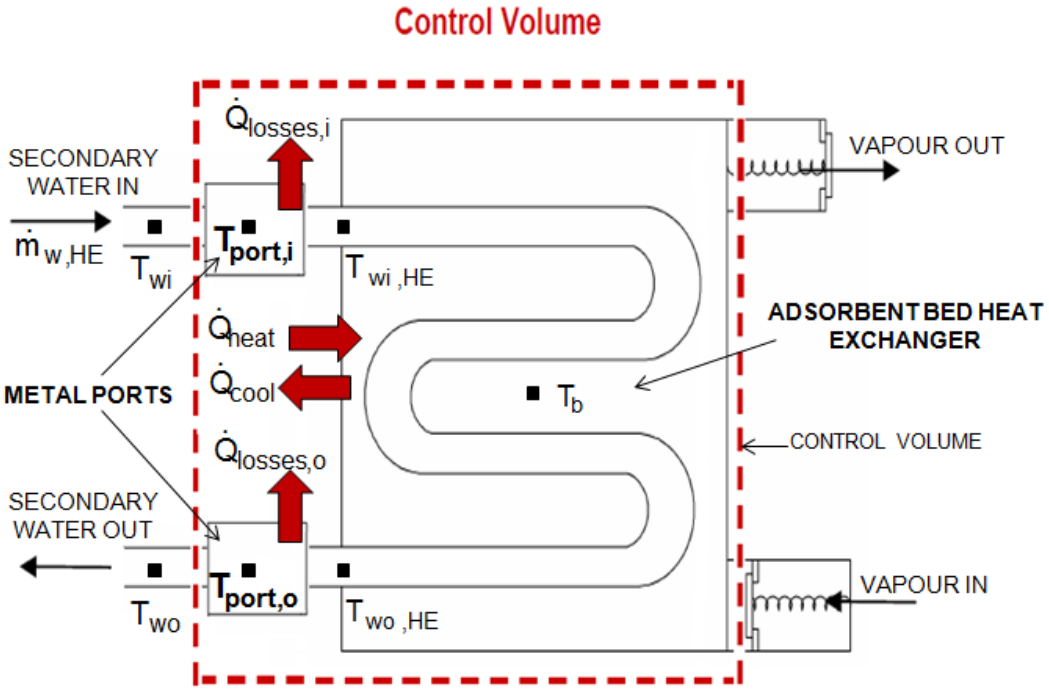

Fig. 39. Schematic design of the adsorbent bed heat exchanger basic elements.

The governing equations of the model describe the energy balance for all the elements mentioned above, and the mass transfer balance for the adsorbent

material, related to the vapour phase through the pores of the adsorbent. The energy balance applies to the control volume approach as illustrated in Fig. 39 by the dashed line, and it represents a single adsorbent bed heat exchanger plus the inlet and outlet ports.

In order to simplify the analysis, the following assumptions are made:

- As mentioned in subsection 5.1, the general modelling approach is the use of zero-dimensional models (uniform temperature distribution in each operating unit at any instant).

- The two sorption beds have identical thermo-physical, structural and geometric characteristics.

- The sorption bed has an empty space (due to particle porosity, clearance volume, etc.) which is partially filled with water vapour. Consequently, the pressure at the sorption bed depends on the instantaneous mass of vapour contained inside. The vapour pressure throughout the bed is uniform but varies with time.

- The temperature of the water vapour is calculated as the saturation temperature corresponding to the instantaneous pressure in the bed.

- The water vapour in the bed behaves as an ideal gas.

- The refrigerant (water vapour) is adsorbed uniformly in the sorption bed and is liquid in the adsorbent.

- The physical properties of all the metal parts are constant.

- The physical properties of the refrigerant (water vapour) as well as those of the adsorbent are considered to be temperature dependant, apart from the density of dry adsorbent which is considered constant.

- The flow of refrigerant (water vapour) among the beds, the condenser and the evaporator is governed by the pressure difference between these elements and the position of the valves.

- The heat/thermal losses during the heating and cooling of the inert masses of the bed such as the inlet/outlet metal ports and the metal body of the heat exchanger (including fins and tubes) are taken into consideration.

5.5.2. Energy balance for the sorption bed

Mass and heat balances are based on the assumption that both the temperature and the amount of refrigerant adsorbed are uniform in the sorption beds. Since the temperatures during the cycle period are not in a steady state, the energy balance equations must account for the sensible heat input or output. Hence, the energy equations for the sorption bed include sensible heat terms for the metallic parts, the refrigerant and the adsorbent material.

The energy balance on the bed control volume, represented in Fig. 39, yields:

$$C_{HE}\frac{dT_b}{dt} = m_{ads,HE}\cdot\frac{dw_b}{dt}\cdot\Delta h_{ad} - \left(\frac{\dot{m}_{v,i}}{N_{HE}}\right)\cdot cp_v\cdot\left(T_b - T_{evap}\right) + \dot{Q}_{heat/cool} \qquad (5.21)$$

where C_{HE} is the thermal capacity of the adsorbent bed heat exchanger [J/K] ; N_{HE} is the number of heat exchangers per bed; $m_{ads,HE}$ is the mass of dry adsorbent per heat exchanger [kg] ; $\dot{m}_{v,i}$ stands for the refrigerant mass flow from the evaporator to the bed during adsorption [kg/s]; w_b is the instantaneous uptake [kg/kg]; Δh_{ad} is the heat of adsorption [J/kg]; T_b is the bed temperature [K]; T_{evap} the evaporation temperature [K]; $\dot{Q}_{heat/cool}$ is the heat transferred between the secondary water and the adsorbent bed heat exchanger. Eq. (5.21) is valid for the bed in adsorption mode as well in desorption mode.

The term on the left-hand side of the bed energy balance equation (Eq. (5.21)) represents the amount of sensible heat required to cool or heat the adsorbent, the adsorbate as well as the metallic parts in the bed during adsorption and

desorption process. The first tem on the right-hand side of Eq. (5.21) refers to the heat due to the adsorption or desorption process, depending on the operation mode of the bed. The second term on the right-hand side of Eq. (5.21) represents the sensible heat of the adsorbed vapour, which is the sensible heat required to heat up the vapour from the evaporation temperature up to the bed temperature during adsorption. Finally, the third term on the right-hand side of Eq. (5.21) represents the total amount of heat released to the cooling water or provided by the heating water depending on the operation mode of the bed (cooling-adsorption/heating-desorption).

The thermal capacity of the adsorbent bed heat exchanger which includes the dry adsorbent, adsorbate and metallic parts can be estimated by the following equation:

$$C_{HE} = m_{ads,HE} \cdot (1 + w_b) \cdot cp_{ads} + m_{met,HE} \cdot cp_{met} \qquad (5.22)$$

where cp_{ads} is the equivalent specific heat of the adsorbent [J kg^{-1} K^{-1}]; cp_{met} is the specific heat capacity of the metal [J kg^{-1} K^{-1}]; $m_{ads,HE}$ is the mass of dry adsorbent per heat exchanger [kg] and $m_{met,HE}$ is the metal mass per heat exchanger [kg]. In Eq. (5.22), $m_{ads,HE} \cdot (1 + w_b)$ corresponds to the mass of wet adsorbent per adsorbent bed heat exchanger [kg].

The rate of heat transfer between the secondary water and the adsorbent bed heat exchanger $\dot{Q}_{heat/cool}$, in W, can be estimated by the following equation, as proposed in subsection 5.4:

$$\dot{Q}_{heat/cool} = \varepsilon_{HE} \cdot \dot{m}_{w,HE} \cdot cp_w \cdot \left[0.80 \cdot (T_{wi,HE} - T_b) + 0.20 \cdot \left(\frac{T_{wo,HE} - T_b}{1 - \varepsilon_{HE}}\right)\right] \qquad (5.23)$$

where ε_{HE} is the adsorbent bed heat exchanger effectiveness; $\dot{m}_{w,HE}$ is the secondary water mass flow (heating or cooling water) circulating through the adsorbent bed heat exchanger [kg/s]; cp_w is the specific heat capacity of the water [J kg^{-1} K^{-1}] ; $T_{wi,HE}$ and $T_{wo,HE}$ are the temperatures of the secondary water at the inlet and outlet of the adsorbent bed heat exchanger, respectively, in K.

The effectiveness of the adsorbent bed heat exchanger ε_{HE} is given by the following equation, as proposed in subsection 5.4:

$$\varepsilon_{HE} = 1 - \exp\left(-\frac{UA_{total,HE}}{\dot{m}_{w,HE} \cdot cp_w}\right) \quad (5.24)$$

where $UA_{total,HE}$ is the overall thermal conductance of the adsorbent bed heat exchanger [W/K]. An analytical model has been developed in order to estimate accurately the $UA_{total,HE}$ value, depending on the thermal and geometrical characteristics of the bed. A description of this model can be found in chapter 4.

The thermal losses to the inert masses due to the bed heating and cooling have been taken in consideration in the model. Therefore, the thermal masses of the inlet and outlet metal ports which connect the secondary water intake and outtake tubes to the heat exchanger have been taken in to account. The two ports are modelled as simple heat exchangers in series with the adsorbent bed heat exchanger. The following governing equations have been developed in order to calculate the temperature of the inlet and outlet ports and the temperature of the secondary water at the points located in the Fig. 39.

The temperature of the inlet metal port $T_{port,i}$, in K, can be estimated by the following equation:

$$C_{port,i} \frac{dT_{port,i}}{dt} = \dot{Q}_{losses,i} \quad (5.25)$$

where $C_{port,i}$ is the thermal capacity of the inlet port in J/K.

The term on the left-hand side of the Eq. (5.25) represents the sensible heat of the inlet metal port (excluding the secondary water). The term on the right-hand-side of Eq. (5.25) refers to the heat transferred from the cooling water or heating water entering the bed to the port (i.e. the metallic part of the inlet port).

The following equation, given in subsection 5.4, is used to estimate the rate of heat transferred between the secondary water and the inlet port $\dot{Q}_{losses,i}$:

$$\dot{Q}_{losses,i} = \dot{m}_{w,HE} \cdot cp_w \cdot \varepsilon_{port,i} \left[0.8 \cdot \left(T_{wi} - T_{port,i} \right) + 0.20 \cdot \frac{T_{wi,HE} - T_{port,i}}{1 - \varepsilon_{port,i}} \right] \quad (5.26)$$

where, $\varepsilon_{port,i}$ is the surface effectiveness of the inlet port; T_{wi} is the temperature of the secondary water entering the bed [K] ; $T_{wi,HE}$ is the temperature of the secondary water at the inlet of the adsorbent bed heat exchanger [K] and $T_{port,i}$ is the temperature of the inlet port [K].

The temperature of the outlet metal port $T_{port,o}$, in K, can be estimated by the following equation :

$$C_{port,o} \frac{dT_{port,o}}{dt} = \dot{Q}_{losses,o} \quad (5.27)$$

where, $C_{port,o}$ is the thermal capacity of the outlet port in J/K.

The term on the left-hand side of the Eq. (5.27) represents the sensible heat of the outlet metal port (excluding the secondary water). The term on the right-hand-side of Eq. (5.27) refers to the heat transferred from the cooling water or heating water leaving the bed to the port (i.e. the metallic parts of the outlet port).

The following equation, given in subsection 5.4, is used to estimate the rate of heat transferred between the secondary water and the outlet port $\dot{Q}_{losses,o}$:

$$\dot{Q}_{losses,o} = \dot{m}_{w,HE} \cdot cp_w \cdot \varepsilon_{port,o} \left[0.8 \cdot \left(T_{wo,HE} - T_{port,o} \right) + 0.20 \cdot \frac{T_{wo} - T_{port,o}}{1 - \varepsilon_{port,o}} \right] \quad (5.28)$$

where, $\varepsilon_{port,o}$ is the surface effectiveness of the outlet port; $T_{wo,HE}$ is the temperature of the secondary water at the outlet of the adsorbent bed heat

exchanger [K] ; T_{wo} is the temperature of the secondary water at the outlet of the bed [K] and $T_{port,o}$ is the temperature of the outlet port [K].

The temperatures of the secondary water at the inlet of the adsorbent bed heat exchanger $T_{wi,HE}$, in K, can be estimated by the following equation:

$$C_{wport,i}\frac{dT_{wi,HE}}{dt} = \dot{m}_{w,HE}\cdot cp_w\cdot\left(T_{wi}-T_{wi,HE}\right)-\dot{Q}_{losses,i} \qquad (5.29)$$

where, $C_{wport,i}$ is the thermal capacity of the secondary water inside the inlet port [J/K]; $\dot{m}_{w,HE}$ is the secondary water mass flow circulating through the adsorbent bed heat exchanger [Kg/s]; cp_w is the specific heat capacity of the water [J kg^{-1} K^{-1}]; T_{wi} is the secondary water temperature at the inlet of the bed [K]; $\dot{Q}_{losses,i}$ is the heat transferred between the secondary water entering the bed and the inlet metal port [W].

The term on the left-hand side of the Eq. (5.29) refers to the sensible heat of the water inside the inlet port. The first term on the right-hand side of Eq. (5.29) represents the enthalpy change of the water across the inlet port. Finally, the second term on the right-hand side of Eq. (5.29) represents the amount of heat transferred from the water entering the bed to the port (i.e. the metal part of the inlet port).

The temperature of the secondary water at the outlet of the adsorbent bed heat exchanger $T_{wo,HE}$, in K, can be estimated by the following equation :

$$C_{wHE}\frac{dT_{wo,HE}}{dt} = \dot{m}_{w,HE}\cdot cp_w\cdot\left(T_{wi,HE}-T_{wo,HE}\right)-\dot{Q}_{heat/cool} \qquad (5.30)$$

where, C_{wHE} is the thermal capacity of the secondary water inside the heat exchanger [J/K]; $\dot{m}_{w,HE}$ is the secondary water mass flow circulating through the heat exchanger [Kg/s]; cp_w is the specific heat capacity of the water [J kg^{-1} K^{-1}]; $T_{wi,HE}$ is the secondary water temperature at the inlet of the adsorbent bed heat

exchanger [K]; $\dot{Q}_{heat/cool}$ is the heat transferred between the secondary water and the adsorbent bed heat exchanger [W].

The term on the left-hand side of the Eq. (5.30) refers to the sensible heat of the water in the adsorbent bed heat exchanger. The first term on the right-hand side of Eq. (5.30) represents the enthalpy change of the water across the bed. Finally, the second term on the right-hand side of Eq. (5.30) represents the amount of heat transferred from the water to the bed (i.e. the adsorbent, the adsorbate and the metallic parts of the bed).

Finally, the temperature of the secondary water leaving the bed T_{wo} in K, can be estimated by the following equation:

$$C_{wport,o}\frac{dT_{wo}}{dt} = \dot{m}_{w,HE} \cdot cp_w \cdot \left(T_{wo,HE} - T_{wo}\right) - \dot{Q}_{losses,o} \qquad (5.31)$$

where, $C_{wport,o}$ is the thermal capacity of the secondary water inside the outlet port [J/K]; $\dot{m}_{w,HE}$ is the secondary water mass flow circulating through the heat exchanger [Kg/s]; cp_w is the specific heat capacity of the water [J kg^{-1} K^{-1}]; $T_{wo,HE}$ is the secondary water temperature at the outlet of the heat exchanger [K]; $\dot{Q}_{losses,o}$ is the heat transferred between the secondary water leaving the bed and the outlet port [W].

The term on the left-hand side of the Eq. (5.31) refers to the sensible heat of the secondary water inside the outlet port. The first term on the right-hand side of Eq. (5.31) represents the enthalpy change of the water flow across the outlet port. Finally, the second term on the right-hand side of Eq. (5.31) represents the amount of heat transferred from the water leaving the bed to the port (i.e. the metal part of the outlet port).

5.5.3. Mass balance for the sorption bed

Since the amount of refrigerant adsorbed is uniform in the bed, and there is an empty space partially filled with water vapour, the mass balance for the

refrigerant (water vapour) in the sorption bed, represented in Fig. 38, can be expressed as:

$$\frac{dm_{v,b}}{dt} = -m_{ads,b} \cdot \frac{dw_b}{dt} + \dot{m}_{v,i} - \dot{m}_{v,o} \tag{5.32}$$

where $m_{ads,b}$ is the total mass of dry adsorbent packed in each bed [kg]; $m_{v,b}$ is the total mass of vapour in the bed [kg]; $\dot{m}_{v,i}$ is the water vapour flow from the evaporator to the bed [kg/s] and $\dot{m}_{v,o}$ is the water vapour flow from the bed to the condenser [kg/s]. Eq. (5.32) provides the necessary link between the uptake variation in the bed (w_b) and the vapour flow rates leaving or entering the bed.

5.5.4. Pressure in the sorption bed

The pressure in the sorption bed is based on a state equation as well as mass conversation. Hence, the state equation for the water vapour inside the sorption bed can be described as:

$$P_b = P_a + P_v = \frac{R_v \cdot T_b}{V_{v,b}} \cdot \left(\frac{m_a}{M_a} + \frac{m_{v,b}}{M_w}\right) \tag{5.33}$$

where P_a is the pressure due to the non-condensable gases in the bed; P_v is the pressure due to the water vapour inside the bed; M_w is the water molar mass [kg/mol]; M_a is the molar mass of the non-condensable gases [kg/mol]; R is the universal gas constant [$mbar \cdot m^3 \cdot kg^{-1} \cdot K^{-1}$]; m_a is the non-condensable gases mass [kg]; $m_{v,b}$ is the water vapour mass in the bed [kg]; $V_{v,b}$ is the volume of water vapour in the bed [m^3].

As it has been assumed that the non-condensable gases have been totally removed from the bed, Eq. (5.33) can be simplified to:

$$P_b = \frac{R}{V_{v,b} \cdot M_w} \cdot (T_b \cdot m_{v,b}) \rightarrow dP_b = \frac{R}{V_{v,b} \cdot M_w} \cdot d(T_b \cdot m_{v,b}) \tag{5.34}$$

By the product rule, the differential equation for the pressure in the bed then results:

$$\rightarrow \frac{dP_b}{dt} = \frac{R}{V_{v,b} \cdot M_w} \cdot \frac{d}{dt}\left(T_b \cdot m_{v,b}\right) \leftrightarrow$$

$$\leftrightarrow \frac{dP_b}{dt} = \frac{R}{V_{v,b} \cdot M_w} \cdot \left(m_{v,b} \cdot \frac{dT_b}{dt} + T_b \cdot \frac{dm_{v,b}}{dt}\right) \leftrightarrow$$

$$\leftrightarrow \frac{dP_b}{dt} = \frac{R}{V_{v,b} \cdot M_w} \cdot \left[\left(m_{v,b} \cdot \frac{1}{T_b} \cdot T_b\right) \cdot \frac{dT_b}{dt} + \left(T_b \cdot m_{v,b} \cdot \frac{1}{m_{v,b}}\right) \cdot \frac{dm_{v,b}}{dt}\right] \leftrightarrow$$

$$\leftrightarrow \frac{1}{P_b} \cdot \frac{dP_b}{dt} = \frac{1}{T_b} \cdot \frac{dT_b}{dt} + \frac{1}{m_{v,b}} \cdot \frac{dm_{v,b}}{dt} \tag{5.35}$$

Finally, the differential equation for the pressure in the bed can be written as:

$$\frac{dP_b}{dt} = P_b \cdot \left(\frac{1}{T_b} \cdot \frac{dT_b}{dt} + \frac{1}{m_{v,b}} \cdot \frac{dm_{v,b}}{dt}\right) \tag{5.36}$$

5.5.5. Refrigerant flow and vapour valves operation strategy

As mentioned previously, the refrigerant (vapour) flow between the components is based on the pressure difference between them, which makes the model able to follow the full dynamics of the system. In order to calculate the vapour flow through the interconnecting pipes and valves and between the sorption beds, the condenser and the evaporator, the following assumptions have been considered:

- The vapour check valves are considered fully opened or fully closed, depending on the pressure difference. They are assumed to react instantaneously.

- The vapour valve connected between the bed and the condenser is only open when the pressure upstream is higher than the one at the condenser. Otherwise it remains closed.

- The vapour valve connected between the bed and the evaporator is only open when the pressure downstream is lower than in the evaporator. Otherwise it remains closed.

Consequently, the instantaneous refrigerant flow rate, $\dot{m}_{v,i}$ and $\dot{m}_{v,o}$, is estimated by means of the set of Eqs. (5.37) to (5.40):

$$\dot{m}_{v,o} = \begin{cases} 0 & (5.37) \quad \text{if} \quad P_b < P_{cond} \\ A_{cond} \cdot \sqrt{2 \cdot \rho_v(T_b, P_b) \cdot (P_b - P_{cond})} & (5.38) \quad \text{if} \quad P_b \geq P_{cond} \end{cases}$$

$$\dot{m}_{v,i} = \begin{cases} 0 & (5.39) \quad \text{if} \quad P_b > P_{evap} \\ A_{evap} \cdot \sqrt{2 \cdot \rho_v(T_{evap}, P_{evap}) \cdot (P_{evap} - P_b)} & (5.40) \quad \text{if} \quad P_b \leq P_{evap} \end{cases}$$

where A_{cond} and A_{evap} is the effective flow area of the vapour valves connected between the bed and the condenser or the evaporator, respectively [m^2]; ρ_v is the water vapour density at (T,P); P_b is the pressure in each bed [mbar]; P_{evap} is the evaporator pressure [mbar]; P_{cond} is the condenser pressure [mbar].

By solving the set of differential Eqs. (5.21) to (5.36) in time, the following unknowns are found for each bed: uptake distribution, w_b ; bed temperature, T_b ; inlet metal port temperature, $T_{port,i}$; outlet metal port temperature, $T_{port,o}$; water temperature at the inlet of the heat exchanger, $T_{wi,HE}$; water temperature at the outlet of the heat exchanger, $T_{wo,HE}$; water temperature at the outlet of the bed T_{wo} ; total mass of vapour in the bed, $m_{v,b}$; bed pressure, P_b. Furthermore, it is possible to calculate the refrigerant flow between the sorption beds and the evaporator/condenser according to the operation mode of the bed.

5.6. Condenser equations

5.6.1. Assumptions

The following governing equations (ODEs) describe the energy balance for the condenser and the mass balance for the refrigerant (water). Fig. 40 shows a schematic design of the modeled condenser.

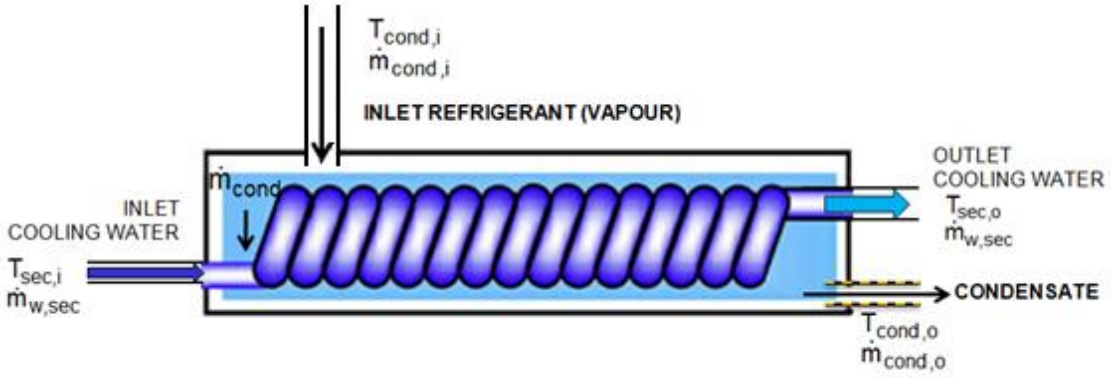

Fig. 40. Schematic design of the condenser under study.

In order to simplify the analysis, the following assumptions are made:

- The water vapour is assumed to be a perfect gas.

- Fluid is considered always in thermodynamic equilibrium corresponding to saturation conditions.

- Pressure is dependent on the amount of vapour existing in the top of the condenser. It is then assumed that temperature of the liquid condensing around the cold surfaces reacts instantaneously to the variation of pressure keeping it under saturation conditions. This assumption is perfectly reasonable for the condenser, since the water liquid film around the tube is very thin. It is also assumed that the amount of water liquid stored in the condenser is small. Therefore, the condenser temperature is calculated as

the saturation temperature corresponding to the instantaneous pressure of the condenser.

- It is assumed that the temperature of the liquid is the same as the condensation temperature at any time.

5.6.2. Energy balance for the condenser

During the desorption process, the condenser is connected to the bed where the refrigerant (desorbed vapour) can be condensed and delivered to the evaporator through an expansion valve. Since the refrigerant comes from the bed as vapour at higher temperature $T_{cond,i}$ and at the same pressure as in the condenser P_{cond}, the energy balance equation for the vapour region surrounding the condenser tubes can be expressed as follows:

$$\dot{Q}_C = \dot{m}_{cond} \cdot \left[cp_v \cdot \left(T_{cond,i} - T_{cond}\right) + \Delta h_{fg}(T_{cond})\right] \quad (5.41)$$

where $\dot{m}_{cond}$ is the condensation rate [kg/s]; $T_{cond,i}$ is the temperature of the refrigerant (vapour) from the bed to the condenser [K]; T_{cond} is the condensing temperature [K]; cp_v is the water vapour specific heat capacity [J kg^{-1} K^{-1}] and Δh_{fg} is the specific heat of vaporization at T_{cond} [J/kg].

The left-hand side of the condenser energy balance equation (Eq. (5.41)) represents the total amount of heat transferred to the heat transfer fluid (i.e. cooling water). The first term on the right-hand side of Eq. (5.41) represents the sensible heat of the vapour being cooled from the temperature of the refrigerant leaving the bed (desorbed vapour) to the temperature of condensation. The second term on the right-hand side of Eq. (5.41) represents the total amount of latent heat involved in the change of state from saturated vapour to saturated liquid.

Eq. (5.41) does not take into account the energy required for the variation of temperature for the condensed liquid. In any case, this amount is very small. A

trial to include such a term into the equations was attempted, but then a new ODE was deemed necessary, with strong coupling with the other equations. Unfortunately, no available solver was able to find the solution to the resulting system of equations. Anyhow, this term can be neglected since the instantaneous variation of the liquid temperature is very small. Accordingly, and in order to close the system of equations, it has been assumed that the liquid in the condenser follows the condensing temperature variations.

As commented above, the following expression is used to estimate the rate of heat released from the refrigerant to the secondary water, $\dot{Q}_C$, in W, as proposed in subsection 5.4:

$$\dot{Q}_C = -\varepsilon_{cond} \cdot \dot{m}_{w,sec} \cdot cp_w \cdot \left[0.80 \cdot \left(T_{sec,i} - T_{cond}\right) + 0.20 \cdot \left(\frac{T_{sec,o} - T_{cond}}{1 - \varepsilon_{cond}}\right)\right] \qquad (5.42)$$

where ε_{cond} is the condenser effectiveness; $\dot{m}_{w,sec}$ is the secondary water mass flow circulating through the condenser [Kg/s]; cp_w is the specific heat capacity of the water [J kg^{-1} K^{-1}]; $T_{sec,i}$ and $T_{sec,o}$ are the inlet and outlet temperatures of the condenser secondary water (i.e. condenser cooling water) [K].

Finally, the temperature of the secondary water at the outlet of the condenser $T_{sec,o}$, in K, can be estimated by the following equation:

$$C_{cond} \frac{dT_{sec,o}}{dt} = \dot{m}_{w,sec} \cdot cp_w \cdot \left(T_{sec,i} - T_{sec,o}\right) + \dot{Q}_C \qquad (5.43)$$

where, C_{cond} is the thermal capacity of the condenser (water included) [J/K]; $\dot{m}_{w,sec}$ is the cooling water mass flow circulating through the condenser [Kg/s]; cp_w is the heat capacity of the water [J kg^{-1} K^{-1}]; $T_{sec,i}$ and $T_{sec,o}$ are the inlet and outlet temperatures of the condenser secondary water (i.e. cooling water) in [K]; $\dot{Q}_C$ is the heat transferred from the refrigerant to the secondary water [W].

The term on the left-hand side of the equation (Eq. (5.43)) refers to the energy variation of the metallic tubes and secondary water in the condenser. The first term on the right-hand side of Eq. (5.43) represents enthalpy change of the water flow across the condenser. Finally, the second term on the right-hand side of Eq. (5.43) represents the amount of heat transferred from the water flow to the condenser.

5.6.3. Mass balance for the condenser

The mass balance equation for the vapour, which links the variation of vapour mass in the condenser with the incoming mass flow from the bed ($\dot{m}_{v,o}$) and the condensation rate ($\dot{m}_{cond}$) can be written as:

$$\frac{dm_{v,cond}}{dt} = \dot{m}_{cond,i} - \dot{m}_{cond} \tag{5.44}$$

where $\dot{m}_{cond,i}$ is the refrigerant flow entering the condenser which corresponds to the total flow of water vapour desorbed from the bed ($\dot{m}_{cond,i} = \dot{m}_{v,o}$), in kg/s, and $\dot{m}_{cond}$ is the condensation rate in kg/s.

The mass balance equation for the liquid in the condenser can be written as:

$$\frac{dm_{l,cond}}{dt} = \dot{m}_{cond} - \dot{m}_{cond,o} \tag{5.45}$$

where $m_{l,cond}$ is the mass of liquid water in the condenser [kg]; $\dot{m}_{cond}$ is the condensation rate [kg/s]; $\dot{m}_{cond,o}$ is the refrigerant (liquid water) flow from the condenser to the evaporator [kg/s].

Hence, the volume of liquid water in the condenser $V_{l,cond}$, in m^3, can be estimated as:

$$\frac{dV_{l,cond}}{dt} = \frac{1}{\rho_w}\frac{dm_{l,cond}}{dt} \rightarrow \frac{dV_{l,cond}}{dt} = \frac{\dot{m}_{cond} - \dot{m}_{cond,o}}{\rho_w} \quad (5.46)$$

Furthermore, the vapour volume comes from the variation of the liquid level in the condenser vessel. Finally, the following equation provides the link between the liquid volume ($V_{l,cond}$) and the vapour volume in the condenser ($V_{v,cond}$):

$$\frac{dV_{v,cond}}{dt} = -\frac{dV_{l,cond}}{dt} \quad (5.47)$$

5.6.4. Pressure in the condenser

The pressure in the condenser is based on state equation which provides a way to evaluate the variation of the pressure as a function of the vapour mass, vapour volume and temperature. Hence, the state equation for the water vapour inside the condenser can be described as:

$$P_{cond} = \frac{R \cdot T_{cond}}{V_{v,cond}} \cdot \frac{m_{v,cond}}{M_w} \rightarrow \frac{d}{dt}\left(P_{cond} \cdot V_{v,cond}\right) = \frac{R}{M_w} \cdot \frac{d}{dt}\left(T_{cond} \cdot m_{v,cond}\right) \quad (5.48)$$

where M_w is the water molar mass [kg/mol]; R is the universal gas constant [$mbar \cdot m^3 \cdot kg^{-1} \cdot K^{-1}$]; $m_{v,cond}$ is the water vapour mass in the condenser [kg]; $V_{v,cond}$ is the volume of water vapour in the condenser [m^3]; T_{cond} is the temperature in the condenser [K] ; is the pressure in condenser [mbar].

By the product rule, the Eq. (5.48) can be written as:

$$\frac{dP_{cond}}{dt} \cdot V_{v,cond} + P_{cond} \cdot \frac{dV_{v,cond}}{dt} = \frac{R}{M_v}\left(m_{v,cond} \cdot \frac{dT_{cond}}{dt} + T_{cond} \cdot \frac{dm_{v,cond}}{dt}\right) \quad (5.49)$$

Finally, the following differential equation for the pressure in the condenser is obtained:

$$\frac{dP_{cond}}{dt} = P_{cond}\left(\frac{1}{T_{cond}}\cdot\frac{dT_{cond}}{dt} + \frac{1}{m_{v,cond}}\cdot\frac{dm_{v,cond}}{dt} - \frac{1}{V_{v,cond}}\cdot\frac{dV_{v,cond}}{dt}\right) \quad (5.50)$$

Since the refrigerant (water vapour) inside the condenser is in a saturated state, the following equation provides a way to relate the temperature variation with the pressure in the condenser:

$$T_{cond} = T_{sat}(P_{cond}) \rightarrow \frac{dT_{cond}}{dt} = \frac{dT_{sat}(P_{cond})}{dP_{cond}}\cdot\frac{dP_{cond}}{dt} \quad (5.51)$$

Replacing Eq. (5.51) into Eq. (5.50) and rearranging the following equation is obtained:

$$\frac{dP_{cond}}{dt} = \frac{\frac{P_{cond}}{m_{v,cond}}\left(\frac{dm_{v,cond}}{dt}\right) - \frac{P_{cond}\left(\frac{dV_{v,cond}}{dt}\right)}{V_{v,cond}}}{1 - \frac{P_{cond}}{T_{cond}}\left(\frac{dT_{sat}}{dP_{cond}}\right)} \quad (5.52)$$

By solving the set of differential Eqs. (5.43) to (5.52) in time, the following unknowns are found for each bed: condenser pressure, P_{cond} ; mass of water vapour in the condenser, $m_{v,cond}$; volume of water vapour in the condenser, $V_{v,cond}$; secondary water temperature at the outlet of the condenser, $T_{sec,o}$. Furthermore, it is possible to calculate the condensation rate, the volume of the liquid in the condenser and the temperature in the condenser according to the saturation hypothesis.

5.7. Evaporator equations

5.7.1. Assumptions

The following governing equations (ODEs) describe the energy balance for the evaporator and the mass balance for the refrigerant (water). Fig. 41 shows a schematic design of the modeled evaporator.

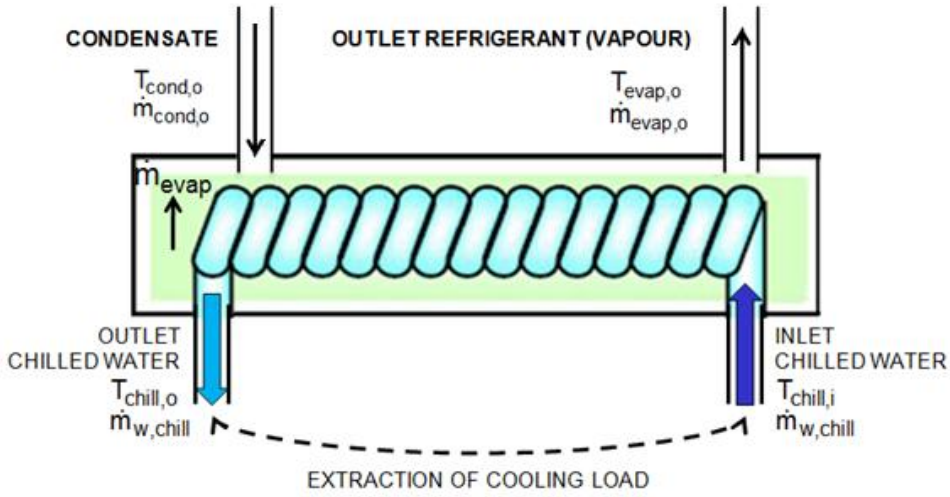

Fig. 41. Schematic design of the evaporator under study.

In order to simplify the analysis, the same assumptions valid for the condenser model have been considered for the evaporator:

- The water vapour is assumed to be a perfect gas

- Fluid is always considered in thermodynamic equilibrium corresponding to saturation conditions.

- Pressure is dependent on the amount of vapour existing in the top of the evaporator.

- The evaporator temperature is calculated as the saturation temperature corresponding to the instantaneous pressure in the evaporator. This hypothesis is maybe be less accurate for the evaporator since the amount of liquid in the evaporator could be higher than in the condenser. However, this simplification is justified since the pressure variations during the operation are rather small.

- The entire water flow rate coming from the condenser to the evaporator is instantly evaporated. In other words, it is assumed that there is an expansion device which keeps a constant liquid level at the evaporator, so that the amount of incoming liquid exactly balances the evaporation rate.

This means that the outlet water flow rate of the condenser is controlled by the evaporation rate: $\dot{m}_{cond,o} = \dot{m}_{evap}$.

5.7.2. Energy balance for the evaporator

Since the refrigerant enters the evaporator as liquid at higher pressure and temperature ($P_{cond,0}$, $T_{cond,o}$) , the energy balance equation for the refrigerant in the evaporator can be written as follows:

$$\dot{Q}_E = \dot{m}_{evap}\left[h_v(T_{evap}) - h_l(T_{cond,0})\right] \tag{5.53}$$

where $\dot{m}_{evap}$ is the evaporation rate [kg/s] ; h_v is the specific enthalpy of the vapour at T_{evap} [J/kg] ; h_l is the specific enthalpy of the liquid at $P_{cond,o}$ [J/kg].

And by assuming that:

$$h_l(T_{cond}) = h_l(T_{evap}) + cp_w(T_{cond,o} - T_{evap}) \tag{5.54}$$

Then, Eq. (5.53) can be rewritten as:

$$\dot{Q}_E = \dot{m}_{evap}\left[\Delta h_{fg}(T_{evap}) - cp_w(T_{cond,o} - T_{evap})\right] \tag{5.55}$$

where $\dot{m}_{evap}$ is the evaporation rate [kg/s] $T_{cond,o}$ is the temperature of the refrigerant (liquid water) entering the evaporator [K]; T_{evap} is the evaporator temperature [K], Δh_{fg} is the specific heat of vaporization at T_{evap} [J/kg].

The first term on the right-hand side of Eq. (5.55) represents the total amount of latent heat involved in the change of state from saturated liquid to saturated vapour. The second term on the right-hand side of Eq. (5.55) represents the sensible heat required to cool down the incoming condensate from the

condensation temperature to the evaporation temperature. Another important assumption is that the level of the liquid in the evaporator is held constant in order to maximize the heat transfer between the evaporator and the heat transfer fluid.

The following equation is used to estimate the rate of heat provided by the secondary water (i.e. chilled water) to the refrigerant, $\dot{Q}_E$, in W, as proposed in subsection 5.4 :

$$\dot{Q}_E = \varepsilon_{evap} \cdot \dot{m}_{w,chill} \cdot cp_w \cdot \left[0.80 \cdot \left(T_{chill,i} - T_{evap}\right) + 0.20 \cdot \left(\frac{T_{chill,o} - T_{evap}}{1 - \varepsilon_{evap}}\right)\right] \qquad (5.56)$$

where ε_{evap} is the evaporator effectiveness; $\dot{m}_{w,chill}$ is the chilled water mass flow [Kg/s]; cp_w is the specific heat capacity of the water [J kg^{-1} K^{-1}]; $T_{chill,i}$ and $T_{chill,o}$ are the inlet and outlet temperatures of the evaporator secondary water (i.e. chilled water) [K].

Finally, the temperature of the chilled water at the outlet of the evaporator $T_{chill,o}$, in K, can be estimated by the following equation:

$$C_{evap} \frac{dT_{chill,o}}{dt} = \dot{m}_{w,chill} \cdot cp_w \cdot \left(T_{chill,i} - T_{chill,o}\right) - \dot{Q}_E \qquad (5.57)$$

where, C_{evap} is the thermal capacity of the evaporator (metal mass and water included) [J/K] ; $\dot{m}_{w,chill}$ is the chilled water mass flow circulating through the evaporator [Kg/s] ; cp_w is the specific heat capacity of the water [J kg^{-1} K^{-1}] ; $T_{chill,i}$ and $T_{chill,o}$ are the inlet and outlet temperatures of the chilled water [K] ; $\dot{Q}_E$ is the heat transferred from the chilled water to the refrigerant [W].

The term on the left-hand side of the equation (Eq. (5.57)) refers to the temporal variation of the internal energy contained in the metal tubes and the water mass in the evaporator. The first term on the right-hand side of Eq. (5.57) represents the amount of sensible heat provided by the secondary water. Finally, the

second term on the right-hand side of Eq. (5.57) refers to the total amount of heat exchanged with the refrigerant.

5.7.3. Mass balance for the evaporator

The mass balance equation for the vapour, which links the variation of vapour mass in the evaporator with the outcoming mass flow from the evaporator ($\dot{m}_{evap,o}$) and the evaporation rate ($\dot{m}_{evap}$) can be written as:

$$\frac{dm_{v,evap}}{dt} = \dot{m}_{evap} - \dot{m}_{evap,o} \tag{5.58}$$

where $\dot{m}_{evap}$ is the evaporation rate, in kg/s, and $\dot{m}_{evap,o}$ is the refrigerant flow leaving the evaporator which corresponds to the total flow of vapour adsorbed by the bed ($\dot{m}_{evap,o} = \dot{m}_{v,i}$), in kg/s.

Furthermore, the volume of liquid water in the evaporator $V_{l,evap}$, in m^3, can be estimated as:

$$\frac{dV_{l,evap}}{dt} = \frac{1}{\rho_w}\frac{dm_{l,evap}}{dt} \rightarrow \tag{5.59}$$

$$\rightarrow \frac{dV_{l,evap}}{dt} = \frac{\dot{m}_{cond,o} - \dot{m}_{evap}}{\rho_w} \tag{5.60}$$

Since the vapour volume comes from the variation of the liquid level in the evaporator, the following equation is used to estimate the volume variation of the water vapour in the evaporator, $V_{v,evap}$:

$$\frac{dV_{v,evap}}{dt} = -\frac{dV_{l,evap}}{dt} \rightarrow \tag{5.61}$$

$$\rightarrow \frac{dV_{v,evap}}{dt} = \frac{\dot{m}_{evap} - \dot{m}_{cond,o}}{\rho_w} \quad (5.62)$$

where $\dot{m}_{evap}$ corresponds to the evaporation rate and $\dot{m}_{cond,o}$ is the refrigerant (liquid water) flow from the condenser to the evaporator. As it has been assumed that the entire water flow coming from the condenser to the evaporator is instantly evaporated ($\dot{m}_{cond,o} = \dot{m}_{evap}$), the variation of vapour volume in the evaporator, given by Eq. (5.62), is zero.

5.7.4. Pressure in the evaporator

The pressure in the evaporator is based on state equation which provides a way to evaluate the variation of the pressure as a function of the vapour mass, vapour volume and temperature. Hence, the state equation for the water vapour inside the evaporator can be described as:

$$P_{evap} = \frac{R \cdot T_{evap}}{V_{v,evap}} \cdot \frac{m_{v,evap}}{M_w} \rightarrow \frac{d}{dt}\left(P_{evap} \cdot V_{v,evap}\right) = \frac{R}{M_w} \cdot \frac{d}{dt}\left(T_{evap} \cdot m_{v,evap}\right) \quad (5.63)$$

where M_w is the water molar mass [kg/mol]; R is the universal gas constant [$mbar \cdot m^3 \cdot kg^{-1} \cdot K^{-1}$]; $m_{v,evap}$ is the water vapour mass in the evaporator [kg]; T_{evap} is the temperature in the evaporator [K]; P_{evap} is the pressure in the evaporator [mbar].

By the product rule, the Eq. (5.63) can be written as:

$$\frac{dP_{evap}}{dt} = P_{evap}\left(\frac{1}{T_{evap}} \cdot \frac{dT_{evap}}{dt} + \frac{1}{m_{v,evap}} \cdot \frac{dm_{v,evap}}{dt} - \frac{1}{V_{v,evap}} \cdot \frac{dV_{v,evap}}{dt}\right) \quad (5.64)$$

As it has been assumed that the level of the liquid in the evaporator is held constant in order to maximize the heat transfer between the evaporator and the heat transfer fluid, the Eq. (5.64) can be simplified to:

$$\frac{dP_{evap}}{dt} = P_{evap}\left(\frac{1}{T_{evap}} \cdot \frac{dT_{evap}}{dt} + \frac{1}{m_{v,evap}} \cdot \frac{dm_{v,evap}}{dt}\right) \quad (5.65)$$

Since the refrigerant (water vapour) inside the evaporator is in a saturated state, the following equation provides a way to relate the variation of the temperature with the pressure in the evaporator:

$$T_{evap} = T_{sat}(P_{evap}) \rightarrow \frac{dT_{evap}}{dt} = \frac{dT_{sat}(P_{evap})}{dP_{evap}} \cdot \frac{dP_{evap}}{dt} \quad (5.66)$$

Replacing Eq. (5.66) into Eq. (5.65) and rearranging, the following differential equation for the pressure in the evaporator is obtained:

$$\frac{dP_{evap}}{dt} = \frac{\frac{P_{evap}}{m_{v,evap}}\left(\frac{dm_{v,evap}}{dt}\right)}{1 - \frac{P_{evap}}{T_{evap}}\left(\frac{dT_{sat}}{dP_{evap}}\right)} \quad (5.67)$$

By solving the set of differential Eqs. (5.57) to (5.67) in time, the following unknowns are found for each bed: pressure in the evaporator, P_{evap} ; mass of water vapour in the evaporator, $m_{v,evap}$; volume of water vapour in the evaporator, $V_{v,evap}$; chilled water temperature at the outlet of the evaporator, $T_{chill,o}$. Furthermore, it is possible to calculate the evaporation rate, the volume of the liquid in the evaporator and the temperature in the evaporator accordingly with the saturation hypothesis.

5.8. System Performance

The model proposed in this PhD study is able to calculate the amounts of heat exchanged in each component and, consequently, the performance of the adsorption cooling system. The performance of the adsorption system under study is characterized by the cooling effect produced at the evaporator (Q_{chill}) and the coefficient of performance (COP).

5.8.1. Cooling capacity of the system

The cooling capacity of the adsorption cooling system $\dot{Q}_{chill}$, in W, is given by the following equation:

$$\dot{Q}_{chill} = \dot{m}_{w,chill} \cdot cp_w \cdot \int_0^{t_{cycle}} \left(T_{chill,i} - T_{chill,o}\right) dt \qquad (5.68)$$

where $\dot{m}_{w,chill}$ is the chilled water flow [kg/s]; $T_{chill,i}$ is the inlet chilled water temperature [K]; $T_{chill,o}$ is the outlet chilled water temperature [K]; τ_{cycle} is the cycle time.

5.8.2. Condenser capacity

The condenser capacity $\dot{Q}_{cond}$, in W, is given by the following equation:

$$\dot{Q}_{cond} = -\dot{m}_{w,sec} \cdot cp_w \cdot \int_0^{\tau_{cycle}} \left(T_{sec,i} - T_{sec,o}\right) dt \qquad (5.69)$$

where $\dot{m}_{w,sec}$ is the condenser secondary water flow [kg/s]; $T_{sec,i}$ is the inlet condenser cooling water temperature [K]; $T_{sec,o}$ is the outlet condenser cooling water temperature [K]; τ_{cycle} is the cycle time.

5.8.3. Heating capacity of the bed

The heating capacity of the bed $\dot{Q}_{heat}$, in W, is given by the following equation:

$$\dot{Q}_{heat} = \dot{m}_{hw,b} \cdot cp_w \cdot \int_0^{\tau_{cycle}} \left(T_{hw,i} - T_{hw,o}\right) dt \qquad (5.70)$$

where $\dot{m}_{hw,b}$ is the heating water mass flow circulating through the bed [kg/s]; $T_{hw,i}$ is the inlet heating water temperature [K] ; $T_{hw,o}$ is the outlet heating water temperature [K]; τ_{cycle} is the cycle time.

5.8.4. Cooling capacity of the bed

The cooling capacity of the bed $\dot{Q}_{cool}$, in W, is given by the following equation:

$$\dot{Q}_{cool} = -\dot{m}_{cw,b} \cdot cp_w \cdot \int_0^{\tau_{cycle}} \left(T_{cw,i} - T_{cw,o}\right) dt \qquad (5.71)$$

where $\dot{m}_{cw,b}$ is the cooling water mass flow circulating through the bed [kg/s] ; $T_{cw,i}$ is the temperature of the cooling water entering the bed [K] ; $T_{cw,o}$ is the temperature of the cooling water leaving the bed [K]; τ_{cycle} is the cycle time.

5.8.5. Coefficient of performance

The coefficient of performance of the adsorption cooling system is given by the following equation:

$$COP = \frac{\dot{Q}_{chill}}{\dot{Q}_{heat}} = \frac{\dot{m}_{w,chill} \cdot cp_w \cdot \int_0^{\tau_{cycle}} \left(T_{chill,i} - T_{chill,o}\right) dt}{\dot{m}_{hw,b} \cdot cp_w \cdot \int_0^{\tau_{cycle}} \left(T_{hw,i} - T_{hw,o}\right) dt} \qquad (5.72)$$

5.9. Numerical solver

The system of first-order ordinary differential equations (ODEs) mentioned above was implemented in MATLAB® as an S-Function and solved dynamically in Simulink® by the solver ode23tb (stiff/TR-BDF2). The solver uses a method from the Runge-Kutta family to solve the system of ODEs and it gives accurate solutions with high speed of convergence.

Fig. 42 shows a simplified structure of the adsorption cooling system model. The model requires a set of inputs, a set of state variables, and a set of outputs.

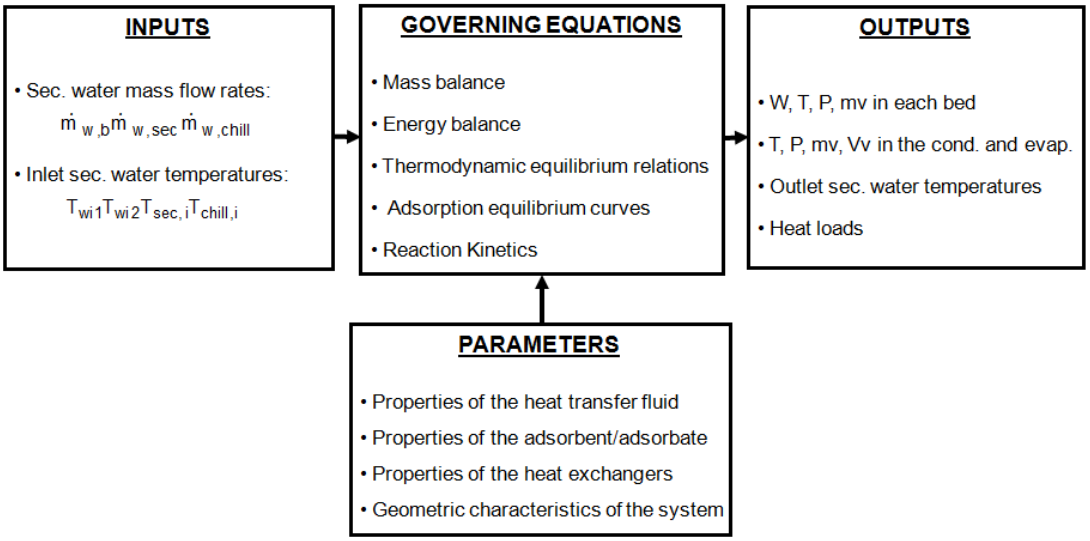

Fig. 42. Simplified structure of the adsorption system model.

Furthermore, the model requires several parameters which are constant throughout the simulation as e.g. the parameters which are related to the thermophysical properties of the water, adsorbent and other components of the system (such as the specific heat, adsorption equilibrium constants, kinetic constants, etc…) and the parameters which are related to the physical design of the system (such as the geometry of the bed, the adsorbent and metallic mass in each heat exchanger, etc.). The main parameters used in the model are listed in Table 7.

Table 7. Main parameters used in the model.

Symbol	Value	Units	Observations
cp_w	4182	J Kg^{-1} K^{-1}	Taken from [94]
ρ_w	1014	J Kg^{-1} K^{-1}	Taken from [94]
h_w	2248	W m^{-2} K^{-1}	Taken from [94]
$cp_{ads,0}$	750	J kg^{-1} K^{-1}	Taken from [90]
k_{ads}	0.13	W m^{-1} K^{-1}	Assumed
cp_{met}	890	J kg^{-1} K^{-1}	Taken from [94]
k_{met}	160	W m^{-1} K^{-1}	Taken from [94]
k_1	0.019	s^{-1}	Taken from [7]
k_2	906	K	Taken from [7]
$m_{w,HE}$	0.3276	kg	ECN onboard prototype
$m_{w,porti}$	0.0938	kg	Assumed to be 1/3 of $m_{w,HE}$
$m_{w,porto}$	0.0938	kg	Assumed to be 1/3 of $m_{w,HE}$
$m_{met,HE}$	1.012	kg	ECN onboard prototype
$m_{port,i}$	0.1518	kg	Assumed to be 1/6 of $m_{met,HE}$
$m_{port,o}$	0.1518	kg	Assumed to be 1/6 of $m_{met,HE}$
$m_{ads,HE}$	1	kg	ECN onboard prototype
N_{HE}	3	-	ECN onboard prototype
W	0.255	m	ECN onboard prototype
D	0.038	m	ECN onboard prototype
H	0.210	m	ECN onboard prototype
p	0.0067	m	ECN onboard prototype
t	0.0017	m	ECN onboard prototype
N_{ch}	38	-	ECN onboard prototype
p_f	0.0015	m	ECN onboard prototype
t_f	0.001	m	ECN onboard prototype
e_{met}	0.0003	m	ECN onboard prototype
V_b	0.0108	m^3	ECN onboard prototype
V_{cond}	0.0231	m^3	ECN onboard prototype
V_{evap}	0.0128	m^3	ECN onboard prototype

The model requires the time dependent inputs which are related to the operative conditions of the system, in order to make a direct comparison between simulating results and experimental results. These type of inputs correspond to experimental data such as the secondary water temperature entering the beds (i.e. bed 1 and bed 2), condenser and evaporator, and the water mass flow rate in each secondary water circuit (i.e. heating, cooling and

chilled water circuit). The input data used in the model is reported at the topside of Table 8.

The state variables are those variables in the model that change over time and are reported at the bottom of Table 8. The solver computes the derivatives of the continuous states at the current time step, and then it integrates the state derivatives with respect to time. The state variables must be defined at the initial time. Starting from the known states at the initial time, the simulation model calculates, in time: the temperature and pressure in the beds, condenser and evaporator; the vapour mass in the beds, evaporator and condenser; the vapour volume in the condenser and evaporator; the uptake variation in each bed; the outlet temperature of the secondary water circuits (i.e. heating water, cooling water and chilled water). Furthermore, it is possible to calculate the condensation and evaporation rate; the liquid volume in the condenser and evaporator, the temperature in the condenser and evaporator; the amounts of heat exchanged and, consequently, the overall performance of the adsorption cooling system under study.

Table 8. Input data and state variables of the model.

	Symbol
Input variables:	
Temperature of the secondary water entering the bed 1	T_{wi1}
Temperature of the secondary water entering the bed 2	T_{wi2}
Temperature of the secondary water entering the condenser	$T_{sec,i}$
Temperature of the chilled water entering the evaporator	$T_{chill.i}$
Bed 1 secondary water mass flow	$\dot{m}_{w,b1}$
Bed 2 secondary water mass flow	$\dot{m}_{w,b2}$
Condenser secondary water mass flow	$\dot{m}_{w,sec}$
Evaporator secondary water mass flow	$\dot{m}_{w,chill}$
State variables:	
Temperature in the bed 1	T_{b1}
Pressure in the bed 1	P_{b1}
Uptake in the bed 1	w_{b1}
Total vapour mass in the bed 1	$m_{v,b1}$
Temperature of the inlet metal port (for the bed 1)	$T_{port,i1}$
Inlet water temperature at the heat exchanger of the bed 1	$T_{wi,HE1}$
Outlet water temperature at the heat exchanger of the bed 1	$T_{wo,HE1}$
Temperature of the outlet metal port (for the bed 1)	$T_{port,o1}$
Temperature of the secondary water leaving the bed 1	T_{wo1}
Temperature in the bed 2	T_{b2}
Pressure in the bed 2	P_{b2}
Uptake in the bed 2	w_{b2}
Total vapour mass in the bed 2	$m_{v,b2}$
Temperature of the inlet metal port (for the bed 2)	$T_{port,i2}$
Inlet water temperature at the heat exchanger of the bed 2	$T_{wi,HE2}$
Outlet water temperature at the heat exchanger of the bed 2	$T_{wo,HE2}$
Temperature of the outlet metal port (for the bed 2)	$T_{port,o2}$
Temperature of the secondary water leaving the bed 2	T_{wo2}
Pressure in the condenser	P_{cond}
Temperature of the cooling water leaving the condenser	$T_{sec,o}$
Vapour mass in the condenser	$m_{v,cond}$
Vapour volume in the condenser	$V_{v,cond}$
Pressure in the evaporator	P_{evap}
Temperature of the chilled water leaving the evaporator	$T_{chill,o}$
Vapour mass in the evaporator	$m_{v,evap}$
Vapour volume in the evaporator	$V_{v,evap}$

6. VALIDATION OF THE DYNAMIC MODEL

6.1. Introduction

The mathematical model of the double-bed adsorption cooling system driven by low grade waste heat (80-90 °C) for automobile air-conditioning purposes (see chapter 5) had to be validated before employing it as a simulation tool for the design optimization study. First, the consistency of the mathematical model has been checked based on an energy balance analysis. Secondly, the model has been validated by comparison with experimental results of the prototype system tested under dynamic conditions. The calculated results demonstrate that the model is self-consistent and that it is in good agreement with the experiments, showing the excellent capabilities of the model to predict the dynamic behaviour of the systems.

The experimental tests were performed on the onboard adsorption chiller prototype at the ECN laboratories during the TOPMACS project [65]. A description of the prototype system is presented in chapter 3. The experimental tests were conducted for two different operation modes. The mathematical model was adapted to simulate the dynamic behaviour of the system under any of both operation modes. In both modes, the calculated results are in very good agreement with the experiments, proving the good capabilities of the model to predict the system performance.

The validation of the model has been carried out at the ECN institute, where the PhD author spent several months as part of her thesis. The validation of the mathematical model and the good results attained show that the use of this kind of model is essential for the optimization of the design of the adsorption system layout as well as for the optimization of its operation and control.

6.2. Consistency checking of the model

The consistency of the mathematical model has been analysed by checking the energy balance of the system. In particular, the amount of energy provided or removed from a specific component has been calculated considering the energy transferred between the component and the external heat transfer fluid (i.e. water). Fig. 43 illustrates the energy balances in the main components (i.e. beds, condenser and evaporator) of the adsorption cooling system.

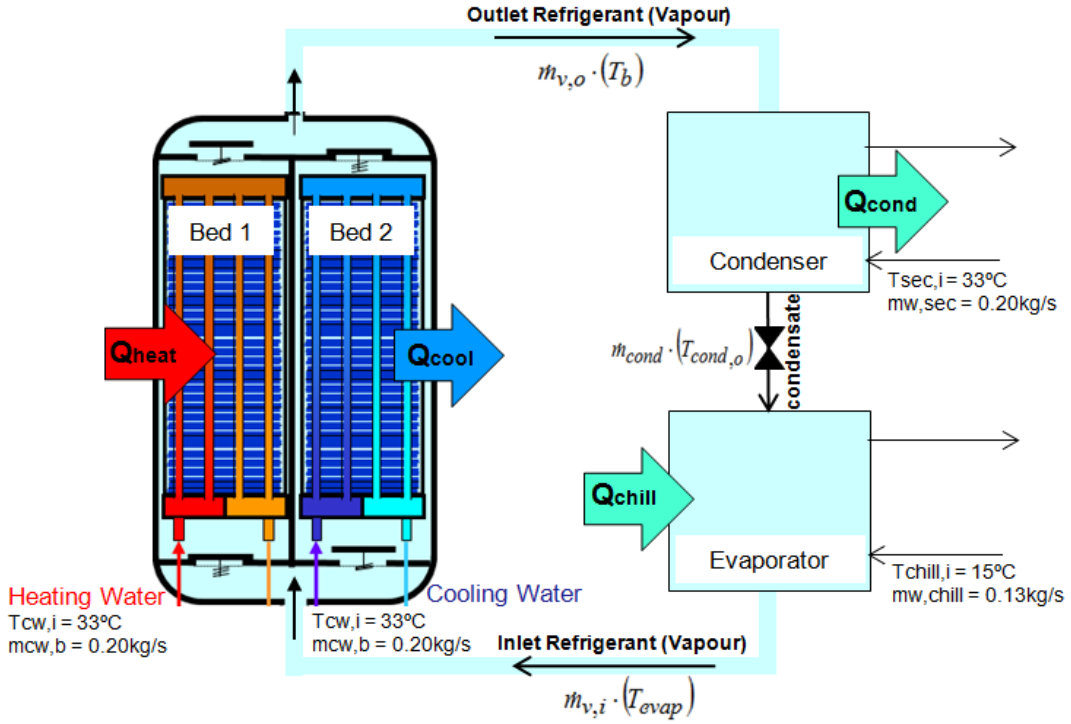

Fig. 43. Energy Balance of the system.

Where: $T_{hw,i}$ is the inlet heating water temperature of the bed ; $T_{cw,i}$ is the inlet cooling water temperature of the bed; $T_{sec,i}$ is the inlet cooling water temperature of the condenser; $T_{chill,i}$ is the inlet temperature of the chilled water.

Hence, the energy balance of the overall system is given by the following relation:

$$\underbrace{\dot{Q}_{heat} + \dot{Q}_{chill}}_{\textbf{Balance In}} = \underbrace{\dot{Q}_{cond} + \dot{Q}_{cool}}_{\textbf{Balance Out}} \quad (6.1)$$

where, the total amount of energy supplied to the system, named “Balance In”, as detailed in Eq.(6.1), is given by the sum of the amount of heat supplied to the bed ($\dot{Q}_{heat}$) and the cooling effect at the evaporator ($\dot{Q}_{chill}$). The total amount of energy removed from the system, named “Balance Out”, as detailed in Eq.(6.1), is given by the sum of the amount of heat removed from the bed by the cooling water ($\dot{Q}_{cool}$) and the amount of heat transferred from the condenser to the secondary water ($\dot{Q}_{cond}$). The energy balances were estimated at the operating conditions shown in Fig. 43. Table 9 shows the total heat consumed and cooling effect produced, calculated by the model for the last cycle, which best approaches steady state conditions.

Table 9. Energy balance estimated for the last computed cycle.

$\dot{Q}_{heat}$ [W]	$\dot{Q}_{chill}$ [W]	$\dot{Q}_{cool}$ [W]	$\dot{Q}_{cond}$[W]	Energy Balance In	Energy Balance Out
6475.98	1607.44	6354.43	1698.72	**8083.42**	**8053.16**
Residual Balance [%]:			**0.37**		

As it can be seen in Table 9, the heat amount transferred at the condenser is slightly higher than the one transferred at the evaporator. This is due to the vapour temperature entering the condenser being above its saturation temperature, therefore carrying a larger amount of sensible heat.

Fig. 44 shows the model’s calculation result of the instantaneous thermal power of the heat transfer fluid for more than 20 cycles. As it can be seen on Fig. 44, the thermal power for heating and cooling the bed is similar to each other but not the same. The thermal power extracted from the heating water circuit and the power rejected to the cooling water circuit shows very rapid variations, especially after switching the beds, where the spikes in thermal power are very high. These sudden variations represent a problem for the evaluation of the transferred heat along a cycle, since during those switching periods the integrals cannot be solved with high precision. This numerical problem of the integration of the results explains the small error obtained for the energy

balance, which corresponds to 0.37%. However, the error is always monitored during the calculations, and its value always remains smaller than 0.5%. This error is very small, and therefore allows an accurate optimization and analysis of the system.

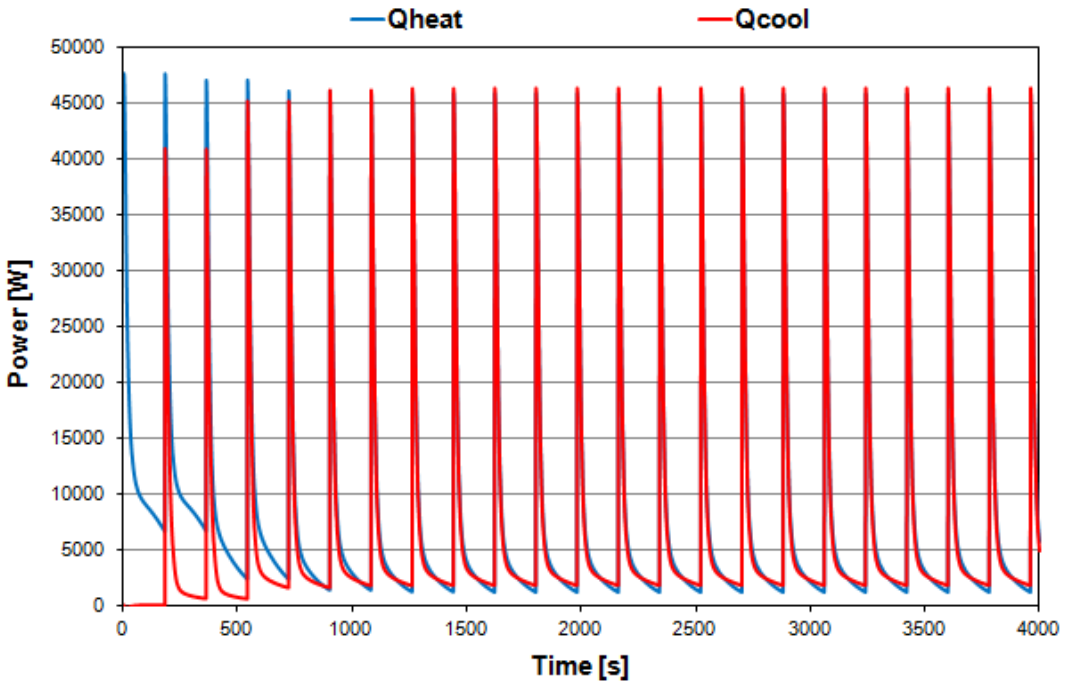

Fig. 44. Instantaneous thermal power of the heat transfer fluid (heating and cooling water).

6.3. Validation of the model with experimental tests

6.3.1. Operation of the system

The experimental tests have been carried out applying two different operation modes of the liquid valves of the heating and cooling water circuits, which are represented in Fig. 45. The first operation mode had no time delay between the switching of the outlet and inlet valves, so that there was no heat recovery. The second operation mode included a delay time between the switching of the liquid circuit valves. Note that the system uses additional temperature sensors at the inlet and outlet of the beds. If the temperature difference between inlet and outlet is smaller than a predefined value (e.g. 1K), the inlet valves (V-241

and V-231) will switch. The outlet valves (V-242 and V-232) will switch with a time delay with respect to the inlet valves. The time delay is set to such a value that at the moment of switching the outlet temperatures are almost identical, and within the range of the average temperatures of the heating and cooling water circuit. This time delay prevents hot water remaining inside the hot bed to be sent directly to the cooling circuit, and cooling water remaining in the cold bed to be sent to the heating circuit. The result is that some heat of the water stored in the bed is always returned to the hot water circuit, and the cold water stored in the other bed is sent to the cooling water circuit. In this operation mode a part of the sensible heat contained in the liquid circuits is recovered, with the aim to increase the COP.

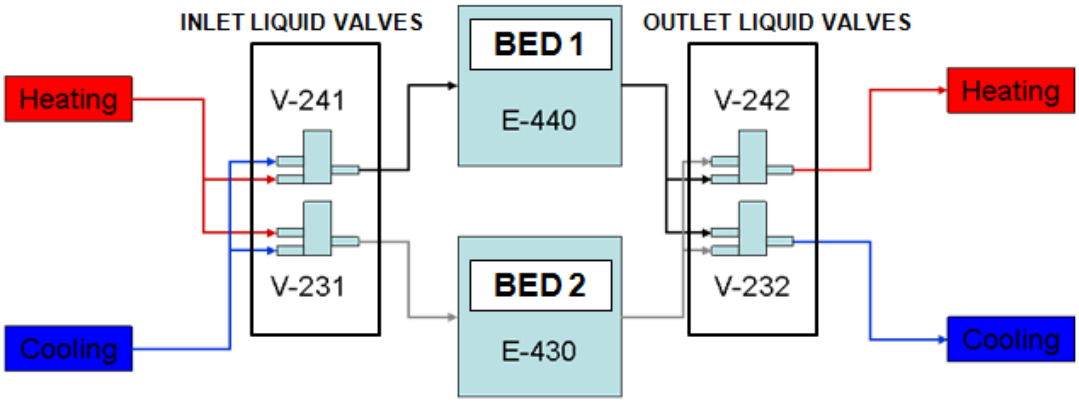

Fig. 45. Layout of the liquid valves of the heating and cooling circuits.

6.3.2. Testing conditions

A sample of the experimental results obtained with inlet water temperature of 90 ºC, condensing temperature of 33 ºC and evaporating temperature of 15 ºC is presented in comparison with the simulation results for both operation modes. The total cycle time, which comprises of the adsorption and desorption cycle times, is set to 6 min.

6.3.3. 1st – Operation mode : Tests performed without heat recovery

Fig. 46 shows the comparison between the simulated and experimental results for the first operation mode (without heat recovery). All the data shown in this figure are obtained from the experiments and simulations for the system at the operating conditions shown in Table 3 of chapter 3 (see subsection 3.4.2). The figures show four peaks, each of them corresponding to half a cycle. Accordingly, two complete cycles are shown, each with a fixed cycle time of 6 minutes (360 s).

Fig. 46(a) shows the comparison between bed pressure and outlet temperature predicted by the model, and experimental results. The experimental results show some differences between the temperature profiles of the beds. They are clearly distinguishable for pressures at the highest values range, which corresponds to the desorption phase. This difference could be caused by different pressure losses in the flow from the condenser to the bed across the corresponding valves, or simply be due to some slight uncertainty in the measurements. Furthermore, the water temperature at the outlet of the bed is asymmetric, showing slight differences between both beds. This can be due to a different permeability and compactness of the adsorbent material in the bed, leading to the observed differences in behaviour. The model is not able to reproduce those differences, since it assumes that both beds are identical. However, the model adequately describes the behaviour of the test facility. Overall, the model predicted fairly well the experimental values.

Fig. 46(b) shows the simulated and measured pressure and temperature level in the evaporator and condenser. According to the simulated results, the average temperature and pressure in the condenser are 35.6 ºC and 58.2 mbar respectively, and the average temperature and pressure in the evaporator are 8.8 ºC and 11.4 mbar. The adjustment between calculated and measured results is very good in phase and amplitude, regardless of the hypothesis assumed for the modelling.

Fig. 46(c) shows the simulated and measured cooling capacity of the evaporator and the condenser capacity. At stable conditions, the cooling

capacity of the evaporator remained stable with an average of 2113 W. Switching caused the cooling capacity to collapse briefly to a minimum of about 750 W. Overall, the average condenser capacity was 2217 W. The adjustment is remarkably good, taking into account the approximate nature of the model.

Fig. 46(d) shows the equilibrium value of the uptake, calculated from the bed pressure and temperature for both experimental measurements and simulations. The equilibrium uptake for the experimental results has been evaluated from the instantaneous recordings of bed pressure and temperature. However, there is high uncertainty in the evaluation of the bed temperature, since the experimental value corresponds only to the readings of a single temperature point. The inertia of the temperature measurement together with temperature variation across the heat exchanger, could explain the differences with the model results. Probably due to the difficulty of measuring the temperature inside the bed, the calculated and measured equilibrium uptake is not very similar, although the agreement in the total variation of uptake is remarkable. According to the simulation results, the minimum temperature reached by the bed at the end of the adsorption phase was 36 ºC, with a maximum uptake of about 10 wt%, while the maximum temperature reached by the bed at the end of the regeneration phase was 88 ºC, with a minimum uptake of about 3 wt%.

Fig. 46(e) shows the equilibrium and non-equilibrium uptake evolution calculated from the bed pressure and temperature obtained from the simulations. As it can be seen from the non-equilibrium uptake curve, the desorption phase is found to be slower than the adsorption one. From the equilibrium uptake variation, it seems that both adsorption/desorption phases run faster than the non-equilibrium uptake variation. Therefore, the adsorbed/desorbed amount of refrigerant could be increased if the kinetics would be faster, since it would reach the maximum and minimum uptake in a shorter amount of time.

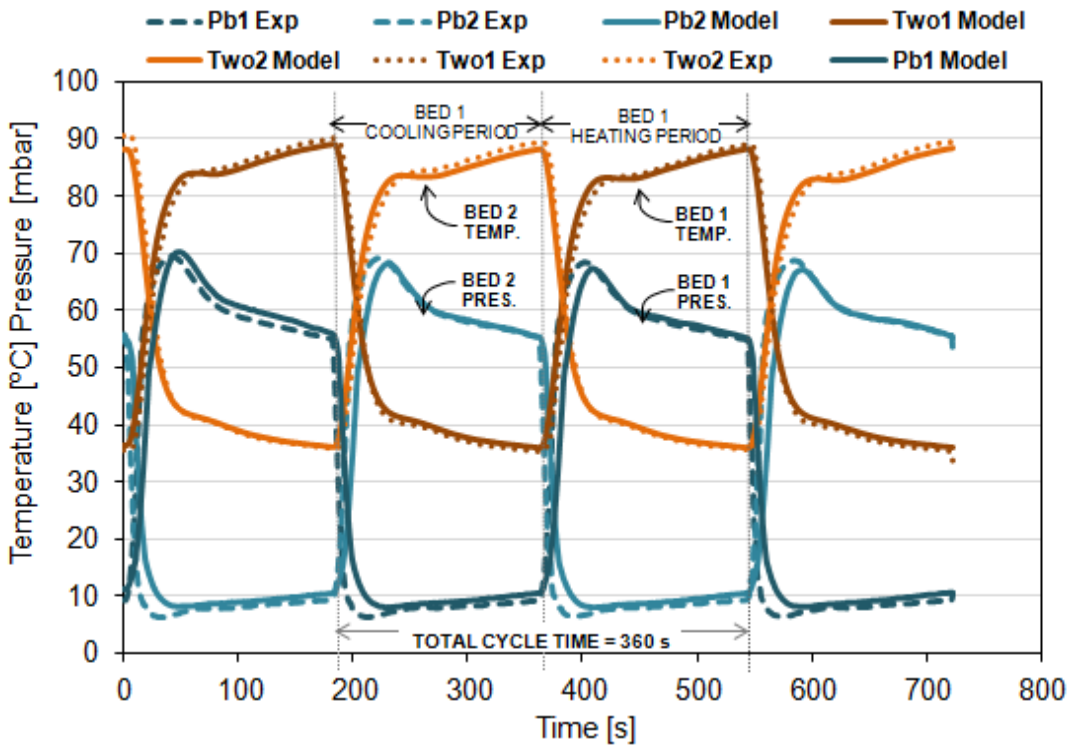
Pb1 Exp
Pb2 Exp
Pb2 Model
Two1 Model
Two2 Model
Two1 Exp
Two2 Exp
Pb1 Model
BED 1 COOLING PERIOD
BED 1 HEATING PERIOD
BED 2 TEMP.
BED 1 TEMP.
BED 2 PRES.
BED 1 PRES.
TOTAL CYCLE TIME = 360 s
Temperature [°C] Pressure [mbar]
Time [s]

(a)

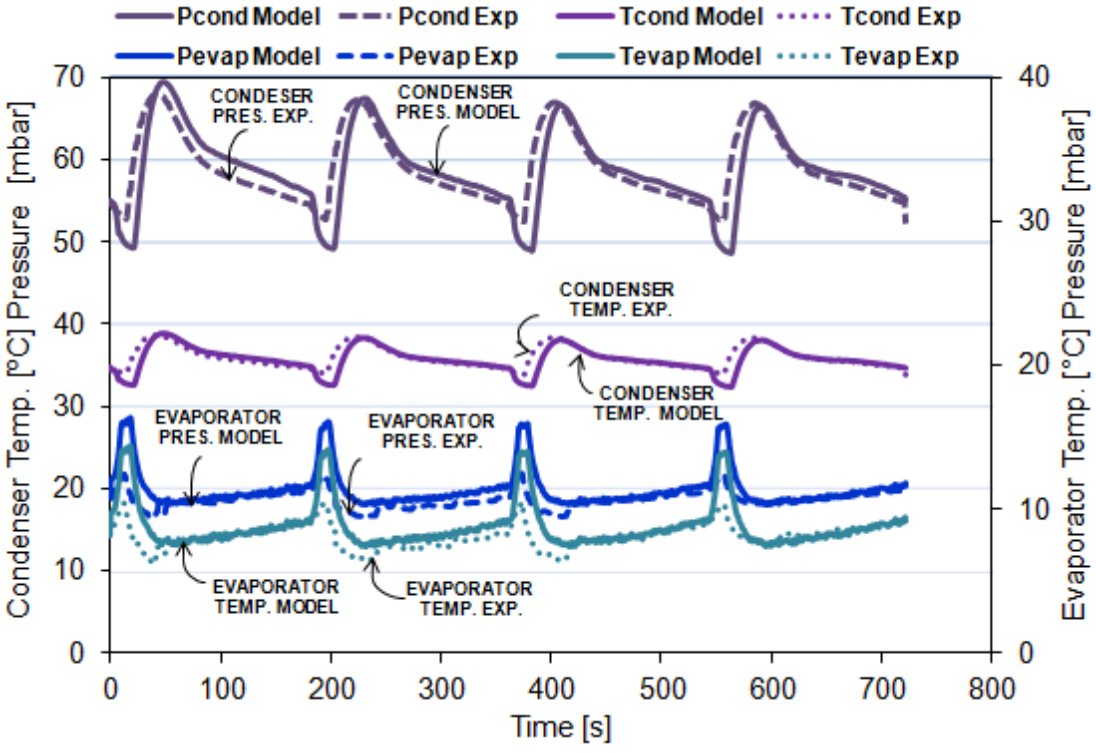
Pcond Model
Pcond Exp
Tcond Model
Tcond Exp
Pevap Model
Pevap Exp
Tevap Model
Tevap Exp
CONDESER PRES. EXP.
CONDENSER PRES. MODEL
CONDENSER TEMP. EXP.
CONDENSER TEMP. MODEL
EVAPORATOR PRES. MODEL
EVAPORATOR PRES. EXP.
EVAPORATOR TEMP. MODEL
EVAPORATOR TEMP. EXP.
Condenser Temp. [°C] Pressure [mbar]
Evaporator Temp. [°C] Pressure [mbar]
Time [s]

(b)

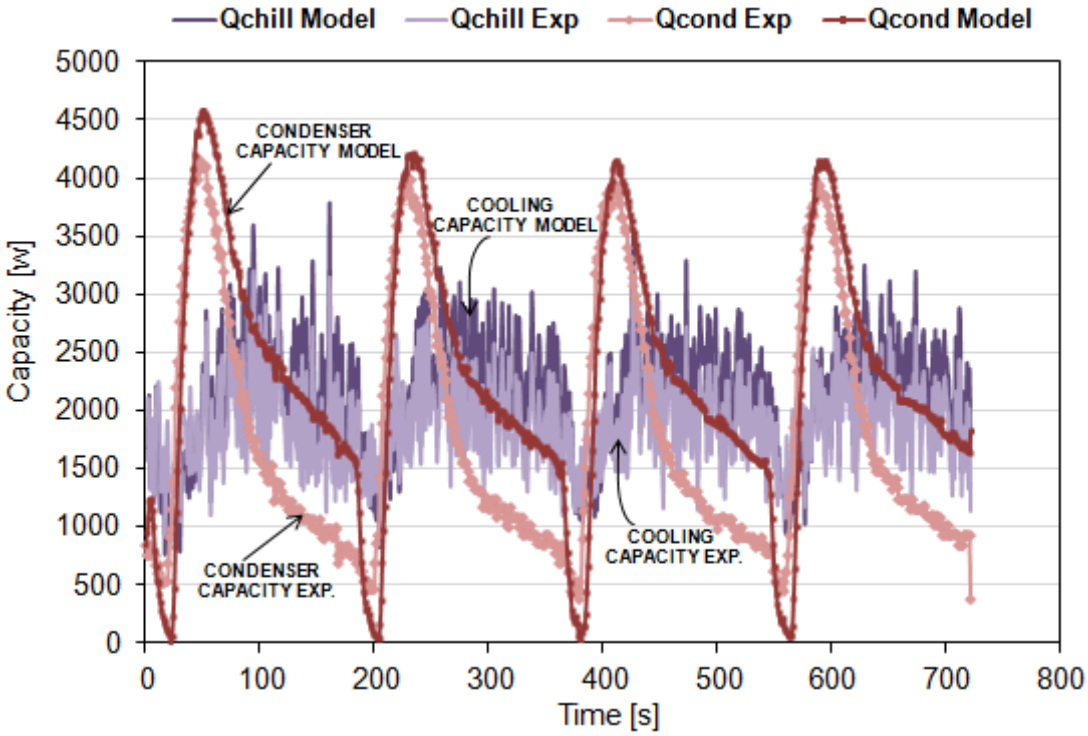
Qchill Model
Qchill Exp
Qcond Exp
Qcond Model
CONDENSER CAPACITY MODEL
COOLING CAPACITY MODEL
CONDENSER CAPACITY EXP.
COOLING CAPACITY EXP.
Capacity [w]
Time [s]
0
500
1000
1500
2000
2500
3000
3500
4000
4500
5000
0
100
200
300
400
500
600
700
800

(c)

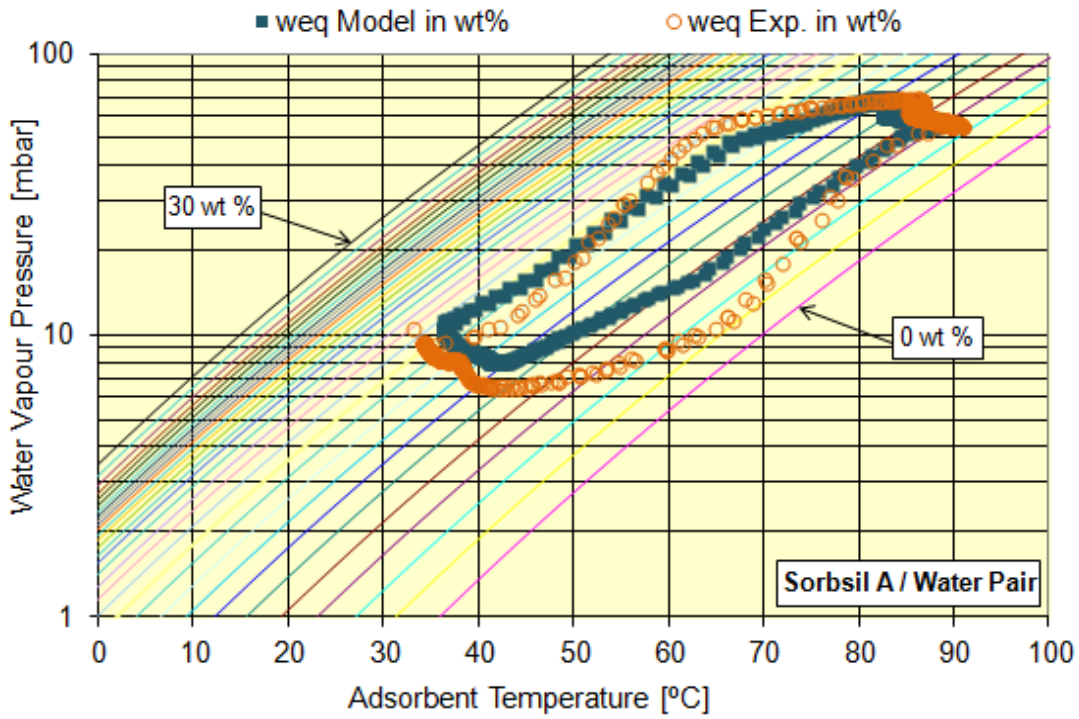
weq Model in wt%
weq Exp. in wt%
30 wt %
0 wt %
Sorbsil A / Water Pair
Water Vapour Pressure [mbar]
Adsorbent Temperature [ºC]
1
10
100
0
10
20
30
40
50
60
70
80
90
100

(d)

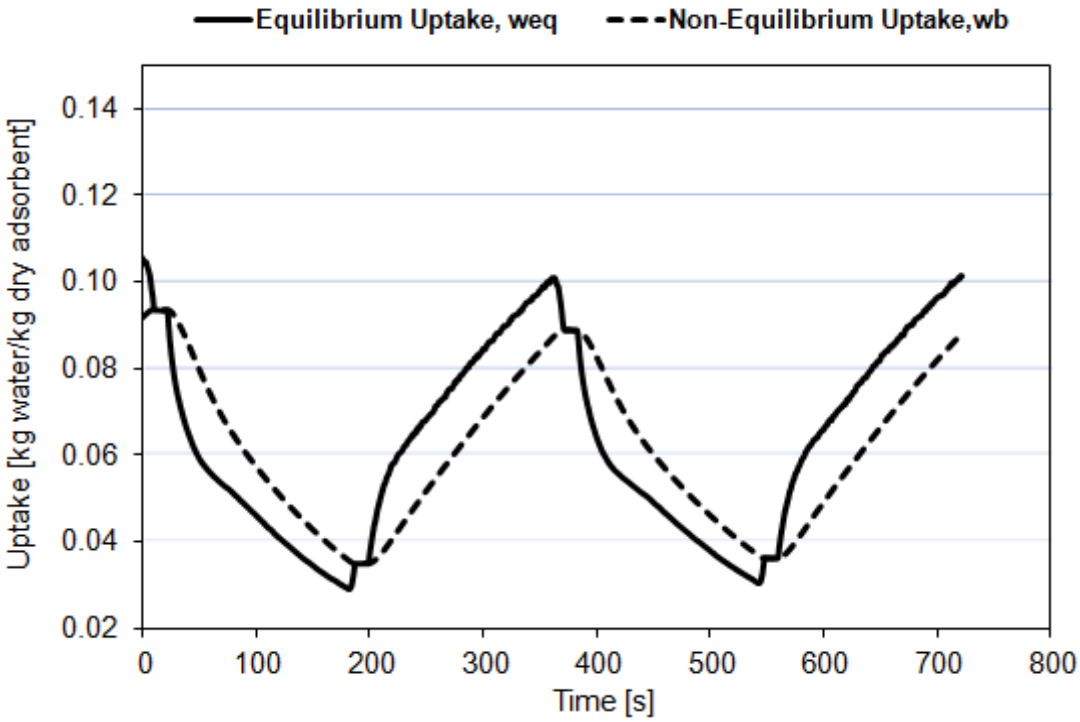

(e)

Fig. 46. Comparison between calculated and experimental results - 1st Operation Mode (No Heat Recovery): (a) Bed 1 and Bed 2 pressures and outlet water temperatures; (b) Temperature and pressures at condenser and evaporator; (c) Cooling capacity and condenser capacity; (d) Thermodynamic cycle for a sorption bed (Bed1) on the Dühring diagram; (e) Equilibrium and non-equilibrium uptake evolution in the bed (Bed 1).

6.3.4. 2nd – Operation mode : Tests performed with heat recovery

Fig. 47 shows the comparison between the simulated and experimental results for the second operation mode (heat recovery mode), at the above mentioned operating conditions. As it can be observed, the agreement between measured and experimental results is good for both operation modes, indicating that the model has good prediction capability for transient conditions and that it is able to capture most of the dynamics of the system.

Comparing the results obtained for the tests carried out with heat recovery to the previous ones, it can be seen that there are almost no differences in the behaviour of the beds, especially with regards to cycle time. This is because the time delay when switching between inlet and outlet valves of the beds'

secondary water circuits is very small (around 20 s). The major differences in the system when operating in heat recovery mode are due to the amount of heat that is saved when heating the secondary water, and not due to the operation of the beds.

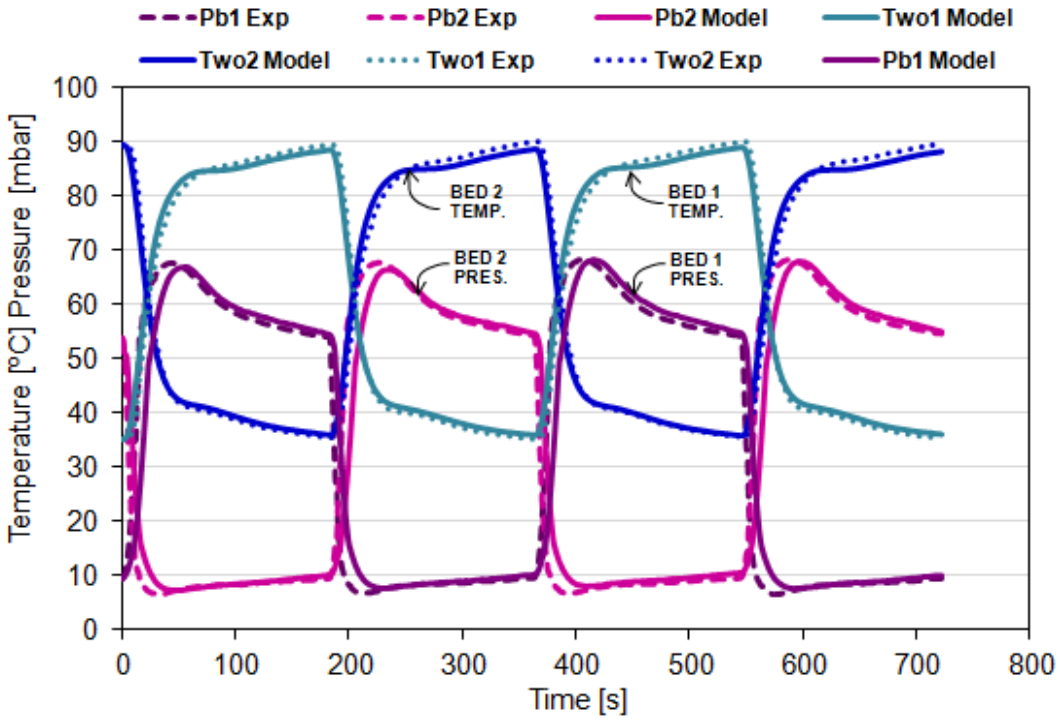

(a)

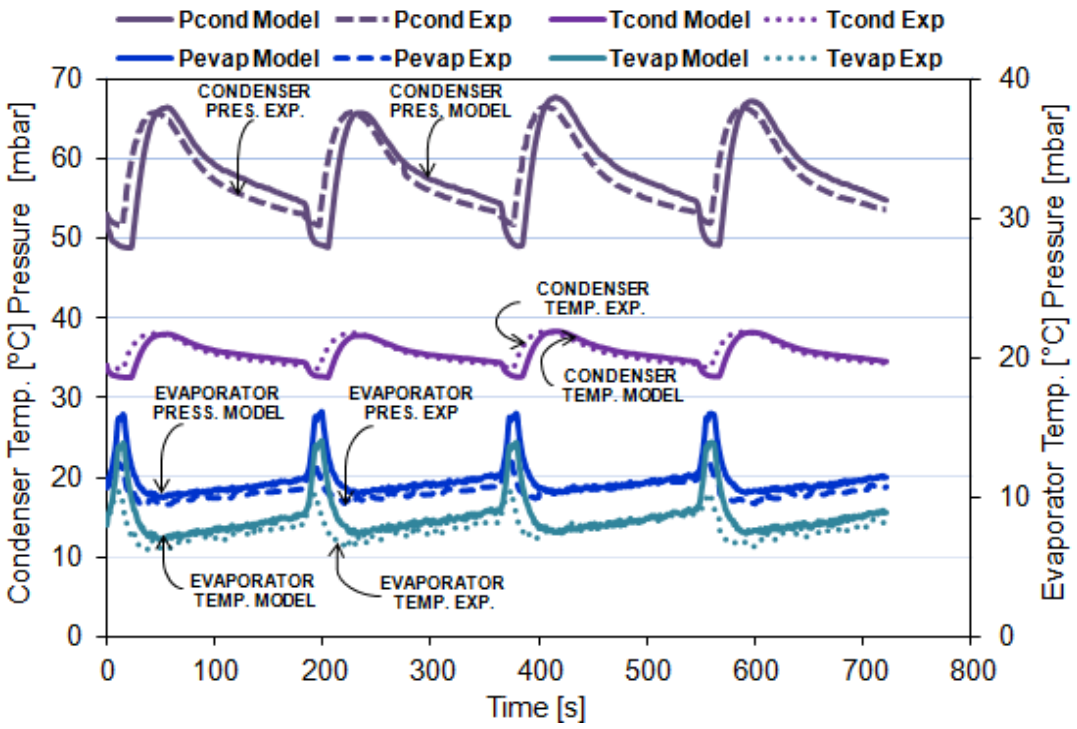
Pcond Model
Pcond Exp
Tcond Model
Tcond Exp
Pevap Model
Pevap Exp
Tevap Model
Tevap Exp
CONDENSER PRES. EXP.
CONDENSER PRES. MODEL
CONDENSER TEMP. EXP.
CONDENSER TEMP. MODEL
EVAPORATOR PRESS. MODEL
EVAPORATOR PRES. EXP
EVAPORATOR TEMP. MODEL
EVAPORATOR TEMP. EXP.
Condenser Temp. [°C] Pressure [mbar]
Evaporator Temp. [°C] Pressure [mbar]
Time [s]

(b)

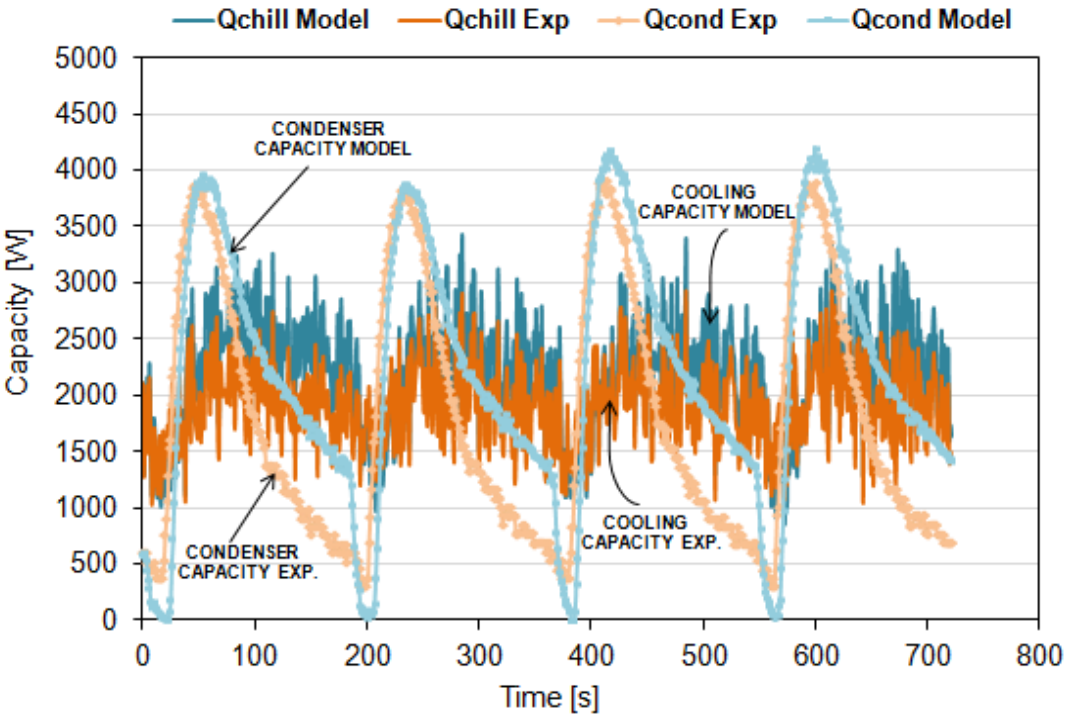
Qchill Model
Qchill Exp
Qcond Exp
Qcond Model
CONDENSER CAPACITY MODEL
COOLING CAPACITY MODEL
CONDENSER CAPACITY EXP.
COOLING CAPACITY EXP.
Capacity [W]
Time [s]

(c)

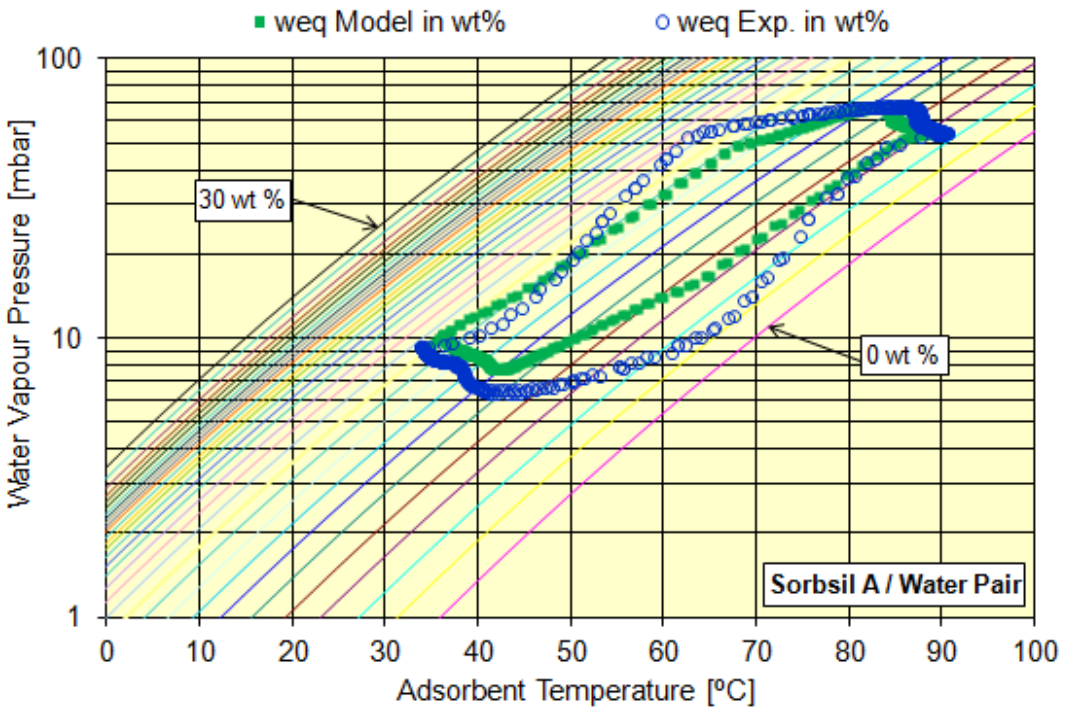

(d)

Fig. 47. Comparison between calculated and experimental results – 2nd Operation Mode (Heat Recovery Mode): (a) Bed 1 and Bed 2 pressures and outlet water temperatures; (b) Temperature and pressures at condenser and evaporator; (c) Cooling capacity and condenser Capacity; (d) Thermodynamic cycle for a sorption bed (Bed1) on the Dühring diagram.

6.3.5. System performance evaluation

In this PhD study, the system performance calculated by the experimental data is presented in comparison to the system performance obtained by the model. The experimental data, measured for each operation mode, were properly treated in order to evaluate the performance of the system in terms of COP and cooling capacity. In particular, the adsorption chiller was considered as a black box, in which the only parameters known were the temperatures and flow rates of the heat transfer fluid going into the system, as well as the cycle time in question. As a result, the amount of heating power consumed by the bed and the amount of cooling capacity produced at the evaporator were calculated from the changes in the temperature of the heat transfer fluid (heating water or chilled water), the mass flow rate, and the heat capacity of the fluid. Hence, the

COP was obtained from the measurements of heat transfer fluid temperatures and mass flow rates at a fixed cycle of 6 minutes, which is the optimum for the characteristics of the system, as:

$$\mathrm{COP_{Exp}} = \frac{\dot{Q}_{\mathrm{chill_{Exp}}}}{\dot{Q}_{\mathrm{heat_{Exp}}}} = \frac{\dot{m}_{\mathrm{w,chill}} \cdot \mathrm{cp_w} \cdot \left(\mathrm{T_{chill,i}} - \mathrm{T_{chill,o}}\right)}{\dot{m}_{\mathrm{hw,b}} \cdot \mathrm{cp_w} \cdot \left(\mathrm{T_{hw,i}} - \mathrm{T_{hw,o}}\right)} \tag{6.2}$$

where the experimentally obtained cooling capacity and driving heat input are denoted by $\dot{Q}_{\mathrm{chill_{Exp}}}$ and $\dot{Q}_{\mathrm{heat_{Exp}}}$, respectively.

Table 10 shows the obtained system performance for both operation modes. Based on the simulation results, the system is able to produce a mean cooling capacity of 2096 W and a COP of 0.33 without heat recovery. If the auxiliary heat recovery circuit is considered, the system is able to produce a mean cooling capacity of 2180 W and a COP of 0.48. Based on experimental results, the system is able to produce a mean cooling capacity of 1893 W and a COP of 0.29 for the first configuration mode, and a mean cooling capacity of 1912 W and a COP of 0.44 for the second configuration mode. The model predicts the same improvement in terms of COP when comparing the simulation results with the experimental results. Therefore, the model can also be used to predict how much the performance can be improved when using a different system configuration.

As it can be observed, an important agreement between the model predictions and the experiments is found for the global performance of the system. This means that the model can effectively be employed for the optimization of the design of the system layout, as well as for the optimization of its operation and control.

Table 10. System Performance.

	Experimental		Simulation	
Operation Mode:	$\dot{Q}_{chill_{Exp}}$ **[W]**	COP_{Exp}	$\dot{Q}_{chill_{Model}}$ **[W]**	COP_{Model}
1st: No Heat Recovery	1893	0.29	2096	0.33
2nd: Heat Recovery	1912	0.44	2180	0.48

From the obtained results, it is clear that the heat recovery has a strong positive effect on the system´s COP, and a slight positive effect on the cooling capacity, so it is one of the design key points to improve the performance of adsorption systems.

7. PERFORMANCE ESTIMATION OF AN ONBOARD ADSORPTION A/C SYSTEM

7.1. Introduction

In order to assist the design of the onboard adsorption chiller prototype realized at the ECN laboratories, a lumped parameter model of the vehicle (with all the sub-systems that have interaction with the adsorption A/C system) was developed under the framework of the Topmacs project [65]. The development of an overall model for the proposed system was a particular challenging task since the system is extremely complex and comprises of a great number of different components. The overall model was developed under MATLAB® Simulink® environment and it has been employed to estimate the performance of the onboard adsorption A/C system under real driving conditions, the results of which are presented in this chapter. Since the control strategy of the beds implemented on the overall model was based on the cycle time, a parametric study was carried out at constant operating conditions in order to find the optimum cycle time that achieves best system performance. Furthermore, parametric studies have been carried out for a different design configuration in order to explore further improvements of the system performance. The results obtained for the alternative system design have been compared with the ones obtained for the system layout implemented in the car prototype.

7.2. Onboard adsorption A/C system implemented in the overall model

The overall model developed under the Topmacs project [65] can provide estimations of the performance of the adsorption A/C system seen in Fig. 48, which is essentially the system layout proposed by ECN and implemented in the reference vehicle. The system involves a secondary water loop to cool in series first the condenser and then the sorption bed (Cooling Water Loop, in Fig. 48) and a secondary water loop to cool the air cabin (Chilled Water Loop, in Fig. 48). The term radiator in Fig. 48 refers to the heat exchanger that is used to cool down the condenser as well as the sorption beds by means of an auxiliary

hydraulic loop, which dissipates heat to the environment. The term air cooler in Fig. 48 refers to the heat exchanger that is used to cool down the cabin air by means of the water secondary fluid that is “absorbing heat” from the air cooler, producing a chilling effect in the cabin.

Heat is supplied to one of the beds by the engine waste heat and the cooling water (some degrees higher than ambient temperature) is provided to the other bed thanks to an auxiliary cooler (Radiator, in Fig. 48).

The water flow rate available to activate the adsorption system is the same that normally goes through the radiator (Engine Radiator, in Fig. 48) to cool down the engine. The engine needs to warm up as fast as possible in order to reduce emissions and increase the efficiency. During the warming up period there is no waste heat available. When the engine water temperature reaches an adequate level, the thermostat opens the cooling circuit to the engine radiator. The hot water is then sent to activate the adsorption system. This means that during the engine warm up no desorption can be carried out until the engine is sufficiently warm. Nonetheless, cooling the cabin is still possible provided that one or two beds have been kept dry, so that it can absorb vapour from the evaporator and produce a cooling effect from the beginning of a driving cycle.

The engine coolant system includes a thermostat which controls the engine temperature in order to first allow for the fastest warming up of the engine, and then just dissipate the excess heat on the engine radiator, therefore keeping constant the engine operating temperature. The engine radiator will be employed to dissipate the excess heat in the case that the adsorption system is not able to employ all the available waste heat in order not to overheat the engine. Additionally, a way to monitor the water temperature at the outlet of the adsorption system, and measures to ensure that it returns to the engine at an appropriate temperature have been implemented in the overall model. This corresponds to the constraints of engine design, which dictate a maximum acceptable temperature drop through the adsorption system in order not to decrease the engine operation temperature. This would negatively affect both engine efficiency and emissions.

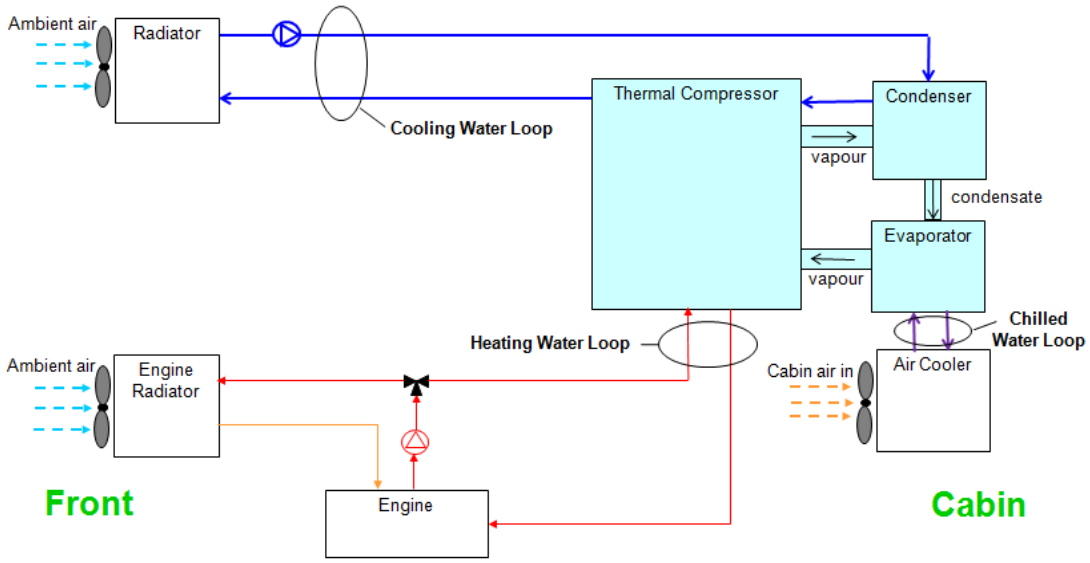

Fig. 48. Layout of the onboard adsorption A/C system proposed by ECN under the framework of the Topmacs project.

7.3. Overall system model – Brief description

7.3.1. Overall model structure

The main purpose of developing the overall model is to simulate the performance of the entire system (engine, adsorption cooling system and cabin). The developed overall model takes into account all the systems and subsystems, from the engine to the air cabin, in such a way that the entire A/C system can be virtually assessed, similarly to the real system during typical standard characterization tests. The developed model is completely dynamic and is able to reproduce the operation of the engine throughout the driving cycle. Particularly, it is able to evaluate the waste heat available at the engine cooling hydraulic loop and at the exhaust gases, calculate the sequential operation of a double-bed adsorption chiller, calculate the condensation of the vapour at the condenser and the cooling effect produced at the evaporator, and finally, monitor the temperature and humidity evolution of the air at the cabin, as a function of the external sun radiation, ambient temperature and vehicle velocity.

The overall model has been developed under MATLAB® Simulink® programming environment and includes models for each of the mentioned systems. Fig. 49 shows the main structure of the overall model. As it can be observed, the overall model is structured in modules, each representing one of the following systems:

- Engine thermal model;
- Adsorption cooling system model;
- Cabin thermal model;

All those systems exchange information through flows of different fluids and control parameters. Each system model is additionally composed by submodels, representing the different subsystems included in it.

The systems defined in the overall model have been studied in detail in order to understand their operation and constraints, and also simple models were developed for them, taking into account their most important design and operation parameters. CRF provided the necessary information for the models. The UPV then developed the models for the engine, the engine cooling hydraulic system and the thermal model for the cabin. The other partners of the Topmacs project [65] cooperated in the definition of the models and have provided input data and experimental data when available. Then, the different models have been combined in the MATLAB® Simulink® environment, and have been integrated into the overall model. The developed models were continuously improved and updated throughout the project by means of the experimental results and information obtained from the testing of the adsorption system at the laboratories of the other partners. The UPV team worked on the checking of all the models, on the development of the dynamic model of the adsorption cooling system, already described in chapter 5, on the implementation of all the models in the Simulink® environment, and on their integration on the overall model.

Furthermore, models for the radiator and air cooler, represented in Fig. 48, have been developed and incorporated in the dynamic model of the adsorption system. The radiator and air cooler were modeled according to the equations presented in the subsection 5.4. of chapter 5. The heat exchangers in question were characterized by their overall thermal conductance (UA). A detailed analysis has been carried out and adequate values of UA for the radiator and air cooler, depending on water and air mass flow rates, have been estimated from experimental results provided by CRF.

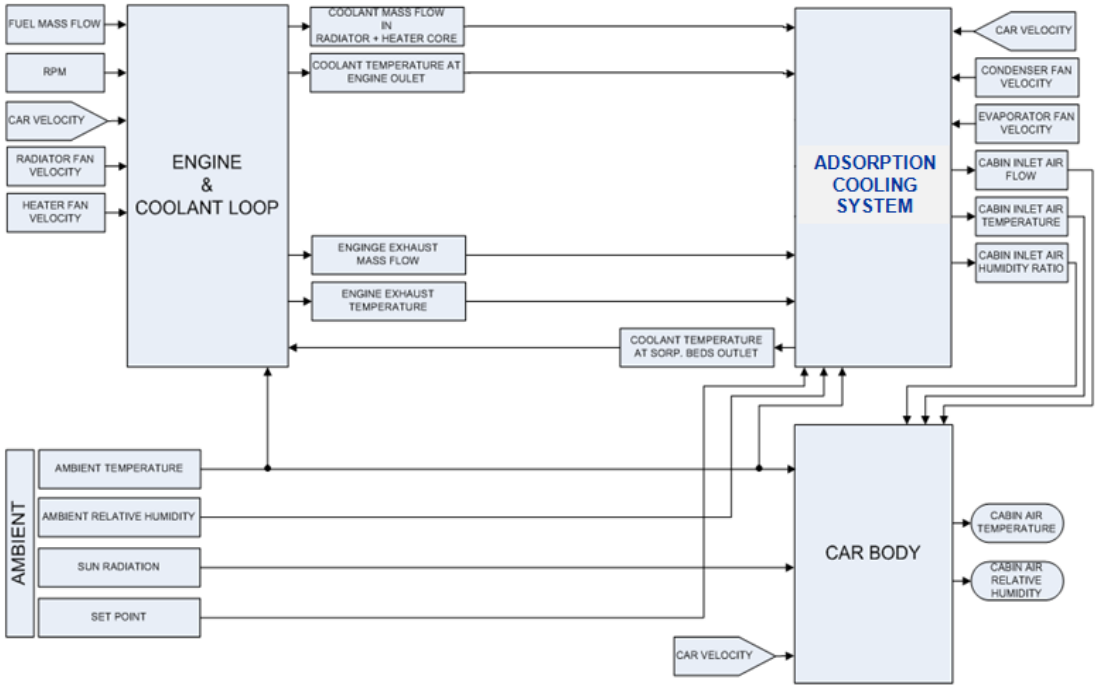

Fig. 49. Overall Model structure under MATLAB® Simulink®

7.3.2. Assessment tests – Brief description

7.3.2.1. Testing facility

A series of tests were performed on the reference vehicle (Fiat Grande Punto) at the CRF laboratories, in order to provide experimental data that was used to identify the mathematical model of the car and to define the thermal comfort performances of the reference vehicle. By performing these tests it was possible to define the amount of waste heat in the engine cooling loop. This waste heat was recovered and transformed into cooling capacity by the

adsorption system. The reference vehicle has been tested under different conditions.

Fig. 50 shows a scheme of the vehicle during the assessment tests. Tests were performed in a climatic chamber equipped with a roll bench. The assessment test for the model follows the same routine as the usual A/C characterization tests performed for cars. More specifically:

- The vehicle is run on a roll test bench following a programmed standard driving cycle.
- The air is blown at the front of the vehicle in order to simulate ambient air around the vehicle on the road.
- Sun radiation is simulated with artificial lamps.
- Ambient temperature is kept at the desired condition.
- The A/C system is in operation following a standard procedure.
- Temperature of the air provided by the A/C system and temperatures at several positions of the cabin air are recorded during the tests. These measurements allow characterizing the thermal performance of the cabin and the A/C system.

The inputs to the overall model are the same as the inputs for a conventional A/C system during the assessment tests. Fig. 50 shows those inputs, constituting the set of operating conditions for the tests, which consist of: ambient temperature and humidity, A/C fan velocity, instantaneous power, engine speed (rpm), and finally, gear and accelerator position. The overall model predicts the evolution of the air temperature inside the cabin throughout the assessment test.

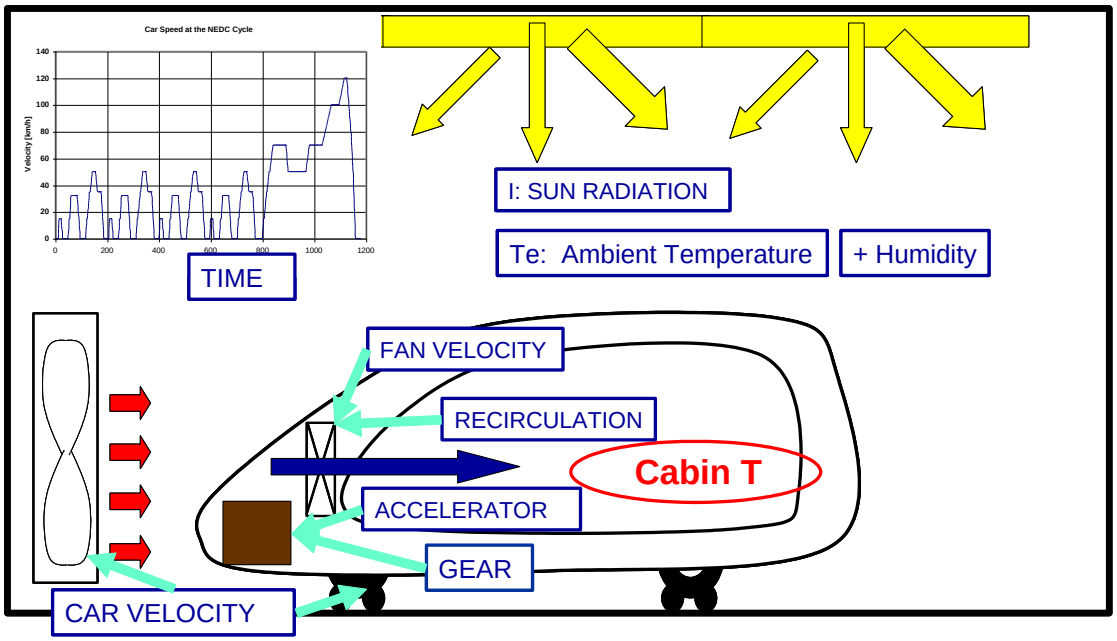

Fig. 50. Scheme of a climatic chamber with rolling bench suitable to perform the A/C assessment tests.

7.3.2.2. Testing cycle

The testing cycle chosen is the Normal European Driving Cycle (NEDC cycle), since in Europe passenger vehicles are normally qualified in terms of fuel consumption using this particular type of cycle. The overall model is capable of simulating the whole A/C characterization test for the car under a NEDC cycle. The NEDC cycle is represented in Fig. 51 and is constituted of four repetitions of elementary urban cycles at low speed (ECE) and one higher speed extra urban cycle (EUDC).

The driving cycle assessment is performed under MATLAB® Simulink® mathematical programming environment.

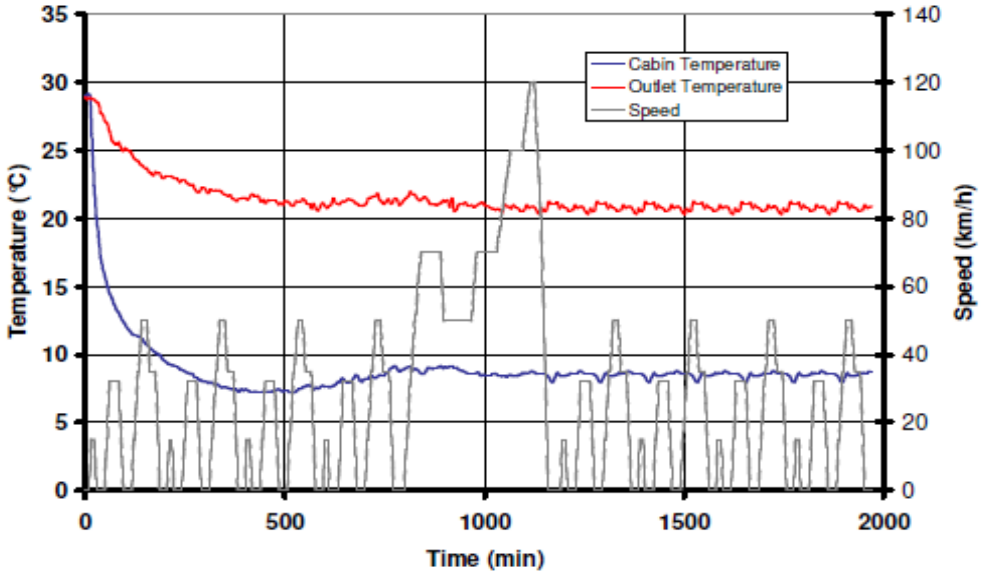

Fig. 51. NEDC-2ECE cycle

7.3.2.3. Thermal Testing Conditions

Different conditions have been simulated in order to assess the performance of the whole system (engine, adsorption cooling system and cabin). The tests have been performed at the ambient conditions presented in Table 11.

Table 11. Assessment tests performed at CRF.

	Ambient Conditions	
	Temperature [ºC]	R.H. [%]
Test Nº 1 – Equivalent European Summer Conditions	28	50
Test Nº 2 – Severe Summer Conditions	35	60
Test Nº 3 – Cooldown Test	+43	35

As mentioned before, the following tests have been performed:

Test Nº 1:

- Equivalent European Summer conditions: these conditions are the ones suggested to classify the air conditioning systems with regards to fuel consumption and thermal comfort
- Ambient conditions: 28°C, 50% RH

- Driving cycle: NEDC cycle
- A/C way of use: auto, with 20 ºC internal set point
- Recirculation: only renewal air

Test Nº 2:

- Severe Summer conditions: these conditions can be considered for non-European countries, where the thermal load is normally higher.
- Ambient conditions: 35°C, 60% RH
- Driving cycle: NEDC cycle
- A/C way of use: auto, with 23 ºC internal set point
- Recirculation: only renewal air

Test Nº 3:

- Severe European climate conditions during the day.
- Ambient conditions: + 43°C, 35% RH
- Cabin soaking temperature: 63° C;
- A/C way of use: auto, with 25 ºC internal set point
- Recirculation: only renewal air
- Car manufacturers assess the potential of the A/C system on a cooldown test, in very hot conditions. The testing site for the cooldown cycle is a wind tunnel equipped with lamps to simulate the solar load. The car is soaked into the wind tunnel under the lamps until the air temperature reaches 63°C. After that, A/C is turned on, along with the artificial wind.

7.3.3. Start-up conditions

The assessment tests have been carried out assuming three different start-up conditions:

- Saturated Beds: The first start-up condition is assuming that both beds are saturated. This means that all the valves of the adsorption system have remained open or do not close hermetically, so that the system is in

equilibrium with the water stored in it at ambient temperature. Under these conditions, the beds and the water are at ambient temperature; the pressure is the one corresponding to saturation, and the uptake corresponds to the equilibrium value at that pressure and temperature. This strategy is the worst case scenario because it does not allow the system to produce any cooling effect at the driving cycle start. First, the bed must be dried out before any evaporation is produced in it.

- 1 Dry Bed: The second start-up condition considers one of the beds as dry, which is possible by keeping the valves of that bed closed and isolated from the rest of the system. In this way, one bed remains at saturated equilibrium conditions, while the other bed remains with the minimum uptake and dry, ready to adsorb water vapour when the valve connecting the evaporator and the bed opens.

- Dry Beds: The third start-up condition is keeping both beds dry by using the same strategy. In real operation, the beds could be initially dry if, after using the system during car operation, the beds are dried with the remaining waste heat stored in the engine once it has been switched off. As mentioned above, this could only be possible if the valves communicating the beds with the condenser and evaporator are able to practically seal the beds when closed. The analysis of the system has covered the whole range of variation of ambient conditions at the different start-up conditions mentioned above, in order to evaluate their influence on the obtained performance.

7.4. Optimization of the onboard adsorption A/C system at constant operating conditions

7.4.1. Introduction

Under real driving conditions the available waste heat from the engine can vary greatly. This happens due to the fact that, firstly, the heat cannot be used by the adsorption A/C system before the engine has been warmed up, and secondly, the water which is sent back to the engine, during normal operation, cannot be neither too cool nor too hot. The engine operation requirements mentioned above make the input temperature and mass flow rate to the adsorption A/C system quite variable. On the other hand, the conditions at the cabin are not constant either. The initial temperature is quite high and it drops as the adsorption A/C system starts to operate. This leads to a considerable variation of the temperature and humidity at the cabin until the comfort conditions are attained. Consequently, this variation is transmitted from the cabin to the evaporator and then to the beds. Hence, the optimization of the design and operation of the system in such variable operating conditions becomes a considerably difficult task. Therefore, parametric studies have been carried out in order to find an optimum cycle time that ensures the system can reach its maximum performance at constant operating conditions.

7.4.2. Cycle time optimization

In this PhD study, a parametric study has been carried out in order to find the optimum cycle time that yields the maximum cooling capacity. The parametric study has been carried out at different ambient temperatures (28 / 35 / 43 ºC) for the adsorption system layout implemented in the car prototype, as shown in Fig. 52, assuming a constant temperature of 90 ºC for the engine coolant water. In this study, the values assumed for the ambient temperatures correspond to the ones considered by CRF for the assessment tests (see subsection 7.3.2.3). Furthermore, the mass flow rates values for the heating water (i.e. engine-bed water loop in Fig. 52), cooling water (i.e. radiator-condenser-bed water loop in Fig. 52) and chilled water (i.e. evaporator-air cooler water loop in Fig. 52) are

settable, constant, and correspond to the values provided by CRF implemented in the car prototype. The air flow rate values passing through the radiator and cabin cooler are taken from the experimental data given by CRF.

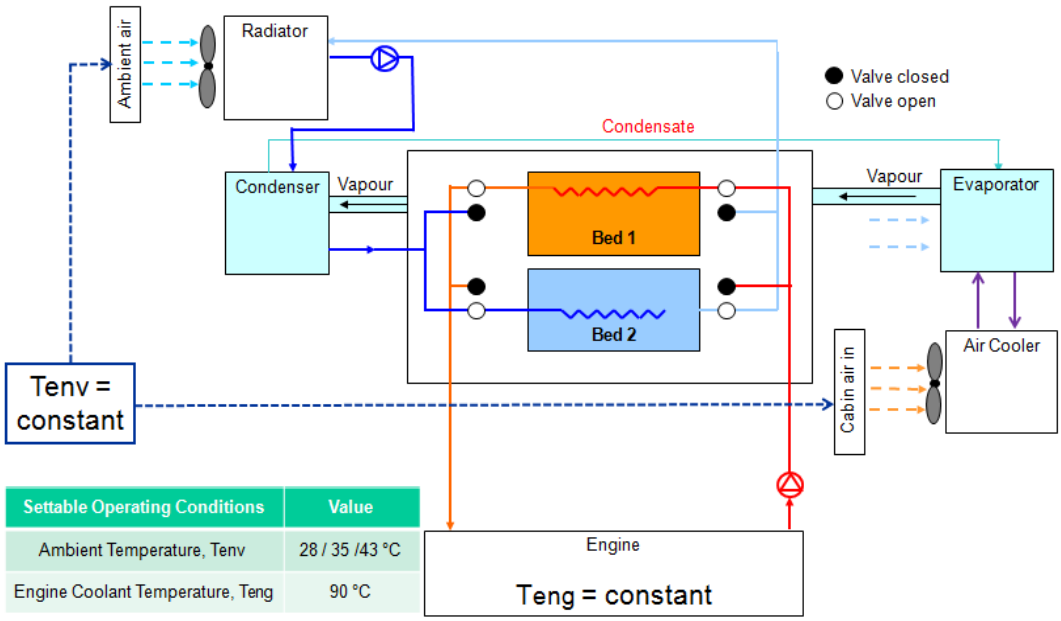

Fig. 52. Scheme of the onboard adsorption A/C system (ECN system design) and operating temperatures considered for the parametric studies.

The effect of the cycle time on the cooling capacity and COP at different ambient temperatures is presented in Fig. 53. The cycle time is defined here as the sum of the adsorption and desorption times. Since the beds operate alternately (one bed is in regeneration mode while the other in cooling mode), the desorption and adsorption times must be the same. The cooling capacity and COP are calculated by the model as the average for the last cycle, once the system is operating in steady-state conditions and the initialization period does not have an effect over the performance anymore.

As it can be seen on Fig. 53(a), the cooling capacity decreases abruptly when cycle times are shorter than 350 s, and this is due to the fact that there is not enough time for adsorption or desorption to occur satisfactory. On the other hand, when cycle times are longer than the optimum values, the cooling capacity decreases gradually since adsorption tends to become less intensive as the adsorbent approaches to its equilibrium condition. However, for ambient

temperatures at 35 and 43 ºC, the cooling capacity does not decrease significantly when the cycle time is longer than its optimum value. On the contrary, the COP increases uniformly as the cycle time increases (see Fig. 53(b)). This occurs because the final part of the adsorption/desorption process increases the cooling produced but requires a longer time, therefore the cooling capacity decreases.

Furthermore, the outdoor air temperature also has an effect on the performance. As can be seen on Fig. 53(a) the cooling capacity increases with decreasing ambient temperature. When the outdoor air temperatures are high (such as 43 ºC), the cooling down of the bed is taking place at a higher temperature. This has a negative effect on the cooling capacity, since a less amount of water vapour is therefore adsorbed in the sorption bed. It can be said that the refrigeration effect will be improved when the system is operating at lower environmental temperatures since the cooling process of the beds will be more efficient, allowing faster cycling times. In contrast the COP decreases with decreasing ambient temperatures. This occurs because the system requires more engine waste energy to heat the sorption bed when working at lower ambient temperatures, since it will be more difficult to heat the bed after it has been cooled down at lower cooling temperatures. However, the impact of the cycle time on the COP is more significant than the environmental temperatures.

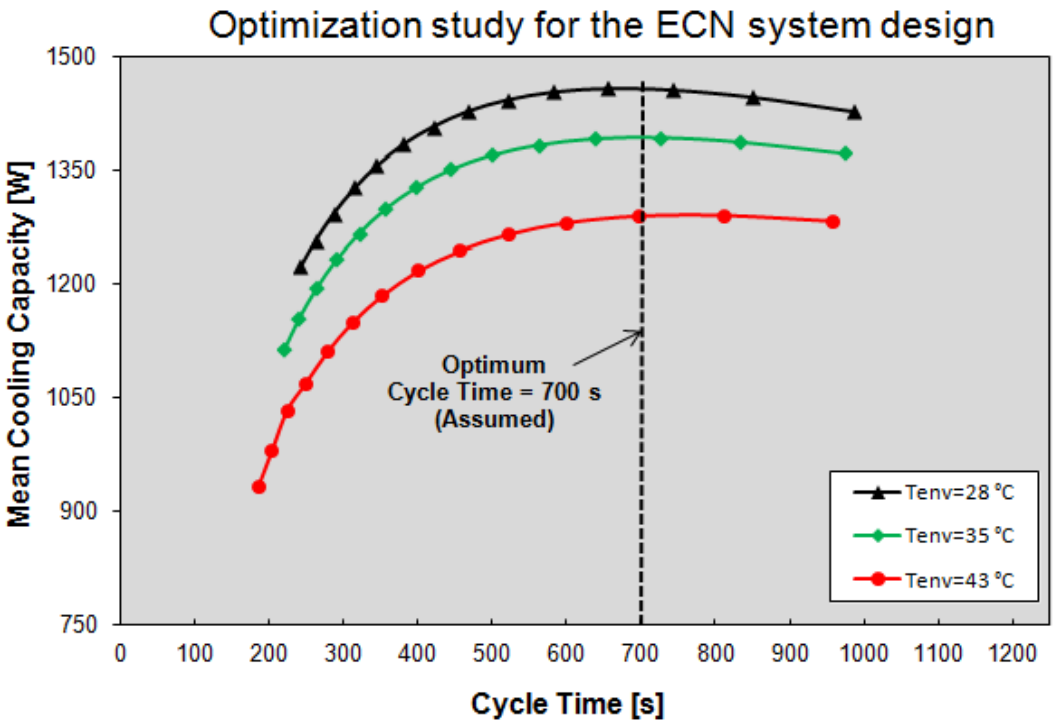

(a)

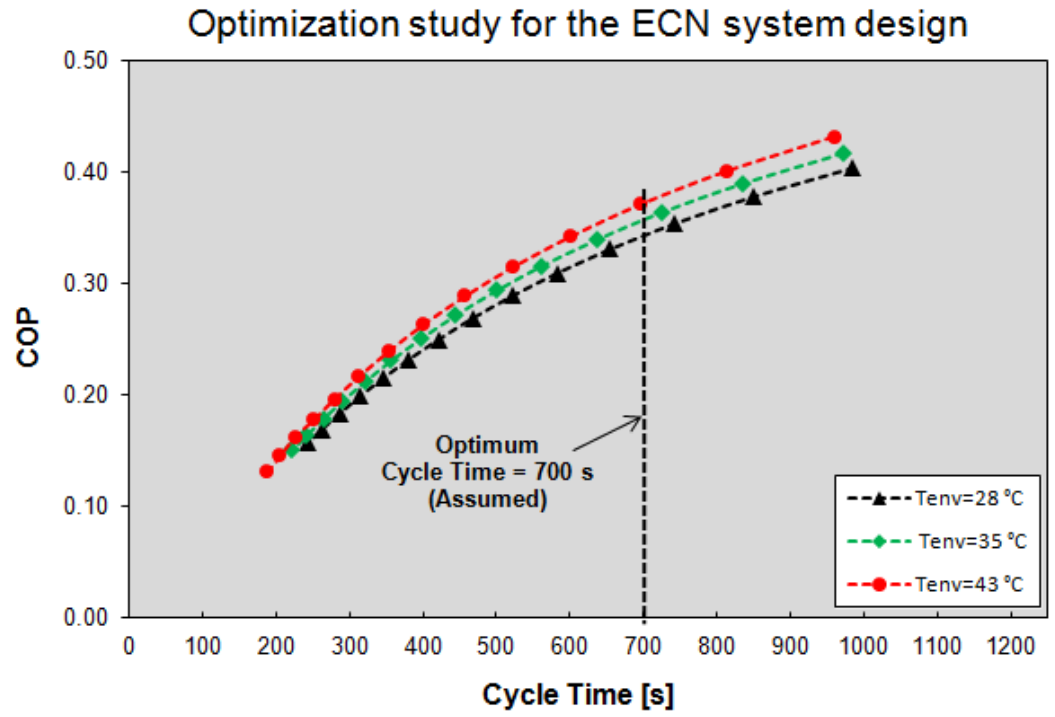

(b)

Fig. 53. Effect of the cycle time on the system performance at different ambient temperatures: (a) Cooling Capacity and (b) COP.

Table 12 summarizes the optimum value for the cycle time, and corresponding maximum cooling capacity and COP at different ambient temperatures. From

the results obtained, when the ambient temperature drops from 43 ºC to 28 ºC, the maximum cooling capacity increases from 1291 W to 1459 W and the COP decreases from 0.39 to 0.33. On the other hand, the optimum cycle time maximizing the capacity increases from 656 to 812 s when the environmental temperature increases from 28 to 43 ºC.

Table 12. Results of the cycle time optimization study.

Tenv [ºC]	Optimum Cycle Time [s]	Optimum Ad/Desorption Time [s]	Maximum Cooling Capacity [W]	COP
28	656	328	1459	0.33
35	726	363	1393	0.36
43	812	406	1291	0.39

The results obtained from the parametric studies provide a guideline for the design and optimization of a control system aimed to provide the maximum cooling output at different operating conditions. It can be said that an optimum value around 700 s for the cycle time (i.e. an ads/desorption time of 350 s) could make the system achieve a good performance for the range of ambient temperatures studied (from 28 ºC to 43 ºC).

7.4.3. System layout modification

During the Topmacs project [65], an alternative layout for the adsorption A/C system, different from the one implemented in the car prototype, has been studied in order to further increase the system performance. The only difference between this system layout and the one designed by ECN is the number of radiators. Instead of using one radiator to cool in series first the condenser and then the bed, the proposed system is comprised of two radiators working in independently cooling loops, where one radiator is used to cool down the bed and another is used to cool down the condenser. Fig. 54 shows the alternative system layout and the operating conditions considered for the parametric studies.

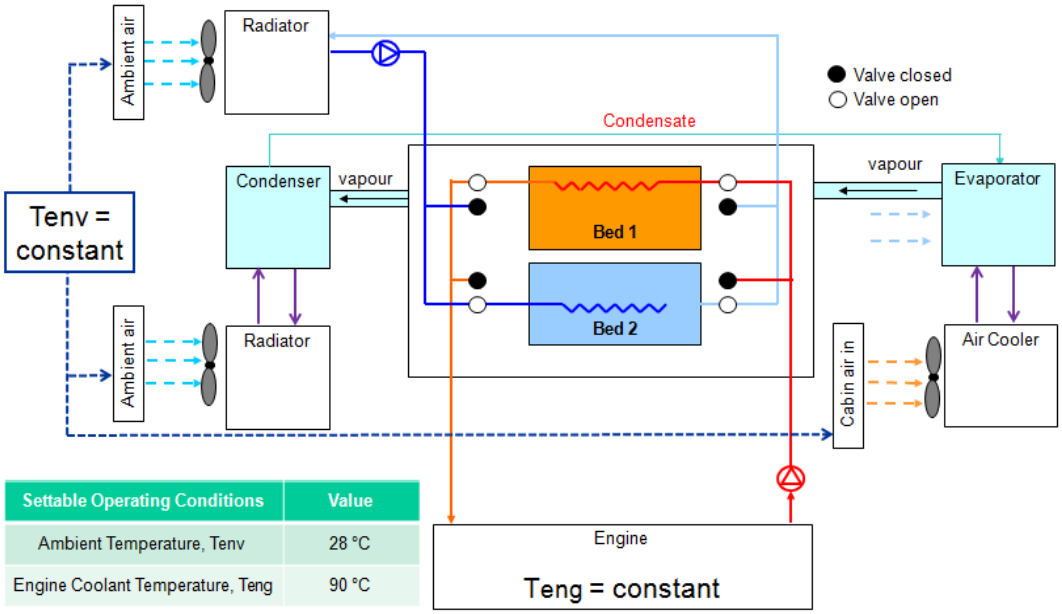

Fig. 54. Scheme of the proposed system (alternative system design) and operating temperatures considered for the parametric studies.

The parametric study described above has been carried out for the system layout sketched in Fig. 54 (named here alternative system design), assuming a constant temperature of 90 ºC for the engine coolant water and an ambient temperature of 28 ºC. The results presented here have been compared to the results obtained previously for the ECN system layout sketched in Fig. 52.

The effect of the cycle time on the cooling capacity and COP for the conditions mentioned above is presented in Fig. 55. If the maximum cooling capacity obtained for the alternative system layout is compared with the one obtained for the ECN system layout, it can be observed a clear increase of the system performance. From the results obtained, when using one secondary water loop to cool in series first the condenser and then the bed (see ECN system layout) instead of two independent cooling loops (see alternative system layout), the cooling capacity decreases from 1638 to 1459 W and the optimum cycle time increases from 511 to 656 s. This occurs because the cooling water enters the bed at higher temperature since it has previously absorbed heat from the condenser, consequently, less amount of water vapour will be adsorbed by the bed. This will negatively affect the performance of the system. On the other hand, for the alternative system layout, the cooling of the beds will take place at

lower temperature, allowing faster cycling times. This will further improve the system's performance. On the contrary, the system COP will slightly decrease when having two independent cooling loops instead of one. This occurs because the system requires more engine waste energy to heat the sorption bed when working at lower cooling temperatures. This happens as it will be more difficult to heat the bed after it has been cooled down at lower cooling temperatures.

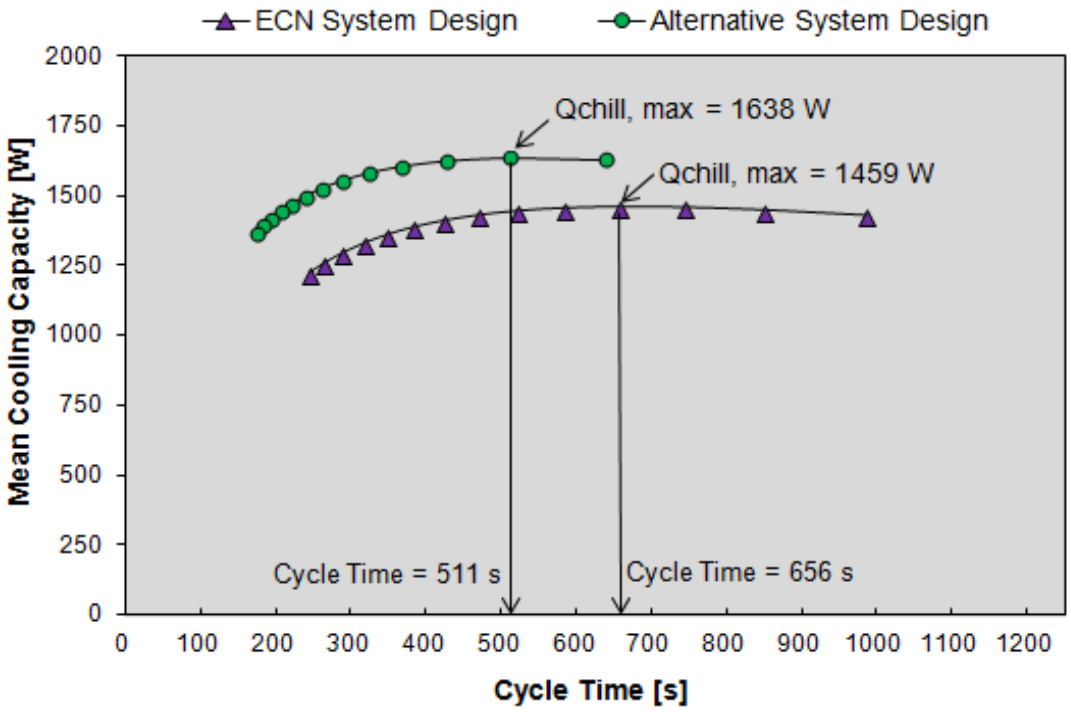

(a)

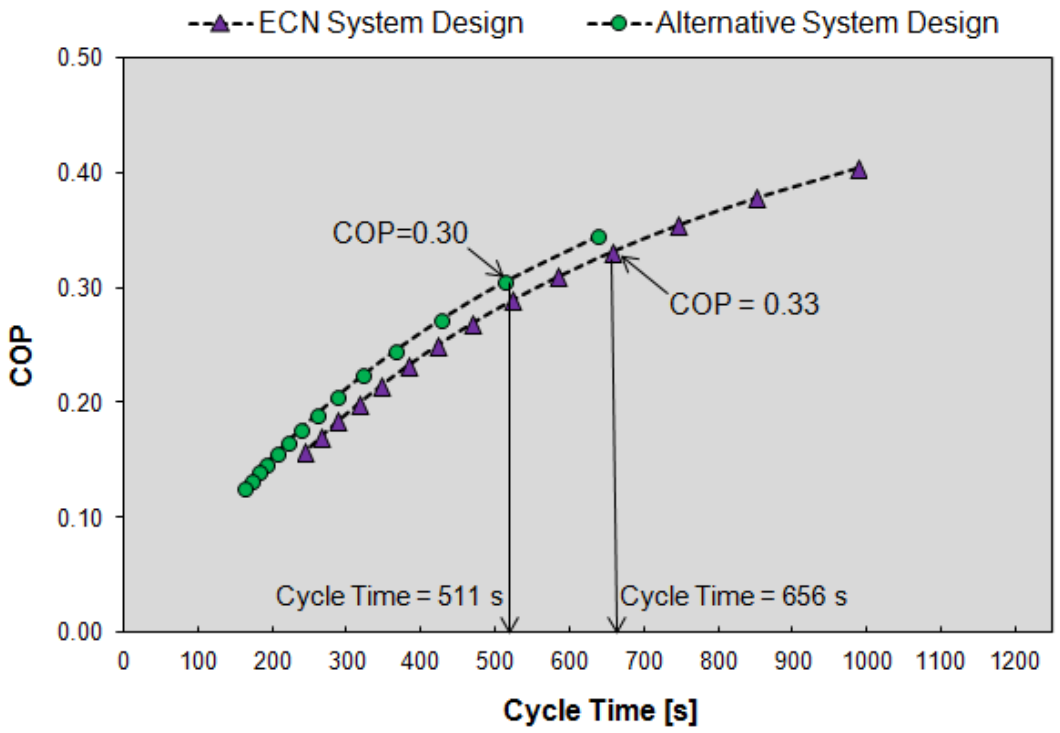

(b)

Fig. 55. Effect of the cycle time on the system performance for different system layouts: (a) Cooling Capacity and (b) COP.

The variation of the bed heating and cooling water temperatures with the cycle time for the system layouts mentioned before is presented in Fig. 56. From the results obtained, when using one secondary water loop to cool in series first the condenser and then the bed (see ECN system layout) instead of two independent cooling loops (see alternative system layout), the inlet cooling water temperature slightly increases from 36 to 37.6 ºC (at the optimum cycle time). This happens because the cooling water entering the bed absorbs first the heat from the condenser, coming back to the bed at a higher temperature. Also, the difference between the inlet and outlet cooling water temperature is smaller, which means that the bed is being cooled less efficiently and it takes longer time to cool down. Consequently, the cycle time is longer in comparison with the alternative system. On the other hand, the cooling water leaving the bed slightly decreases from 39.9 to 38.7 ºC (at the optimum cycle time) when using two independent cooling loops instead of one. Also, the difference between the inlet and outlet heating water temperature is higher in comparison with the ECN system. The outlet heating water temperature is lower in the case

of having two independent cooling loops, since the bed absorbs more heat from the engine so it returns at lower temperature (87.2 ºC at the optimum cycle time). This happens since it is more difficult to heat the bed after it has been cooled down at lower cooling water temperatures.

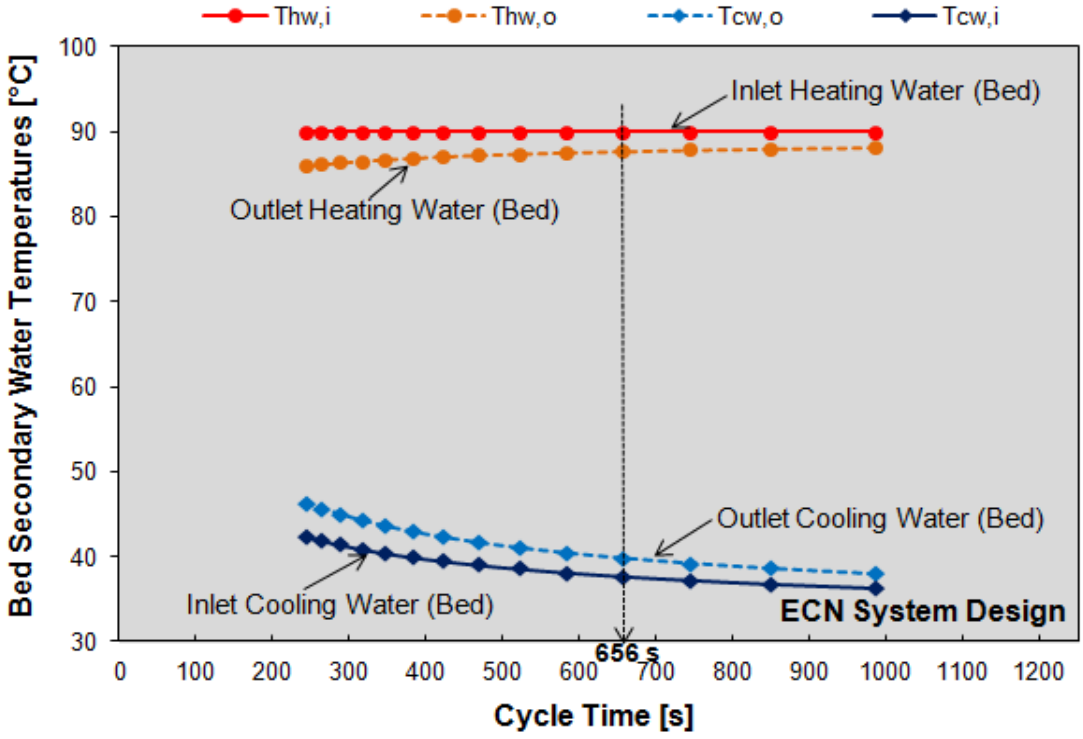

(a)

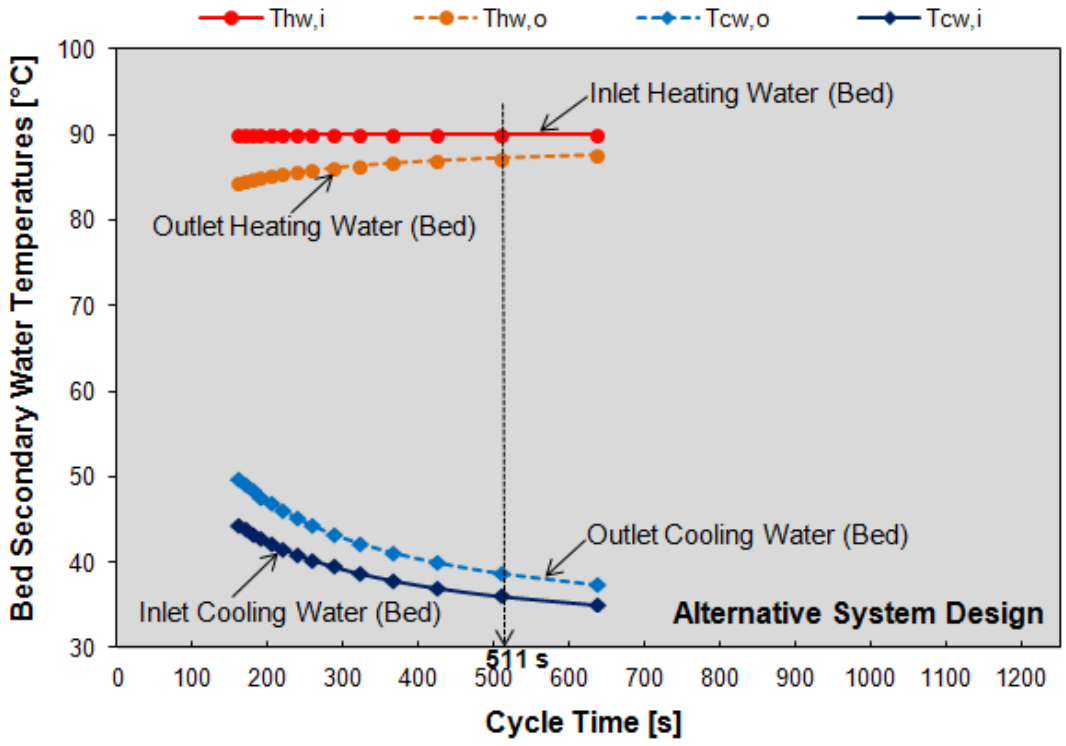

(b)

Fig. 56. Variation of the bed heating and cooling water temperatures with cycle time for different system layouts: (a) ECN system design; (b) Alternative system design.

The variation of the condenser and evaporator secondary water temperatures with the cycle time for the system layouts mentioned before is presented in Fig. 57. From the results obtained, when using one secondary water loop to cool in series first the condenser and then the bed (see ECN system layout) instead of two independent cooling loops (see alternative system layout), the inlet condenser cooling water temperature increases from 30.59 to 36.86 ºC, and as a consequence the condenser temperature increases from 33.26 to 39.24 ºC. This happens because the cooling water entering the condenser first absorbs the heat from the bed coming back to the condenser at higher temperature. When using two independent cooling loops instead of one, the condenser is cooled down at lower temperature, and as a consequence the condenser temperature decreases as the condenser is able to reject more heat, in turn improving the performance. Moreover, the chilled water temperature entering the evaporator decreases from 14 to 12.3 ºC and the evaporator temperature decreases from 11 to 9 ºC when having two independent cooling loops instead of one. When having a single cooling water loop, the refrigerant comes from the condenser to the evaporator at a higher temperature, which results in an increase of the evaporator temperature. Also, it absorbs less amount of vapour from the evaporator since it is more difficult to cool down the bed. Consequently, the evaporator pressure increases. This negatively affects the overall performance of the system.

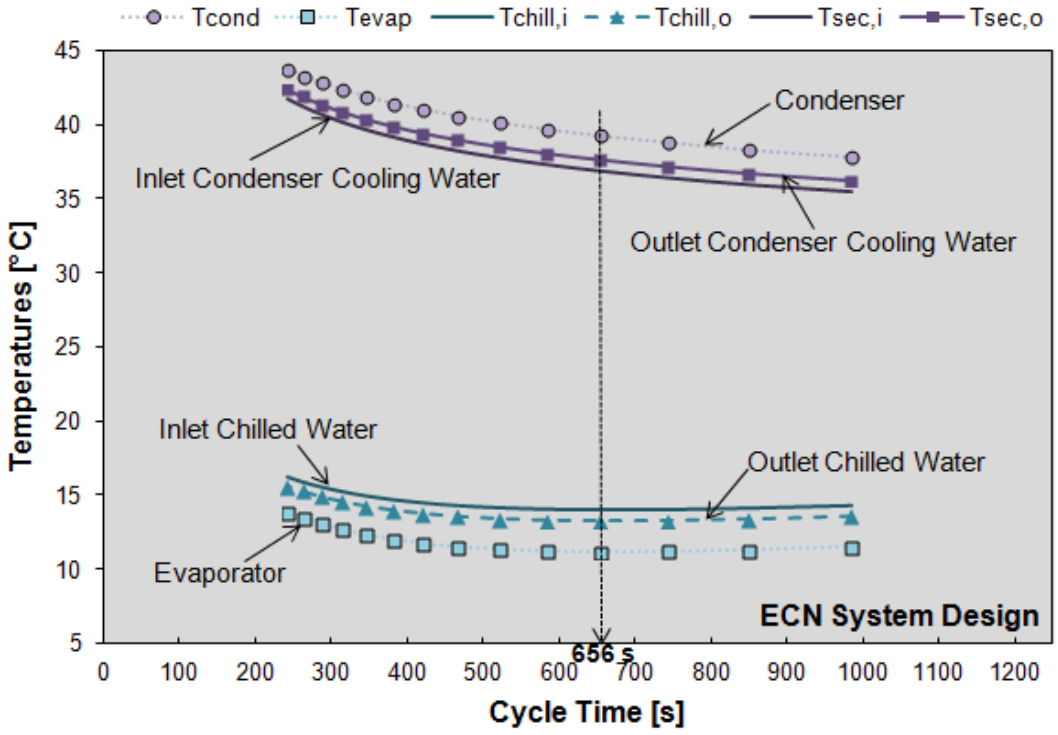

(a)

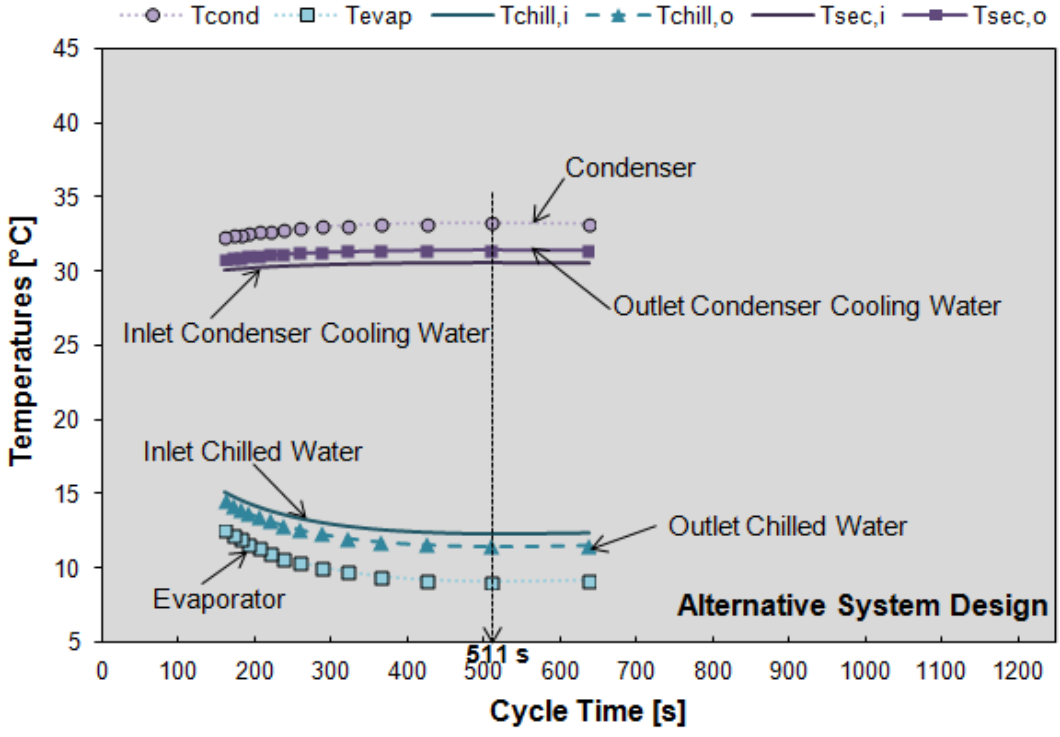

(b)

Fig. 57. Variation of the evaporator and condenser secondary water temperatures with cycle time for different system layouts: (a) ECN system design (b) Alternative system design.

7.5. Performance estimation of the onboard adsorption A/C system at real driving conditions

7.5.1. Introduction

Different test conditions have been simulated in order to assess the performance of the whole adsorption A/C system (engine, adsorption cooling system and cabin). The system under evaluation is the one corresponding to the onboard system (see Fig. 48). A sample of results for the test performed at ambient temperature of 28ºC and relative humidity of 50% (Test Nº 1), and also for the Cooldown test at severe conditions is presented in this chapter. For all the tests it is assumed that the A/C system is working in recirculation mode. This means that the inlet air temperature to the cabin cooler is at the cabin temperature, which will be decreasing with the time. This is the usual mode of operation for the A/C system in summer conditions.

7.5.2. Beds control strategy

The control strategy of the beds implemented on the overall model was based on a fixed cycle time. This means that the adsorption/desorption cycle will be reversed when it reaches a settable value which is 350 s. The value assumed for the adsorption/desorption cycle time corresponded to the optimum value obtained from the parametric studies already presented in subsection 7.4.2. However, the simulation results showed a poor performance when a fixed cycle time was implemented in the model. This happened because the bed could not be heated up efficiently once the bed temperature at the end of the cycle was not close to 90 ºC, and as consequence the system could not adsorb enough vapour. This fact negatively affected the system performance. Therefore, a different bed control strategy was implemented which was not only based on the cycle time but also on the maximum temperature of the bed. This strategy is based on a double condition: the cycle will be reversed when the bed in heating mode reaches at least 85 ºC, and the cycle time reaches at least its optimum value (350 s). The results obtained showed a good operation of the system so

this double condition has been implemented in the overall model for all assessment tests.

7.5.3. Test nº 1 - Equivalent European Summer Conditions

Fig. 58 shows the simulation results obtained for the test at an ambient temperature of 28 ºC and relative humidity of 50% (Test Nº 1) for the most favourable start-up condition, which means that both beds are completely dry. In this case, it is assumed that all the valves of the adsorption system remain closed, and there is no leakage in the system, so that it is capable to maintain both beds completely dry until the following driving cycle.

Fig. 58(a) shows the temperature and pressure in the bed, at the above mentioned conditions. As discussed previously, the available waste heat from the engine under real driving conditions is very variable, especially during the engine warming up period. Therefore, the behaviour of the system during the initial period is influenced by the fact that there is no available waste energy at the engine to activate the adsorption system. In the first approximately 660 s after engine start-up, the outlet coolant temperature of the engine is below 90 ºC, so it is not possible to use the engine coolant as a heat source. Except at 550 s where there is a first activation peak and the engine coolant temperature reach 90 ºC for the first time. However, the bed is very cold and absorbs a lot of heat, producing a sudden drop of the engine coolant temperature. Consequently, the thermostat which controls the engine coolant flow to be used by the system is switched off, causing a deactivation of the adsorption system. After 660 s, the adsorption system is activated again and is able to use the waste energy from the engine coolant at temperature between 85-90 ºC, until time reaches 850 s. After the 850 s, the engine outlet coolant temperature goes above 90 ºC, insuring high engine efficiency. The adsorption system is then able to use the engine coolant as a higher temperature heat source, which lies between 90-95 ºC. Given that the car operates in quite constant driving conditions, the engine is able to provide a considerable amount of hot water at almost constant flow rate along the rest of the driving cycle. Therefore, the adsorption-desorption cycles become more regular.

Fig. 58(b) shows the uptake evolution in the beds. As it can be observed, Bed 1, which is being heated up, is kept dry (with the minimum uptake). Bed 2 is being cooled during this period and is adsorbing water vapour from the evaporator until the cycle is reversed. When Bed 2 almost reaches equilibrium conditions, at 520 s after the engine start-up, the cycle is reversed. Bed 1 then starts to adsorb since it is dry and empty of water, and Bed 2 starts to desorb as it is fully loaded with water. For the last stable cycle (from 1500 s to 1950 s) the uptake variation ranges from 6.5 % to 13 %.

Fig. 58(c) shows the produced cooling capacity as a function of time. As it can be seen, the system is able to produce a cooling effect since the very beginning. In this case, the heat from the engine is not needed to start producing cooling since the beds are assumed to be initially dry. In this way, once one of them is cooled down and connected to the evaporator, it starts to adsorb and produces a cooling effect immediately. This start-up strategy is the best case scenario since it allows the production of cold since the beginning of the driving cycle without the necessity of the engine coolant temperature to reach 90ºC. The adsorption system is able to produce an average cooling capacity of approximately 925 W.

Fig. 58(d) shows the cabin temperature as a function of time. As it can be seen, the temperature decreases during each cooling cycle. Then, during the reversing period, it slightly increases due to heat transferred from the cabin to the inner air. As it can be observed, the system is able to cool down the air quite fast, reaching a quite low temperature. The final cabin temperature depends on the test. In this case, the system is able to decrease the cabin temperature from 28 ºC down to 17.5 ºC. As such, the comfort conditions will be achieved, since the final cabin temperature is below the target value, which is 20 ºC. In real use, the cabin thermostat would switch off the system once the comfort temperature has been reached.

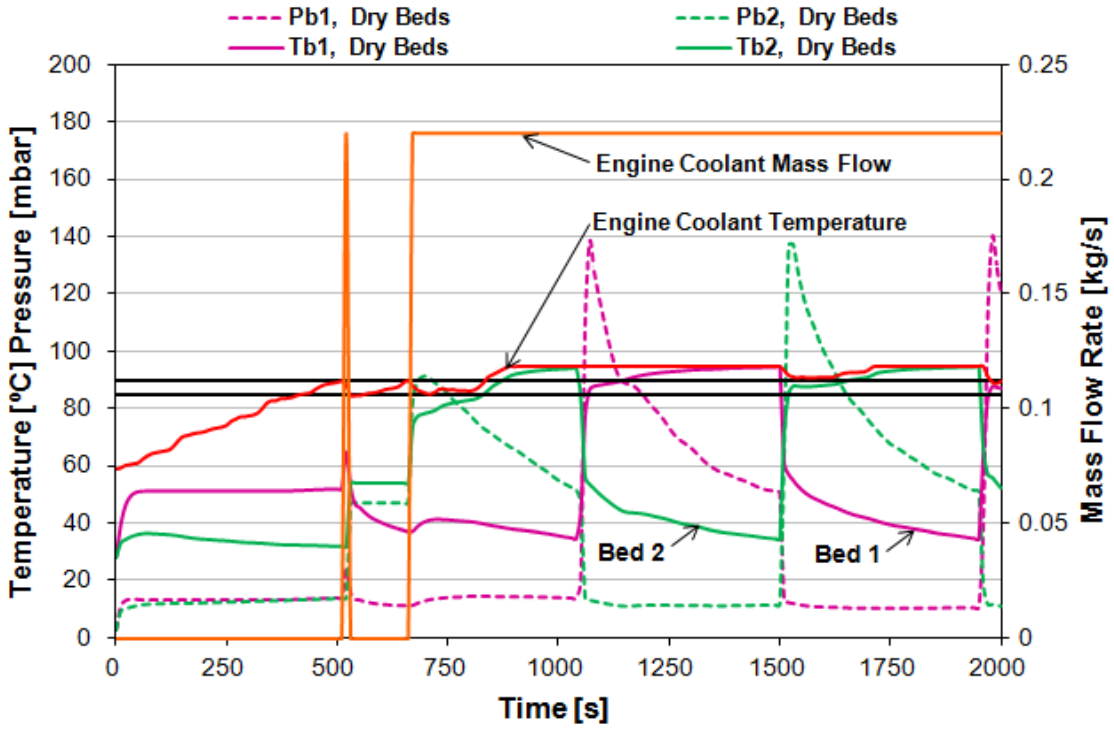
Pb1, Dry Beds
Tb1, Dry Beds
Pb2, Dry Beds
Tb2, Dry Beds
Engine Coolant Mass Flow
Engine Coolant Temperature
Bed 2
Bed 1
Temperature [ºC] Pressure [mbar]
Mass Flow Rate [kg/s]
Time [s]
0
20
40
60
80
100
120
140
160
180
200
0
0.05
0.1
0.15
0.2
0.25
0
250
500
750
1000
1250
1500
1750
2000

(a)

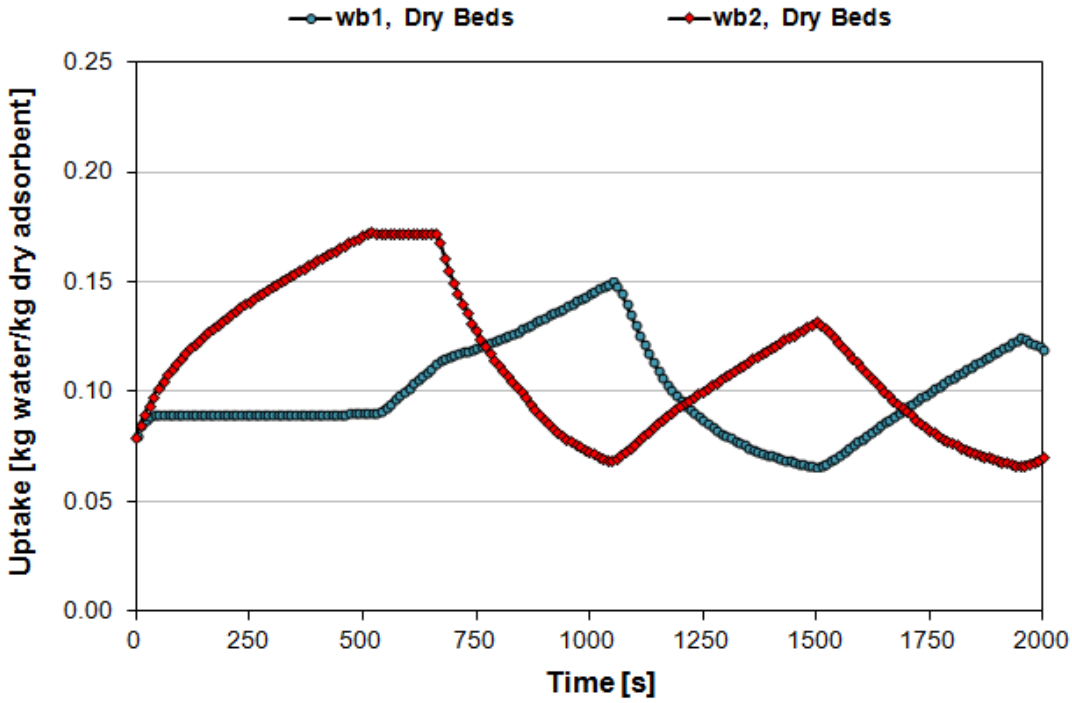
wb1, Dry Beds
wb2, Dry Beds
Uptake [kg water/kg dry adsorbent]
Time [s]
0.00
0.05
0.10
0.15
0.20
0.25
0
250
500
750
1000
1250
1500
1750
2000

(b)

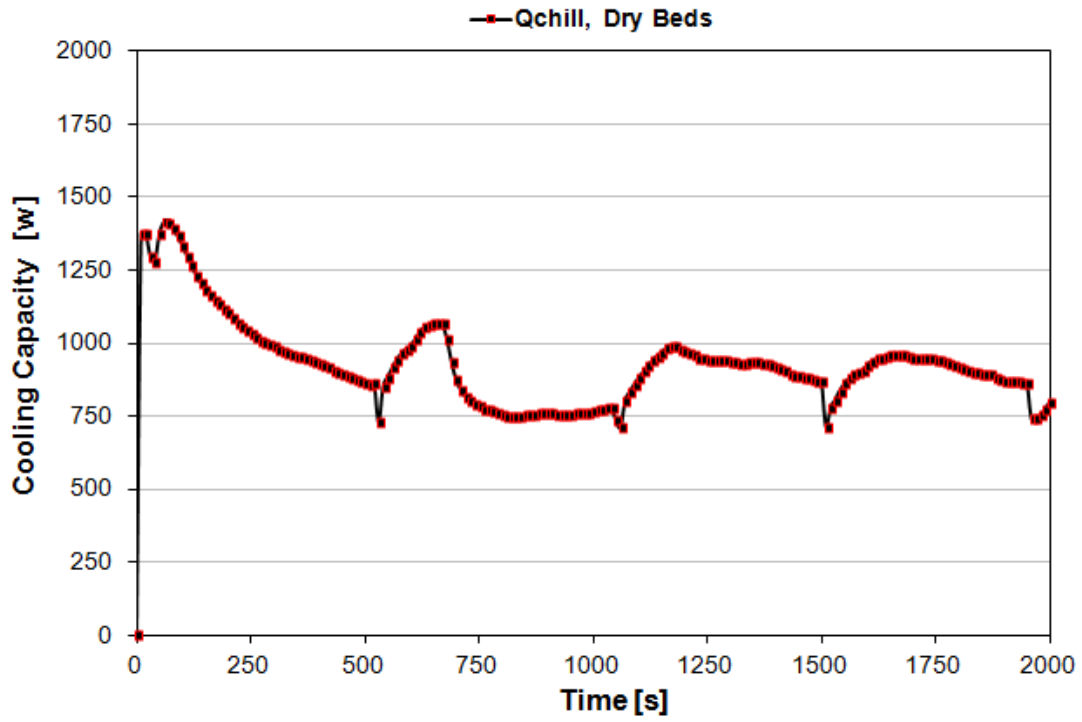

(c)

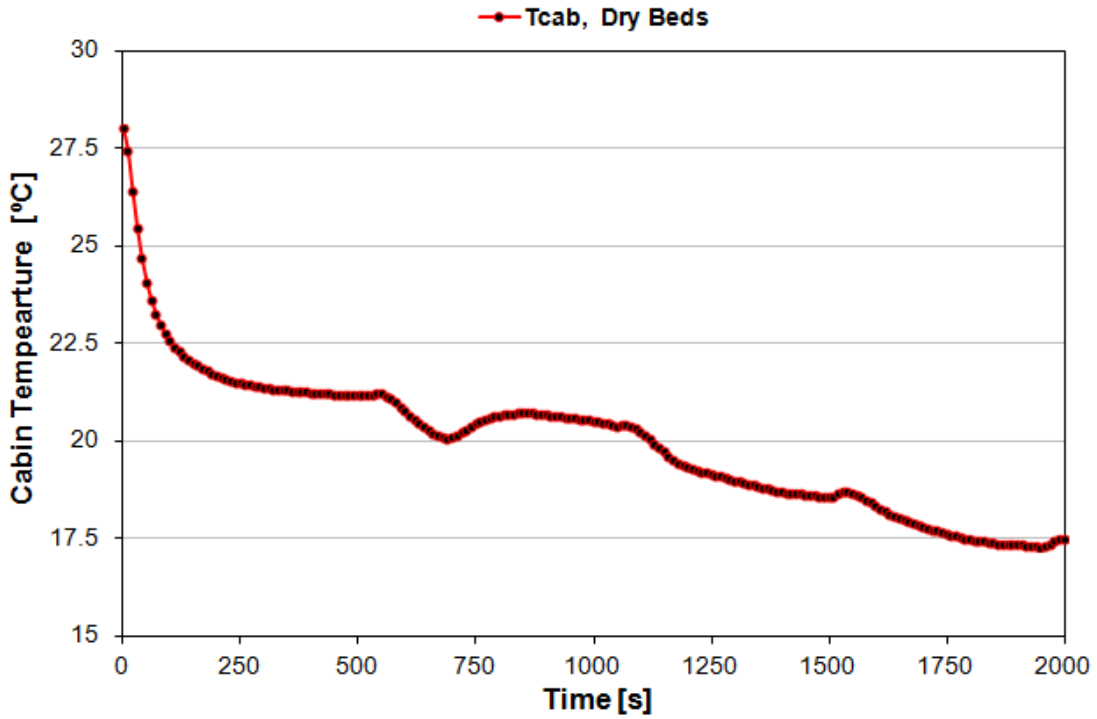

(d)

Fig. 58. Test Nº 1: Equivalent European Summer Conditions (28 ºC and 50% RH). Start-Up Strategy: Dry Beds. Calculated values: (a) Temperature and pressure evolution at bed 1 and bed 2; Engine coolant temperature and mass flow rate evolution; (b) Uptake evolution; (c) Cooling capacity evolution; (d) Cabin temperature evolution.

Fig. 59 shows the simulation results obtained along the test at an ambient temperature of 28 º C and relative humidity of 50 % (Test Nº 1) for the three studied start-up conditions: Dry Beds, 1 Dry Bed and Saturated Beds.

Fig. 59(a) shows the cooling capacity evolution predicted by the model for the different start-up conditions. As it can be observed, when the two beds are saturated, the system takes a long time to start producing a cooling effect (around 1100s), while if at least one bed is dry it is possible to have cold production since the beginning of the driving cycle. With both beds initially dry, the system is logically able to produce an increased cooling effect, and therefore a faster decrease of the cabin temperature. Nevertheless, the difference between having one or two beds dry is not so important. This indicates that in order to have good performance it would only be necessary that, after the engine is switched off, one of the beds is dried and sealed. The system with two dry beds is able to produce a mean cooling capacity of 925 W, with one dry bed is able to produce a mean cooling capacity of 700 W, and with both beds saturated it is able to produce a mean cooling capacity of 300 W.

Fig. 59(b) shows the cabin temperature evolution predicted by the model for the different start-up conditions. As it can be observed, if at least one of the beds is dried, the adsorption cooling system is able to reach a cabin temperature lower than 20 ºC, which is the comfort temperature. Keeping both beds dry results in more efficiency for the system performance, and also the comfort conditions are reached quicker.

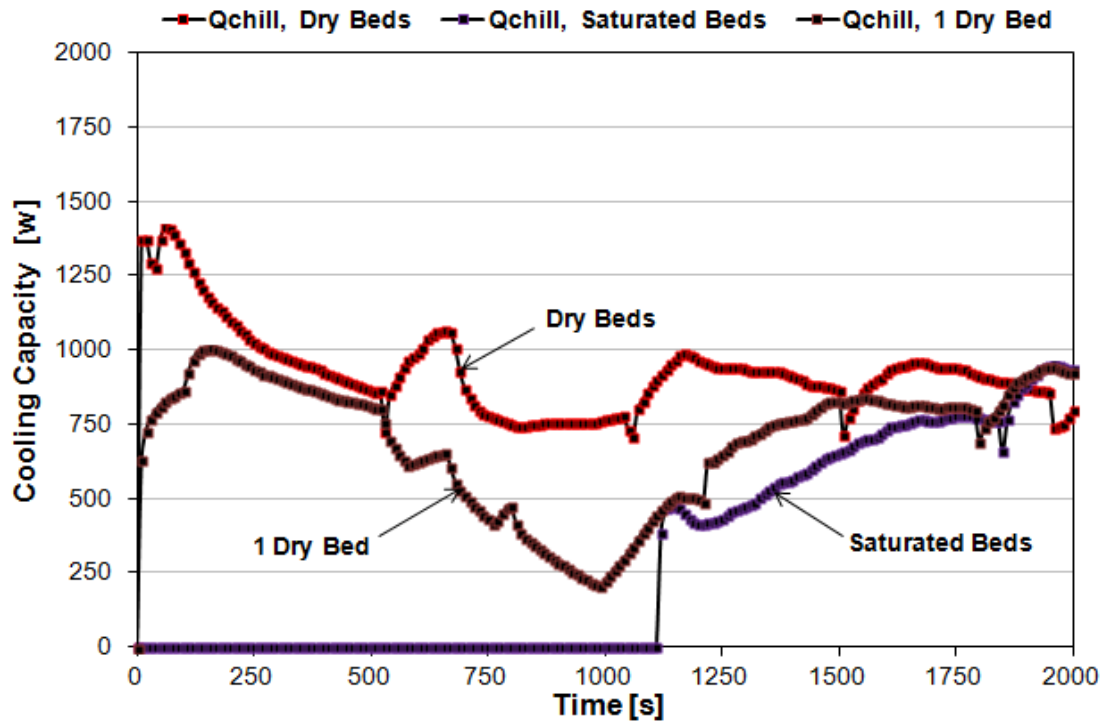

(a)

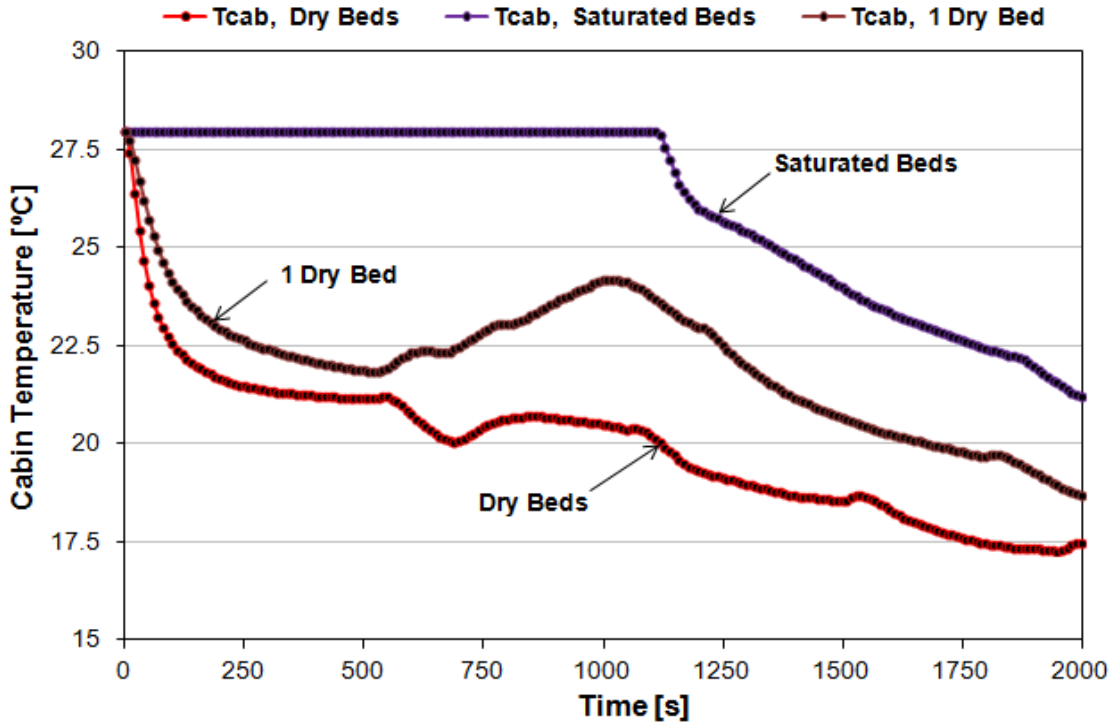

(b)

Fig. 59. Test Nº 1: Equivalent European Summer Conditions (28 ºC and 50% RH). Three Start-Up Strategies: Dry Beds, 1 Dry Bed and Saturated Beds. Calculated values: (a) Cooling capacity evolution; (b) Cabin temperature evolution.

7.5.4. Test Nº 3 - Cooldown

Fig. 60 shows the simulation results obtained along the cooldown test (Test Nº 3), again for the best start-up condition: Dry Beds. The cooldown test is the most severe test of all assessment tests. The ambient temperature is set at 43 ºC; however, the temperature of the cabin is higher due to soaking (46 ºC). These are highly severe conditions for the thermal compressor.

As it can be seen in Fig. 60(a), the adsorption-desorption cycles are more stable, in comparison with previous results, due to the characteristics of the assessment test. For the cooldown cycle test, the car is in highway driving mode, which guarantees that a more constant engine coolant mass flow rate is sent to the adsorption system. Furthermore, the cycle time is shortened since the system performs at higher cooling temperature, so that it tends to follow quite fast adsorption-desorption cycles, and the range of uptake variation becomes very small (see Fig. 60(b)). As a consequence, the number of cycles per driving cycle and their frequency increase, which leads to a slight increase of the cooling capacity. Thus, the system is able to produce a mean cooling capacity of approximately 1100 W (see Fig. 60(c)). Nevertheless, the cooling effect produced by the system is not enough to carry the cabin temperature to comfort conditions (target value 25 ºC), and is only able to keep the cabin at around 37 ºC (see Fig. 60(d)). The system is obviously undersized if it has to cope with these severe conditions. The operation could be improved by modifying the switching criterion and increasing the cycle time.

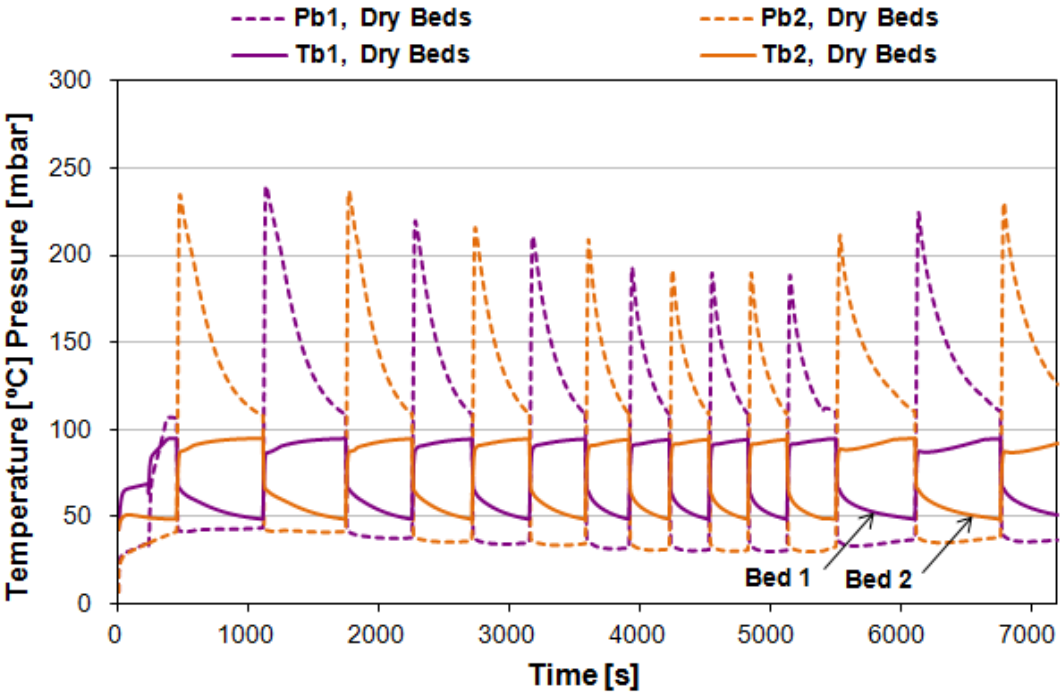
Pb1, Dry Beds
Pb2, Dry Beds
Tb1, Dry Beds
Tb2, Dry Beds
Temperature [ºC] Pressure [mbar]
300
250
200
150
100
50
0
0
1000
2000
3000
4000
5000
6000
7000
Time [s]
Bed 1
Bed 2

(a)

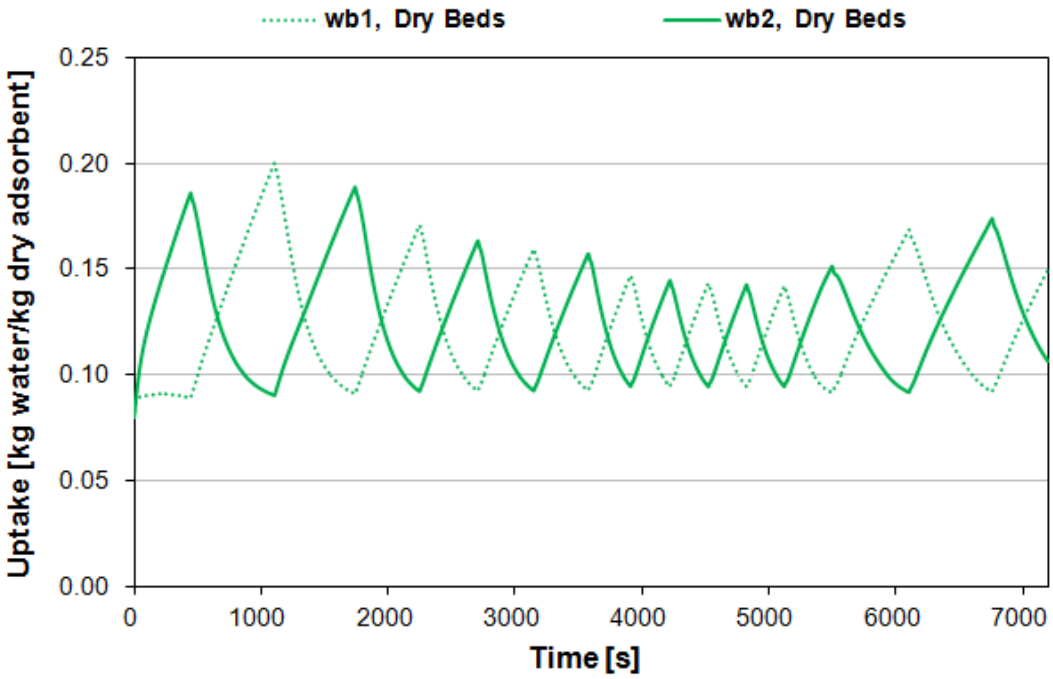
wb1, Dry Beds
wb2, Dry Beds
Uptake [kg water/kg dry adsorbent]
0.25
0.20
0.15
0.10
0.05
0.00
0
1000
2000
3000
4000
5000
6000
7000
Time [s]

(b)

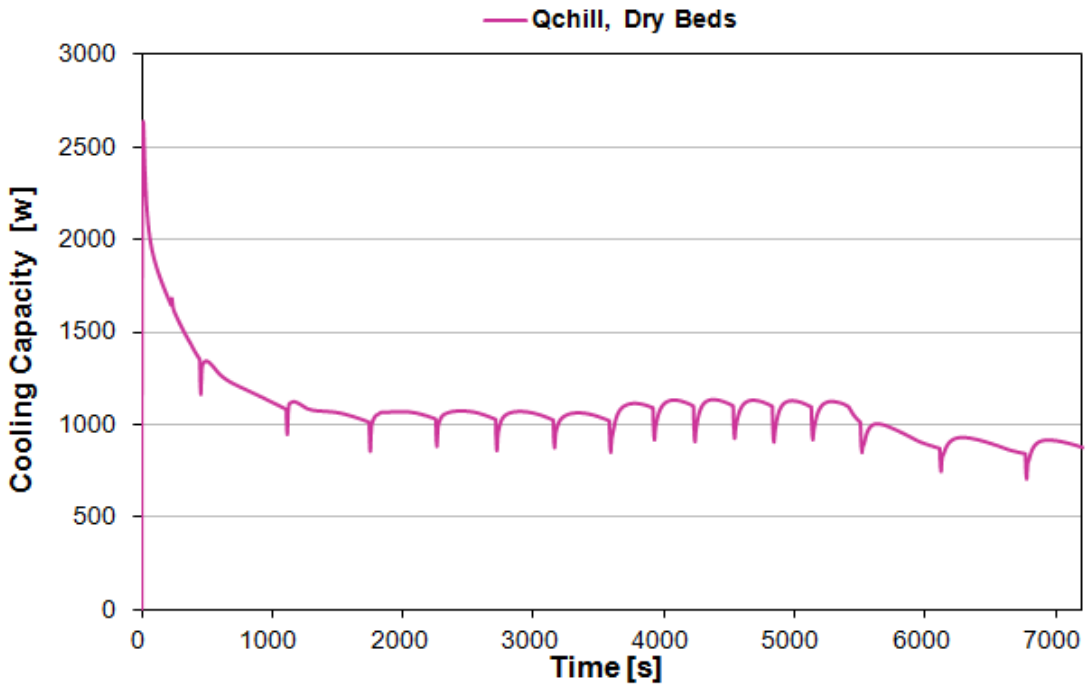

(c)

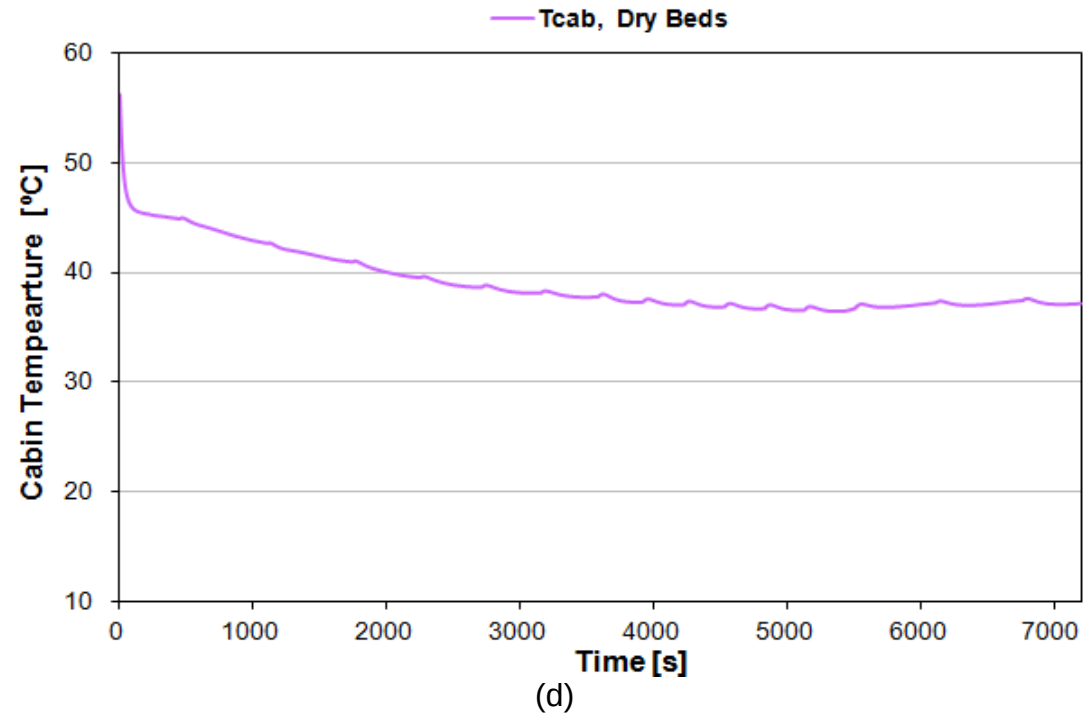

(d)

Fig. 60. Test Nº 3: Cooldown (+43 ºC and 35 % RH). Start-Up Strategy: Dry Beds. Calculated values: (a) Temperature and pressures evolution at bed 1 and bed 2; (b) Uptake evolution; (c) Cooling capacity evolution; (d) Cabin temperature evolution.

7.5.5. System performance comparison at different test conditions

A comparison between the system performances obtained at different test conditions, for the best start-up scenario (Dry Beds), is shown in Table 14.

Results obtained showed that, for Test Nº 1 (Equivalent European Summer Conditions), the adsorption cooling system is able to deliver a cooling capacity of 925 W with a COP of 0.40. For these testing conditions, the system was able to keep the cabin temperature at 17.5 ºC, which means that comfort conditions can be perfectly achieved.

A mean cooling capacity of 930 W with a COP of 0.42 was obtained for Test Nº 2 (Severe Summer Conditions). Under these conditions, the system is able to produce a reasonable cooling effect but not enough to carry the cabin temperature to comfort conditions (target value 23 ºC), and is only able to keep the cabin at around 24.4 ºC.

For the most severe of all assessment tests (Test Nº 3), the system is able to produce a mean cooling capacity of 1100 with a COP of 0.44. However, the cooling effect produced by the system is not enough to carry the cabin temperature to comfort conditions (target value 25 ºC). As it can be observed in Table 13, under severe conditions the COP of the system tends to increase. This is simply due to the fact that the system performs at a higher cabin temperature, which leads to an increase of the evaporation temperature.

Table 13. System performance at different operating conditions for the best start-up condition: Dry Beds.

TEST	T_{env} [ºC]	RH [%]	Final T_{cab} [ºC]	Target T_{cab} [ºC]	$\dot{Q}_{chill}$ [W]	COP
Nº 1: Equivalent European Summer Conditions	28	50	17.5	20	925	0.40
Nº 2: Severe Summer Conditions	35	60	24.4	23	930	0.42
Nº 3: Cooldown	43	35	37	25	1100	0.44

7.5.6. Performance of an adsorption A/C system for a truck

As it has been mentioned in chapter 3, a prototype of a truck driver-cabin adsorption air conditioner, which employs zeolite-water as working pairs and is driven by the waste heat from the engine coolant loop, was realized by CNR-ITAE under the framework of the Topmacs project [65]. The overall size of the prototype was 170 dm^3 and its weight 60 kg, so it was deemed suitable for mobile applications. Performance tests under different driving conditions have been simulated in order to assess the performance of the whole system (engine adsorption system and cabin). The same kind of assessment tests (already mentioned in subsection 7.3.2) have been carried out for the truck. However, the input temperature and mass flow rate of the engine coolant sent to the adsorption system is more constant, in comparison with the previous system, since the truck is mostly operating in highway driving conditions. Simulated results obtained along the test under Equivalent European Summer Conditions (Test Nº 1), for the different considered start-up conditions, showed that the system is able to reach a cabin temperature lower than 20 ºC, which is the target comfort temperature. The system with both beds dry is able to produce a mean cooling capacity of 1400 W with a COP of 0.40, with one bed dry is able to produce a cooling capacity of 1295 W with a COP of 0.30, and with both beds saturated it is able to produce a cooling capacity of 974 W with a COP of 0.20.

7.5.7. Effect on the performance when using two radiators

The possibility of employing two radiators to increase the performance of the adsorption system has been considered as an option from the beginning of the Topmacs project [65]. However, the decision was made not to proceed with this option, since it would increase the complexity of the onboard system in terms of size and cost. Despite this, the overall model has been built in such a way that it is possible to test different layouts and therefore it was decided to study this possibility as well. The system layout, which includes two radiators (named here as alternative system design) can be seen in Fig. 54.

The effect on the performance when using two radiators to independently cool down the condenser and the bed, instead of using one radiator to cool in series first the condenser and then the bed has already been discussed in subsection 7.4.3. The study presented here is the same, but for dynamic conditions. The effect of using two independent radiators on the performance is presented for the test performed at ambient temperature of 28 ºC and relative humidity of 50% (Test Nº 1). The results obtained have been compared to the results obtained previously for the system layout with only one radiator, which corresponds to the ECN system layout (see Fig. 52) implemented in the car prototype.

Fig. 61 shows the cooling capacity and cabin temperature evolution, at the conditions mentioned above, for the most favourable start-up condition, meaning that both beds are completely dry. As it can be observed, when using two radiators working in independently cooling loops, the system gains some cooling capacity. The system using two radiators is able to reduce the cabin temperature to 16.5 ºC with a mean cooling capacity of 990 W with a COP of 0.30, while when using one radiator the system is able to reduce it to 17.5 ºC with a mean cooling capacity of 925 W with a COP of 0.40 for the best start-up scenario (Dry Beds). This happens because in the case of using the same radiator to cool in series first the condenser and then the bed, it becomes more difficult to cool down the beds with water coming from the condenser at a higher temperature. As a consequence, a less amount of water vapour is adsorbed, resulting in a lower refrigeration effect. On the contrary, when using two radiators instead of one, the COP decreases. This happens due to the fact that the system using two radiators performs at a lower evaporation temperature due to a decrease of the cabin temperature. The COP is very sensitive to the evaporation temperature.

From the obtained results, it is clear that using two independent radiators is more efficient, leading to better performance in terms of cooling capacity. However, the difference is not high, and whether this option is cost effective or not would depend on the increase of the cost to include the second radiator.

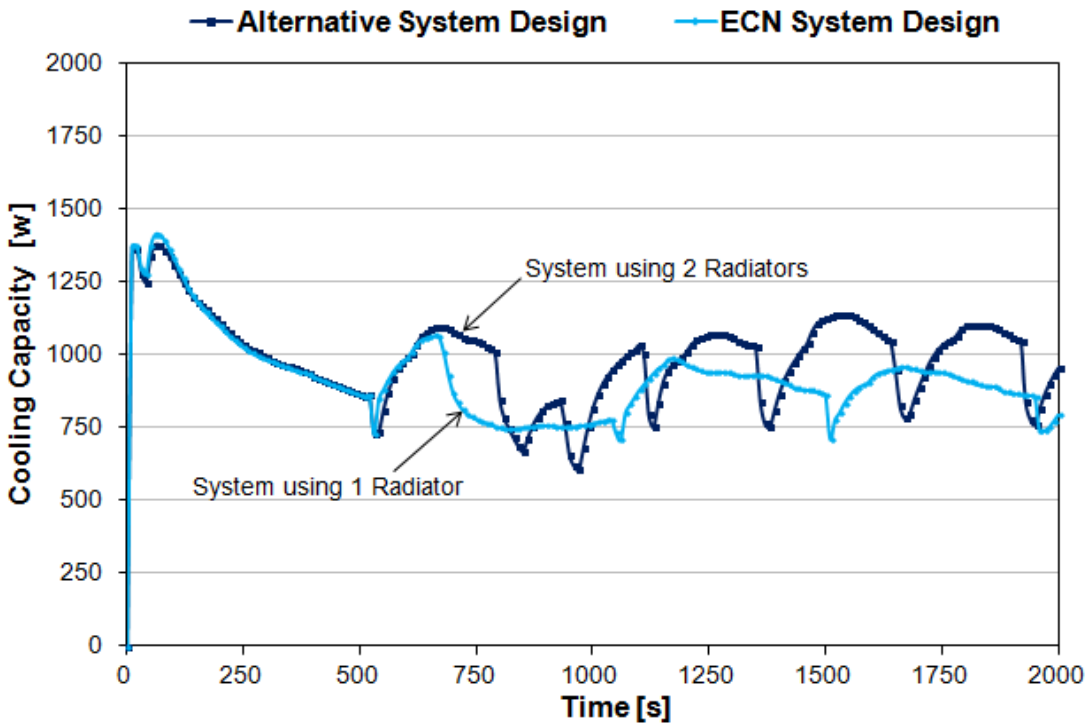

(a)

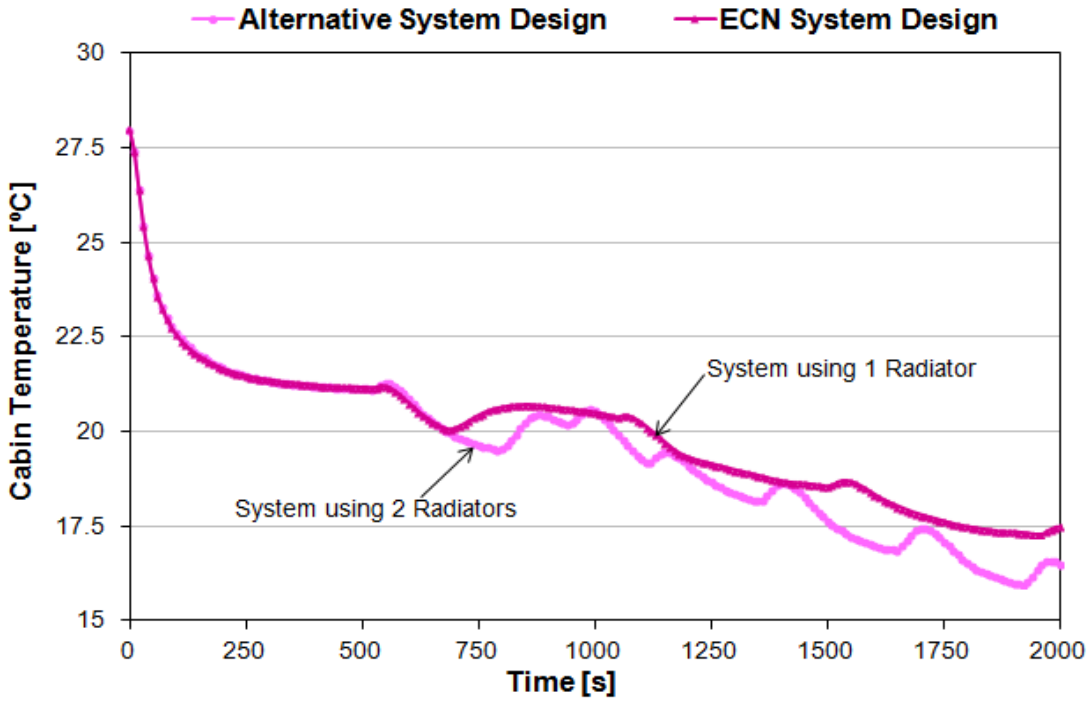

(b)

Fig. 61. Performance of the system at 28 ºC (Test Nº1, Start-Up Strategy: Dry Beds) for different system layouts: (a) Cooling capacity evolution; (b) Cabin temperature evolution.

8. CONCLUSIONS

In this PhD study, a dynamic model of a silica gel/water adsorption cooling system for automotive A/C applications has been developed. The model was subsequently used to optimize the design and operation of the system, and improve its performance. The adsorption cooling system under study was developed and experimentally evaluated under the framework of an R&D project called “Thermally Operated Mobile Air Conditioning Systems – TOPMACS” [65]. The adsorption system in question was designed to be driven by waste heat coming from the engine cooling loop to produce a cooling effect in the cabin of the vehicle. The main reason behind the development of this system is to reduce the fuel consumption and the impact on the environment with respect to traditional mobile air conditioning systems. Modeling such a system is extremely complex since it involves a great number of different components and its operation is fully dynamic with sharp variations of the conditions. Due to this high complexity, and the need of reasonably low computing time, the model has been based on a series of zero-dimensional lumped parameter models (uniform temperature distribution in each component at any instant), which were able to track the dynamics of the system and at the same time provide sufficient accuracy in the estimation of its instantaneous operation and performance.

Simulation results of the sorption system have been compared with experimental results obtained from the adsorption chiller prototype tested at laboratory conditions during the Topmacs project [65]. This comparison proved that the model is able to capture the most important characteristics of the transient behaviour of this kind of adsorption system, as well as its global performance. The experimental tests were conducted using two different operation modes. The first mode did not include a time delay between the switching of the outlet and inlet valves, so no heat recovery was considered. The second operation mode included a delay time in between the on/off switching of the liquid circuit valves. In this operation mode, a part of the sensible heat contained in the liquid circuits was recovered, with the aim to

increase the coefficient of performance (COP). In both operation modes, the calculated results are in very good agreement with the experimental results, proving the good capabilities of the model to predict the system performance at different operation modes. This means that the model can effectively be employed for the optimization of the design of the system layout, as well as for the optimization of its operation and control. Both experimental and model results showed a considerable increase in the coefficient of performance (COP) when the heat recovery is performed, without incurring any loss on the system cooling capacity.

In parallel to the development of the overall system model, an analytical model was developed in order to analyse the influence of the properties of the employed materials and the main design parameters of the beds on the overall thermal conductance of the bed as well as on the maximum performance that could be achieved with a properly designed and operated system. The maximum performance was estimated in terms of maximum specific cooling capacity ($SCC_{m,p}$) and maximum coefficient of performance ($COP_{m,p}$) that could be achieved in practice.

The effects of important parameters such as the channel pitch (p), the channel thickness/channel pitch ratio (t/p), the fin thickness/channel pitch ratio (t_f/p), the fin pitch/channel pitch ratio (p_f/p), the water channel wall thickness/channel pitch ratio (e_{met}/p), the adsorbent thermal conductivity (k_{ads}), the metal thermal conductivity (k_{met}) and the water thermal conductivity (k_w) on the specific thermal conductance of the bed and maximum specific cooling capacity of the system have been investigated thoroughly. The obtained results clearly showed that the maximum specific cooling capacity is proportional to the specific thermal conductance, and this is the reason why both parameters have been studied together.

The most important geometrical parameters affecting the specific thermal conductance of the bed, and hence the maximum specific cooling capacity, are the channel pitch (p), the channel thickness/pitch ratio (t/p) and the fin pitch/ channel pitch ratio (p_f/p). Therefore, the heat transfer performance of the bed

can be improved by reducing the channel pitch. However, it should be taken into consideration that the adsorbent granules must still be able to fit in between the channels. Results also showed that a decrease in the t/p and p_f/p ratios provide higher heat transfer rate throughout the bed. On the other hand, increasing the t_f/p and the e_{met}/p ratios positively affects the specific thermal conductance of the bed; however, it does not yield significant improvements.

From all the thermal parameters that have been studied, the adsorbent thermal conductivity is the most sensitive parameter. It can be concluded that the heat transfer rate inside the bed is strongly affected by the adsorbent thermal conductivity. Increasing the adsorbent thermal conductivity clearly results in better system performance. An effective adsorbent thermal conductivity of at least 0.15 W m^{-1} K^{-1} is desirable. This analysis confirms that the adsorbent conduction constitutes the largest thermal resistance in the system. Therefore, efforts should be focused on reducing the thermal resistance through the adsorbent.

On the other hand, it can be concluded that the plate-side conduction heat transfer resistance has a very small contribution on the total thermal resistance, so that the heat transfer performance of the bed is not significantly affected by the metal conductivity. In any case, a metal thermal conductivity of at least 140 W m^{-1} K^{-1} is desirable. Furthermore, it turns out that the fluid-side convection heat transfer resistance has a very small contribution on the total thermal resistance in the bed. Therefore, changing the heat transfer fluid from water to a mixture of glycol-water will result in a small influence on the heat transfer performance of the bed.

The influence of the properties of the adsorbent material and of the main design parameters of the employed beds were also analyzed. In particular, the effects of the desorption heat (Δh_{des}), the heat transfer fluid/adsorbent mass ratio ($m_{w,tot}/m_{ads,HE}$) and the metal/adsorbent mass ratio ($m_{met,tot}/m_{ads,HE}$) on the maximum performance of the system in terms of $SCC_{m,p}$ and $COP_{m,p}$ have been investigated. The obtained results showed that the desorption heat of the working pair used in the system is the most sensitive parameter from all those

mentioned previously. It is convenient to choose a working pair with low desorption heat and low adsorbent specific heat capacity. For instance, changing the adsorbent used in the bed (Sorbsil A) to a different type of silica gel named SWS-1L could significantly increase both $COP_{m,p}$ and $SCC_{m,p}$. This analysis confirms that the water/adsorbent mass ratio and the metal/adsorbent mass ratio should be kept as low as possible in order to minimize the associated alternate heating/cooling losses. Interestingly, the effect of reducing the water mass is slightly higher than reducing the metal mass, therefore the bed design should target the minimization of the amount of fluid inside. Moreover, the performance of the system could be significantly enhanced by considering metal components and adsorbents for the bed construction that have low specific heat capacities in order to minimize heat losses and other energy losses associated to the alternate heating and cooling.

Finally, the effects of the operating temperatures on the $SCC_{m,p}$ and $COP_{m,p}$ have been investigated. This analysis confirms that the $SCC_{m,p}$ and $COP_{m,p}$ are positively affected if the temperature of the cooling loop decreases. However, the improvement in the SCC is more significant than in the COP. As expected, both $COP_{m,p}$ and $SCC_{m,p}$ increase when increasing the chilled water temperature. This study also shows that increasing the heating water temperature results in higher SCC. However, the COP decreases with higher heating temperatures since the system requires larger heat inputs. It seems that the $SCC_{m,p}$ is more sensitive to heating water variations. In this analysis, it can be concluded that the system under study can achieve a maximum practical COP between 0.4 and 0.6 depending on the operating conditions.

After being validated by experimental results, the model of the adsorption cooling system was then incorporated into the overall model of the vehicle in order to estimate the performance of the onboard adsorption chiller prototype at different operating and driving conditions. Moreover, a parametric study was performed in order to optimize the system operation at constant operating conditions. The effect of the cycle time on the maximum cooling capacity and COP of the system was investigated. The results obtained showed that there is an optimum cycle time for which the system achieves its best performance. The

value obtained for the optimum cycle was taken into consideration for the control strategy of the beds implemented on the overall model of the vehicle.

The overall model has been developed under the MATLAB® Simulink® programming environment, and includes the adsorption cooling system model, plus the engine and cabin models. It is able to reproduce the operation of the engine throughout a standard driving cycle, evaluate the waste heat available at the engine cooling hydraulic loop, simulate the sequential operation of the double-bed adsorption chiller, estimate the condensation of the vapour at the condenser and the cooling effect produced at the evaporator, and finally, the temperature and humidity evolution of the air at the cabin as a function of the external sun radiation, ambient temperature and vehicle velocity.

The overall model has been able to reproduce the behaviour of the engine and the available waste heat throughout a standard driving cycle, and has been employed to estimate the performance of the adsorption air conditioning system under different initial and ambient conditions.

The simulation results showed that the during the warming up period there is no waste heat available to activate the adsorption system, so the engine needs to warm up as fast as possible. When the engine coolant reaches an adequate temperature value, it can then be employed to activate the adsorption system. Nevertheless, cooling the cabin is still possible provided that one or two beds have been kept dry from a previous driving cycle. In this case, they can immediately absorb vapour from the evaporator and produce a cooling effect since the beginning of the new driving cycle.

The simulation results show that the system would be able to provide a significant amount of the required cooling, although it turned out to be slightly undersized for the vehicle.

An alternative layout for the adsorption A/C system has been also studied in order to further increase the system performance. This layout employed two radiators instead of one for the loop providing the cooling for the beds and the

condenser, and its performance has been evaluated using the overall model. This was made possible since the overall model permits different system configurations to be tested. The results obtained have been compared to the results for the system layout with only one radiator, which corresponds to the system installed in the car prototype. It has been made clear that using two radiators is more efficient, leading to better performance. However, during the TOPMACS project [65] this option was discarded mainly because it would have implied a non-negligible extra size and cost.

9. FUTURE WORK

From the results obtained in this PhD study, it is clear that an improved design for the adsorption A/C system prototype is required in order to achieve an increase in system performance. A new, more efficient adsorption system prototype could be designed and built according to the findings obtained from the design optimization study. An improved system layout should include two independent secondary water loops for cooling the beds and the condenser, and a heat recovery option in order to achieve higher cooling capacity. The model developed in this PhD study could be used to optimize the operation of the new system, and to assist in the development of an adequate control for the vehicle. Finally, the new system prototype should be installed in a vehicle and tested at laboratory conditions in order to predict the maximum performance that could be achieved in practice. Perhaps the most important aspect of further developments on adsorption A/C system design is the reduction of size and weight.

Even though the adsorption A/C system presented in this thesis has shown an interesting alternative to conventional MAC systems, any commercial versions must be able to physically fit in a commercial vehicle without restricting passenger space and comfort. Furthermore, the actual weight of the unit must be such that it will not cause an excessive consumption of fuel, or else the benefits of the system described here could be outweighed by potential losses in fuel economy. It would be perhaps advisable to prioritize the installation of the system on larger vehicles, such as trucks, where its weight and volume will not have a significant impact on total vehicle weight and loss of space.

REFERENCES

[1]. Demir, H., Mobedi, M. and Ülkü, S. (2008). A review on adsorption heat pump: problems and solutions, Renewable and Sustainable Energy Reviews, 12, pp. 2381-2403.

[2]. Wang, R.Z., Ge, T.S., Chen, C.J., Ma, Q. and Xiong, Z.Q. (2009). Solar sorption cooling systems for residential applications: options and guidelines, International Journal of Refrigeration, 32, pp. 638-660.

[3]. Zhu, R., Han, B., Lin, M. and Yongzhang, Y. (1992). Experimental investigation on an adsorption system for producing chilled water, Rev. Int. Froid, 15, 1, pp. 31-34.

[4]. Wang, L.W., Wang, R.Z., Wu, J.Y., Xu, Y.X. and Wang, S.G. (2006). Design, simulation and performance of a waste heat driven adsorption ice maker for fishing boat, Energy, 31, pp. 244-259.

[5]. Jiangzhou, S., Wang, R.Z., Lu, Y.Z., Xu, Y.X. and Wu, J.Y. (2002). Experimental investigations on adsorption air-conditioner used in internal-combustion locomotive driver-cabin, Applied Thermal Engineering, 22, pp. 1153-1162.

[6]. Lu, Y.Z., Wang, R.Z., Jianzhou, S., Xu, Y.X. and Wu, J.Y. (2004). Practical experiments on an adsorption air conditioner powered by exhausted heat from a diesel locomotive, Applied Thermal Engineering, 24, pp. 1051-1059.

[7]. Wang, D.C., Xia, Z.Z. and Wu, J.W. (2006). Design and performance of a novel zeolite-water adsorption air conditioner, Energy Conversion and Management, 47, pp. 590-610.

[8]. Zhang, L.Z. (2000). Design and testing of an automobile waste heat adsorption cooling system, Applied Thermal Engineering, 20, pp. 103-114.

[9]. Suzuki, M. (1993). Application of adsorption cooling systems to automobiles, Heat Recovery Systems & CHP, 13, 4, pp. 335-340.

[10]. Grisel, R.J.H., Smeding, S.F. and de Boer, R. (2010). Waste heat driven silica gel/water adsorption cooling in trigeneration, Applied Thermal Engineering, 30, pp. 1039-1046.

[11]. Vasta, S., Freni, A., Sapienza, A., Costa, F. and Restuccia, G. (2012). Development and lab-test of a mobile adsorption air conditioner, International Journal of Refrigeration, 35, pp. 701-708.

[12]. Poyelle, F., Guilleminot, J.J. and Meunier, F. (1999). Experimental tests and predictive model of an adsorptive air conditioning unit, Industrial & Engineering Chemistry Research, 38, pp. 298-309.

[13]. Lambert, M.A. and Jones, B.J. (2005). Review of regenerative adsorption heat pumps, Journal of Thermophysics and Heat Transfer, 19, 4, pp. 471-485.

[14]. Wang, R.Z. and Oliveira, R.G. (2006). Adsorption refrigeration – an efficient way to make good use of waste heat and solar energy, Progress in Energy and Combustion Science, 32, 4, pp.424-458.

[15]. Wang, D.C., Li, Y.H., Li, D., Xia, Y.Z. and Zhang, J.P. (2010). A review on adsorption refrigeration technology and adsorption deterioration in physical adsorption systems, Renewable and Sustainable Energy Reviews, 14, 1, pp. 344-353.

[16]. Yong, L. and Wang, R.Z. (2007). Adsorption refrigeration: A survey of novel technologies, Recent Patents on Engineering, 1, pp. 1-21.

[17]. Chua, K.J., Chou, S.K. and Yang, W.M. (2010). Advances in heat pump systems: A review, Applied Energy, 87, pp. 3611-3624.

[18]. Chekirou, W., Boussehain, R., Feidt, M., Karaali, A. and Boukheit, N. (2011). Numerical results on operating parameters influence for a heat recovery machine, Energy Procedia, 6, pp. 202-216.

[19]. Cerkvenik, B. and Ziegler, F. (2006). The influence of periodic operation on the characteristics of adsorption devices, Energy Conversion and Management, 47, pp. 2020-2033.

[20]. Maggio, G., Freni, A. and Restuccia, G. (2006). A dynamic model of heat and mass transfer in a double-bed adsorption machine with internal heat recovery, International Journal of Refrigeration, 29, pp. 589-600.

[21]. Akahira ,A., Alam, K.C.A., Hamamoto, Y., Akisawa, A. and Kashiwagi, T. (2005). Experimental investigation of mass recovery adsorption refrigeration cycle, International Journal of Refrigeration, 28, pp. 565-572.

[22]. Akahira, A., Alam, K.C.A., Hamamoto, Y., Akisawa, A. and Kashiwagi, T. (2004). Mass recovery adsorption refrigeration cycle – improving cooling capacity, International Journal of Refrigeration, 27, pp. 225-234.

[23]. Wang, R.Z. (2001). Performance improvement of adsorption cooling by heat and mass recovery operation, International Journal of Refrigeration, 24, pp. 602-611.

[24]. Leong, K.C. and Liu, Y. (2004). Numerical study of a combined heat and mass recovery cooling cycle, International Journal of Heat and Mass Transfer, 47, pp. 4761-4770.

[25]. Leong, K.C. and Liu, Y. (2006). System performance of a combined heat and mass recovery adsorption cooling cycle: A parametric study, International Journal of Heat and Mass Transfer, 49, pp. 2703-2711.

[26]. Saha, B.B. and Kashiwagi, T. (1997). Experimental investigation of an advanced adsorption refrigeration cycle, ASHRAE Transactions, 103, 2, pp. 50-58.

[27]. Saha, B.B., Akisawa, A. and Kashiwagi, T. (2001). Solar/waste heat driven two-stage adsorption chiller: the prototype, Renewable Energy, 23, pp. 93-101.

[28]. Alam, K.C.A., Akahira ,A., Hamamoto, Y., Akisawa, A., Kashiwagi, T., Saha, B.B., Koyama, S., Ng, K.C. and Chua, H.T. (2003). Multi-bed multi-stage adsorption refrigeration cycle-reducing driving heat source temperature, ASHRAE Transactions, 20, 3, pp. 413-420.

[29]. Khan, M.Z.I., Alam, K.C.A., Saha, B.B., Hamamoto, Y., Akisawa, A. and Kashiwagi, T. (2006). Parametric study of a two-stage adsorption chiller using re-heat – The effect of overall thermal conductance and adsorbent mass on system performance, International Journal of Thermal Sciences, 45, pp. 511-519.

[30]. Saha, B.B., Koyama, S., Lee, J.B., Kuwahara, K., Alam, K.C.A., Hamamoto, Y., Akisawa, A. and Kashiwagi, T. (2003). Performance evaluation of a low-temperature waste heat driven multi-bed adsorption chiller, International Journal of Multiphase Flow 29, pp. 1249-1263.

[31]. Saha, B.B., El-Sharkaway, I., Koyama, S., Lee, J.B. and Kuwahara, K. (2006). Waste heat driven multi-bed adsorption chiller: Heat exchangers overall thermal conductance on chiller performance, Heat Transfer Engineering, 27, 5, pp. 80-87.

[32]. Miyazaki, T., Akisawa, A. and Saha, B.B. (2010). The performance analysis of a novel dual evaporator type three-bed adsorption chiller, International Journal of Refrigeration, 33, pp. 276-285.

[33]. Cacciola, G., Hajji, A., Maggio, G. and Restuccia, G. (1993). Dynamic simulation of a recuperative adsorption heat pump, Energy, 18, 11, pp. 1125-1137.

[34]. Cacciola, G. and Restuccia, G. (1995). Reversible adsorption heat pump: a thermodynamic model, International Journal of Refrigeration, 18, 2, pp. 100-106.

[35]. Cacciola, G., Restuccia, G. and van Benthem, G.H.W. (1999). Influence of the adsorber heat exchanger design on the performance of the heat pump system, Applied Thermal Engineering, 19, pp. 255-269.

[36]. van Benthem, G.H.W., Cacciola, G. and Restuccia, G. (1995). Regenerative adsorption heat pumps: optimization of the design, Heat Recovery Systems & CHP, 15, 6, pp. 531-544.

[37]. Douss, N., Meunier, F.E. and Sun, L.-M. (1988). Predictive model and experimental results for a two-adsorber solid adsorption heat pump, Industrial & Engineering Chemistry Research, 27, pp. 310-316.

[38]. Schicktanz, M. and Núñez, T. (2009). Modelling of an adsorption chiller for dynamic system simulation, International Journal of Refrigeration, 32, pp.588-595.

[39]. Miyazaki, T., Akisawa, A., Saha, B.B., El-Sharkawy, I.I. and Charkraborty, A. (2009). A new cycle time allocation for enhancing the performance of two bed adsorption chillers, International Journal of Refrigeration, 32, pp. 846-853.

[40]. Miyazaki, T. and Akisawa, A. (2009). The influence of heat exchanger parameters on the optimum cycle time of adsorption chillers, Applied Thermal Engineering, 29, pp. 2708-2717.

[41]. Zhang, L.Z. and Wang, L. (1997). Performance estimation of an adsorption cooling system for automobile waste heat recovery, Applied Thermal Engineering, 17, 12, pp. 1127-1139.

[42]. Sami, S.M. and Tribes, C. (1996). An improved model for predicting the dynamic behaviour of adsorption systems, Applied Thermal Engineering 16, 2, pp. 149-161.

[43]. Saha, B.B., Boelman, E.C. and Kashiwagi, T. (1995). Computer simulation of a silica gel-water adsorption refrigeration cycle – The influence of operating conditions on cooling output and COP, ASHRAE Transactions, 101, 2, pp. 348-357.

[44]. Cho, S.-H. and Kim J.-N. (1992). Modeling of a Silica gel/water adsorption-cooling system, Energy, 17, 9, pp. 829-839.

[45]. Hajji, A. (1991). Simulation of a regenerative, closed-cycle adsorption cooling/heating system, Energy, 16, 3, pp. 643-654.

[46]. Alam, K.C.A., Saha, B.B., Kang, Y.T., Akisawa, A. and Kashiwagi, T. (2000). Heat design effect on the performance of silica gel adsorption refrigeration systems, International Journal of Heat and Mass Transfer, 43, pp. 4419-4431.

[47]. Alam, K.C.A., Kang, Y.T., Saha, B.B., Akisawa, A. and Kashiwagi, T. (2003). A novel approach to determine optimum switching frequency of a conventional adsorption chiller, Energy, 28, pp. 1021-1037.

[48]. Chua, H.T., Ng, K.C., Wang, W., Yap, C. and Wang, X.L. (2004). Transient modeling of a two-bed silica gel-water adsorption chiller, International Journal of Heat and Mass Transfer, 47, pp. 659-669.

[49]. Alam, K.C.A., Saha, B.B., Akisawa, A. and Kashiwagi, T. (2000). A novel parametric analysis of a conventional silica gel – water adsorption chiller, ASHRAE Transactions, 17, 3, pp. 323-332.

[50]. Zheng, W. and Worek, W.M. (1995). Effect of operating conditions on the performance of two-bed closed-cycle solid-sorption heat pump systems, Journal of Solar Energy Engineering, 117, pp. 181-186.

[51]. Sakoda, A. and Suzuki, M. (1986). Simultaneous transport of heat and adsorbate in closed type adsorption cooling system utilizing solar heat, Journal of Solar Energy Engineering, 108, pp. 239-245.

[52]. Sakoda, A. and Suzuki, M. (1984). Fundamental study on solar powered adsorption cooling system, Journal of Chemical Engineering of Japan, 17, 1, pp. 52-57.

[53]. Zhang, L.Z. (2000). A three dimensional non-equilibrium model for an intermittent adsorption cooling system, Solar Energy, 69, pp. 27-35.

[54]. Wu, W.-D., Zhang, H. and Sun, D.-W. (2009). Mathematical simulation and experimental study of a modified zeolite 13X-water adsorption refrigeration module, Applied Thermal Engineering, 29, pp. 645-651.

[55]. Voyiatzis, E., Pavlos, J.A. and Markatos, N.-C. (2008). Heat-exchanger design and switching-frequency effects on the performance of a continuous type solar adsorption chiller, Applied Energy, 85, pp.1237-1250.

[56]. Miltkau, T. and Dawoud, B. (2002). Dynamic modeling of the combined heat and mass transfer during the adsorption/desorption of water vapor into/from a zeolite layer of an adsorption heat pump, International Journal of Thermal Sciences, 41, pp. 753-762.

[57]. Melkon, T., Birgul, T.-E. and Ayse, E.-S. (1999). A novel approach to enhance heat and mass transfer in adsorption heat pumps using the zeolite-water pair, Microporous and Mesoporous Materials, 27, pp. 1-10.

[58]. Liu, Y. and Leong, K.C. (2005). The effect of operating conditions on the performance of zeolite/water adsorption cooling systems, Applied Thermal Engineering, 25, pp. 1403-1418.

[59]. Marletta, L., Maggio, G., Freni, A., Ingrasciotta, M. and Restuccia, G. (2002). A non-uniform temperature non-uniform pressure dynamic model of heat and mass transfer in compact adsorbent beds, International Journal of Heat and Mass Transfer, 45, pp. 3321-3330.

[60]. Leong, K.C. and Liu, Y. (2004). Numerical modeling of combined heat and mass transfer in the adsorbent bed of a zeolite/water cooling system, Applied Thermal Engineering, 24, pp. 2359-2374.

[61]. Restuccia, G., Freni, A., Maggio, G., (2002). A zeolite-coated bed for air conditioning adsorption systems: parametric study of heat and mass transfer by dynamic simulation, Applied Thermal Eng., 22, pp. 619-630.

[62]. Niazmand, H. and Dabzadeh, I. (2012) Numerical simulation of heat and mass transfer in adsorbent beds with annular fins, Int. Journal of Refrigeration, 35, pp. 581-593.

[63]. Rezk, A.R.M. and Al-Dadah, R.K. (2011). Physical and operating conditions effects on silica gel/water adsorption chiller performance, Applied Energy, 89, pp 142-149.

[64]. Solmus, I., Rees, D.A.S., Yamali, C., Baker, D., Kaftanoglu, B. (2012). Numerical investigation of coupled heat and mass transfer inside the adsorbent bed of an adsorption cooling unit, Int. Journal of Refrigeration, 35, pp. 652-662.

[65]. European project TOPMACS – Thermally Operated Mobile Air – Conditioning Systems, funded by the European Comission under the 6th European Community framework program (Contract Ref. TST4-CT-2005-012471).
Retrieved from:
http://ec.europa.eu/research/transport/projects/items/topmacs_en.htm

[66]. Miller, A.R., (1949). *The adsorption of gases on solids*. Cambridge University Press, Cambridge.

[67]. Ruthven, Douglas M. (1984). *Principles of adsorption and adsorption processes*. John Wiley & Sons, Canada.

[68]. Rouquerol F. (1999). *Adsorption by powders and porous solids: principles, methodology and applications.* Academic Press, London.

[69]. Gregg, S.J. (1997). *Adsorption, surface area and porosity.* 2nd edition, Academic Press, London.

[70]. Verde, M. , Cortés, L., Corberán , J.M., Sapienza, A., Vasta, S. and Restuccia, G. (2010). Modelling of an adsorption system driven by engine waste heat for truck cabin A/C. Performance estimation for a standard driving cycle, Applied Thermal Engineering, 30, pp. 1511-1522

[71]. Mola S., (2005). *TOPMACS Project - Description of Work.* Research report, Centro Ricerche Fiat - CRF, Italy.

[72]. de Boer R., (2006). *TOPMACS Project - Component design and models for sorption cooling systems.* Deliverable 12, Energy research Center of the Netherlands - ECN, The Netherlands.

[73]. Mitsubishi Corporation. Technical information on adsorbent materials (FAM-Z02). Retrieved from: http://www.mitsubishicorp.com/

[74]. Sapienza, A., Freni, A., Vasta, S., Restuccia, G. and Cacciola G. (2007). Performance of a novel functional adsorbent material for automotive adsorption air conditioning, International Symposium on Innovative Materials for Processes in Energy Systems - IMPRES, Kyoto, Japan, October 28-31

[75]. Ineos Group Limited, Technical information on adsorbent materials (Sorbsil A). Retrieved from: http://www.ineos.com/

[76]. Smeding, S.F. and de Boer R., (2009). *Adsorption cooling systems analysis: Future improvement potential.* Research Report ECN-0-09-000, Energy research Center of the Netherlands - ECN, The Netherlands.

[77]. Denso Corporation, Technical information on heat exchangers.
Retrieved from: http://www.globaldenso.com/en/

[78]. Valeo, Technical information on heat exchangers.
Retrieved from: http://www.valeo.com/]

[79]. Behr, Technical information on heat exchangers.
Retrieved from: www.behrhellaservice.com

[80]. Sapienza, A., Santamaria, S., Frazzica, A. and Freni, A. (2011). Influence of the management strategy and operating conditions on the performance of an adsorption chiller, Energy, 36, pp. 5532-5538.

[81]. Raymond, A. and Garimella, S. (2011). Annular-finned sorption bed heat exchanger design for adsorption heat pump optimization, In: Proc. of the International Sorption Heat Pump Conference ISHPC11, Padua, Italy.

[82] Critoph, R.E., Telto, T.Z. and Davies, L.N.G. (2000). A prototype of a fast cycle adsorption refrigerator utilizing a novel carbon–aluminium laminate, In: Proc. of the Institution of Mechanical Engineers, 214.

[83]. Guilleminot, J. J., Choisier, A. , Chalfen, J. B. , Nicolas S. and Reymoney J. L., (1993). Heat transfer intensification in fixed bed adsorbers, Heat Recovery Systems & CHP, 13, pp. 297-300.

[84]. Gui, Y.B., Wang, R.Z., Wang, W., Wu, J.Y. and Xu, Y.X., (2002). Performance modelling and testing on a heat-regenerative adsorptive reversible heat pump, Applied Thermal Engineering, 22, pp. 309–320.

[85]. Saha, B.B., Koyama, S., El-Sharkawy, I.I., Kuwahara, K., Kariya, K., Ng, K.C., (2006). Experiments for measuring adsorption characteristics of an activated carbon fiber/ethanol pair using a plate-fin heat exchanger, HVAC&R Research, 12, pp. 767–782.

[86]. Bou, P., Guilleminot, J.J., Pons, M. (1996). Composite actif à structure feuilletée comprenant un agent actif sous forme de granules. Elf Aquitaine Patent, 9612762.

[87]. Lambert, M. A. and Jones, B. J. (2006). Automotive adsorption air conditioner powered by exhaust heat. Part 1: conceptual and embodiment design, Journal of Automobile Engineering, 220, pp. 959-972.

[88]. Incropera, F.P., 1990. *Fundamentals of Heat and Mass Transfer*, 3rd Edition, Wiley, New York, pp. 501.

[89]. Sharonov, V.E., Aristov, Y., (2008). Chemical and adsorption heat pumps: Comments on the second law efficiency, Chemical Eng. Journal, 136, pp. 419-424.

[90]. Restuccia, G., Aristov, Y., Maggio, G., Cacciola, G. and Tokarev, M.M. (1999). Performance of sorption systems using selective water sorbents, In: Proc. of the International Sorption Heat Pump Conference – ISHPC99, Munich, Germany, pp. 219-223.

[91]. Rohsenow, W.M, Hartnett and Ganic, E.N. (1985). *Handbook of Heat Transfer Fundamentals*, 2nd Edition, McGraw-Hill, New York.

[92]. Freni, A., (2013). *Personal communication*, Istituto di Tecnologie Avanzate per l´Energia 'Nicola Giordano' CNR-ITAE, Messina, Italy.

[93]. Melinder Ake, Ed. (1997). *Thermophysical Properties of Liquid Secondary Refrigerants*, IIR – International Institute of Refrigeration.

[94]. Mills, A.F. (1999). *Heat Transfer.* 2nd Edition, Prentice Hall, Upper Saddle River.